

Endothelial Cell Apoptosis

Adrian Thomas Churchman

A thesis submitted in partial fulfilment of the requirements of the University of Hertfordshire for the degree of Doctor of Philosophy.

School of Life Sciences
University of Hertfordshire
College Lane Campus
Hatfield
Herts.

December 2005

Acknowledgements

I would like to thank my supervisors Dr. Richard Hoffman and Prof. Anwar Baydoun for all their support and guidance over the past three years, their experience has been invaluable throughout my studies.

I would like to thank all the people in the labs who have given me support and help especially Gareth, Dirk, and Jen; they were always there when I needed them. Special thanks must be given to Di, Jon and Jenny for all their hard work, encouragement and technical support (even at short notice!) during my PhD.

Special thanks go to the nurses and midwives at the Queen Elizabeth II hospital, Welwyn Garden City, for all their cooperation in acquiring samples for this study.

I would also like to thank my family and friends, who made it possible for me to complete my studies. All their encouragement and help was always gratefully received and will not be forgotten. Special thanks go to my Mum, Dad and Emma, without their support I would have not made it this far.

Abstract

Endothelial cell apoptosis is an important process during vasculature remodelling, angiogenesis and inflammation. Medical interest in endothelial cell apoptosis as a target for arthritis and solid tumour treatment has prompted biochemical and pharmacological investigation into the mechanisms controlling endothelial cell survival and angiogenesis. In recent years it has been hypothesised that control of endothelial cell apoptosis and the induction of angiogenesis may in part be due to the enzyme cyclooxygenase (COX)-2.

COX-2 is involved in the metabolism of arachidonic acid to prostaglandins in mammals. This pathway has been implicated in controlling inflammation and angiogenesis through prostaglandin (PG) production and more recently has been shown to inhibit endothelial cell death. It was the aim of this study to investigate endothelial cell apoptosis and angiogenesis focussing on the role of COX-2, prostaglandins and endogenous apoptotic inhibitors in these pathways.

Endothelial cell apoptosis was assessed by chromatin condensation, DNA fragmentation and caspase activation. Angiogenesis was investigated by examining capillary-like tubule formation. Endothelial cell apoptosis induction and angiogenesis inhibition was observed using the selective COX-2 inhibitor 5-bromo-2-(4-fluorophenyl)-3-(methylsulfonyl) thiophene (DuP-697) at a concentration 100 times lower than has previously been reported. Apoptosis was confirmed by induction of caspases 8, 9 and 3 over 8 hr and DNA fragmentation and condensation over 24 hr. The effects observed may be due to a selective inhibition of COX-2 as apoptosis induction and angiogenic

inhibition only occurred when COX-2 was inhibited by selective and non-selective COX inhibitors.

Induction of endothelial cell death was induced by treatment with two natural products that inhibit COX-2, namely curcumin and 6-shogaol (from turmeric and ginger respectively) although only at concentrations higher than were required to inhibit COX-2. Both compounds induced chromatin condensation in endothelial cells and Jurkat E6.1 cells with no DNA laddering or caspase induction.

Further examination of the mechanisms of endothelial cell survival were investigated by assessing the endogenous expression of the apoptosis repressor with a caspase recognition domain (ARC) protein through examining reverse transcriptase (RT) - PCR, native protein expression and transgenic over-expression in the endothelial cells. Endogenous expression of ARC was found in endothelial cells. However this expression declined during *in vitro* culture. Transgenic expression of ARC was found to increase levels of ARC *in vitro*. However it had no effect on apoptosis inhibition after 24 hr.

The underlying mechanisms of cell death induction may be compound dependent in endothelial cells. Pharmacological inhibition of COX-2 and possibly PGE₂ generation has detrimental effects on angiogenesis and endothelial cell survival. However inhibition of COX-2 by natural products at low concentrations may be advantageous in preventing tumour angiogenesis with no apoptosis induction.

Contents

1.0 Introduction

1.1 Endothelial cells and angiogenesis	1
1.1.1 Endothelial cells	1
1.1.2 Angiogenesis	1
1.1.3 Breakdown of the extracellular matrix (ECM)	5
1.1.4 Endothelial cell migration	5
1.1.5 Lumen formation and vessel maturation	6
1.1.6 The effect of VEGF of endothelial cells	6
1.1.7 Induction of gene expression in endothelial cells by VEGF	7
1.2 Cyclooxygenase enzymes	9
1.2.1 Catalysis of arachidonic acid to prostaglandin H ₂	10
1.2.2 Cyclooxygenase 1	12
1.2.3 Expression and function of COX-1	14
1.2.4 Cyclooxygenase 2	16
1.2.5 Cyclooxygenase 2 induction	17
1.2.6 Induction of cyclooxygenase 2 during inflammation	19
1.2.7 Induction of cyclooxygenase 2 during angiogenesis	20
1.2.8 Regulation of COX-2 expression	23
1.2.9 Prostaglandins	25
1.2.10 Prostaglandin E ₂ (PGE ₂)	27
1.2.11 Inhibitors of cyclooxygenase 2	28
1.2.11.1 Non-specific cyclooxygenase inhibitors	28
1.2.11.2 Specific cyclooxygenase 2 inhibitors	29
1.2.11.3 Celecoxib (Celebrex ®)	31
1.2.11.4 Rofecoxib (Vioxx ®)	32
1.2.11.5 5-bromo-2- (4-fluorophenyl)-3-(methylsulfonyl) thiophene (DuP-697)	33
1.2.12 Dietary natural products	35
1.2.12.1 Curcumin (Diferuloylmethane)	35
1.2.12.2 6-Shogaol	38

1.3 Cell death	39
1.3.1 Necrosis	39
1.3.2 Apoptosis	39
1.3.2.1 Morphological changes associated with apoptosis	40
1.3.2.2 Apoptotic bodies	41
1.3.2.3 Phosphatidylserine translocation	41
1.3.2.4 Cell shrinkage	42
1.3.2.5 Condensation of the chromatin and DNA cleavage	42
1.3.3 Caspases	44
1.3.3.1 Caspase 8	45
1.3.3.2 Caspase 9	46
1.3.3.3 Caspase 3	46
1.3.3.4 Caspases 6 and 7	47
1.3.4 The Bcl-2 proteins	47
1.3.5 The pathways of apoptosis	51
1.3.5.1 The mitochondrial pathway of apoptosis	51
1.3.5.2 The death receptor pathway of apoptosis	53
1.3.5.3 Interlinking of the apoptotic pathways	55
1.3.6 Endogenous inhibitors of apoptosis	57
1.3.6.1 Apoptosis repressor with caspase recruitment domain (ARC)	57
1.4 Angiogenesis, Cyclooxygenase 2 and Apoptosis	60
1.4.1 Angiogenesis and apoptosis	60
1.4.2 Angiogenesis and cyclooxygenase 2	60
1.4.3 Angiogenesis and cyclooxygenase 2 inhibition	62
1.4.4 Cyclooxygenase 2 and apoptosis	63
1.4.4.1 Cyclooxygenase 2 and apoptosis inhibition	63
1.4.4.2 Cyclooxygenase 2 and apoptosis induction	64
1.4.4.3 Cyclooxygenase 2 inhibition and apoptosis induction	64
2.0 Materials and Methods	66
2.1 Cell culture	66

2.1.1 Isolation of Human Umbilical Vein Endothelial Cells (HUVECs)	66
2.1.2 Growth and maintenance of HUVECs	67
2.1.3 Passage and plating of HUVECs	67
2.1.4 Growth and maintenance of J774 macrophages	68
2.1.5 Growth and maintenance of Jurkat E6.1 cells	68
2.2 Matrigel HUVEC tubule formation assay	69
2.3 Induction of apoptosis in HUVEC and Jurkat E6.1 cells	69
2.4 Determination of induced cell apoptosis	70
2.4.1 Cytospinning and fluorescent staining of condensed chromatin	70
2.4.2 DNA laddering assay using a DNA suicide track ® kit	72
2.4.3 DNA laddering assay following phenol/chloroform DNA extraction	72
2.4.4 Analysis of caspase 3 activity	73
2.5 Western blotting and protein analysis	75
2.5.1 BCA assay for protein concentration	75
2.5.2 Sample preparation	76
2.5.3 Sodium dodecyl sulphate polyacrylamide gel electrophoresis (SDS-PAGE)	76
2.5.4 Western Blotting of SDS-PAGE gel	78
2.5.5 Immunodetection of proteins on nitrocellulose membranes	79
2.5.6 Enhanced chemiluminescence detection of antibody bound proteins	80
2.5.7 Analysis of immunoblotting by densitometry	80
2.6 Prostaglandin E ₂ enzyme linked immunosorbent assay (ELISA)	81
2.6.1 Sample preparation	81
2.6.2 Detection of PGE ₂	81
2.7 Apoptosis repressor with CARD domain plasmid isolation and analysis	82
2.7.1 Culture of competent cells	82
2.7.2 Preparation of plasmid pCDNA3-ARC	83
2.7.3 Transformation of the competent DH5α <i>E.coli</i> cells	83

2.7.4 Bacterial growth and maintenance	83
2.7.5 Isolation of pCDNA3-ARC using Qiagen Miniprep plasmid isolation kit.	84
2.7.6 Digestion of pCDNA3-ARC with endonucleases	85
2.7.7 Polymerase chain reaction (PCR)	85
2.7.8 Transfection of HUVECs using the JetPEI-HUVEC reagent	86
2.8 Agarose gel analysis and detection of DNA	86
2.8.1 Agarose gel electrophoresis	86
2.8.2 Ethidium Bromide staining of an agarose gel	87
2.9 Statistical analysis of data	87
2.9.1 Student's unpaired t-test	87
2.9.2 One way analysis of variance (ANOVA)	88
3.0 Calibration and optimisation of apoptosis analysis techniques	91
3.1 Introduction	91
3.1.1 Membrane blebbing	91
3.1.2 DNA condensation staining	92
3.1.3 DNA cleavage and strand breaks	94
3.2 Aims	95
3.3 Methods	95
3.4 Results	96
3.4.1 The induction of apoptosis by multiple stimuli	96
3.4.2 Effect of paclitaxel in Jurkat E6.1 cells	106
3.4.3 Effects of paclitaxel on HUVECs	108
3.4.4 Effects of actinomycin-D on HUVECs	110
3.5 Discussion	114
4.0 Effects of curcumin and 6-shogaol on VEGF ₁₆₅ induced cyclooxygenase-2 expression and apoptosis induction in HUVECs	118
4.1 Introduction	118
4.2 Aims	119
4.3 Methods	119
4.4 Results	120
4.4.1 Induction of COX-2 with VEGF ₁₆₅ in HUVECs	120

4.4.2	Inhibition of COX-2 by curcumin and 6-shogaol in HUVECs	120
4.4.3	Induction of HUVEC apoptosis with curcumin and 6-shogaol	124
4.4.4	Effects of PGE ₂ on curcumin and 6-shogaol induced HUVEC chromatin condensation	127
4.4.5	Induction of Jurkat E6.1 apoptosis with curcumin and 6-shogaol	130
4.5	Discussion	133
5.0	Comparison of selective and non-selective COX-2 inhibitors on angiogenesis and induction of apoptosis in HUVECs	138
5.1	Introduction	138
5.2	Aims	139
5.3	Methods	139
5.4	Results	140
5.4.1	Expression of COX-2 in HUVECs	140
5.4.2	Inhibition of prostaglandin E ₂ production in unstimulated and VEGF ₁₆₅ stimulated HUVECs by DuP-697	141
5.4.3	Effects of DuP-697 on chromatin condensation in HUVECS	145
5.4.4	Induction of apoptosis in HUVECs by indomethacin	147
5.4.5	Effects of DuP-697 on caspase activation	150
5.4.6	Effects of indomethacin on caspase activation	152
5.4.7	Effects of PGE ₂ , VEGF ₁₆₅ and CHO-DEVD on DuP-697 induced apoptosis in HUVECs	153
5.4.8	Induction of HUVEC membrane permeability by DuP-697	161
5.4.9	Effects of DuP-697 and indomethacin on tubule formation	162
5.5	Discussion	167
6.0	Isolation, growth and transfection of the apoptosis repressor with caspase recruitment domain (ARC)	175
6.1	Introduction	175
6.2	Aims	176
6.3	Methods	176
6.4	Results	177

6.4.1 Expression of the ARC protein in HUVECs	177
6.4.2 Analysis of ARC RNA transcription in HUVECs	180
6.4.3 Isolation of pCDNA3-ARC from filter paper and transformation into competent DH5 α <u>E.coli</u>	182
6.4.4 Restriction of the plasmid pCDNA3-ARC and sizing of the <u>ARC</u> gene	183
6.4.5 Transfection of HUVECs with pCDNA3-ARC	187
6.4.6 Inhibition of DuP-697 induced apoptosis in pCDNA3-ARC transfected HUVECs	190
6.5 Discussion	192
7.0 General Discussion	196
8.0 References	206
9.0 Appendix A	228
10.0 Appendix B	231

List of figures

Figure 1.1.1	Overview of the stages of angiogenesis	4
Figure 1.2.1	Schematic representation of the catalysis of arachidonic acid to prostaglandins and thromboxanes indicating the points of catalysis by the cyclooxygenase and peroxidase enzymes	9
Figure 1.2.2	Overview of arachidonic acid catalysis to prostaglandin G ₂	11
Figure 1.2.3	Schematic representation of the catalytic conversion of arachidonic acid to prostaglandin H ₂ (PGH ₂)	12
Figure 1.2.4a	Schematic diagram of cyclooxygenase 1 protein structure	12
Figure 1.2.4b	Ribbon diagram of ovine COX-1 active homodimer	13
Figure 1.2.5	Schematic diagram of cyclooxygenase 2 protein structure	15
Figure 1.2.6	Cartoon of the cyclooxygenase 2 monomer	16
Figure 1.2.7	Schematic representation of the COX-2 promoter sequence	18
Figure 1.2.8	Lipopolysaccharide (LPS) signalling in the induction of COX-2	20
Figure 1.2.9	VEGF signalling in the induction of COX-2	22
Figure 1.2.10	Regulation of COX- 2 expression by negative feedback loop	23
Figure 1.2.11	Positive feedback loop of COX- 2 expression	24
Figure 1.2.12	Inhibition of the COX- 2 enzyme identifying the binding of the inhibitor to the “side-pocket” in the cyclooxygenase active site	30
Figure 1.2.13	Chemical structure of celecoxib (Celebrex ®)	32
Figure 1.2.14	Chemical structure of rofecoxib (Vioxx ®)	33
Figure 1.2.15	Chemical structure of DuP-697	34
Figure 1.2.16	Molecular structure of curcumin from <i>curcuma longa</i>	35
Figure 1.2.17	Inhibition of the signalling pathways involved in COX-2 induction	37
Figure 1.2.18	Chemical structure of 6-shogaol	38
Figure 1.3.1	Structural conversion of pro-caspase to active caspase	44
Figure 1.3.2	Structure of the Bcl-2 superfamily members showing the <i>Bcl-2</i> homology (BH) domains	48

List of figures

Figure 1.1.1	Overview of the stages of angiogenesis	4
Figure 1.2.1	Schematic representation of the catalysis of arachidonic acid to prostaglandins and thromboxanes indicating the points of catalysis by the cyclooxygenase and peroxidase enzymes	9
Figure 1.2.2	Overview of arachidonic acid catalysis to prostaglandin G ₂	11
Figure 1.2.3	Schematic representation of the catalytic conversion of arachidonic acid to prostaglandin H ₂ (PGH ₂)	12
Figure 1.2.4a	Schematic diagram of cyclooxygenase 1 protein structure	12
Figure 1.2.4b	Ribbon diagram of ovine COX-1 active homodimer	13
Figure 1.2.5	Schematic diagram of cyclooxygenase 2 protein structure	15
Figure 1.2.6	Cartoon of the cyclooxygenase 2 monomer	16
Figure 1.2.7	Schematic representation of the COX-2 promoter sequence	18
Figure 1.2.8	Lipopolysaccharide (LPS) signalling in the induction of COX-2	20
Figure 1.2.9	VEGF signalling in the induction of COX-2	22
Figure 1.2.10	Regulation of COX- 2 expression by negative feedback loop	23
Figure 1.2.11	Positive feedback loop of COX- 2 expression	24
Figure 1.2.12	Inhibition of the COX- 2 enzyme identifying the binding of the inhibitor to the “side-pocket” in the cyclooxygenase active site	30
Figure 1.2.13	Chemical structure of celecoxib (Celebrex ®)	32
Figure 1.2.14	Chemical structure of rofecoxib (Vioxx ®)	33
Figure 1.2.15	Chemical structure of DuP-697	34
Figure 1.2.16	Molecular structure of curcumin from <i>curcuma longa</i>	35
Figure 1.2.17	Inhibition of the signalling pathways involved in COX-2 induction	37
Figure 1.2.18	Chemical structure of 6-shogaol	38
Figure 1.3.1	Structural conversion of pro-caspase to active caspase	44
Figure 1.3.2	Structure of the Bcl-2 superfamily members showing the Bcl-2 homology (BH) domains	48

Figure 1.3.3	Potential arrangement of the pro-apoptotic Bcl-2 proteins during apoptosis	50
Figure 1.3.4	The mitochondrial pathway of apoptosis	52
Figure 1.3.5	The death receptor pathway of apoptosis	54
Figure 1.3.6	Positive feedback loop of caspase activation	56
Figure 1.3.7	Pathways of apoptosis and site of action of ARC protein	59
Figure 1.4.1	Schematic diagram of the positive feedback loop of vascular endothelial growth factor (VEGF) and COX-2 expression	62
Figure 2.4.1	Cartoon of a cytospin vessel and cytospinning	71
Figure 2.5.1	SDS-PAGE resolving gel forming equipment	77
Figure 2.5.2	SDS-PAGE stacking gel and well formation equipment	78
Figure 2.5.3	Schematic of the arrangement of the filter paper, nitrocellulose membrane, and gel for western blotting	79
Figure 3.1a	Induction of chromatin condensation in Jurkat E6.1 cells with serum free RPMI 1640 medium	97
Figure 3.1b	Induction of chromatin condensation in Jurkat E6.1 cells with hydrogen peroxide	98
Figure 3.1c	Induction of chromatin condensation in Jurkat E6.1 cells with curcumin	99
Figure 3.1d	Induction of chromatin condensation in Jurkat E6.1 cells with paracetamol	100
Figure 3.1e	Induction of chromatin condensation in Jurkat E6.1 cells with staurosporine	101
Figure 3.1f	Induction of chromatin condensation in Jurkat E6.1 cells with paclitaxel	102
Figure 3.2	DNA fragmentation in Jurkat E6.1 cells treated with multiple inducers of apoptosis	103
Figure 3.3a	Caspase 3 activity by multiple stimuli in Jurkat E6.1 cells after 24 hr	104
Figure 3.3b	Caspase 3 activity by multiple stimuli in Jurkat E6.1 cells after 48 hr	105

Figure 3.4a	Dose response curve chromatin condensation in Jurkat E6.1 cells treated with paclitaxel	106
Figure 3.4b	Apoptotic DNA fragmentation in Jurkat E6.1 cells treated with paclitaxel	107
Figure 3.5a	Dose response curve of chromatin condensation in HUVECs treated with paclitaxel	108
Figure 3.5b	Apoptotic DNA fragmentation in HUVECs treated with paclitaxel	109
Figure 3.6a	Dose response curve of chromatin condensation in HUVECs treated with actinomycin-D	111
Figure 3.6b	DNA fragmentation in HUVECs treated with actinomycin-D	112
Figure 3.6c	Trypan blue staining of HUVECs treated with actinomycin-D	113
Figure 4.1	Induction of COX-2 expression in HUVECs with VEGF ₁₆₅	120
Figure 4.2a/b	Inhibition of VEGF ₁₆₅ induced COX-2 expression in HUVECs by curcumin and 6-shogaol	121
Figure 4.2c	Densitometry of the inhibition of VEGF ₁₆₅ induced COX-2 expression in HUVECs by curcumin and 6-shogaol	122
Figure 4.3	MTT assay of HUVECs treated with 6-shogaol	123
Figure 4.4a	Chromatin condensation in HUVECs with curcumin and 6-shogaol	125
Figure 4.4b-f	Photographs of chromatin condensation in HUVECs with curcumin and 6-shogaol	126
Figure 4.5	DNA fragmentation in HUVECs treated with 6-shogaol	127
Figure 4.6a	Induction of chromatin condensation in HUVECs treated with curcumin, 6-shogaol and PGE ₂	128
Figure 4.6b-e	Photographs of the induction of chromatin condensation in HUVECs treated with curcumin, 6-shogaol and PGE ₂	129
Figure 4.7a	Chromatin condensation in Jurkat E6.1 cells by curcumin and 6-shogaol	131
Figure 4.7b	Apoptotic DNA fragmentation in Jurkat E6.1 cells treated with curcumin and 6-shogaol	132
Figure 5.1	Cyclooxygenase-2 expression in HUVECs	140
Figure 5.2	Inhibition of prostaglandin E ₂ production in HUVECs by DuP-697 in serum free medium	142

Figure 5.3	Inhibition of prostaglandin E ₂ production in HUVECs by DuP-697 in 20% foetal calf serum medium	199	143
Figure 5.4	Inhibition of prostaglandin E ₂ production in HUVECs cultured in serum free medium by indomethacin		144
Figure 5.5a	Dose response curve of chromatin condensation in HUVECs treated with DuP-697		145
Figure 5.5b-g	Photographs of the dose response curve of chromatin condensation in HUVECs treated with DuP-697		146
Figure 5.6	Apoptotic DNA fragmentation in HUVECs treated with DuP-697		147
Figure 5.7	Chromatin condensation in HUVECs treated with indomethacin		148
Figure 5.8	Photographs of chromatin condensation in HUVECs treated with indomethacin		149
Figure 5.9	Caspase expression in HUVECs treated with DuP-697		150
Figure 5.9d	Densitometry of caspase expression in HUVECs treated with DuP-697		151
Figure 5.10a/b	Caspase expression in HUVECs treated with indomethacin		152
Figure 5.10c	Densitometry of caspase expression in HUVECs treated with indomethacin		153
Figure 5.11	Reversal of DuP-697 induced chromatin condensation by PGE ₂ and caspase 3 inhibitor (CHO-DEVD) in HUVECs		154
Figure 5.12	Photographs of Reversal of DuP-697 induced chromatin condensation by PGE ₂ and caspase 3 inhibitor (CHO-DEVD) in HUVECs		155
Figure 5.13	Densitometry of caspase expression in HUVECs treated with DuP-697 and PGE ₂		156
Figure 5.14	Apoptotic DNA fragmentation in HUVECs treated with DuP-697, PGE ₂ and CHO-DEVD		157
Figure 5.15a	Reversal of DuP-697 induced chromatin condensation by VEGF in HUVECs		158
Figure 5.15b-e	Photographs of the reversal of DuP-697 induced chromatin condensation by VEGF in HUVECs		159

Figure 5.16	Apoptotic DNA fragmentation in HUVECs treated with DuP-697 and VEGF	160
Figure 5.17	Induction of HUVEC membrane permeability by DuP-697	161
Figure 5.18a	Tubule formation of HUVECs treated with DuP-697, VEGF and PGE ₂	163
Figure 5.18b-h	Photographs of tubule formation of HUVECs treated with DuP-697, VEGF and PGE ₂	164
Figure 5.19a	Inhibition of HUVEC tubule formation by indomethacin	165
Figure 5.19b-i	Photographs of the inhibition of HUVEC tubule formation by indomethacin	166
Figure 6.1	The expression of ARC in freshly isolated HUVECs	177
Figure 6.2	Expression of ARC in passage 0 HUVECs grown in 20% FCS medium 199 for up to 24 hr	178
Figure 6.3	Expression of ARC in passage 1 HUVECs grown in 20% FCS medium 199 for up to 24 hr	178
Figure 6.4	Expression of ARC in passage 5 HUVECs grown in 20% FCS medium 199 for up to 24 hr	179
Figure 6.5	Expression of ARC in passage 5 HUVECs grown in 0% FCS medium 199 for up to 24 hr	179
Figure 6.6	Isolation of passage 5 HUVEC RNA	180
Figure 6.7	Reverse transcriptase (RT)-PCR of passage 5 HUVEC RNA for the <i>ARC</i> gene using specific <i>ARC</i> primers	181
Figure 6.8	Reverse transcriptase (RT)-PCR of passage 5 HUVEC RNA using a gradient of annealing temperatures	182
Figure 6.9	Isolation of pCDNA3-ARC from transfected DH5α <i>E.coli</i>	183
Figure 6.10	The digestion of pCDNA3-ARC with restriction enzymes to size the <i>ARC</i> gene insert in the pCDNA3.1 plasmid	185
Figure 6.11	PCR amplification of <i>ARC</i> gene insert from the isolated pCDNA3-ARC plasmid	186
Figure 6.12	Photographs of the transfection of HUVECs (passage 1-4) with pCDNA3.1-GFP	188
Figure 6.13	Photographs of the transfection of HUVECs (passage 1-4) with pCDNA3.1-GFPc as a positive marker for pCDNA3-ARC	189

Figure 6.14	Expression of recombinant ARC protein in HUVECs	190
Figure 6.15	Induction of chromatin condensation by DuP-697 in HUVECs transfected with pCDNA3-ARC	191
Figure 7.1	Schematic diagram of the role of COX-2 in the apoptosis and angiogenesis pathways	197

List of tables

Table 1	The effects of different prostaglandins produced from arachidonic acid	26
Table 2	The interactions of the anti-apoptotic Bcl-2 proteins with the pro-apoptotic Bcl-2 proteins antagonising the induction of apoptosis	49
Table 3	Reagents required for the caspase 3 activity assay	74
Table 4	Advantages and disadvantages of cell and DNA staining to identify apoptosis	93

Abbreviations

AA	arachidonic acid
ANT	adenosine nucleotide translocator
APAF	apoptotic protease activating factor
ARC	apoptosis repressor with caspase recruitment domain
ATP	adenosine triphosphate
bFGF	basic fibroblast growth factor
BH	Bcl-2 homology
cAMP	cyclic adenosine mono-phosphate
CAD	caspase activated DNase
CARD	caspase recruiting domain
COX	cyclooxygenase
cyt-c	cytochrome-c
DAPI	4' 6 - Diamino-2 phenylindole
DD	death domain
DED	death effector domain
DFF	DNA fragmentation factor
DISC	death inducing signalling complex
DMSO	dimethyl sulphoxide
DNA	deoxyribose nucleic acid
ECM	extracellular matrix
EGR	early growth response
ERK	extracellular regulated kinase
EtOH	ethanol
FADD	fas-associated death domain
FCS	foetal calf serum
GM-CSF	granulocyte macrophage colony stimulating factor
GPCR	G- protein coupled receptors
H ₂ O ₂	hydrogen peroxide
HIF-1	hypoxia inducible factor-1
hr	hour(s)

IFN	interferon
I κ K	I-kappaB kinase
IL	interleukin
Kb	Kilo base(s)
KDa	Kilo Dalton(s)
LPS	lipopolysaccharide
MAPK	mitogen activated protein kinase
min	minute(s)
MPTP	mitochondrial permeability transition pore
mRNA	messenger RNA
NF- κ B	nuclear factor- κ B
NSAIDs	Non-steroidal anti-inflammatory drugs
PARP	poly(ADP-ribose) polymerase
PAGE	polyacrylamide gel electrophoresis
PBS	phosphate buffered saline
PG	prostaglandin
PIGF	placental growth factor
PPAR	peroxisome proliferator-activated receptor
RNA	ribose nucleic acid
ROS	reactive oxygen species
TLR	toll-like receptor
TNF	tumour necrosis factor
TNFR	tumour necrosis factor receptor
TRADD	trail associated death domain
TRAIL	TNF related apoptosis inducing ligand
TUNEL	Terminal deoxynucleotide transferase mediated dUTP- biotin nick end labelling
TX	thromboxane(s)
UV	ultraviolet
VDAC	voltage dependent anion selective channel
VEGF	vascular endothelial growth factor
VEGFR	VEGF receptor

1 Introduction

1.1 *Endothelial cells and angiogenesis*

1.1.1 *Endothelial cells*

Vascular endothelial cells are found as a monolayer in the internal surface of blood vessels in the body. In the vasculature of the arteries the endothelial cells are elongated forming a smooth luminal surface. Venous vessels however have endothelial cells that are rounded indented and bulge in to the lumen. Endothelial cells have three surfaces (i) a cohesive surface that adjoin endothelial cells to each other (ii) an adhesive surface which bind the cells to the basement membrane and (iii) a luminal surface that has specific binding proteins for the regulation of blood cells (Pasyk and Jakobczak, 2004). Vascular endothelium is found to regulate blood pressure by releasing vasodilators such as nitric oxide and prostacyclin and vasoconstrictors e.g. thromboxane A₂ and platelet activating factor. Endothelial cells are also found to secrete prostaglandins and numerous growth factors including vascular endothelial growth factor and basic fibroblast growth factor, which aid in the process of angiogenesis (Pasyk and Jakobczak, 2004).

1.1.2 *Angiogenesis*

Hertig described angiogenesis originally in 1935 as the formation of new blood vessels from pre-existing blood vessels during physiological development. Angiogenesis occurs physiologically in the female reproductive system, embryogenesis and in normal

angiogenic turnover (Hertig, 1935; Paper, 1998; Carmeliet, 2000; Dor *et al.*, 2003). In healthy adults angiogenic turnover is slow requiring 3 to 12 months (Paper 1998). Angiogenesis also occurs in pathological states such as wound healing, tumour formation, inflammation, and rheumatoid arthritis (Carmeliet, 2000; Cao, 2001; Chavakis and Dimmeler, 2002; Folkman, 2003). In 1971 Judah Folkman observed that angiogenesis was required for the growth of tumours beyond 1-3 cubic millimetres (mm) (Folkman, 1971). It is due to this that angiogenesis is the most studied form of blood vessel formation in adults.

Initiation of angiogenesis is controlled by the balance of pro and anti angiogenic molecules in the surrounding cellular environment. Endothelial cells remain in the normal quiescent state due to anti-angiogenic factors out balancing the pro-angiogenic factors. The activation of angiogenesis is initiated by the turning on of the “angiogenesis master switch”, which induces the production of pro-angiogenic inducers and the formation of new blood vessels (Carmeliet and Jain, 2000). Some of these inducing “switches” can include mechanical stress produced by proliferating cells, hypoxia, hypoglycaemia and inflammation (Carmeliet, 1999; Carmeliet, 2000; Lingen, 2001).

Angiogenic stimuli cause the release of pro-angiogenic molecules such as vascular endothelial growth factor (VEGF), basic fibroblast growth factor (bFGF), and granulocyte macrophage colony stimulating factor (GM-CSF) (Rak *et al.*, 2000; Folkman, 2003). The stimulated endothelial cells secrete proteases that breakdown the basement membrane of the parental blood vessels extracellular matrix (ECM). The endothelial cells then migrate through the gaps in the basement membrane toward the site of the chemotactic angiogenic

stimuli. Proliferation of the endothelial cells occurs and the endothelial cells form vessels by lining up bipolarly. The two sprouts of endothelial cells form a capillary and the basement membrane reform (Fig 1.1.1) (Paper, 1998; Chavakis and Dimmeler, 2002)

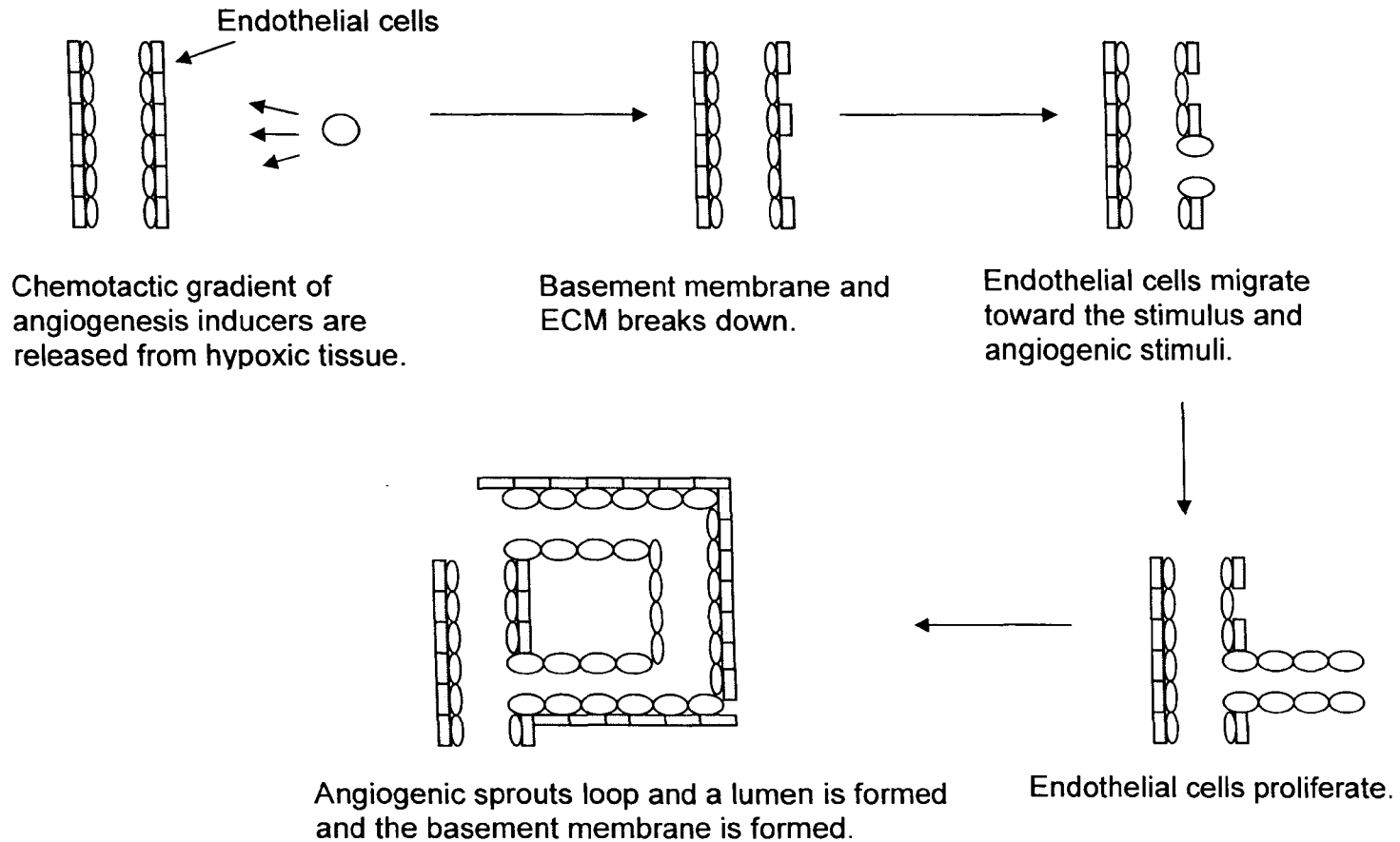


Figure 1.1.1: The stages of angiogenesis showing breakdown of the basement membrane, migration and proliferation of the endothelial cells and the formation of the capillary (Paper,1998)

1.1.3 *Breakdown of the extracellular matrix (ECM)*

Angiogenesis induction by VEGF in wounds or tumours begins with capillary vasodilatation and increased permeability allowing the migration of proteases to cleave the ECM to create space for the new vessels to grow into e.g. matrixmetalloproteases from endothelial or stromal cells (Egeblad and Werb, 2002). Plasma proteins invade the newly formed space and form a provisional scaffold for the migrating endothelial cells to grow onto. The increased protease activity also allows the redistribution of the adhesion molecules e.g. integrins, in the tissue priming the new space for the migration of the endothelial cells (Thurston *et al.*, 2000; Kalluri, 2003). The proteolysis of the ECM releases bound growth factors e.g. VEGF, bFGF to cause a positive feedback effect of the angiogenic process and initiate endothelial cell migration (Carmeliet and Jain, 2000; Akarasereenont *et al.*, 2002; Kalluri, 2003).

1.1.4 *Endothelial cell migration*

Extracellular matrix clearance allows the migration of proliferating endothelial cells forming long chains. Endothelial cells become elongated forming pseudopodia and up-regulating integrin expression allowing binding to ECM adhesion molecules and adhesion molecules e.g. ICAM 1 and 2, VCAM-1 on other cells (Varner, 1995). Integrin binding of endothelial cells to the ECM mediates cell movement and survival with $\alpha v \beta 3$ integrin suppressing the mitochondrial/ intrinsic pathway of apoptosis and promoting endothelial cell survival (Pluda, 1997).

1.1.5 *Lumen formation and vessel maturation*

The new sprouting of endothelial cells into the tissue develops a lumen formed from intercellular vacuoles and cellular surfaces in contact with the endothelial cells. This lumen finally contacts the existing vessels and fuses to give a new vessel. The endothelial cells then return to the original quiescent state (Carmeliet, 2000).

1.1.6 *The effect of VEGF on endothelial cells*

Vascular endothelial growth factor 165, or VEGF-A, is a member of a group of pro-angiogenic molecules, which now includes VEGF-B, C, D, E and placental growth factor (PlGF) (Ferrara, 2001; Bates and Harper, 2003). VEGF is well documented as an inducer of vascular endothelial growth *in vitro* and *in vivo* as well as cellular migration and permeability seen in angiogenesis (Carmeliet and Collen, 2000; Ferrara *et al.*, 2003). Expression of VEGF is regulated by oxygen tension e.g. hypoxia, where the hypoxia inducible factor-1 (HIF-1) binds to the hypoxic response element mediates the expression (Carmeliet, 2000; Giordano and Johnson, 2001; Ferrara *et al.*, 2003) and cytokine/ growth factor binding e.g. FGF, prostaglandins and IL-6 (Ferrara *et al.*, 2003).

VEGF binds to two tyrosine kinase receptors, VEGFR-1 (*flt-1*) and VEGFR-2 (KDR/*flk-1*) but it is the VEGFR-2 receptor that is required in the proliferation and migration of endothelial cells during angiogenesis (Neufeld *et al.*, 1999). The binding of VEGF to VEGFR-2 results in dimerisation of the two VEGFR molecules to activate a ligand

dependent tyrosine phosphorylation of signalling intermediates e.g. PI-3 kinase and mitogen activated protein (MAP) kinases (Ferrara *et al.*, 2003, Neagoe *et al.*, 2005). The activation of these pathways induces pleiotropic responses causing proliferation, tubule formation and survival of endothelial cells through a number of gene activations (Carmeliet and Collen, 2000; Ferrara *et al.*, 2003).

1.1.7 *Induction of gene expression in endothelial cells by VEGF*

Upon stimulation with VEGF it has been shown that 139 genes are activated more than two fold within 24 hr (Abe and Sato, 2001). Only five of these genes are known to be related to the process of angiogenesis and include cyclooxygenase 2, heparin- binding epidermal growth factor like growth factor, early growth response 1 (EGR1), CYR61 a growth factor binding protein that aids the binding of endothelium to $\alpha v\beta 3$ integrins, and angiopoietin-2. Other inducible genes have been found including transcription factors, EGR-2 and 3, nuclear receptors e.g. Nur77, Nurr1 and Nor1, MMPs, DNA replication licensing factor and VEGFR-2 (Abe and Sato, 2001; Akarasereenont *et al.*, 2002; Liu *et al.*, 2003; Wary *et al.*, 2003).

Of the angiogenic related genes that can be activated cyclooxygenase 2 (COX-2) was induced the greatest with a 4.7 fold increase in 0.5 hr, which decreases back to basal levels by 24 hr (Abe and Sato 2001). It can therefore be suggested that the activation of COX-2 is

important in the process of angiogenesis and has been seen to be up-regulated in tumour angiogenesis.

1.2 Cyclooxygenase enzymes

The cyclooxygenase (COX) enzymes, also known as prostaglandin H synthase, are catalytically bifunctional enzymes with a cyclooxygenase and a peroxidase catalytic site (Pairet *et al.*, 1999; Moore and Simmons, 2000). The COX enzyme is found in three isoforms in the body: the constitutive COX-1 and the splice variant COX-3 (not discussed), and the inducible COX-2 enzymes. Cyclooxygenase-1, COX-2 and COX-3 are known to catalyse the conversion of arachidonic acid (AA) to prostaglandins (PG), thromboxanes (TX), and prostacyclins (PGI₂) (Fig. 1.2.1) (Pairet *et al.*, 1999; Moore and Simmons, 2000; Stack and Dubois, 2001; Steele *et al.*, 2003).

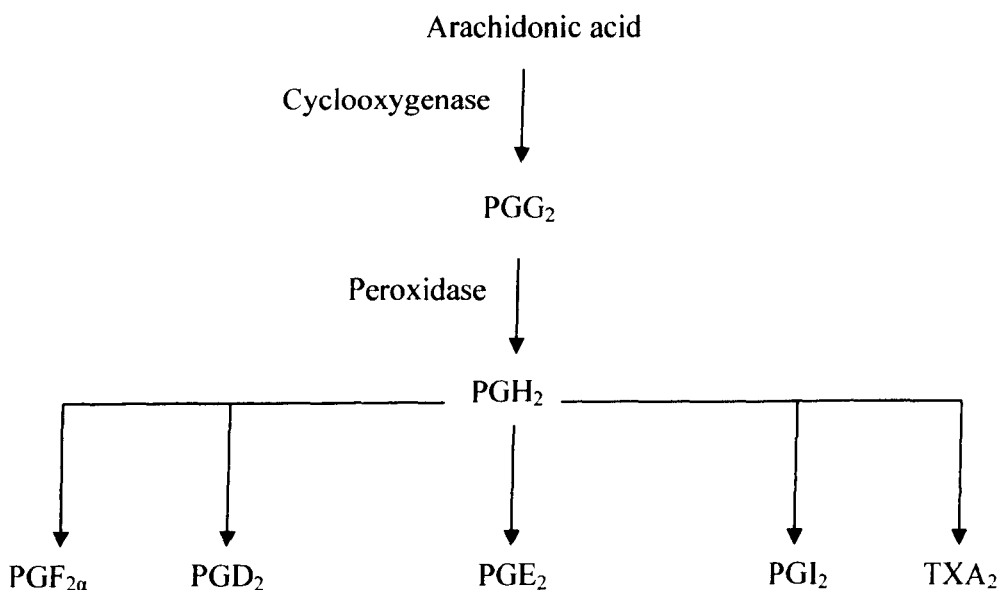


Figure 1.2.1: A schematic representation of the catalysis of arachidonic acid to prostaglandins and thromboxanes indicating the points of catalysis by the cyclooxygenase and peroxidase enzymes (Iniguez *et al.*, 2003).

1.2.1 *Catalysis of arachidonic acid to prostaglandin H₂*

Phospholipase-A₂ catalyses the cleavage of the phospholipid bilayer to release AA into the cytosol of the cell (Masferrer, 2001). A tyrosyl radical formed from the tyrosine²⁸⁵ amino acid residue in the cyclooxygenase active site catalyses the oxidation of arachidonic acid to the peroxy radical precursor, which is then converted to PGG₂ (Fig. 1.2.2). Once produced, PGG₂ is reduced to PGH₂ by the peroxidase catalytic site on the COX enzymes (Fig 1.2.3) (Marnett *et al.*, 1999, Marnett, 2002).

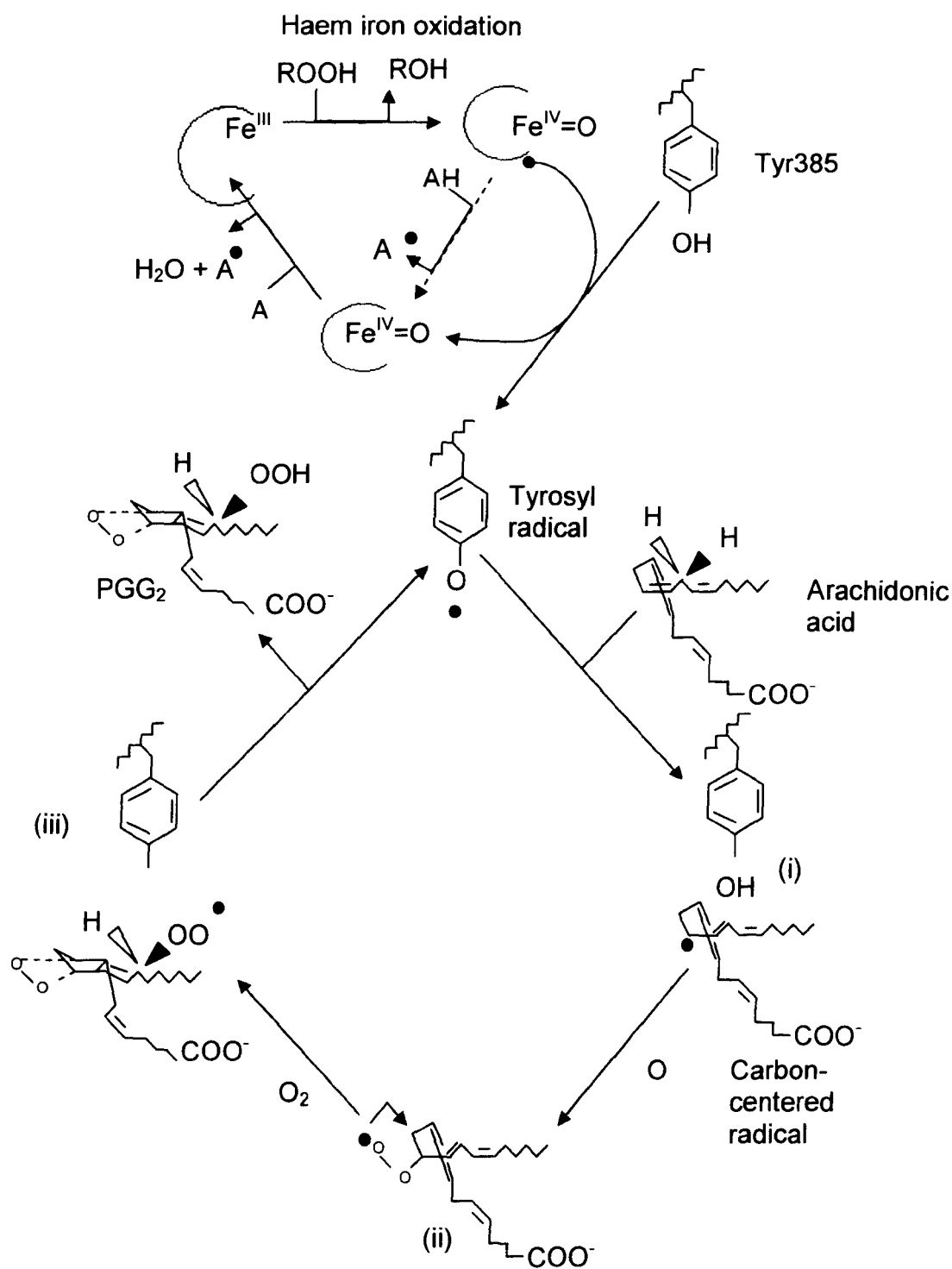
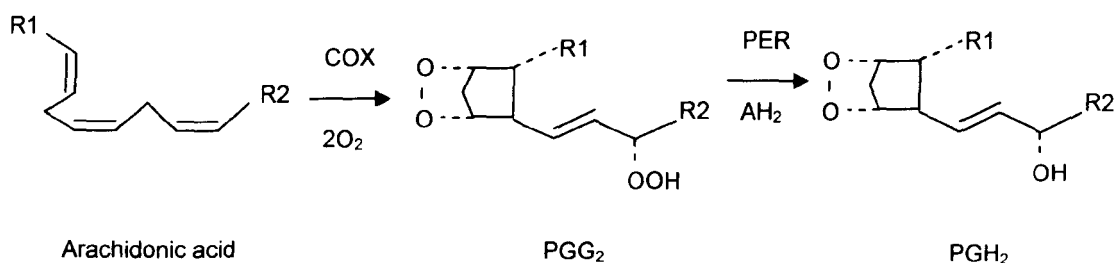


Figure 1.2.2: The catalysis of arachidonic acid (AA) to prostaglandin G₂ (PGG₂) indicating the activation of COX by the formation of a ferryl-oxo complex by oxidising the haem group of COX to give a tyrosyl radical of Tyr385. The tyrosyl radical oxidises AA, allowing the binding of oxygen to form a carbon radical (i). The 11-peroxyl radical cyclises with the oxygen (ii). Molecular oxygen binds to the radical and is subsequently reduced to prostaglandin G₂ (iii) (Marnett, 2002).



R1 = CH₂CH=CH (CH₂)₃CO₂H R2 = C₅H₁₁ AH₂ = Reducing substance

Figure 1.2.3: A schematic representation of the catalytic conversion of arachidonic acid to prostaglandin H₂ (PGH₂) by COX and peroxides enzymes (Marnett, 2002).

1.2.2 Cyclooxygenase 1

Cyclooxygenase 1 isoform is an active homodimer of two 68-80 kDa proteins with four domains. These include a catalytic domain containing two catalytic sites; a cyclooxygenase and peroxidase domain used in the formation of prostaglandins (Fig 1.2.4a and b) (Marnett, *et al.*, 1999; Stack and Dubois, 2001; Lichenburger, 2001; Masferrer, 2001; Marnett, 2002).

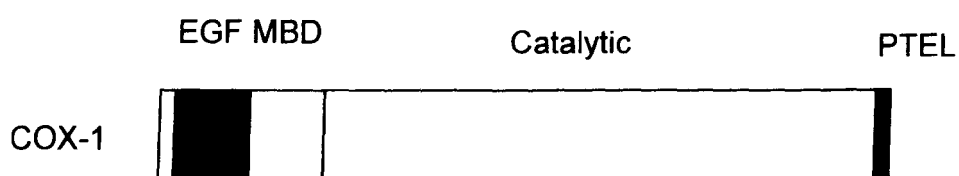


Figure 1.2.4a: A schematic representation of cyclooxygenase 1 showing an epidermal growth factor (EGF)-like domain, a membrane binding domain (MBD) and a catalytic domain. The PTEL signalling peptide allows retention of the enzyme in a lipid membrane (Murakami and Kudo, 2004).

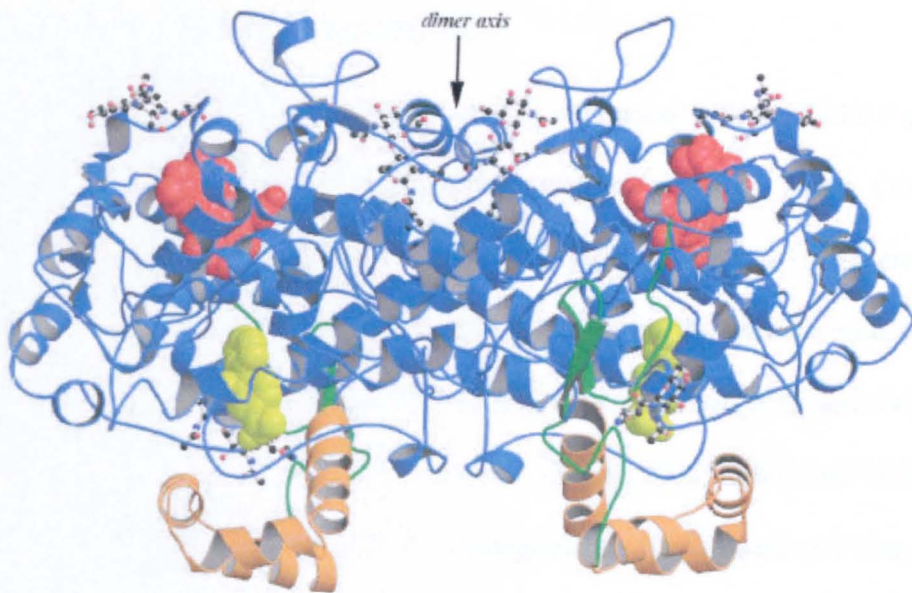


Figure 1.2.4b: A ribbon diagram of ovine COX-1 active homodimer showing the epidermal growth factor like domain (green), the membrane-binding domain (gold), and catalytic domain (blue) with the haem groups shown in red (Garavito *et al.*, 2002).

Cyclooxygenase 1 is the constitutive isoform found in most tissues within the body. It is present at low basal levels, bound to the endoplasmic reticulum and nuclear membrane location (Morita *et al.*, 1995; Gilroy *et al.*, 1998; Ho *et al.*, 1998; Stack and Dubois, 2001; Smith and Langenbach, 2001; Gately, 2003; Steele *et al.*, 2003). It has been reported that COX-1 can be induced under certain conditions. For instance Akarasereenont *et al.*, (2002) reported that exposure of human umbilical vein endothelial cells and bovine aortic endothelial cells to VEGF₁₆₅ resulted in increased COX-1 expression. Murphy and Fitzgerald (2001) also reported an increase in COX-1 expression within 8-10 hr after exposure of endothelial cells to VEGF₁₆₅.

1.2.3 Expression and function of COX-1

Of the three enzymes, COX-1 is the most widely expressed with the *COX-1* gene (9q32-9q33.3) ubiquitously expressed in most cells including platelets where COX-1 is the predominant isoform and converts arachidonic acid to TXA₂ (Fitzgerald, 2002). Cyclooxygenase-1 is also the main isoform expressed in the gastric mucosa where it catalyses the formation of cytoprotective prostaglandins including PGI₂ and PGE₂ (Gilroy *et al.*, 1998; Ho *et al.*, 1998; Colville-Nash and Gilroy, 2000; Stack and Dubois, 2001; Steele *et al.*, 2003). The effects of specific prostaglandins will be discussed later. However the prostaglandins produced in the gastric mucosa are required to maintain blood flow, mucosal integrity and secretions from the gastric mucosa (Riendeau *et al.*, 1997; Gilroy *et al.*, 1998). The renal system is also affected by the activity of COX-1, which maintains homeostasis by ensuring the balance of electrolytes. Prostaglandins produced increase vasodilatation in the renal vascular bed and renal perfusion (Simon, 1999; Wallace, 1999; Weir *et al.*, 2000; Lichenburger, 2001). Another important site of expression of COX-1 is the vascular endothelium where it regulates blood pressure by producing prostaglandins such as prostaglandin I₂ and E₂ (Wallace, 1999; Willoughby *et al.*, 2000; Fitzgerald, 2002).

Apart from its physiological role there is growing evidence that COX-1 may be involved in inflammatory conditions such as rheumatoid arthritis. Evidence in support of this was found when specific COX-2 inhibitors failed to inhibit the inflammatory process in rheumatoid arthritis even though prostaglandin levels were reduced in the inflamed area. In

contrast, dual inhibition of COX-1 and 2 decreased the inflammation, indicating a role for COX-1 (Wallace, 1999; Willoughby *et al.*, 2000, Fitzgerald, 2002).

1.2.4 Cyclooxygenase 2

Cyclooxygenase 2 is an active homodimer similar to COX-1 and is made up of two 68-72 kDa subunits depending on post-translational modifications. Similar to the COX-1 protein, COX-2 has 4 domains that consist of a catalytic domain containing two catalytic sites, an epidermal growth factor like domain, a membrane binding domain and a signalling domain, which allows the retention of COX-2 in the lipid membrane (Fig 1.2.5) (Sakamoto, 1998; Gately, 2000; Masferrer, 2001; Tanabe *et al.*, 2002).

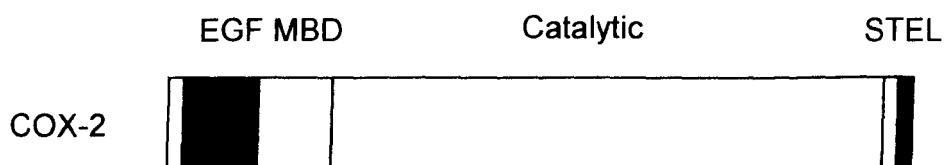


Figure 1.2.5: A schematic diagram of cyclooxygenase 2 showing an epidermal growth factor (EGF)-like domain, a membrane binding domain (MBD) and a catalytic domain. The STEL signalling peptide allows retention of the enzyme in a lipid membrane (Murakami and Kudo, 2004).

The cyclooxygenase active site of COX-1 and COX-2 were found to be 90% similar with only a single amino acid substitution of isoleucine⁵⁹⁰ for valine in the catalytic site of COX-2. This is thought to result in a large side pocket in the substrate-binding site of COX-2 (Fig

1.2.6) (Simon, 1999; Emery, 2001; Zha *et al.*, 2004), which has been exploited in the design of specific COX-2 inhibitors. Some of these inhibitors will be discussed later (Section 1.2.8).

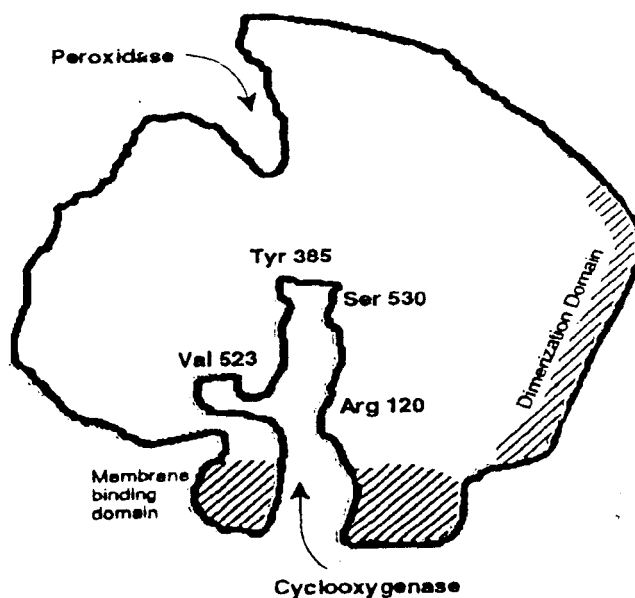


Figure 1.2.6: A cartoon of the cyclooxygenase 2 monomer indicating the peroxidase active site, membrane binding and dimerisation domain and the cyclooxygenase active site with the specific side pocket due to the substitution of isoleucine⁵⁹⁰ for valine (Taken from Moore and Simmons, 2000).

COX-2 is predominantly inducible and generally absent in tissues under normal physiological conditions. The induction of COX-2 can be initiated by multiple stimuli, including inflammatory mediators such as lipopolysaccharide (LPS) and interferon- γ .

angiogenic stimuli such as VEGF, and shear stress. The induction pathways of COX-2 and the effects of COX-2 in angiogenesis will be discussed later (Section 1.4.2). Constitutive expression of COX-2 at low levels is found in the brain tissue and renal system and has a diuretic and natriuretic effect (Smith *et al.*, 1999; Weir *et al.*, 2000; Stack and Dubois, 2001; Akarasereenont *et al.*, 2002; Inoue *et al.*, 2002, Murakami and Kudo, 2004).

1.2.5 Cyclooxygenase 2 induction

The induction of COX-2 has been shown to occur early in inflammation, wound healing, hypoxia, and in normal and tumour angiogenesis. It appears to be induced in a biphasic manner with an early transient induction occurring at 0-8 hr and a delayed expression at 24-48 hr after exposure to LPS (Willoughby *et al.*, 2000; Stack and Dubois 2001). The initial COX-2 induction of 0-8 hr produces pro-inflammatory cytokines that includes PGE₂ and PGI₂, while the second induction at 24-48 hr results in increased production of anti-inflammatory prostaglandins such as PGD₂ and 15-deoxy- $\Delta^{12,14}$ -PGJ₂ (15d-PGJ₂) (Willoughby *et al.*, 2000). It has been suggested that the production of these anti-inflammatory prostaglandins may have a regulatory effects on COX-2 expression and this will be addressed later (Sections 1.4.2 – 1.4.4)

The promoter sequence of the *COX-2* gene has many transcription control elements including nuclear factor- κ B (NF- κ B), cAMP response element (CRE), GATA box, and TATA box (Fig 1.2.7) (Inoue *et al.*, 1995; Yamamoto *et al.*, 1995; Mestre *et al.*, 2001; Perez-Sala and Lamas, 2001). The importance of these elements in the induction of COX-2

was elucidated in reporter gene assay following the deletion of the specific regions on the COX promoter (Kirtikawa *et al.*, 2000). Different regions are vital for COX-2 expression depending on the stimuli used. However, it has been found that the upstream activation sequences could act in synergy to induce COX-2 and the TATA box could independently induce COX-2. The control of COX-2 expression by these mechanisms allows for the induction of the enzyme under specific circumstances e.g. inflammation (Inoue *et al.*, 1995; Yamamoto *et al.*, 1995; Mestre *et al.*, 2001; Perez-Sala and Lamas, 2001).

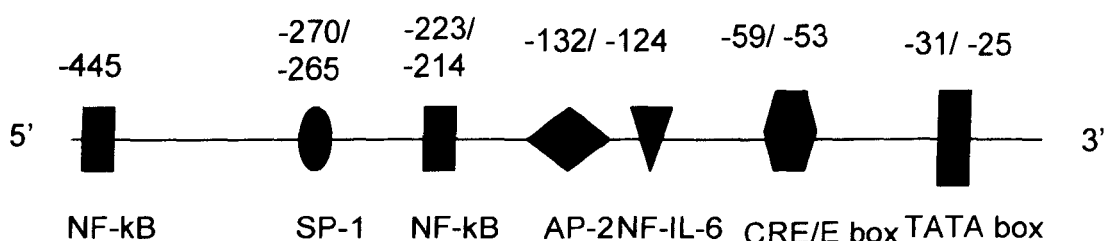


Figure 1.2.7: A schematic representation of the COX-2 promoter sequence showing the regulatory elements present on the promoter region that could induce transcription of the COX-2 gene: nuclear factor-κB (NF-κB), nuclear factor-interleukin 6 (NF-IL6), specificity factor 1 (SP-1) cAMP response element (CRE), E-box, (Adapted from Perez-Sala and Lamas, 2001 and Murakami and Kudo, 2004).

1.2.6 Induction of cyclooxygenase 2 during inflammation

Induction of cyclooxygenase 2 during inflammation has been established to be controlled by many inflammatory mediators including IL-1β, IFN-γ, and TNF-α. However the most documented inflammatory mediator of COX-2 activity is LPS.

Bacterial LPS induction of COX-2 is mediated through the toll-like receptor 4 that activates mitogen MAPK p38. MAPK p38 phosphorylates I-kappaB kinase (IκK) which in turn phosphorylates the inhibitor of NF-κB, I-kappaB (IκB). The latter is normally in a complex with nuclear factor-κB (NF-κB) and upon phosphorylation is targeted for ubiquitination and degradation through the proteosomal pathway. This results in the release of NF-κB, which then translocates to the nucleus and initiates gene transcription (Bierhaus *et al.*, 2000, Chen *et al.*, 2003). A schematic representation of the potential involvement of NF-κB in the induction COX-2 is shown in Fig. 1.2.8.

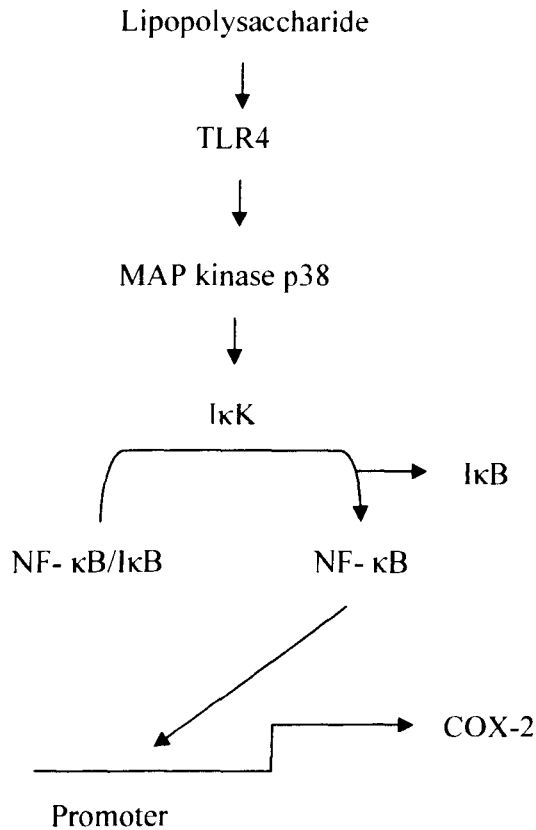


Figure 1.2.8: A schematic representation of lipopolysaccharide (LPS) signalling in the induction of COX-2. Lipopolysaccharide binds to the toll-like receptor 4 (TLR4) activating the phosphorylation of I-kappaB which in turn dissociates from its complex with NF-κB. NF-κB translocates to the nucleus where it binds to the NF-κB recognition site on the COX-2 promoter and activates the transcription and expression of COX-2 (Bierhaus *et al.*, 2000, Chen *et al.*, 2003).

1.2.7 *Induction of cyclooxygenase 2 during angiogenesis*

The expression of *COX-2* is an integral part of angiogenesis, and is expressed within 30 minutes of cellular stimulation with VEGF (Abe and Sato, 2001). Following its release during angiogenesis, VEGF binds to the protein tyrosine kinase receptor, flk-1/VEGFR-2 and activates the mitogen activated protein (MAP) kinase pathway. The binding of VEGF to the VEGFR-2 activates MEK 1/2 which phosphorylates extracellular regulated kinase (ERK) 1/2 or p42/44. This eventually leads to the increase in cyclic adenosine monophosphate (cAMP). Cyclic AMP (cAMP) then activates the *COX-2* promoter inducing expression of *COX-2* (Fig. 1.2.9) (Jones *et al.*, 1999; Tamura *et al.*, 2002; Ruegg *et al.*, 2004). VEGF also activates the production of GATA cis-binding elements that bind to the GATA site on the promoter of the *COX-2* gene. These elements are thought to be essential for the expression *COX-2* (Akarasreenont *et al.*, 2002; Tamura *et al.*, 2002).

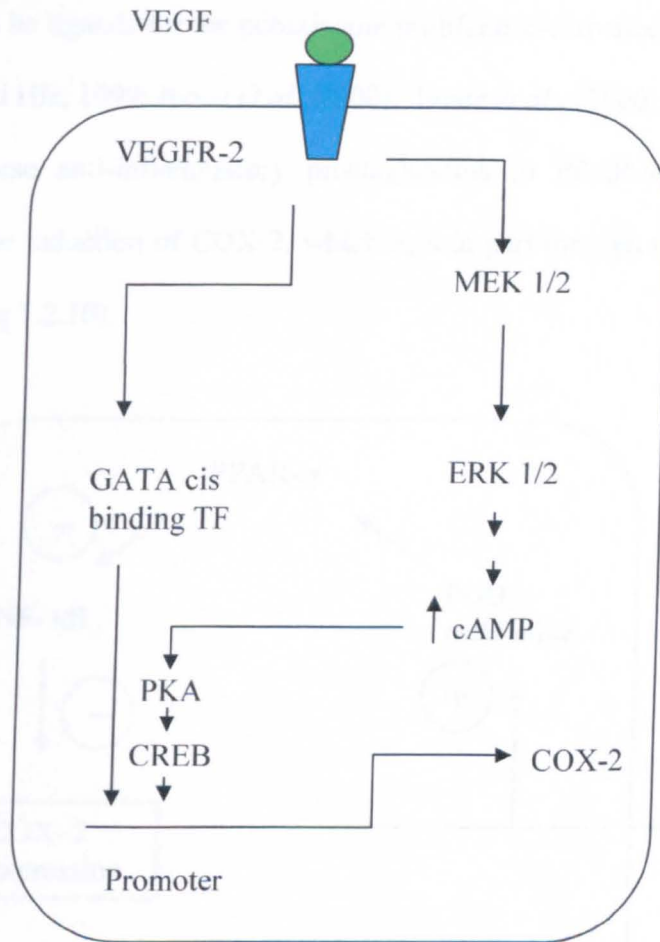


Figure 1.2.9: A schematic diagram of VEGF signalling in the induction of COX-2. VEGF (green) binds to the protein tyrosine kinase VEGFR-2 (blue) that activates the mitogen activated protein (MAP) kinase MEK 1/2. This then activates ERK1/2 (p42/44), increasing the levels of cyclic adenosine mono-phosphate (cAMP) that binds to the COX-2 promoter increasing COX-2 expression. VEGF also activates GATA cis-binding transcription factor (TF), which binds to the GATA box and activates the promoter (Jones *et al.*, 1999; Akarasereenont *et al.*, 2002; Tamura *et al.*, 2002; Chun *et al.*, 2003; Ruegg *et al.*, 2004).

1.2.8 Regulation of cyclooxygenase 2 expression

The anti-inflammatory prostaglandins produced in the second phase of COX-2 induction have been found to be ligands for the peroxisome proliferator-activated receptor (PPAR)- γ (Bishop- Bailey and Hla, 1999; Inoue *et al.*, 2000). Inoue *et al.*, (2000) have suggested that the binding of these anti-inflammatory prostaglandins to PPAR- γ forms a negative feedback loop in the induction of COX-2, which acts in part through the inhibition of the NF- κ B pathway (Fig 1.2.10).

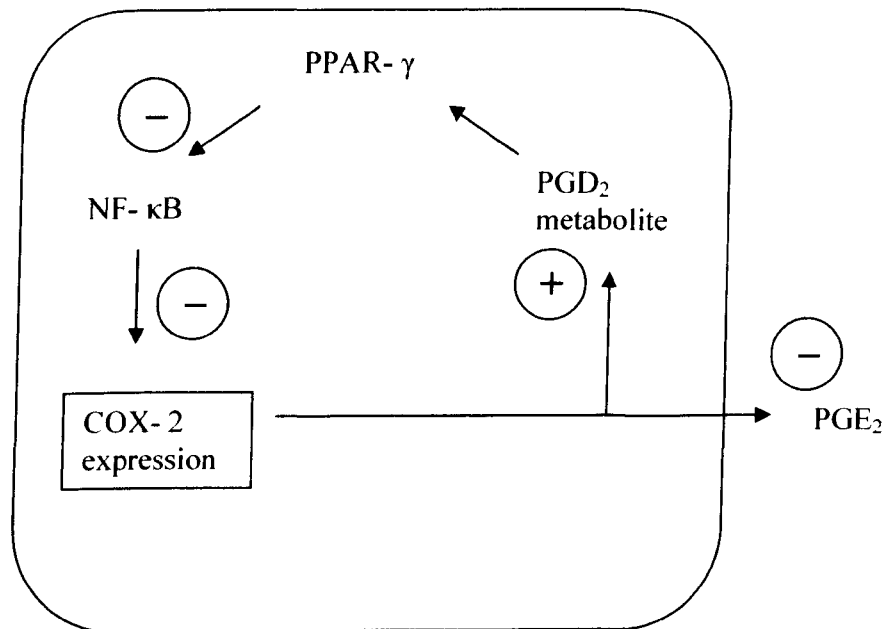


Figure 1.2.10: The regulation of COX- 2 expression by negative feedback loop mediated by PGD₂ production and PPAR- γ binding possibly interfering with NF- κ B pathway and decreasing COX- 2 transcription (Inoue *et al.*, 2000).

It was also suggested that PGE₂ would have a positive effect on COX-2 expression (Inoue *et al.*, 2000). During the initial expression of COX-2 pro-inflammatory prostaglandins such

as PGE₂ are produced and are expelled from the cell. PGE₂ binds EP 2/4 in an autocrine manner, increasing levels of cAMP. The increasing levels of cAMP activate the CRE binding protein (CREB), which binds the CRE region of the COX-2 promoter and induce enzyme expression (Fig 1.2.11) (Inoue *et al.*, 2000).

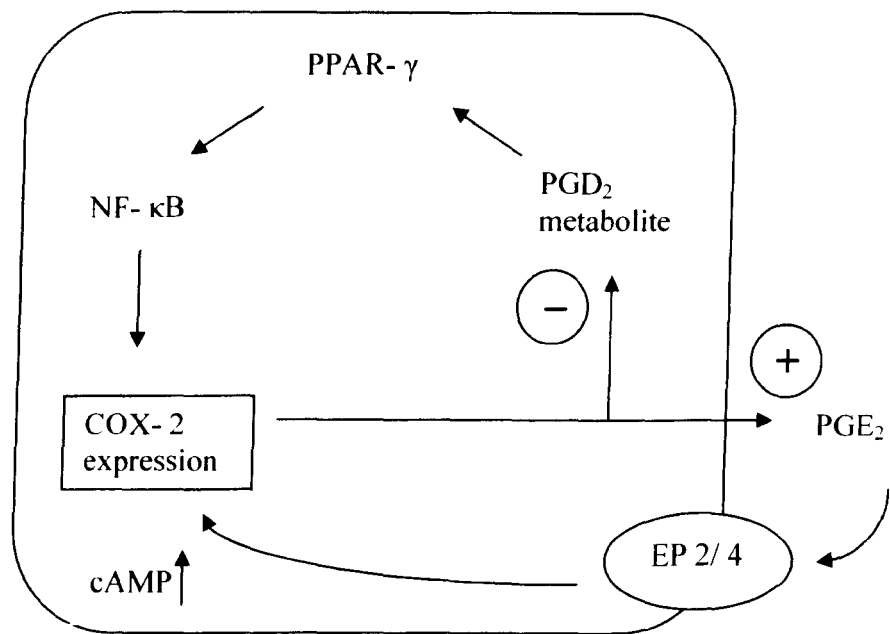


Figure 1.2.11: The positive feedback loop of COX-2 expression by the increases in PGE₂ levels and autocrine binding to the EP 2 or 4 receptor. This increases cAMP levels within the cell and subsequently enhance COX-2 expression by activating the cAMP response element (Inoue *et al.*, 2000).

Other regulatory pathways similar to the positive feedback loop suggested above have been proposed. One such pathway involving VEGF during angiogenesis will be discussed in Section 1.4.2.

1.2.9 Prostaglandins

Prostaglandins are paracrine and autocrine-acting hormones involved in numerous biological processes, including regulation of kidney function, reproduction, vascular tone, angiogenesis and inflammation (Smith *et al.*, 1986; Zhang *et al.*, 1999; Stack and Dubois, 2001). Each prostaglandin is formed from arachidonic acid via the COX pathway to PGH₂ and then to specific prostaglandins via specific synthases. Already stated earlier prostaglandins bind two types of receptors (i) G- protein coupled receptors (GPCR) and, (ii) PPAR, which cause differing effects on cell activity depending on the receptor that the prostaglandin binds (Smith *et al.*, 1986; Ide *et al.*, 2003; Hata and Breyer, 2004). The actions of the different prostaglandins are varied and some of the effects are summarised in Table 1 with PGE₂ being discussed in further detail due to it being used in the current study.

Table 1: The effects of different prostaglandins produced from arachidonic acid (modified from Smith *et al.*, 1986; Bishop-Bailey and Hla 1999; Uracz *et al.*, 2002; Ward *et al.*, 2002; Ide *et al.*, 2003; Dong *et al.*, 2004; Erl *et al.*, 2004; Hata and Breyer, 2004).

Prostaglandin	Receptors	Produced in	Examples of effects
PGI ₂	IP	Endothelium, epithelium, smooth muscle.	Vasodilatation, mediates acute inflammation and oedema, increases/decreases cellular cAMP, activates PPAR β/δ.
PGF _{2α}	FP	Metabolite of PGI ₂	Increases intracellular Ca ²⁺ , found in reproduction and menstrual cycle, used in renal haemodynamics.
PGD ₂	DP and CRTH ₂	Airways, skin, mast cells	Increased bronchoconstriction, eosinophil and leukocyte infiltration, allergic reaction, vasoconstriction and dilation. Increase and decrease cAMP levels. Decreased platelet aggregation.
PGJ ₂	CRTH ₂ and PPAR γ/ δ (Though may be independent of PPAR γ and δ).	Endothelial cells, epithelial cells, granulocytes.	Increases apoptosis, p53 and p38 levels. Decreases IκB degradation and NF-κB binding to DNA. Possible effect in resolution of inflammation and damage of endothelium.
TXA ₂	TPα and β	Endothelial cells, platelets, smooth muscle cells.	Platelet aggregation, increased smooth muscle cell proliferation, bronchoconstriction. Increases and decreases cAMP levels.

1.2.10 Prostaglandin E₂ (PGE₂)

Prostaglandin E₂ is produced in smooth muscle and endothelial cells by the membrane-bound PGE-synthase (Uracz *et al.*, 2002) and its production may be spontaneous (Soler *et al.*, 2000). There are 4 GPCR specific for PGE₂ and these are EP 1, 2, 3 and 4. The effect produced by this prostaglandin may depend on which receptor is bound (Zhang *et al.*, 1999). Receptor 1 and 3 may cause constrictions but via different mechanisms. For instance, in smooth muscle, receptor 1 can cause constriction via an increase in intracellular Ca²⁺ concentration while in the same tissue, receptor 3 signals via an inhibitory G protein that decreases the level of cAMP (Zhang *et al.*, 1999; Purdy *et al.*, 2000). Receptor 2 and 4 causes relaxation of vascular smooth muscle rings by increasing the level of cAMP. There may be coordinated regulation of systemic blood pressure by these receptors, with the actions of receptors 1 and 3 balanced by those of 2 and 4 to maintain the net pressure (Zhang *et al.*, 1999; Purdy *et al.*, 2000). PGE₂ has an effect on inflammation due to the vasodilatation and constriction, and has an important role in the control of renal reabsorption of salt and water (Purdy *et al.*, 2000; Neisisus *et al.*, 2001; Hata and Breyer, 2004). Importantly it has been found that PGE₂ has an effect on angiogenesis by increasing VEGF expression, which is induced by acting through the MAPK pathway (Pai *et al.*, 2001). Apoptosis of cells is also affected by PGE₂, which may decrease apoptosis and promoting cell proliferation by increasing cAMP and the expression of the anti-apoptotic protein Bcl-2 (Ottonello *et al.*, 1998; Sheng *et al.*, 1998; Jabbour *et al.*, 2002; Davis *et al.*, 2004). Cell adhesion by αvβ3 integrin binding may also be enhanced by PGE₂ acting through cAMP (Dormond *et al.*, 2002).

1.2.11 *Inhibitors of cyclooxygenase 2*

Inhibition of the COX-2 may be therapeutically beneficial in inflammation, where this enzyme is found to be expressed, resulting in the production of pro-inflammatory prostaglandins. Drugs that inhibit COX-2 can be segregated into non-specific inhibitors, which inhibit COX-1 and COX-2 and specific inhibitors, which selectively block COX-2. The list of compounds both groups is increasing and now include some natural dietary compounds (e.g. curcumin), which inhibit COX-2 in certain cell types.

1.2.11.1 *Non-specific cyclooxygenase inhibitors*

Non-specific inhibitors of cyclooxygenase were first developed to inhibit COX-2 regulated inflammation but were found to inhibit COX-1 and COX-2. Non-steroidal anti-inflammatory drugs (NSAIDs) such as aspirin are widely used to treat inflammation and pain by decreasing the production of pro-inflammatory prostaglandins and have also been used to treat rheumatoid arthritis and cancer (Masferrer *et al.*, 1994; Smith *et al.*, 1998). Non-steroidal anti-inflammatory drugs have been found to have anti-pyretic, analgesic and anti-inflammatory actions preferentially inhibiting COX-1 to decrease prostaglandin production. These drugs are grouped into 3 classes. Class 1 includes ibuprofen, naproxen and salicylic acid and are reversible competitive inhibitors, class 2 inhibitors such as indomethacin, are competitive inhibitors that can be reversed in a slow time dependent manner and class 3 inhibitors (e.g. aspirin), are irreversible inhibitors (Rosenstock *et al.*, 1999).

Aspirin has been shown to bind transiently via the carboxyl group to arginine¹²⁰ of the active site of the COX enzymes. This weak interaction allows aspirin to diffuse and transfer the acetyl group to serine⁵³⁰. The salicylate produced then diffuses out of the active site leaving the serine bound 2-carbon adduct close to tyrosine³⁸⁵. This is activated in the formation of PGG₂ and has previously been discussed (Section 1.2.1) (Moore and Simmons, 2000).

Unfortunately NSAIDs were found to have undesirable side effects, causing gastrointestinal toxicity and ulcer formation (Allison *et al.*, 1992). Extended administration of NSAIDs inhibits the production of cytoprotective prostaglandins from COX-1 in the gastric mucosa. The decrease in cytoprotective prostaglandins alters gastric homeostasis as discussed (Section 1.2.2.1). The induction of gastric ulcers by NSAID inhibition of COX- 1 led to the development of specific COX- 2 inhibitors to avoid the side effects of NSAIDs.

1.2.11.2 *Specific cyclooxygenase 2 inhibitors*

Specific COX-2 inhibitors were designed to inhibit inflammatory prostaglandin formation by COX-2. The specific inhibitors are designed to bind the unique “side- pocket” found in the active site of COX-2. The selective COX-2 inhibitors inhibit COX-2 specifically in a 2 step inhibition process where the first step involves an initial rapid reversible interaction of the drug with the enzyme and the second step involves the formation of a tight bond that allows a complex to form with a slow dissociation of the drug from the enzyme due to its

binding to the “side-pocket” in the active site of the COX- 2 enzyme (Fig. 1.2.12) (Rosenstock *et al.*, 1999, Urban, 2000).

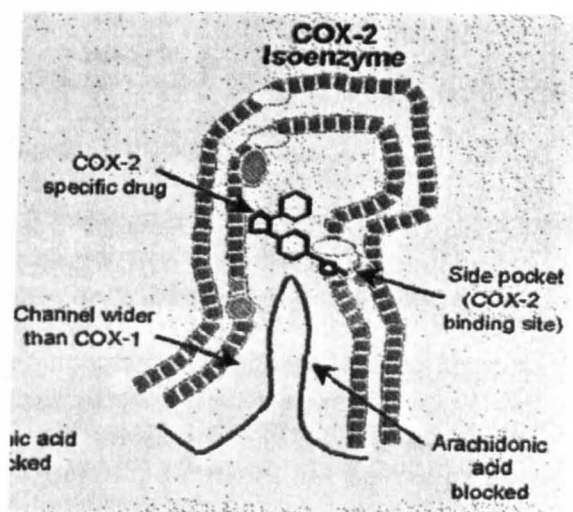


Figure 1.2.12: The inhibition of the COX- 2 enzyme identifying the binding of the inhibitor to the “side-pocket” in the cyclooxygenase active site, preventing arachidonic acid entering the active site (Urban, 2000).

There have been many specific COX-2 inhibitors developed, including celecoxib, rofecoxib, NS-398, and DuP-697. However, only a few of these will be discussed. The structure of specific COX-2 inhibitors is very specific with certain chemical groups vital for COX inhibition. In the tricyclic inhibitor class, which includes celecoxib, rofecoxib and DuP-697, the exact spatial orientation of the aromatic rings is essential for inhibition of the COX enzymes. The aromatic rings must be adjacent to each other on the centre ring for COX-2 inhibition (Penning *et al.*, 1997). Studies of the inhibitors and potential inhibitors were investigated using the rat carrageenan-induced footpad oedema assay and the most

potent inhibitors taken on for further analysis (Penning *et al.*, 1997). It was found that the 4-methyl analogue of the base compound was the most effective and this led to the discovery of celecoxib (Penning *et al.*, 1997).

1.2.11.3 Celecoxib (Celebrex®)

Celecoxib is one of the specific COX-2 inhibitors approved for the treatment of inflammation in rheumatoid arthritis (Fig 1.2.13) (Urban, 2000). Celecoxib has been found to be as effective in reducing prostaglandin formation as ibuprofen (800mg) at half the dose (400mg) *in vivo* and *in vitro* (Fitzgerald, 2002; Wu *et al.*, 2003), and has been shown to be anti-inflammatory and anti-analgesic *in vivo* (Smith *et al.*, 1998). The additional advantage of celecoxib over traditional NSAIDs is the reduced gastrointestinal ulcer complications in the upper GI tract as it is found to have an 8-fold lower incidence of ulceration compared to non-specific COX-2 inhibitors back to placebo levels (Goldstein *et al.*, 2000).

Recently, it has been established that celecoxib has anti-cancer effects reducing cancer cell proliferation *in vitro* and *in vivo*. The administration of celecoxib has been shown to reduce the amount of polyps in familial adenomatous polyposis over a 6 month period (Blanke, 2002), and also decreases the number of prostate cancer cells in treated cell lines (Hsu *et al.*, 2000) and cholangiocarcinoma cells in treated cell lines (Wu *et al.*, 2003). Mostly the decrease in the proliferation of cancer cells is found to be due to the induction of apoptosis of the target cells (see Section 1.3.2 below).

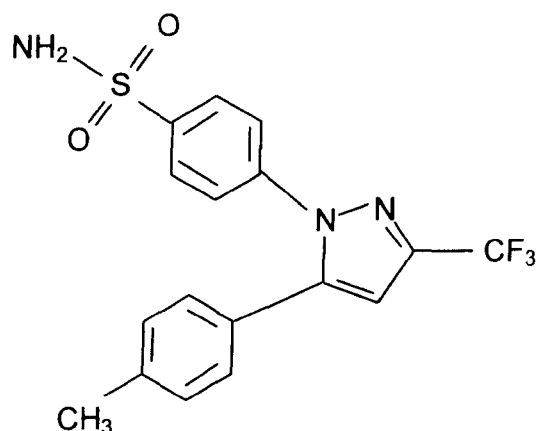


Figure 1.2.13: The chemical structure of Celecoxib (Celebrex ®) indicating the two aromatic rings adjacent on the centre ring (Urban, 2000).

1.2.11.4 Rofecoxib (Vioxx ®)

Rofecoxib is the specific COX-2 inhibitor that has been approved for the treatment of osteoarthritis (Fig 1.2.14) (Urban, 2000). Rofecoxib specifically inhibits COX-2 derived prostaglandin production *in vitro* and *in vivo* (Chan *et al.*, 1999). Rofecoxib also is gastro-protective as it maintains gastrointestinal integrity in rat models over 5 days (Chan *et al.*, 1999). Recently however rofecoxib has been found to increase the risk of cardiovascular disease resulting in the drug being removed from the market. There is now also increasing controversy over the cardiovascular safety of celecoxib as well (Mukherjee *et al.*, 2001; Niederberger *et al.*, 2004).

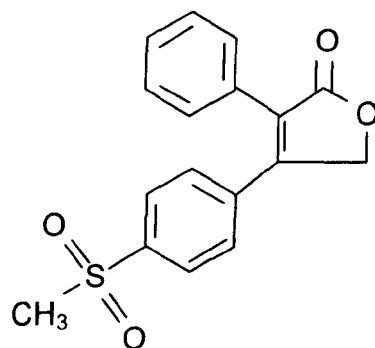


Figure 1.2.14: The chemical structure of rofecoxib (Vioxx ®) indicating the two aromatic rings adjacent on the centre ring (Urban, 2000).

1.2.11.5 5-bromo-2- (4-fluorophenyl)-3-(methylsulfonyl) thiophene (DuP-697)

Structurally similar to celecoxib and rofecoxib, DuP- 697 is a tricyclic COX-2 inhibitor (Fig 1.2.15) (Penning *et al.*, 1997). DuP-697 is an anti-inflammatory drug that promotes gastrointestinal safety similar to other specific COX- 2 inhibitors. Inhibition of inflammation was demonstrated using the inflamed rat paw model in non-established and established adjuvant arthritis (Gans *et al.*, 1990). DuP-697 was also found to be non-ulcerogenic in rat models at concentrations of up to 400mg/ kg and had no effect on renal vasculature prostaglandin production and on renal blood flow (Gans *et al.*, 1990).

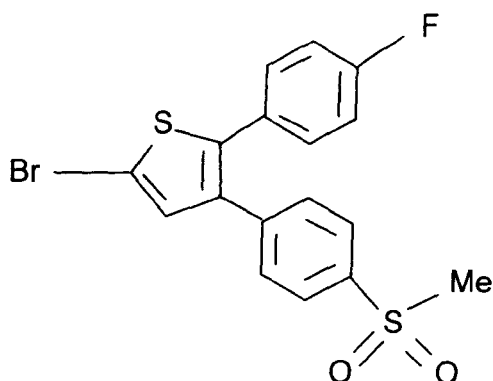


Figure 1.2.15: Chemical structure of DuP-697 showing the tricyclic structure of the inhibitor similar to celecoxib and rofecoxib, which is vital to the inhibition of COX- 2 (Gierse *et al.*, 1995).

The specificity of DuP-697 for COX-2 is very high with the IC_{50} for COX-2 inhibition being 10nM (Gierse *et al.*, 1995). This concentration of DuP-697 (10nM) has been shown to be ineffective against COX-1, with concentrations of 1-100 μ M apparently being required for COX-1 inhibition in bovine aortic endothelial cells (BAEC) (Rosenstock *et al.*, 1999). At high concentrations, DuP-697 can act in synergy with non-specific COX inhibitors to irreversibly inhibit COX-1 (Rosenstock *et al.*, 2001). The specific COX-2 inhibition has been attributed to the DuP-697 altering the enzymatic conformation via an interaction with a site, which is not the active site. This implies a non-competitive inhibition of COX-2 activity by DuP-697, which may act by inhibiting the cleavage of the enzymes by trypsin (Rosenstock *et al.*, 1999).

1.2.12. Dietary natural products

Dietary products have been found to have many effects on the body, with many substances having anti-inflammatory properties. For instance, it has been established that turmeric (*Curcuma longa*) and ginger (*Zingiber officinale*) have anti-inflammatory effects and have been used in alternative therapies in the treatment of rheumatoid arthritis. These properties have been ascribed to certain chemicals found in the foods e.g. curcumin from turmeric and gingerols and shogaols from ginger.

1.2.12.1 Curcumin (Diferuloylmethane)

Curcumin is the yellow pigment of Turmeric (*Curcuma longa*) (Fig 1.2.16), and its anti-oxidant and anti-inflammatory properties have been known for many years (Singh *et al.*, 1996).

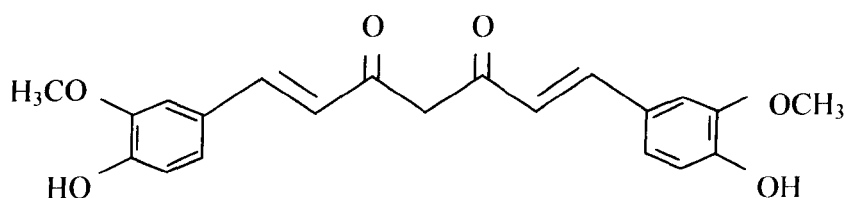


Figure 1.2.16: The structure of curcumin from *curcuma longa*, containing two aromatic moieties and a substituted functional group on an alkyl side chain (Zhang *et al.*, 1999).

The anti-inflammatory properties of curcumin are thought to be due to the inhibition of COX-2 at several levels including at the mRNA, protein expression and functional levels.

This occurs in a concentration-dependent manner (1 μ M to 25 μ M) after 8 hr (Zhang *et al.*, 1999; Chun *et al.*, 2003). Curcumin has been shown to repress the activation of the NF- κ B pathway by inhibiting the phosphorylation and degradation of I κ B α subunit. This prevents the release of NF- κ B from its inhibitory complex with I κ B and thus activation of the COX-2 promoter and *COX-2* gene transcription (Plummer *et al.*, 1999; Surh *et al.*, 2001; Chun *et al.*, 2003) (Fig 1.2.17). The MAPK pathway is also affected by curcumin with inhibition of the p38 and p42/44 pathways resulting in the inhibition of COX-2 induction (Fig 1.2.17). These findings suggest that curcumin may block the induction of COX-2 by inhibiting the phosphorylation of the signalling molecules involved in the activation of the *COX-2* promoter (Chun *et al.*, 2003).

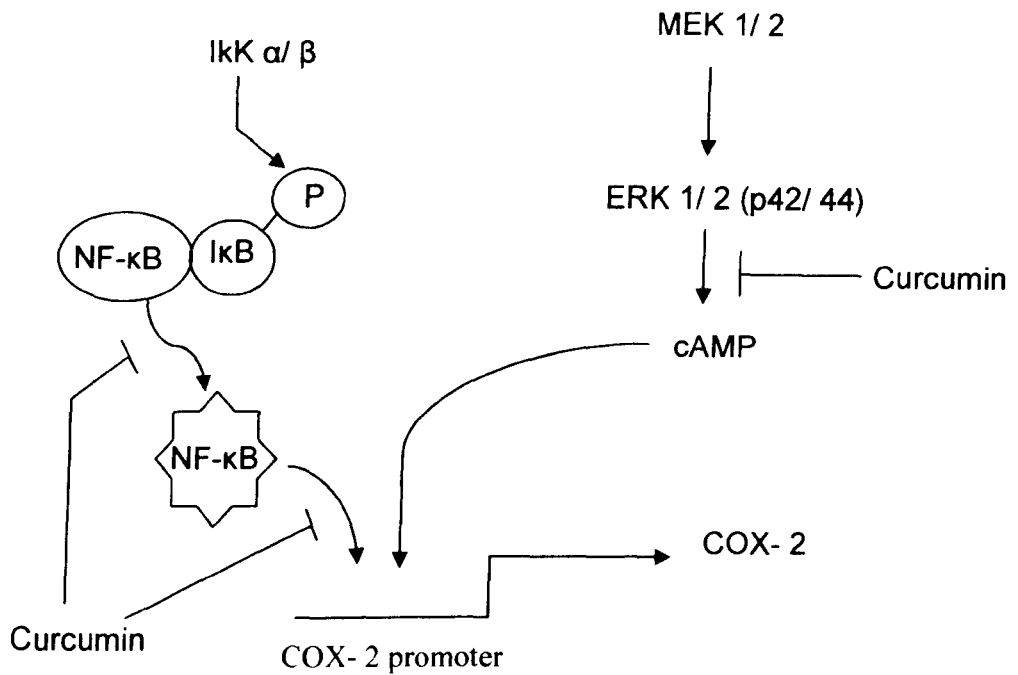


Figure 1.2.17: The inhibition of the signalling pathways involved in COX-2 induction. Curcumin inhibits either the MAP kinase pathways or the dissociation of IκB from NF-κB, resulting in the inhibition of COX-2 induction (adapted from Chun *et al.*, 2003).

Curcumin has pro-apoptotic and anti-proliferative properties in certain cells. It is pro-apoptotic in HL-60 cells and adenocarcinoma cell lines and anti-proliferative in human umbilical vein endothelial cells (Singh *et al.*, 1996). The pro-apoptotic and anti-proliferative effects in these cells may be due to the inhibition of COX-2 and the correlation between apoptosis and COX-2 inhibition is discussed in Section 1.4.4.

1.2.12.2 6-Shogaol

6-Shogaol is one of the metabolites of the shogaol constituent of ginger (*Zingiber officinale*), and has been found to inhibit COX-1 in rat cells (Tjendraputra *et al.*, 2001). 6-shogaol has a similar structure to curcumin (Fig 1.2.18), and has been shown to inhibit prostaglandin production by COX-2 in lung epithelial cells, where it was the most effective of all ginger compounds tested (IC₅₀ of 2.1 μM). The inhibition of COX-2 generated prostaglandins may lead to an increase in apoptosis (see section 1.4.4).

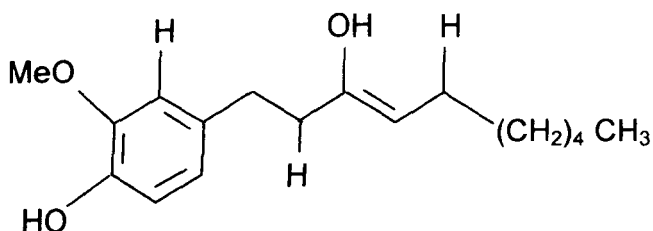


Figure 1.2.18: The chemical structure of 6-shogaol indicating similarities to curcumin with the aromatic moiety, carbon chain and lipophilic alkyl side chain (Tjendraputra *et al.*, 2001)

1.3 *Cell death*

1.3.1 *Necrosis*

Necrosis is the uncontrolled form of cell death. Induction of necrosis has been observed with viral infection, bacterial products such as LPS and immune defence components including the complement system (Proskuryakov *et al.*, 2003). During necrosis cells swell, lose membrane integrity and lyse causing an inflammatory reaction in the body (Proskuryakov *et al.*, 2003). Unlike apoptosis (discussed below) necrosis does not require adenosine triphosphate (ATP) and does not require the production of specific enzymes to occur (Proskuryakov *et al.*, 2003). A specific form of necrosis can occur during the process of apoptosis. This is referred to as “secondary necrosis” and occurs when ATP stores decrease during apoptosis thereby preventing the process of apoptosis to reach completion and the cell enters the process of necrosis instead (Proskuryakov *et al.*, 2003).

1.3.2 *Apoptosis*

Apoptosis was first described by Kerr, Wyllie and Currie in 1972 and is characterised as a set of morphological changes in a dying cell that contrast to a necrotic cell (Kerr *et al.*, 1972). The morphological changes included loss of contact with the ECM cytoplasmic shrinkage, membrane blebbing, the formation of apoptotic bodies, chromatin condensation and nuclear fragmentation resulting in 180bp multimer fragments of DNA (Gupta, 2001).

Apoptosis is essential in embryonic development, the removal of dangerous or damaged cells, and for homeostasis of cellular turnover in adults (Kerr *et al.*, 1972). However

uncontrollable apoptosis has been associated to some pathological states including Parkinson's and Alzheimer's disease, while a complete inhibition of apoptosis in unwanted or dangerous cells can result in an increase autoimmunity and tumour formation leading to cancer.

Induction of apoptosis can begin with an insult to the cell (e.g. ultraviolet (UV) radiation, reactive oxygen species (ROS) or chemical damage), or following ligand-receptor binding (e.g. CD95 ligand binding to the CD95 receptor in T-cells (Ashkenazi and Dixit, 1998)), or by loss of contact with the extra-cellular matrix (e.g. anoikis (Frisch and Francis, 1994)).

The inducers activate two major pathways, which control apoptosis: (1) the mitochondrial pathway and (2) the death receptor pathway, resulting in both pathways causing specific apoptotic morphological changes.

1.3.2.1 *Morphological changes associated with apoptosis*

The characteristic morphological changes associated with apoptosis were first described in 1972 by Kerr, Wyllie and Currie (Kerr *et al.*, 1972). These changes are still being used to define apoptosis with some of the changes being used as the hallmark by which the degree of apoptosis is judged.

1.3.2.2 *Apoptotic bodies*

The formation of apoptotic bodies from a cell is one of the main features of apoptosis. The cell undergoes the blebbing off of “small spherical or ovoid cytoplasmic fragments containing remnants of the nuclei,” (Kerr *et al.*, 1972). The apoptotic bodies have been found to contain not only cytoplasm but also condensed parts of the nuclei and densely packed organelles, which are intact but condensed, depending on the constituents of the cell at the time of the formation (Kerr *et al.*, 1972). This was found to be orchestrated by the cleavage and activation of gelsolin and p21-activated kinase-2 and fodrin in the cell (Martin *et al.*, 1995)

1.3.2.3 *Phosphatidylserine translocation*

As the membrane of the cells blebs, phosphatidylserine moves from its position in the inner membrane to the outer membrane in a calcium dependent manner (Blatt and Glick, 2001). The translocation of phosphatidylserine is required for the recognition of apoptotic cells by phagocytes, so that the apoptotic cells do not under go secondary necrosis and release their contents thereby causing an inflammatory reaction (Savill *et al.*, 1993; Fadok *et al.*, 2001). Recognition of the phosphatidylserine by phagocytes has been thought to be by a specific receptor that is expressed on macrophages and conserved throughout phylogeny of *Caenorhabditis elegans* (*C. elegans*) and *Drosophila melanogaster* (Fadok *et al.*, 2000).

1.3.2.4 *Cell shrinkage*

After the initiation of apoptosis the cell shrinks and loses volume of the cytoplasm (Bortner and Cidlowski; 1998). This is in contrast to necrosis in which the cells swell due to loss in homeostatic functions regulating cell volume. The loss of cellular volume is due to (1) the decrease in potassium ions within the cell causing an osmotic pressure to remove the water from the cytoplasm; (2) A degradation of the macromolecules in the cell due to fragmentation (Bortner and Cidlowski; 1998); (3) Blebbing and the formation of apoptotic bodies decreasing the volume of the cell as the bodies detach.

1.3.2.5 *Condensation of the chromatin and DNA cleavage*

The hallmark morphological change and the most severe change of apoptosis is the condensation and the cleavage of cells DNA into 180bp fragments (Sakahira *et al.*, 2001). Caspase-3 activation causes the cleavage of the heterodimer of DNA fragmentation factor (DFF) 45 and DFF 40. This causes an activation of the intrinsic endonuclease function in DFF 40, which is now referred to as caspase activated DNase (CAD), by cleaving DFF 45, the inhibitor of CAD (iCAD) (Sakahira *et al.*, 2001). The activation of CAD degrades chromatin into multimers of 180bp fragments, due to the cut happening in the linker fragment of the DNA between the histone protein complex, which normally folds the DNA into chromosomes. When resolved on an agarose electrophoresis gel, the fragmented chromatin forms a “DNA ladder” on the gel. This “DNA ladder” is considered the hallmark of apoptosis. This marker of apoptosis should not, however, be taken as the only definitive indicator of apoptosis, as it may not always appear. In some cases, a DNA smear

instead of a ladder may be produced even though the other biochemical changes of apoptosis may be observed (Collins *et al.*, 1992). Drug or serum deprivation induced apoptosis may also cause a different pattern of DNA fragmentation where higher molecular weight fragments (300 and or 50kb fragments) are produced with no lower molecular weight fragments of DNA (Oberhammer *et al.*, 1993; Rusnak *et al.*, 1996; Steiman *et al.*, 1998). The higher molecular weight fragmentation may be inhibited by cyclohexamide, suggesting that the process is endonuclease dependent in a manner similar to other apoptosis mechanism (Rusnak *et al.*, 1996). This indicates that not all inter-chromosomal DNA fragmentation during apoptosis gives the “hallmark” apoptotic biochemical change due to possible release of the chromatin loop domains before full cleavage of the DNA (Oberhammer *et al.*, 1993). The DNA fragmentation has been dissociated from the other apoptotic changes and suggests that fragmentation is not necessary to indicate the induction of apoptosis (Taylor *et al.*, 2001).

These morphological changes associated with apoptosis are due to the activation of a family of cysteine proteases known as “Caspases” (Thornberry *et al.*, 1997), which act in an enzyme activation cascade to target specific cellular proteins including DNases and proteases that result in the specific morphological changes.

1.3.3 Caspases

The caspases are a highly conserved group of cysteine proteases, which initiate and execute the process of apoptosis. The name “Caspase” is derived from the conserved cysteine amino acid residue in the active site and the aspartic acid – xxx target cleavage site of this family of proteins (Nicholson and Thornberry, 1997; Thornberry *et al.*, 1997). In all 14 caspases have been identified, with 13 of them being mammalian (Van loo *et al.*, 2002), 12 human (Shikama *et al.*, 2001), and at least 8 of these are thought to be involved in apoptosis (Salvesen and Dixit 1997; Budihardjo *et al.*, 1999; Earnshaw *et al.*, 1999). As zymogens the pro-caspases are a single chain protein with 3 different domains: (i) N-terminal prodomain (ii) the large subunit, and (iii) the small subunit (Krammer, 1999). Upon activation the small subunit is cleaved off from the peptide chain followed by cleavage of the large subunit from the prodomain. The two subunits heterodimerise and bind a second dimer by hydrophobic interactions to form an enzymatic active tetramer with two active sites (Fig 1.3.1) (Rotonda *et al.*, 1996).

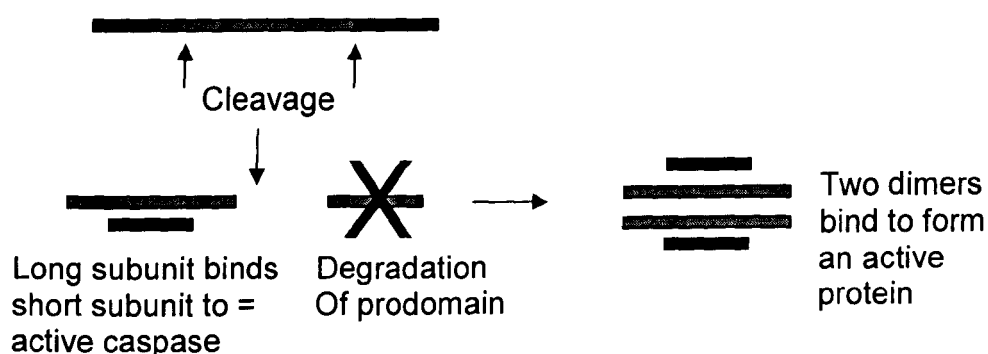


Figure 1.3.1: A schematic diagram of the structural conversion of pro-caspase to active caspase indicating the cleavage of the pro-domain and small subunit from the large subunit and the formation of the tetramer after conversion.

The size of the prodomain for the zymogen is important for the function of the caspase in the activity of an “initiator” caspase or an “effector” caspase. The effector caspases have a shorter prodomain used just to inhibit the activity of the enzyme (Shen and White, 2001). The initiator caspases however have been found to have longer pro-domains in contrast to the effector caspases (90aa: 20-30aa), which can interact with signalling molecules such as death receptors or apoptotic protease activating factor (APAF-1) in apoptosis (Shi, 2002). The active site of the caspase recognises at least 4 amino acids: P4-P3-P2-P1 cleaving at the P1 site, which is an aspartic acid residue (Nicholson and Thornberry, 1997).

The caspase cascade induced in the death receptor pathway of apoptosis involves the activation of caspase 8 that cleaves pro-caspase 3 to active caspase 3 (as discussed in section 1.3.3.1 and 1.3.5.2). The mitochondrial pathway induces caspase 9 activation by the formation of the apoptosome (as discussed in section 1.3.3.2 and 1.3.5.1). Activated caspase 9 cleaves pro-caspase 3 to caspase 3, which targets cellular components (see section 1.3.3.3) to produce the morphological changes associated with apoptosis. Caspase 3 activates caspases 6 and 7, which are possibly required in the amplification of caspase activation as will be discussed in section 1.3.3.4.

1.3.3.1 *Caspase 8*

Caspase 8 is the initiator caspase found in the death receptor pathway of apoptosis. It is found to bind to adaptor molecules (e.g. FADD), and is activated by auto-processing when many zymogens are bound to the adaptor molecules (Ashkenazi and Dixit, 1998) as

discussed below in the death receptor pathway of apoptosis. Caspase 8 activates caspase 3, which subsequently activates other caspases and causes the biochemical and morphological changes found in apoptosis (Nicholson and Thornberry, 1997).

1.3.3.2 *Caspase 9*

Caspase 9 is the initiator caspase in the mitochondrial pathway. It is activated when bound to the adaptor molecule APAF-1 by cytochrome-c (cyt-c) and adenosine triphosphate (ATP). Pro-caspase 9 binds APAF-1 by caspase recruiting domain (CARD)-CARD interactions and dimerises to other pro-caspase 9, forming a large complex called the “apoptosome”. The c-terminal of the pro-caspase 9 inhibits the n-terminal, becoming active. Upon binding ATP and cyt-c a conformational change occurs exposing the n-terminal of pro-caspase 9 allowing it to be activated into caspase 9. Caspase 9 then binds caspase 3 and proteolytically activates it (Zou *et al.*, 1999).

1.3.3.3 *Caspase 3*

Caspase 3 is the general executioner/effector caspase in apoptosis. Activated through the death receptor and mitochondrial pathways by caspases 8 and 9 respectively, it has many targets for proteolytic degradation in apoptosis including cell cycle proteins (e.g. p21), signal transduction molecules (e.g. protein kinase C (PKC)), cytoskeleton proteins (e.g. actin), and anti-apoptotic proteins (e.g. Bcl-2) and iCAD (Enari *et al.*, 1998; Fujita *et al.*, 1998; Kirsch *et al.*, 1999). Caspase 3 also induces other caspases to become active and these include caspase 6 and 7 (Orth *et al.*, 1996).

1.3.3.4 *Caspases 6 and 7*

Classed as executioner/effector caspases downstream in their activation of caspase 3 (Orth *et al.*, 1996). Caspase 6 and 7 have distinct but overlapping substrate preferences and functions (Rao *et al.*, 1996; Zheng and Flavell, 2000), both breaking down lamins in the cytoskeleton. Caspase 7 however is almost synonymous with caspase 3 in its substrate preference, which gives some degree of redundancy in the action of these two caspases (Orth *et al.*, 1996).

1.3.4 *The Bcl-2 proteins*

The Bcl-2 superfamily of proteins is involved in the mitochondrial pathway of apoptosis (Gross *et al.*, 1998; Desagher *et al.*, 1999). The family of at least 19 proteins are split into four sub-groups based on their structure and function. Group 1 contains the anti-apoptotic Bcl-2 family members, with 3 or 4 Bcl-2 homology (BH) domains, and groups 2, 3 and 4 contain the pro-apoptotic proteins, with 1 to 3 of the BH domains (Fig 1.3.2) (Zimmermann *et al.*, 2001). These two types of Bcl proteins interact with each other and organelles within the cell to control the process of apoptosis via the mitochondrial pathway (Marsden and Strasser 2003; Shultz and Harrington 2003).

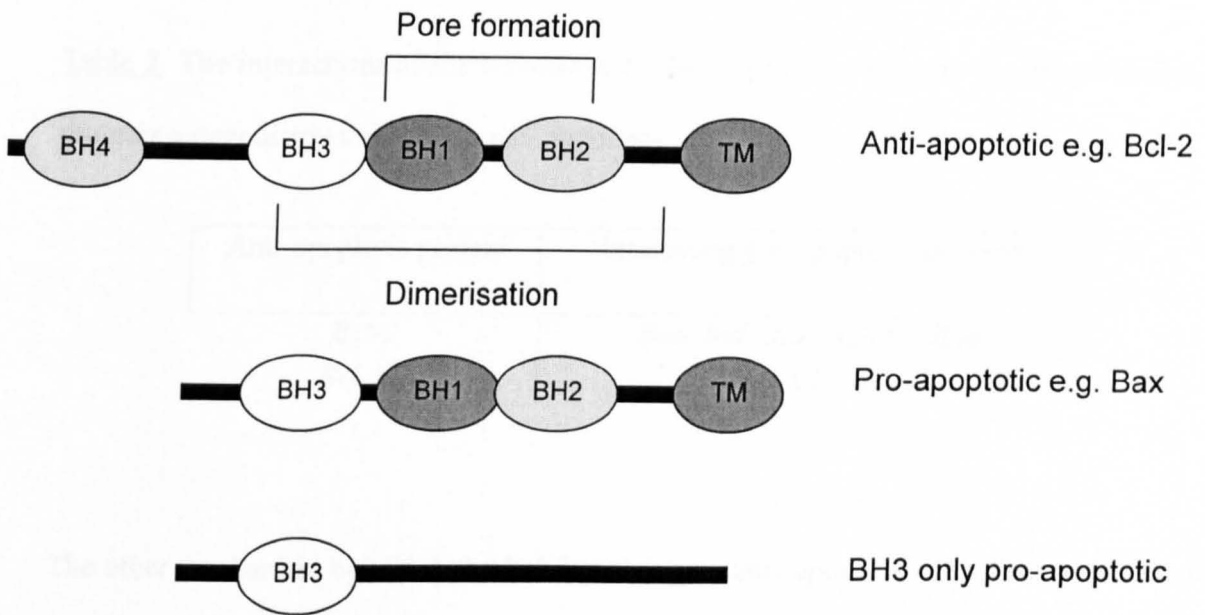


Figure 1.3.2: The structure of the Bcl-2 superfamily members showing the *Bcl-2* homology (BH) domains and their arrangement in the protein and the transmembrane domain TM (Zimmermann *et al.*, 2001)

The anti-apoptotic Bcl-2 proteins bind the mitochondrial outer membrane and prevent the release of *cyt-c* from the mitochondria and thus the induction of apoptosis. It has been suggested that the anti-apoptotic proteins may interact forming heterodimers, via the BH domains, with the pro-apoptotic proteins antagonising their effects on inducing apoptosis (Table 2). This implies that the ratio of anti-apoptotic to pro-apoptotic proteins is important in the induction of apoptosis, as a low ratio of the anti-apoptotic proteins to the pro-apoptotic proteins would allow the induction of apoptosis due to a lack of antagonism from the Bcl-2 and Bcl-XL (Shimizu *et al.*, 2000).

Table 2: The interactions of the anti-apoptotic Bcl-2 proteins with the pro-apoptotic Bcl-2 proteins antagonising the induction of apoptosis.

Anti-apoptotic protein	Interacting pro-apoptotic proteins
<i>Bcl-2</i> <i>Bcl-XL</i>	<i>Bax, Bid, Bak, Bcl-XS, Bad</i> <i>Bcl-XS, Bak</i>

The other mechanism by which the Bcl-2 proteins prevent apoptosis is by the interaction of several anti-apoptotic Bcl-2 proteins with the adenosine nucleotide translocator (ANT) and the voltage dependent anion selective channel (VDAC). The ANT and VDAC form the mitochondrial permeability transition pore (MPTP), which control the release of cyt-c and the transmembrane voltage gradient (Marzo *et al.*, 1998; Shimizu *et al.*, 1999; Shimizu *et al.*, 2000). Upon binding *Bcl-2* and *Bcl-XL* the MPTP closes, preventing the contents of the inter-membrane space of the mitochondria to be released into the cell and initiating apoptosis (Shimizu *et al.*, 2000).

The pro-apoptotic Bcl proteins all contain the BH3 domain that can be exposed or buried in the structure of the protein (Chou *et al.*, 1999). This implies a requirement for some of the proteins to have to undergo post-translational modification to expose the BH3 domain and translocate to specific areas of the cell, thereby inducing apoptosis by the mitochondrial pathway. Some of the pro-apoptotic proteins only have the BH3 domain present in their structure and may activate the process of apoptosis by either forming pores and channels in

the mitochondrial membrane or by influencing the ANT and VDAC to open, releasing the contents of the inter-membrane space of the mitochondria in a pH and voltage dependent manner (Fig 1.3.3) (Green and Reed 1998; Gross *et al.*, 1999; Shimizu, 2000).

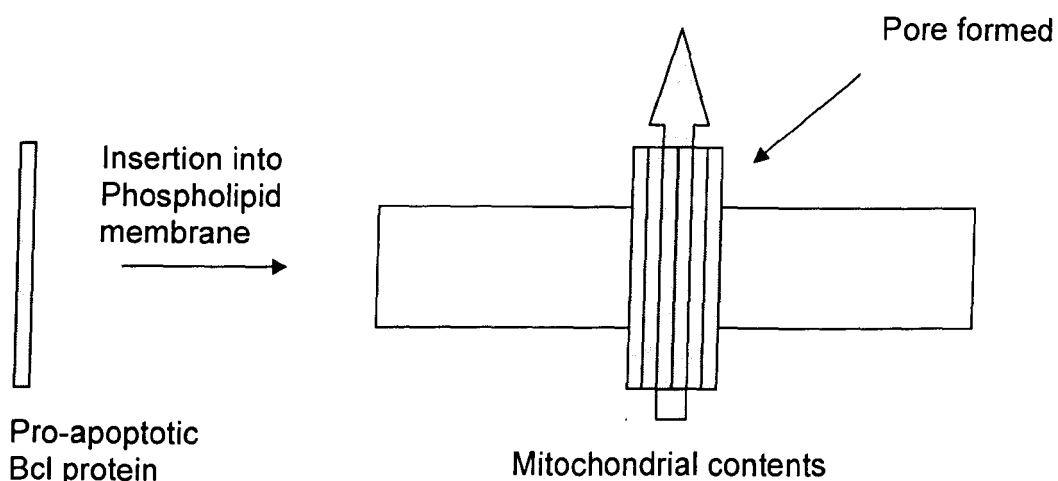


Figure 1.3.3: The potential action of the pro-apoptotic Bcl-2 proteins on the mitochondrial membrane forming a pore in the membrane causing the loss of the intra-membrane contents.

The BH3 domain proteins also form a heterodimer with some of the anti-apoptotic Bcl-2 proteins, inhibiting their anti-apoptotic function. This suggests that the ratio of the pro-apoptotic:anti-apoptotic proteins are important in the induction of apoptosis (Shimizu *et al.*, 2000). If the ratio of pro:anti is high then the anti-apoptotic proteins activity will be sequestered by the pro-apoptotic proteins with enough pro-apoptotic proteins to continue with the induction of apoptosis. Alternatively if the pro:anti ratio is low then the pro-apoptotic proteins will be totally bound to the anti-apoptotic Bcl-2 proteins and will fail to induce apoptosis (Shimizu *et al.*, 2000).

1.3.5 *The pathways of apoptosis*

1.3.5.1 *The mitochondrial pathway of apoptosis*

The mitochondrial pathway of apoptosis is regulated by the changes in mitochondrial potential and permeability and is influenced by the Bcl-2 family of proteins. In a normal situation the anti-apoptotic proteins Bcl-2 and Bcl-XL are inserted into the outer and inner membrane of the mitochondria. These two proteins maintain the mitochondrial potential by reducing the membrane permeability. Exposure of cell to insults such as UV radiation, ROS or chemicals, results in cell damage and an increase in p53 transcription (Chen *et al.*, 1996). Transcription of pro-apoptotic Bcl-2 family members (e.g. Bax and Bcl-XS) is attenuated by p53. These pro-apoptotic proteins undergo a conformational change by dephosphorylation (e.g. Bad) or by proteolytic cleavage (e.g. Bid) and translocate into the mitochondrial membrane (Gross *et al.*, 1998). When the ratio of anti-apoptotic:pro-apoptotic members of the Bcl-2 protein family is too low the pro-apoptotic proteins cause an increase in mitochondrial membrane permeabilisation and release a number of pro-apoptotic factors as discussed earlier (Zamzami and Kroemer, 2003). The permeabilisation of the outer mitochondrial membrane allows the release of pro-apoptotic factors (e.g. cyt-c and APAF-1) from the inter-membrane space. Upon release, APAF-1 and pro-caspase 9 bind via CARD dimerisation (Shi, 2001) forming the “apoptosome”. Addition of ATP and cyt-c converts pro-caspase 9 to the active caspase 9 (Fig 1.1.4). Caspase 9 binds pro-caspase 3 and proteolytically processes pro-caspase 3 to the active form (Fig 1.3.4). Caspase 3 then breaks down target proteins such as iCAD, which induce the morphological

changes associated with apoptosis (Thornberry *et al.*, 1998; Enari *et al.*, 1998; Sakahira *et al.*, 2001).

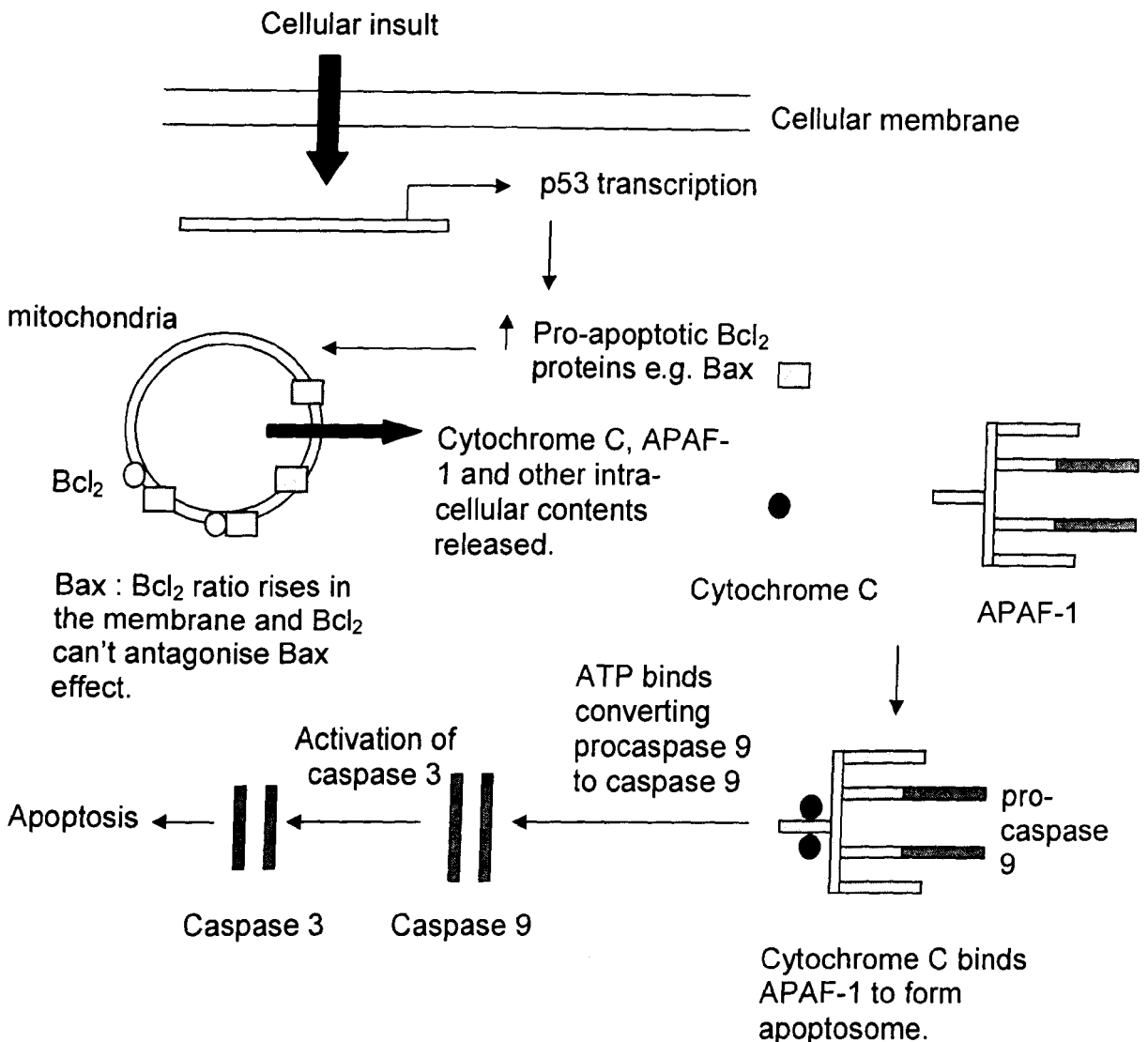


Figure 1.3.4: The mitochondrial pathway of apoptosis induced by cellular stress or insult, increasing p53 expression. This results in increased production of pro-apoptotic Bcl-proteins (e.g. Bax). Binding of these proteins causes the release of cytochrome C that binds to the apoptosome converting pro-caspase 9 to active caspase 9. Caspase 9 proteolytically activates caspase 3 that causes the biochemical changes of apoptosis (adapted from Gupta 2001).

1.3.5.2 *The death receptor pathway of apoptosis*

Activation of apoptosis can be induced by the binding of death receptors to specific ligands (Boldin *et al.*, 1996; Muzio *et al.*, 1996). The receptors are part of the tumour necrosis factor receptor (TNFR) superfamily, with conserved cysteine rich extracellular domain, intracellular death domain (DD; e.g. TNFR1, Fas (CD95)) (Zimmermann *et al.*, 2001), and TNF related apoptosis inducing ligand (TRAIL). The death domain allows the activation of the signal cascade, which causes apoptosis (Boldin *et al.*, 1996).

To understand the death receptor pathway of apoptosis it is best to use the example of the Fas receptor (FasR/ CD95R) and Fas ligand (FasL/ CD95) found on immune cells. FasR is a glycosylated cell surface molecule induced by cytokines including interferon gamma (IFN- γ), and TNF. FasL however is highly regulated, only being expressed on activated immune cells. Upon binding of FasL, FasR trimerizes via the death domain (DD) on each receptor. To this homo-trimer an adaptor protein, Fas-associated death domain (FADD), is recruited using the conserved DD on each protein. The death effector domain (DED) present on FADD allows the recruitment of pro-caspase 8, which binds using homologous DEDs on each of the proteins, forming the death inducing signalling complex (DISC) (Gupta, 2001). In close proximity to each other the pro-caspase 8 autolytically activates each other to active caspase 8. Caspase 8 then catalyses the activation of pro-caspase 3 to caspase 3 (Fig 1.3.5), which then proteolytically destroys its cellular targets including iCAD, poly(ADP-ribose) polymerase (PARP), and lamin (Sakahira *et al.*, 2001).

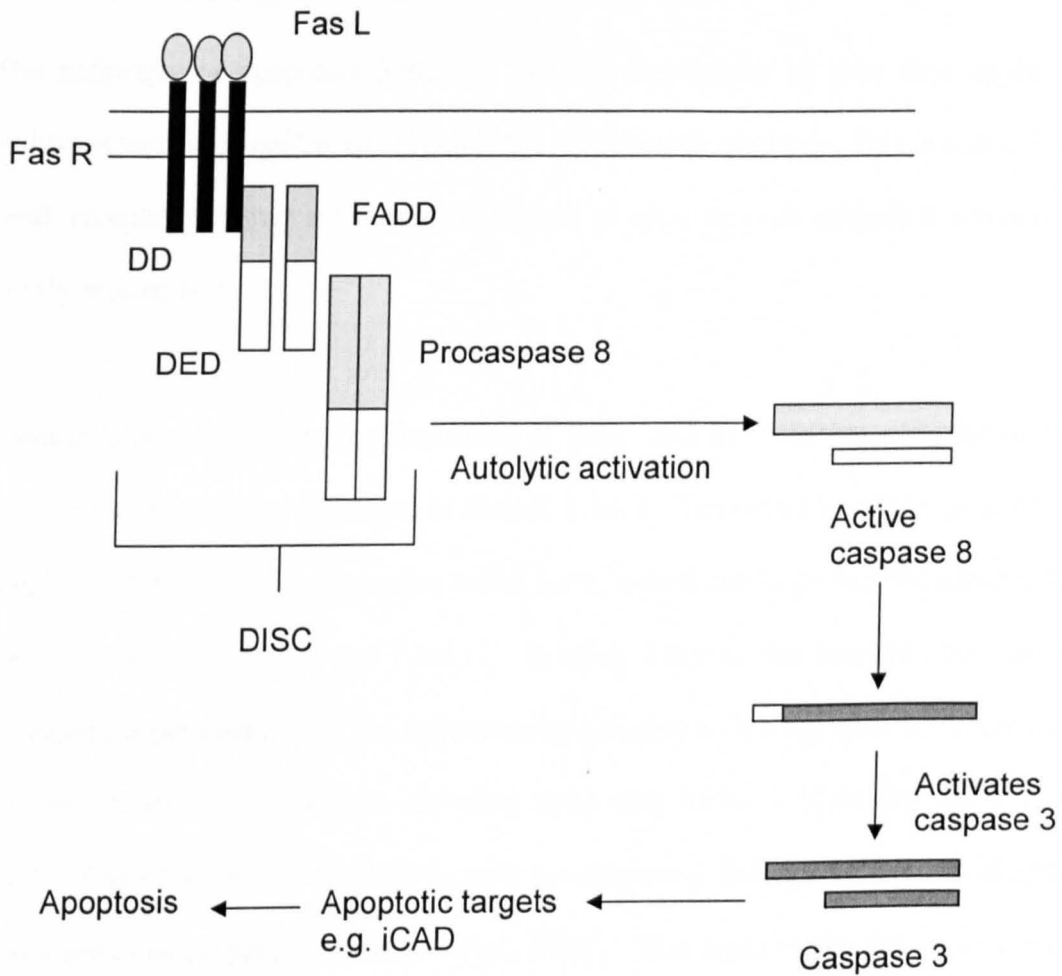


Figure 1.3.5: The death receptor pathway of apoptosis. The diagram indicates the fas ligand (FasL) and receptor (FasR) and the death domains (DD) on the receptor. Fas associated death domain (FADD) with death effector domains (DED) bind pro-caspase 8 forming death inducing signalling complex (DISC) and activating caspase 8 and subsequently caspase 3 (adapted from Gupta 2001).

1.3.5.3 *Interlinking of the apoptotic pathways*

The pathways of apoptosis induction are not as separate as they first appear. Both pathways working together can regulate the induction of apoptosis. This is controlled by the death receptor pathway activating the release of cyt-c through caspase 8 activating Bcl-2 family protein Bid.

Caspase 8 is activated by the formation of DISC and the autolytic cleaving of the pro-caspase 8 zymogens (as described in Section 1.3.5.2). The active caspase 8 cleaves the pro-apoptotic Bid protein to its active t-Bid form, which binds to the mitochondrial outer membrane (Section 1.3.4 and 1.3.5.1). Binding t-Bid to the mitochondrial membrane increases the permeability of the membrane by possibly activating the VDAC, releasing the inter-membrane space contents including cyt-c and APAF-1 (Cowling and Downward, 2002). Cytochrome c and APAF-1, with pro-caspase 9 and ATP, form the apoptosome, which activates caspase 9 (Yoshida *et al.*, 1998). This leads to the further conversion of pro-caspase 3 to caspase 3, which in turn causes the morphological changes associated with apoptosis e.g. DNA laddering, membrane blebbing and cellular shrinkage.

It was however proposed by Cowling and Downward (2002) that a positive feedback loop may occur through this interaction of the pathways increasing the caspase activation in a cell. The positive feedback loop occurs through effector caspases cleaving the initiator caspases. The example being that caspase 8 is involved in the release of cyt-c from the mitochondria due to the cleaving of Bid to t-Bid. In turn the permeabilisation of the

mitochondrial membrane releases cyt-c into the cytosol, activating caspase 9, which then activates the executioner caspases 3. Caspase 3 activates caspase 6 and 7, which activate caspase 8 (Cowling and Downward, 2002) (Fig 1.3.6).

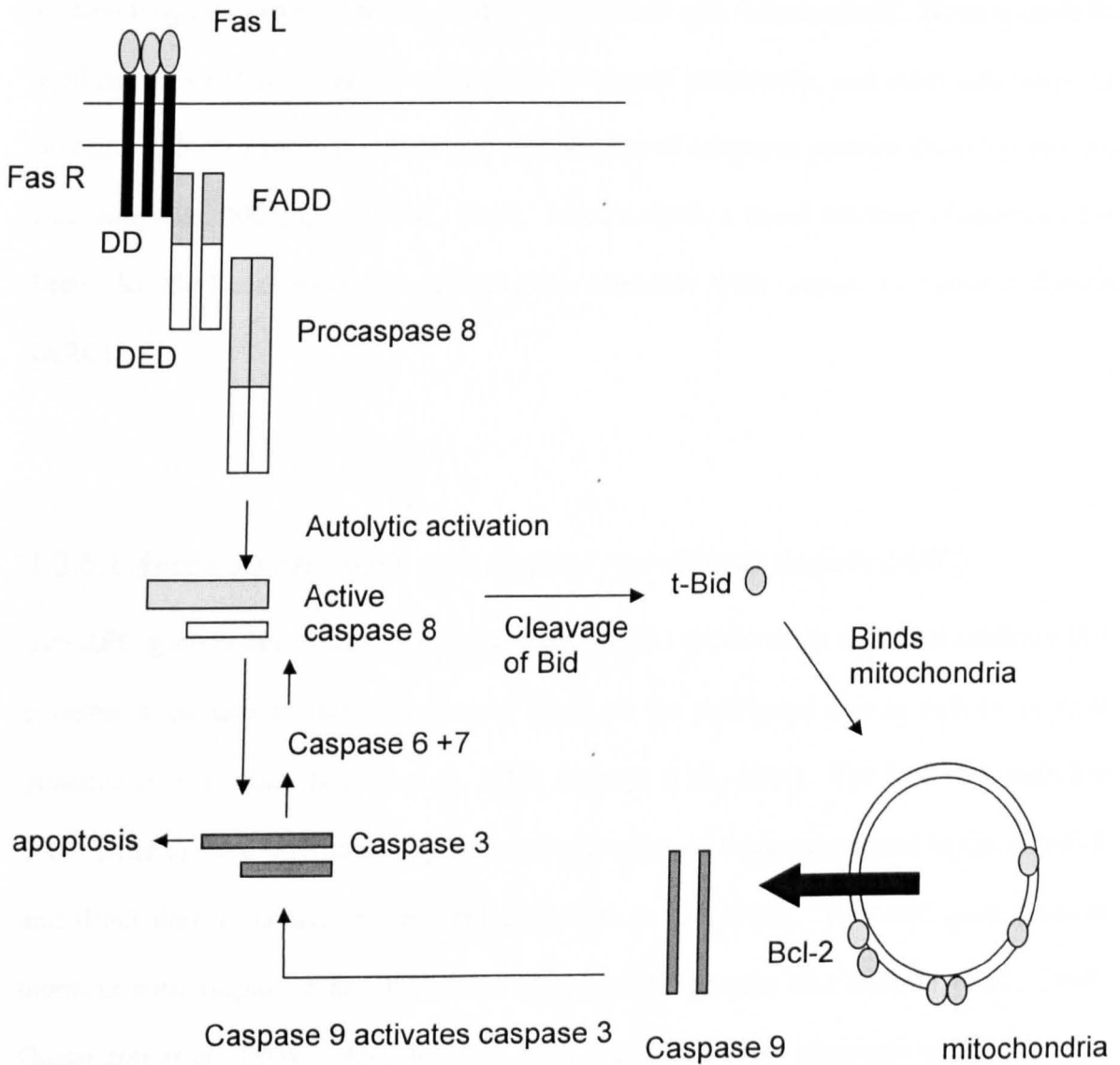


Figure 1.3.6: The activation of caspase 6 by caspase 9 and the subsequent activation of caspase 8 causing a positive feedback loop in the activation of caspase 3, 6, 8 and the truncation of *Bid* to t-Bid (Cowling and Downward, 2002).

1.3.6 *Endogenous inhibitors of apoptosis*

To inhibit apoptosis, signalling pathways are activated by stimuli such as extracellular matrix binding and growth factor binding. The signalling pathways increase the expression of anti-apoptotic proteins, which bind to the caspases and mitochondria. These include the well-documented Bcl-2 family of proteins discussed previously, and other anti-apoptotic proteins including survivin, cFLIP and the inhibitor of apoptosis proteins (IAP) (Chavakis and Dimmeler, 2002; Duval *et al.*, 2003). More recently a novel inhibitor of apoptosis has been identified and referred to as apoptosis repressor with caspase recruitment domain (ARC).

1.3.6.1 *Apoptosis repressor with caspase recruitment domain (ARC)*

The *ARC* gene found on human chromosome 16q22.1 produces an apoptotic inhibitor that contains a caspase recruitment domain fused to the c-terminal region rich in proline/ glutamic acid residues (Koseki *et al.*, 1998; Abmayr *et al.*, 2004). The CARD domain has been found to have high similarity to the pro-domains of the caspases and to the APAF-1 and death domain containing molecules (Koseki *et al.*, 1998). The *ARC* gene product interacts with caspase 2 and 8 and the pro-apoptotic protein Bax (Koseki *et al.*, 1998; Gustafsson *et al.*, 2004). *ARC* has also been found to prevent apoptosis induced by Fas associated death FADD and trail associated death domain (TRADD) containing receptors (Koseki *et al.*, 1998). This indicates that *ARC* induced inhibition of apoptosis occurs predominantly through the death receptor pathway and may be due to the binding of

caspase 8 at the mitochondria and the death domains (Koseki *et al.*, 1998; Li *et al.*, 2002). Binding of ARC to Bax however suggest that it can also suppress parts of the mitochondrial pathway of apoptosis and may include the suppression of cyt-c release from the mitochondria (Fig 1.3.7) (Neuss *et al.*, 2001; Chatterjee *et al.*, 2003; Gustafsson *et al.*, 2004). Activity of ARC is controlled by phosphorylation of threonine¹⁴⁹ by protein kinase CK2 both *in vitro* and *in vivo*. This phosphorylation is required for its anti- apoptotic activity (Li *et al.*, 2002).

Expression of ARC has been found in the heart, skeletal muscle and some brain regions in both human and rats. Its expression however varies, depending on the cellular environment or experimental conditions (Koseki *et al.*, 1998; Dowds and Sabban, 2001). For instance, cells cultured in serum-free medium are found to have elevated expression of ARC, which is localized to the nucleus (Dowds and Sabban, 2001). In areas of hypoxia and ischemia ARC levels in the cytosol may be decreased, allowing apoptosis to occur (Ekhterae *et al.*, 1999; Hong *et al.*, 2003). Other pathological situations also alter the levels of ARC. Alzheimer's disease (AD) causes an increase in the expression of ARC, which may decrease the incidence of apoptosis in the affected cells (Engidawork *et al.*, 2001). By comparison, in Duchenne muscular dystrophy there is no apparent change in levels of ARC but its distribution may be altered in affected muscle fibers (Abmayr *et al.*, 2004). Moreover, ARC expression is decreased under conditions of enhanced caspase-3 expression (Abmayr *et al.*, 2004).

Over expression of ARC in cells has been shown to decrease the incidence of apoptosis and injury. Indeed over expression of ARC in rat heart ventricles decreased apoptosis in ischemic disease models (Chatterjee *et al.*, 2003). Similarly, hypoxia induced apoptosis was reduced by over expression of ARC which also inhibited apoptosis induced by hydrogen peroxide in H9c2 cells (Ekhterae *et al.*, 1999; Neuss *et al.*, 2001; Gustafsson *et al.*, 2004).

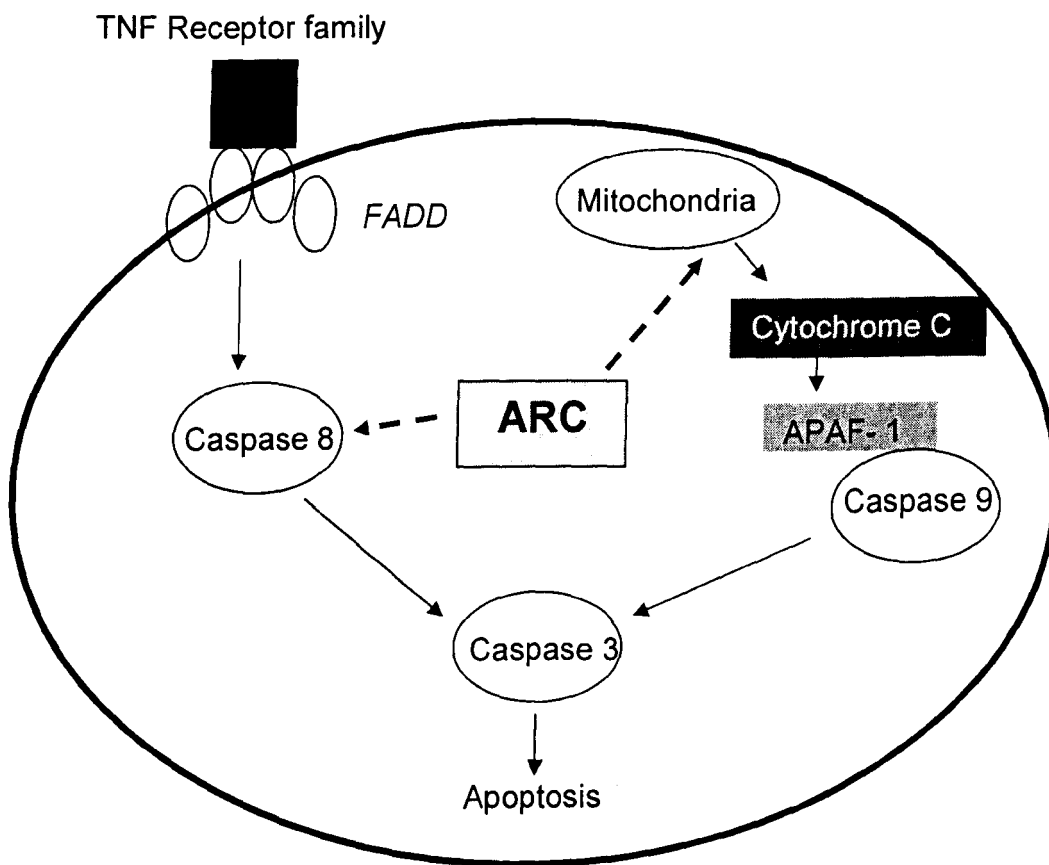


Figure 1.3.7: Pathways of apoptosis and site of action of ARC protein. ARC can inhibit apoptosis by preventing the release of cytochrome c through binding to the pro-apoptotic protein Bax in the mitochondrial pathway, and by preventing the activation of caspase 8 in the death receptor pathway (Chatterjee *et al.*, 2003).-----▶ = inhibition.

1.4 *Angiogenesis, Cyclooxygenase 2 and Apoptosis*

1.4.1 *Angiogenesis and apoptosis*

The processes of angiogenesis and apoptosis are closely linked to each other. During angiogenesis, apoptosis of endothelial cells is reduced allowing the production of fresh blood vessels from existing vessels. Inhibition of apoptosis during angiogenesis is thought to be partially due to the increase in the anti-apoptotic protein Bcl-2 expression caused by VEGF in endothelial cells (Nor *et al.*, 1999). The increase in expression of Bcl-2 was found to be pro-angiogenic in vascular cells, inducing sprouting and proliferation (Nor *et al.*, 2001). Other anti-apoptotic molecules such as ARC have also been shown to inhibit apoptosis of skeletal and cardiac muscle cells (Koseki *et al.*, 1998). It is however not known if ARC is expressed in vascular endothelial cells or whether it can prevent apoptosis during angiogenesis and quiescence of the vasculature.

1.4.2 *Angiogenesis and cyclooxygenase 2*

Induction of angiogenesis during hypoxia by VEGF released from inflammatory cells and the ECM is associated with the induction of expression of COX-2. This occurs in endothelial cells within 30 min of treatment *in vitro* (Carmeliet and Jain, 2000; Abe and Sato, 2001; Akarasereenant *et al.*, 2002; Tamura *et al.*, 2002; Wary *et al.*, 2003).

Vascular endothelial cell growth factor binds to the VEGFR-2 activating protein tyrosine kinase and p42/44 (ERK1/2) MAPK. Induction of ERK1/2 increases the level of cAMP activating COX-2 gene expression (discussed in Section 1.2.5 and 1.2.7). The

ERK1/2 signalling messengers also directly translocate to the nucleus and increase expression of anti-apoptotic proteins including COX-2 (Jones *et al.*, 1999; Ruegg *et al.*, 2004).

Expression of the COX-2 gene by VEGF can cause a positive feedback loop of VEGF expression from endothelial cells (Leung *et al.*, 2003). Prostaglandin E₂, produced by COX-2 and PGE synthase, binds the cell in an auto or paracrine action and activates two possible signalling pathways. PGE₂ stimulates the increase in the expression of VEGF by (i) activating the ERK 2 signalling messenger, which trans-activates JNK 1 and increases levels of VEGF (Lin *et al.*, 2001; Pai *et al.*, 2001), (ii) binding the EP2 receptor releasing HIF-1 α that binds to the hypoxic response element on the promoter of the VEGF gene increasing expression (Carmeliet, 2000; Giordano and Johnson, 2001; Gately and Li, 2004). The increase in VEGF concentration forms the positive feedback loop by inducing further COX- 2 expression (Fig. 1.4.1).

Prostaglandin E₂ has also been found to increase the levels of $\alpha\text{v}\beta\text{3}$ integrins that increases the activation of VEGFR-2 and the binding of VEGF possibly making the cell more sensitive to the VEGF produced thereby increasing angiogenesis (Soldi *et al.*, 1999; Gately and Li, 2004). Other prostaglandins have an effect on angiogenesis. For instance, PGI₂ may increase endothelial cell permeability and sprouting and TXA₂ increases migration of endothelial cells (Gately and Li, 2004).

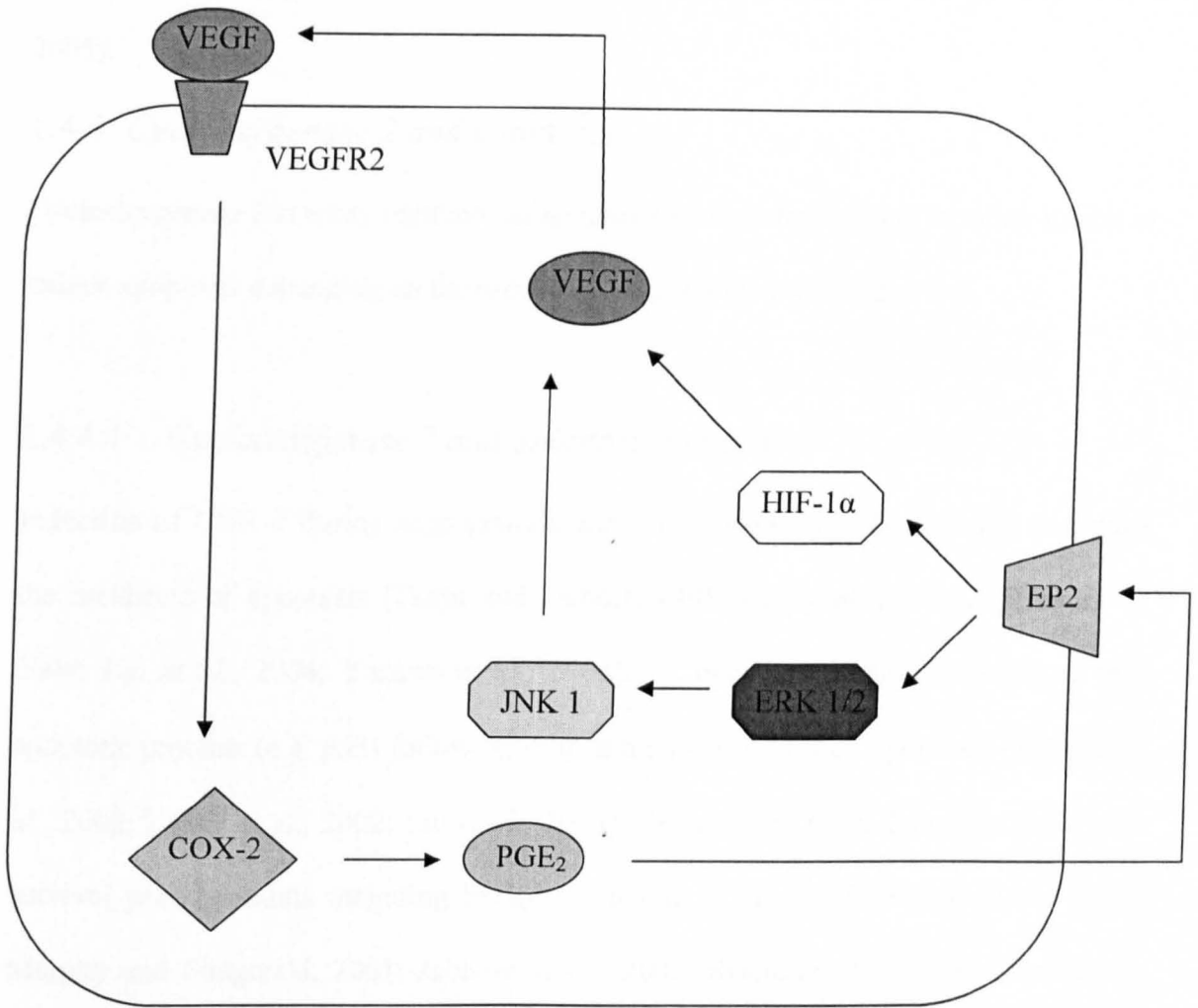


Figure 1.4.1: Schematic diagram of the positive feedback loop of vascular endothelial growth factor (VEGF) and COX-2 expression via PGE₂ (Carmeliet, 2000; Giordano and Johnson, 2001; Lin *et al.*, 2001; Pai *et al.*, 2001; Gately and Li, 2004.).

1.4.3 Angiogenesis and cyclooxygenase 2 inhibition

Selective inhibition of COX- 2 activity has been found to inhibit angiogenesis dose dependently by decreasing growth factor (e.g. VEGF and bFGF) expression and inhibiting proliferation of endothelial cells *in vitro* and *in vivo* (Sawaoka *et al.*, 1999; Leahy *et al.*, 2002; Yazawa *et al.*, 2005). These effects were reversed however by the

addition of PGE₂, allowing endothelial cells to continue to proliferate (Yazawa *et al.*, 2005).

1.4.4 *Cyclooxygenase 2 and apoptosis*

Cyclooxygenase-2 is a key regulator of apoptosis and has been found to either inhibit or induce apoptosis depending on the type of prostaglandins produced.

1.4.4.1 *Cyclooxygenase 2 and apoptosis inhibition*

Induction of COX-2 during angiogenesis and inflammation has been found to reduce the incidence of apoptosis (Tsujii and Dubois, 1995; Leahy *et al.*, 2002; King *et al.*, 2004; Lui *et al.*, 2004; Yazawa *et al.*, 2005). It may inhibit the activation of pro-apoptotic proteins (e.g. p53) following drug and hypoxia induced apoptosis (Jabbour *et al.*, 2002; Leahy *et al.*, 2002; Lui *et al.*, 2004). In addition, COX-2 may increase pro-survival prostaglandins including PGE₂. (Ottonello *et al.*, 1998; Sheng *et al.*, 1998; Murphy and Fitzgerald, 2001; Jabbour *et al.*, 2002; Steele *et al.*, 2003). Increase in PGE₂ has been associated with intracellular increases of pro-survival factors (e.g. Bcl-2) via the PI3K/Akt signalling pathway (Sheng *et al.*, 1998; Parfenona *et al.*, 2001; Gately and Kerbel, 2003). The induction of Bcl-2 inhibits the release of cyt-c from the mitochondria and prevents the activation of caspase 9 (Sun *et al.*, 2002; Jendrossek *et al.*, 2003). The synthesis of PGE₂ or treatment with PGE₂ *in vitro* has also been shown to elevate the levels of cAMP intracellularly. This subsequently results in the activation of the cAMP response element (CRE) on many genes including VEGF and possibly anti-apoptotic proteins (Ottonello *et al.*, 1998), and may also promote $\alpha\beta$ 3 integrin binding of endothelial cells with cAMP signalling preventing cell dissociation from the ECM and subsequent anoikis (Dormond *et al.*, 2002).

1.4.4.2 *Cyclooxygenase 2 and apoptosis induction*

The production of the cyclopentenone prostaglandins during the second induction of COX-2 may be involved in the resolution of inflammation and in the control of angiogenesis. Cyclopentenone prostaglandins such as PGD₂, PGJ₂ and 15-deoxy-Δ^{12,14}-PGJ₂, have been shown to induce apoptosis in many cell types including endothelial cells and granulocytes (Ward *et al.*, 2002; Dong *et al.*, 2004; Erl *et al.*, 2004). These prostaglandins are ligands for PPAR-γ, but may induce apoptosis independently of this receptor (Ward *et al.*, 2002; Erl *et al.*, 2004). Apoptosis induction is accompanied by an inhibition of NF-κB and AP-1 DNA binding (Dong *et al.*, 2004; King *et al.*, 2004), and an increase in p53 and p38 activation that may be pro-apoptotic (Dong *et al.*, 2004).

1.4.4.3 *Cyclooxygenase 2 inhibition and apoptosis induction*

Inhibition of COX-2 by non-steroidal anti-inflammatory drugs (NSAIDs), selective COX-2 inhibitors and other inhibitors of COX-2 such as curcumin, increase apoptosis and inhibit angiogenesis while decreasing PGE₂ levels (Pang and Hoult 1997; Sawaoka *et al.*, 1999; Leahy *et al.*, 2002). The induction of apoptosis by COX-2 inhibitors may be due to the decrease in PGE₂ production and decreasing VEGF production in endothelial cells. The decrease in PGE₂ prevents the PI3K/Akt signalling for the production of anti-apoptotic Bcl-2 proteins promoting the mitochondrial pathway of apoptosis, (Wheeler-Jones *et al.*, 1997; Hsu *et al.*, 2000; Williams *et al.*, 2000; Wu *et al.*, 2003; Zha *et al.*, 2004). The inhibition of COX-2 causes the accumulation of unesterified arachidonic acid in the cell and this may also directly promote apoptosis (Cao *et al.* 2002; Zha *et al.*, 2004).

Inhibitors of COX-2 have been shown to augment apoptosis independently of COX-2 inhibition, suggesting a pro-apoptotic effect through other signalling pathways (Niederberger *et al.*, 2004). COX-2 inhibitors e.g. NS-398, may promote apoptosis through the death receptor pathway independently of COX-2 inhibition (Totzke *et al.*, 2003; Niederberger *et al.*, 2004). The selective COX-2 inhibitors celecoxib and rofecoxib have been found to induce apoptosis by interfering with multiple targets (e.g. Akt, ERK2), with no reversal of the induction of COX-2 (Hsu *et al.*, 2000; Song *et al.*, 2002; Niederberger *et al.*, 2004). These actions of the drugs are observed at concentrations much higher than the IC₅₀ for the inhibition of COX-2, suggesting that at high concentrations COX-2 inhibitors may cause apoptosis in cells with no clinical inhibition of inflammation or angiogenesis.

2. Materials and Methods

A full list of suppliers can be found in Appendix A. A full list of media recipes and solutions can be found in Appendix B.

2.1 *Cell Culture*

2.1.1. *Isolation of Human Umbilical Vein Endothelial Cells (HUVECs)*

HUVECs were isolated using a modification of Morgan, 1999. Human umbilical cords were collected in a sterile container containing phosphate buffered saline (PBS) within a few hr of birth. The umbilical cord was placed on to tissue paper and small sections of the ends of the cord were removed to give a clear surface and unobstructed entry to the vein. To each end of the cord luer lock connectors were placed into the vein and secured using strong thread. A 20ml syringe containing 20ml PBS was attached to one end of the cord and the PBS flushed through the vein to wash out blood cells and also check for leaks or obstructions in the vein. Blood clots present were gently massaged to mechanically break down the clot. If the clot could not be removed the cord was cut beyond the obstruction and the luer lock reattached. A second 20ml syringe containing pre-filter sterilised collagenase solution (0.5mg/ml) was attached to the opposite end of the cord and the vein filled with the collagenase. The cord was wrapped in tin foil and placed in a 37°C incubator for 10 minutes to facilitate dislodging of endothelial cells from the vessel wall. During these 10 minutes a T25 flask was coated with 1% (v/v) gelatin by adding 2ml of 1% gelatin to the flask and incubating at room temperature for 5-10 minutes. Once the incubation was completed the excess gelatin was removed and the flask retained for further use. The cord

was removed from the incubator, gently massaged and the collagenase solution collected into a 50ml centrifuge tube. The cords were flushed with PBS and the wash collected into the same 50ml centrifuge tube. The solution was then centrifuged at 1000rpm for 5 minutes. The supernatant was discarded and the cell pellet resuspended in 5ml of Medium 199 supplemented with 20% foetal calf serum (FCS), 2mM l-glutamine and 100 units penicillin, 0.1 mg/ml streptomycin (complete M199). The cell suspension was then placed into the gelatin-coated T25 flask and incubated for 24 hr at 37°C, 5% CO₂ in a tissue culture incubator. The media was replaced after 24 hr with fresh medium containing endothelial cell growth factor (ECGF; 50µg/ml). Flasks were incubated for a further 2 days.

2.1.2 Growth and Maintenance of HUVECs

Maintenance of HUVECs was carried out by replacing the spent cell culture media with 5ml fresh complete M199 containing ECGF. This process was repeated every two days until cells were confluent.

2.1.3 Passaging and plating of HUVECs

Confluent monolayers of HUVECs were detached with trypsin-EDTA solution (500 units trypsin/ 180µg/ml EDTA). The culture medium was removed from the monolayer and 2ml of trypsin-EDTA added to each flask. The solution was gently swirled around the flask ensuring that the cell monolayer was covered in trypsin. The latter was removed and the process repeated but leaving approximately 200µl of solution in the flask. The flasks were continuously examined under the microscope until the cells rounded up. At this point the

flasks were gently tapped on the bench to dislodge the cells. 1ml of complete M199 was added to each flask to deactivate the trypsin-EDTA. Cells were counted with an improved Neubauer haemocytometer and calculated for plating into 12, 24 or 96 well plates pre-coated with 1% (v/v) gelatin (only 12 and 24 well plates). Cells to be passaged had 2mls of fully supplemented Media 199 added into the flask and divided equally between 3 T25 or placed into a T75 tissue culture flask pre-coated with 1% (v/v) gelatin (see section 2.1.1) and ECGF was then added to each well or flask and incubated at 37°C, 5% CO₂ until ready for use.

2.1.4 Growth and maintenance of J774 macrophages

J774 macrophage cultures were maintained by removing spent Dulbeccos modified eagle media (DMEM) and replacing with 5ml fully supplemented DMEM every two days. Passaging of confluent cells was done by removing culture media and scrapping the cells into 1ml of fully supplemented DMEM. Cells were counted and either plated into 12/24/96 well plates for treatment or into fresh T25 culture flasks for growth and incubated at 37°C, 5% CO₂ until used.

2.1.5 Growth and maintenance of Jurkat E6.1 cells

Jurkat E6.1 cells were maintained in T25 tissue culture flasks in 2mM l-glutamine and 100 units penicillin, 0.1 mg/ml streptomycin (complete RPMI 1640). Upon reaching confluence the media containing the cells was placed into a 15ml centrifuge tube and centrifuged at 1000rpm for 5 minutes. The supernatant was removed and the pellet resuspended into 1 ml

of fresh supplemented media for counting. Cells were distributed into 3 T25 flasks containing 4mls of fresh supplemented media for passaging or plated into 12, 24 or 96 well tissue culture plates for experimentation.

2.2 *Matrigel HUVEC tubule formation assay*

Matrigel was defrosted at 4-8°C until liquid and 40µl applied to each well of a -20°C pre-cooled 96 well plate with -20°C pre-cooled tips ensuring a level covering of the well, followed by an incubation of the 96 well plate at 37°C for 30 minutes. To each well 100µl of a 2×10^5 cells/ml suspension of HUVECs were added. Treatment was then spiked in to the media and the plate incubated to allow tubule formation at 37°C in a 5% CO₂ tissue culture incubator. Tubules were counted and photographed after 8 hrs of incubation with only full tubules being counted as positive.

2.3 *Induction of apoptosis in HUVECs and Jurkat E6.1 cells*

Apoptosis was induced by removing the complete M199 and replacing it with 0% FBS M199. To the negative control wells the vehicle for the drug was added at the highest concentration used. In the treated wells the drug was added directly to give the final concentration required. The samples were incubated for up to 8 hr for caspase activation and for 24 hr when investigating caspase activity, DNA condensation and laddering.

2.4 Determination of induced cell apoptosis

Floating cells in the culture medium were removed and counted. The cells were centrifuged at 13,000 rpm for 5 minutes in a microcentrifuge and resuspended in PBS at 1×10^5 / ml. Adherent cells were trypsinised and counted. The percentage of floating cells was then worked out. The floating cells were subsequently used in chromatin condensation assays, determination of DNA laddering or analysis of caspase induction.

2.4.1 Cytospinning and fluorescent staining of condensed chromatin

Cell suspensions of Jurkat E6.1 cells or HUVECs were pipetted into cytospin chambers (Fig 2.4.1) and centrifuged at 750rpm for 10 minutes to pellet cells onto a glass slide.

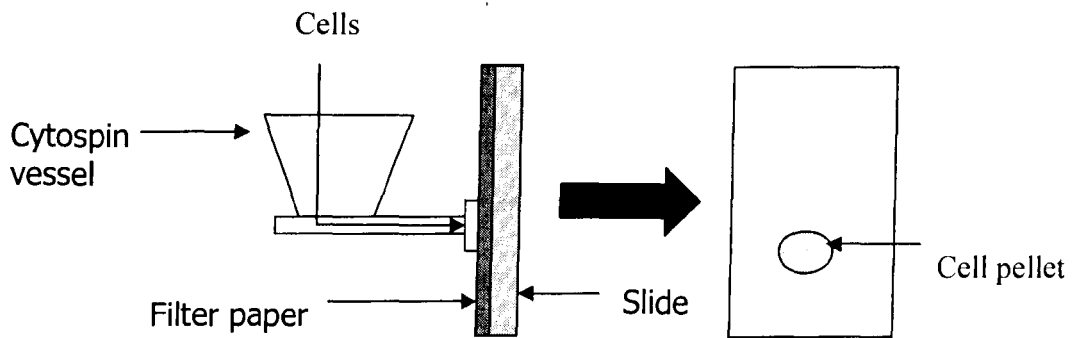


Figure 2.4.1 The cartoon of a cytopsin vessel. Cells were pipetted into the cytopsin vessel and centrifuged to form a pellet of cells on the glass slide. The pellet was then fixed and stained

Slides were fixed by pipetting 20µl of 3.7% formaldehyde on to the cells for 10 minutes and washed 10 times in PBS to remove any excess formaldehyde. Acridine orange (4µM) was added to the fixed cells and incubated in the dark for 3 minutes. Slides were again washed in PBS (10 times) to remove excess stain. 500 cells were counted at random, identifying and counting fluorescent stained cells which were taken as positives for condensed chromatin. The percentage of total cells that had condensed chromatin was then calculated using the equation below:

$$\frac{\text{Cells with condensed chromatin}}{\text{Cells counted on slide (500)}} \times 100 = \% \text{ of floating cells with condensed chromatin}$$

$$(\% \text{ of floating cells} / 100) \times \% \text{ of floating cells with condensed chromatin} \\ = \% \text{ of total cells with condensed chromatin.}$$

These values were then plotted graphically and statistical analysed.

2.4.2 DNA laddering assay using a DNA suicide track[®] kit

The assay was performed according to the manufacturer's protocol. Cell pellet was resuspended in 500µl of extraction buffer and incubated on ice for 30 minutes. The samples were centrifuged at 13,000rpm for 5 minutes and the supernatant retained. To the samples 20µl of solution 2, an RNase solution, was added and incubated at 37°C for 60 minutes. Twenty five microlitres of solution 3, used to aid isolation of the DNA from the cell lysate, was then added and mixed gently before incubating at 50°C for 60 minutes. To the solution 2µl of pellet paint[™], 60µl 3M sodium acetate (pH 5.2), and 662µl of 2-propanol were added, mixed by inversion and incubated at room temperature for 2 minutes. Samples were centrifuged at 13,000rpm for 5 minutes, the supernatant removed and the pellet washed with 500 µl 70% ethanol and re-centrifuged. The supernatant was removed from the samples and the pellet was washed with 500µl 100% ethanol and centrifuged. The pellet was allowed to dry, resuspended in 50µl of resuspension buffer and retained at 4°C until analysed by agarose gel electrophoresis.

2.4.3 DNA laddering assay following phenol/chloroform DNA extraction

Treated cells were lysed in 100µl DNA lysis buffer (10mM EDTA, 50mM Tris – HCl, 0.5% SDS) for 30 minutes on ice. Proteinase K (0.5mg/ml) was added and the samples incubated for a further 1 hour at 50°C. 5µl of 1mg/ml RNase A was added and again incubated at 50°C for 1 hour. An equal volume of phenol: chloroform: isomoyl alcohol

(24:25:1) was added to the samples and gently mixed for 2 minutes. The samples were centrifuged at 13,000 rpm for 5 minutes. The aqueous top layer was transferred into a clean microcentrifuge tube. An equal volume of the phenol:chloroform mixture was added and centrifuged. The aqueous top layer was saved and 2.5 volumes of ice cold absolute ethanol plus 0.1 volumes of 3M sodium acetate (pH 5.8) added. The samples were incubated overnight at -70°C to precipitate the DNA. The precipitates were centrifuged for 5 minutes at 13,000 rpm and the supernatant discarded. Pelleted DNA was washed in 70% ethanol, centrifuged at 13,000 rpm for 5 minutes and left to air dry. The pellet was subsequently resuspended in 50µl of TE buffer and analysed by agarose gel electrophoresis.

2.4.4 *Analysis of caspase-3 activity*

Treated cell cultures were trypsinised and counted using a haemocytometer. The samples were centrifuged at 1000rpm for 10 minutes and resuspended in ice-cold lysis buffer (50mM HEPES, 1mM Dithiothreitol (DTT), 0.1mM EDTA, 10% (v/v) glycerol, 0.1% (w/v) CHAPS) (pH7.4) to the concentration of 1×10^7 cells/ml before incubating on ice for 5 minutes. The lysates were then centrifuged at 1000rpm for 10 minutes at 4°C. The supernatant was retained on ice or at -70°C until required.

To determine caspase activity in samples, a conversion factor for sample activity was required and was determined by adding 100µl of 50µM p-nitroaniline to duplicate wells in a 96-well plate. Assay buffer added to other duplicate wells was used as blanks. The absorbance of each sample was read at 405nm using a Labsystems Multiscan RC

spectrophotometer. The blank values were subtracted from the p-nitroaniline readings and the conversion factor calculated as follows:

$$\text{Conversion factor } (\mu\text{M}/A_{405}) = 50\mu\text{M}/\text{average } A_{405} \text{ (of p-nitroaniline - blank)}$$

A 96-well assay plate was set up as follows using the cell supernatant derived from above:

Table 3: Reagents required for the caspase 3 activity assay

Sample	Assay buffer (μl)	Cell extract (μl)	Human recombinant Caspase-3 ($2\text{U}/\mu\text{l}$)	Caspase-3 inhibitor Ac-DEVD-CHO (μl)	Substrate Ac-DEVD-pNA (μl)
Blank	90	0	0	0	10
Cell sample	60	30	0	0	10
Caspase-3 positive control	60	0	30	0	10
Caspase-3 + cell extract	30	30	30	0	10
Cell extract + inhibitor	40	30	0	20	10

Prior to adding the substrate the 96 well plate was incubated at 37°C with the other reagents in order to allow the inhibitor to interact with the enzyme. The substrate was subsequently added and the absorbance read at 405nm every 10 minutes for up to 2 hr.

Following the absorbance readings the data for each sample was plotted against time (mins). The slope of the lines ($\text{OD at } 405\text{nm}/\text{min}$) was calculated from the linear portion

of the lines and the sample replicates mean averaged. Blank values were subtracted from the sample values. Activity of the samples (pmol/ min) was calculated using the equation below;

$$\text{Activity (pmol/min)} = \text{slope (A/min)} \times \text{conversion factor (50}\mu\text{M/average 405nm)} \times \text{assay volume.}$$

Specific activity (pmol/min/number of cells) of the samples was calculated by dividing the activity (pmol/ min) by the number of cells suspended in 30 μ l of the lysis buffer and plotted for graphically analysis.

2.5 Western blotting and protein analysis

Culture media was discarded from treated wells. Treated cells were lysed in 20-100 μ l 20% (v/v) glycerol, 10%(v/v) SDS, and 0.1 M Tris-Hcl (pH6.8) on ice for 5 min. Protein samples were frozen (-20oC) until required for protein concentration analysis or western blotting.

2.5.1 BCA assay for protein concentration

Stock solutions of protein standards (0-1000 μ g/ μ l) were prepared from bovine serum albumin (BSA) in sterile distilled water (SDW). 0.1 μ l of the lysis buffer used for western blotting was added to each stock solution. A protein standard curve was then constructed by adding 10 μ l of each standard to duplicate wells in a non-sterile 96-well plate. 10 μ l of a

1:10 dilution of the samples were added into the sample wells of the same 96-well plate. The Bicinchoninic acid (BCA) reagent was prepared by mixing a 50:1 ratio of solutions A: B. 200 μ l of the reagent was then added to each well and incubated for 30 mins at 37°C. The plate was read on a Labsystems Multiscan RC spectrophotometer at 595nm. The concentration of protein in each sample was determined from the standard curve constructed.

2.5.2 Sample preparation

Samples were thawed and aliquoted to give an equal concentration of protein for analysis. To the aliquot a volume of dithiothreitol (DTT) (1 M) was added to give a 1:5 dilution of DTT in the final sample (200 mM). This was used to reduce the proteins. 1 μ l of bromophenol blue dye was also added. The samples were then boiled at 95°C for 5 mins to denature the proteins and then loaded immediately onto an SDS-PAGE gel in a mini-protean II system (Biorad).

2.5.3 Sodium dodecyl sulphate polyacrylamide gel electrophoresis (SDS-PAGE)

The resolving gel solution was made (appendix B) and poured leaving approximately 2.5 cm from the top of the glass (Fig 2.5.1).

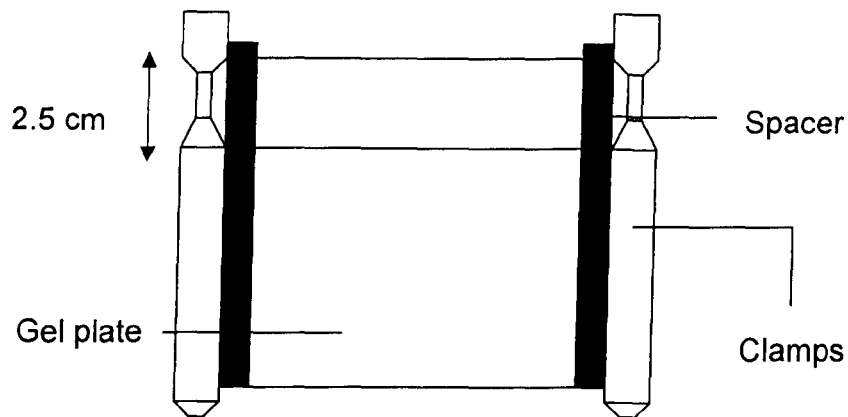


Figure 2.5.1: A cartoon of the gel forming equipment used to set the resolving gel in SDS-PAGE.

500 μ l of isopropanol was applied to the top of the gel to stop oxygen preventing the polymerisation of the gel. Once set, the isopropanol was poured off of the resolving gel and any remaining isopropanol removed with a 3M Whatman filter paper. The stacking gel was prepared and poured on top of the resolving gel with the well forming comb placed into the top (Fig 2.5.2).

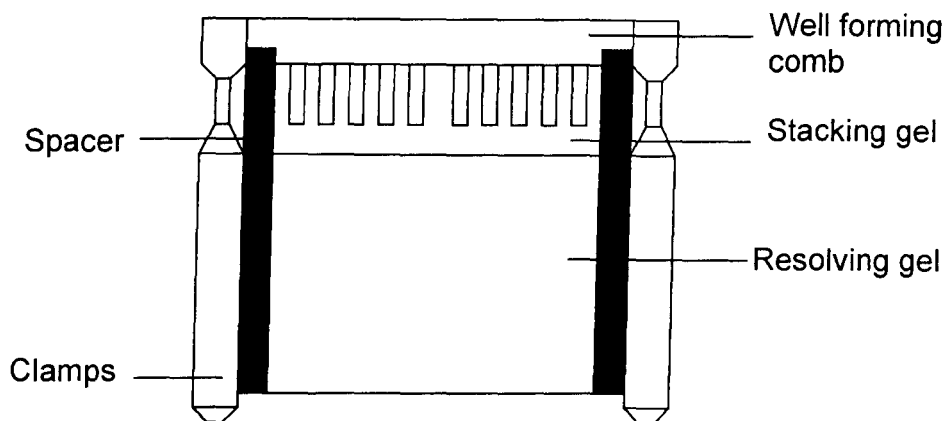


Figure 2.5.2: A cartoon of the stacking gel and well formation used in SDS-PAGE

When the stacking gel was set the gel was placed into the electrode apparatus and then into the gel tank. The tank was filled with gel running buffer and the combs removed. The samples were pipetted into the wells and run at 200 volts for 45-60 mins, until the sample buffer had run through the gel.

2.5.4 *Western Blotting of SDS-PAGE gel*

The gels were removed from the tank, the stacking gel cut and the resolving gel incubated in transfer buffer for 5 mins. Two Whatman filter papers and the nitrocellulose membrane were then cut to size and incubated in transfer buffer for 5-10 mins. After the incubation the nitrocellulose membrane and gel were placed into the transfer cassette as shown (Fig 2.5.3)

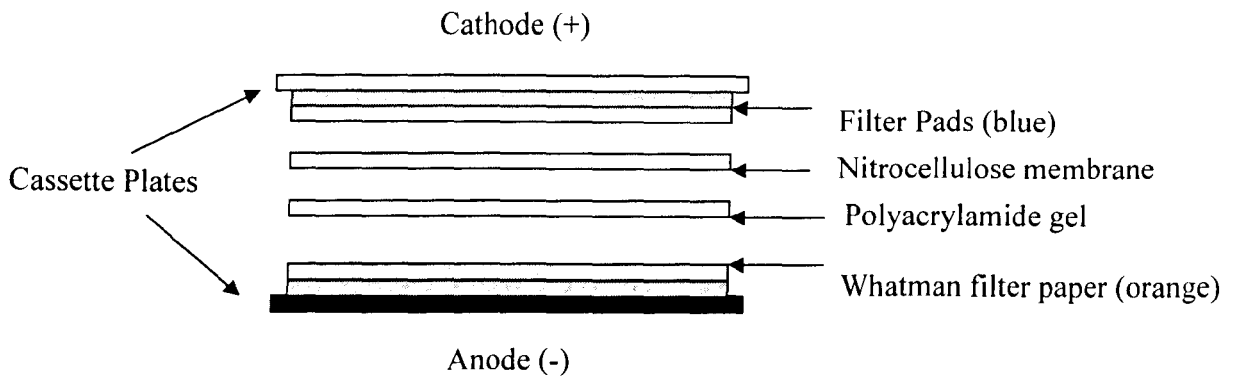


Figure 2.5.3: A schematic of the arrangement of the filter paper, nitrocellulose membrane, and gel for the western blot.

Air bubbles were removed between the gel and the membrane by rolling them out. The cassette was then closed and placed into the transfer apparatus with cooling tubes used to maintain the temperature. The transfer was carried out at 350mA for 1 hour. Following completion of transfer, the nitrocellulose membranes was placed in blocking buffer for 2-3 hr at room temperature on an orbital shaker.

2.5.5 Immunodetection of proteins on nitrocellulose membranes

Blocked nitrocellulose membranes were incubated with primary antibody overnight. Each antibody used was diluted as required in 10mls of PBS-Tween 20. Incubations were followed by four washes with PBS-Tween 20 for 10 mins each wash. Horseradish peroxidase (HRP) conjugated secondary antibody was then incubated with the membrane in 10mls of PBS-Tween 20 at a dilution of 1:5000 for 30 mins. The secondary antibody was specifically targeted at the primary antibody to avoid cross reactivity with other non-related

proteins. After the incubation of secondary antibody the nitrocellulose membrane was again washed four times for 10 mins in PBS-Tween 20 to remove any excess antibody.

2.5.6 Enhanced chemiluminescence detection of antibody bound proteins

Protein bands were visualised using chemiluminescence detection. The two solutions obtained in the ECL kit were mixed in equal parts and incubated on the membrane for one minute. The excess solution was removed by tipping the membrane to its side and onto a paper towel. The membrane was then wrapped in clingfilm ensuring no air bubbles were present trapped. The membrane was exposed to Hyperfilm ECL (Amersham biosciences) for 5 to 20 mins depending on the intensity of the bands. The film was developed for 1-3 mins until bands could be visualised, washed in water to remove any excess developing solution and fixed for 5 mins to prevent any further development of the film.

2.5.7 Analysis of immunoblotting by densitometry

Protein bands identified by specific antibodies and ECL detection were analysed using densitometry. Blots were analysed using the Gene Genius Bioimaging system and the Syngene Genesnap program. All blots were analysed and compared to control values before graphical representation.

2.6 Prostaglandin E₂ enzyme linked immunosorbent assay (ELISA)

2.6.1 Sample preparation

HUVECs were treated with DuP-697 or indomethacin in serum free media (SFM) or complete media 199 and incubated at 37°C for 24 hr. Sample media was then removed from the tissue culture plate and retained for analysis of prostaglandin E₂ (PGE₂) or stored at -70°C until required.

2.6.2 Detection of PGE₂

Wash buffer was prepared by diluting 30ml of 10x buffered surfactant concentrate into 270ml distilled water giving a 1:10 dilution. Standards were serially diluted in cell culture media (CCM) to give a range of standards from 0pg/ml to 2500pg/ml. The standards were then used within 60 mins of dilution.

All samples and standards were analysed in duplicate. One hundred and fifty microlitres of CCM was added to the non-specific binding wells and 100µl of CCM was added to the zero standard wells. Samples and standards (100µl) were added to the remaining wells. To each well, excluding the total activity and substrate blank wells, 50µl of PGE₂ conjugate was added, followed by 50µl of PGE₂ antibody, excluding the total activity, non-specific binding and substrate blank wells. The plate was then covered and incubated for 2 hr at room temperature on an orbital shaker at high speed. Wells were decanted and washed ensuring that all the liquid was fully removed. This was repeated 3 times. 5µl of PGE₂

conjugate was added to the total activity wells. Two hundred micro-litres of pNPP substrate was added to all of the wells and the plate incubated for 1 hour at room temperature on the bench. After the incubation, 50µl of trisodium phosphate stop solution was pipetted into each well and the optical density measured at 405nm immediately.

Duplicates of samples and standards were averaged and the non-specific binding subtracted from the values. A standard curve was then produced and the concentration of PGE₂ in the samples calculated from the curve. These values were then expressed as a percentage of the control concentration of PGE₂ to allow for comparison of different treatments. The wells for total activity, non-specific binding and substrate blank were used for quality control of the assay.

2.7 Apoptosis repressor with CARD domain plasmid isolation and analysis

2.7.1 Culture of competent cells

A single DH5 α *E.coli* colony was used to inoculate 10mls of tryptone-yeast extract media (TYM) and grown at 37°C for 3 hr. After the incubation 1ml of the culture was added to 100ml of fresh TYM and cultured for between 4 to 6 hr until the culture reached an optical density of 550 of 0.5-0.7. Cultures were centrifuged at 4000 \times g for 15 mins at 4°C. The supernatant was removed and the pellet resuspended in 30ml of Tfb 1 buffer (30mM potassium acetate, 50mM manganese chloride, 100mM potassium chloride, 10mM calcium chloride, 15% (w/v) glycerol), and then put on ice for 30 mins. The cells were then

centrifuged at $500 \times g$ for 20 mins at 4°C and the supernatant discarded. The cell pellet was resuspended in 4ml of cold Tfb 2 buffer (10mM MOPS (pH7), 10mM potassium chloride, 75mM calcium chloride, 15% (w/v) glycerol) and aliquoted into 200ul aliquots to be stored at -70°C .

2.7.2 Preparation of plasmid pCDNA3-ARC

The filter paper holding the pcDNA3-ARC plasmid was placed into 100ul of sterile TE buffer for 10 mins at room temperature allowing the plasmid to transfer from the filter paper to the buffer. The plasmid in solution was stored at 4°C and -20°C until required.

2.7.3 Transformation of the competent DH5 α E.coli cells

A 200 μl aliquot of DH5 α cells was defrosted on ice. The plasmid was added and the cells incubated for a further 30 mins on ice before subjecting to heat shock by incubating at 42°C in a water bath for 2 mins. The cells were then placed back on ice and 800 ul of LB broth added before incubating at 37°C for 1hour to allow the bacterial to recover. The transformed bacteria were spread onto an LB agar plate supplemented with ampicillin and incubated overnight at 37°C . The plate was stored at 4°C to be used as a transformed bacteria master plate from which all experimental bacteria would be grown.

2.7.4 Bacterial growth and maintenance

A single colony was selected at random from the transformed bacteria master plate and streak plated onto fresh LB agar plate containing ampicillin and was incubated overnight at

37°C. The fresh streak plate was used as the master plate of transformed bacteria and stored for 3-4 weeks at 4°C until a new master plate was produced.

2.7.5 Isolation of pCDNA3-ARC using Qiagen Miniprep plasmid isolation kit.

Transformed DH5α *E.coli*, with the pCDNA-ARC plasmid, were grown in 10 ml ampicillin containing LB on a rotary shaker at 37°C overnight. 1.5 ml bacterial suspensions were transferred into a microfuge tube and centrifuged at 13,000 rpm for 5 mins. The supernatant was removed and the pellet resuspended in 250µl of buffer P1 (resuspension buffer containing RNase A 0.1% (v/v) (Qiagen)) followed by 250µl of buffer P2 (alkaline lysis buffer containing sodium hydroxide (Qiagen)). The suspension was inverted 5 times until clear. To precipitate the bacterial debris from the solution, 350µl buffer N3 (neutralising guanidine hydrochloride and acetic acid buffer (Qiagen)) was added and mixed by inversion 5 times followed by the tube being centrifuged at 13,000 rpm for 10 mins. The supernatant was retained and passed through the QIA prep spin column by centrifuging at 13,000 rpm for 60 seconds with the flow through discarded. The column was washed in 750µl of buffer PE (Qiagen) and centrifuged 13,000rpm for 60 seconds and the flow through discarded. Centrifuging the column at 13,000rpm for 60 seconds dried the column membrane. Elution of the plasmid in a clean 1.5 microfuge tube was carried out by addition of 50µl of buffer EB (High salt elution buffer (Qiagen)) to the middle of the column membrane and incubating for 1 minute at room temperature followed by centrifuging at 13,000rpm for 1 minute. Plasmid suspensions were stored at 4°C until

required. The eluted DNA was quantified by spectrophotometry at 260nm, using the equation:

$$\text{Absorbance value } 1.000 = 50\text{ng}/\mu\text{l DNA.}$$

2.7.6 Digestion of pCDNA3-ARC with endonucleases

The pCDNA3 plasmid was assessed for endonucleases digestion sites using webcutter program. The reaction mixtures for digestions were set up containing 2 μ l plasmid, 1 μ l 10x buffer mix, 1 μ l of 5U/ μ l restriction enzyme, 7 μ l SDW. The reaction tubes were then placed at 37°C for 1 hour to allow restriction of the DNA to occur. The reaction was placed on ice and 2 μ l of stop mix/loading buffer was added to each reaction. The digestions were visualised using a 1% agarose gel and ethidium bromide staining. The sizing of the restricted plasmid was analysed by the Gene snap program (Syngene).

2.7.7 Polymerase chain reaction (PCR)

PCR amplification of DNA was carried out using a Master Cycler Gradient Thermocycler (Eppendorf) and specific PCR protocols for the target region of DNA. Standard PCR reactions were carried out in a total volume of 50 μ l with the standard PCR mix consisting of; 0.2mM of each dNTP (dATP, dCTP, dTTP, dGTP) (Invitrogen Ltd.), 1mM MgCl₂ (Invitrogen Ltd.), 1x Taq buffer (Invitrogen Ltd.), 1 Unit of Taq polymerase (Invitrogen Ltd.), 0.2 μ M forward primer, 0.2 μ M reverse primer, and DNA template. Nuclease free water (Promega) was used to make the total volume to 50 μ l. Amplified DNA was analysed

using 2 μ l PCR product + 8 μ l agarose gel loading buffer on 0.8% agarose gel electrophoresis at 100V until the dye front was 3cm from the end of the gel.

2.7.8 Transfection of HUVECs using the JetPEI-HUVEC reagent

HUVECs were plated into 24 well plates coated with 1% gelatin using 35,000 cells per well and incubated at 37°C in a tissue culture incubator. Plasmid DNA (2 μ g) was diluted in 50 μ l of 150mM sterile NaCl then briefly vortexed and centrifuged. The JetPEI-HUVEC reagent (4 μ l) was diluted in 50 μ l of sterile NaCl then briefly vortexed and centrifuged. Mixing the two solutions by gently vortexing them together and gathering the liquid to the bottom of the tube by centrifuging followed by an incubation at room temperature for 30 min formed the DNA-JetPEI complex. During this time the 20% FCS medium 199 was removed from the HUVECs and replaced with 500 μ l 2% FCS optiMEM. The DNA-JetPEI complex (100 μ l) was added to the well and homogenized by gently swirling the plate then incubating the plate at 37°C in a tissue culture incubator for 4 hr. The transfection media was removed and replaced with 1ml 20% FCS medium 199 for 24 hr. Transfections were photographed in the well and then prepared for western blot analysis.

2.8 Agarose gel analysis and detection of DNA

2.8.1 Agarose gel electrophoresis

To 1 x TAE buffer 1-2 % (w/v) agarose was added and boiled to dissolve the agarose. The molten agarose was poured in to the gel cassette and the comb placed in the gel to form the sample wells. Once the gel was set 1 x TAE buffer was added to the tank to cover the

wells. Twenty-one micro-litres of the samples were transferred to new microcentrifuge tubes and to each of the samples 4 μ l of sample buffer was added. The samples were then loaded on to the gel and run at 60 – 80 volts until the dye front was 1-2cm from the bottom of the gel.

2.8.2 Ethidium Bromide staining of an agarose gel

Ethidium bromide was added to TAE buffer at a concentration of 1 μ g/ml. The agarose gel was then incubated in a tank containing 1 μ g/ml ethidium bromide for 20-30 mins. Once stained the gel was placed in distilled water for 2 mins and then visualised under UV light to detect the DNA.

2.9 Statistical analysis of data

All statistical analysis was conducted using Microsoft Excel and Graphpad Prism computer programs for all of the data used.

2.9.1 Student's unpaired t-test

Student's t-test was used for the statistical analysis of two independent sets of samples to conclude if the two sets of samples fell into two distinct populations. The two sets of samples that were tested were hypothesised to be under the null hypothesis and then underwent student's t-test to disprove the null hypothesis. Calculating t was done using the calculation below:

$$t = \frac{[\text{Mean}_1 - \text{Mean}_2]}{\sqrt{\frac{[(n_1-1)s_1^2 + (n_2-1)s_2^2]}{[n_1+n_2-2]}}} \times \frac{[\frac{1}{n_1} + \frac{1}{n_2}]}$$

n_1 = number of values in set 1

n_2 = number of values in set 2

s_1 = standard deviation of set 1

s_2 = standard deviation of set 2

Comparing the value produced from the calculation and the degrees of freedom (df) for the calculation ($df = (n_1 + n_2 - 2)$) to a t- table of values (Appendix C) gave a probability value (p value) of the null hypothesis being correct. If the t value was above the value stated for 5% confidence the null hypothesis was discarded and the two groups of samples were considered significantly different.

2.9.2 One way Analysis of Variance (ANOVA)

One way Analysis of Variance (ANOVA) was used to compare more than two sets of sample mean averages. The null hypothesis was again tested for the population of samples and rejected if at least any two of the samples were significantly different from each other. This was concluded by the variance between the mean values of the samples being greater than the variability between the individual sets of data. Analysis of the data was done by calculating the “within-samples sum of squares” (SS_w);

$$SS_w = \sum (x - \bar{x})^2$$

The overall mean of every sample to be compared was calculated and the total sum of squares (SS_t) calculated using each sample value and the overall mean value using the

calculation above. Using the two values gained for the SS_w and SS_t , the value for the “between samples sum of squares” (SS_b) was calculated as below;

$$SS_b = SS_t - SS_w$$

The degrees of freedom of the “within samples” and “between samples” variance were calculated by;

$$df_w = \text{Number of samples in total} - \text{number of samples in the groups}$$

$$df_b = \text{Number of sets of samples} - 1$$

These values were then used to calculate the mean square of the “within samples” (MS_w) and “between samples” (MS_b) data;

$$MS_w = SS_w / df_w$$

$$MS_b = SS_b / df_b$$

A ratio of the two mean square values was then calculated to give F, which was then compared to the F-table (Appendix C):

$$F = \frac{MS_b}{MS_w}$$

If the value gained for F was greater than the value quoted for 5% confidence the null hypothesis was discarded and the data was significantly different.

3.0 Optimisation of apoptosis assays

3.1 *Introduction*

The morphological and biochemical changes associated with apoptosis are very specific. Identification of apoptosis within the cell is done by the assessment of the morphological changes that are associated with apoptosis. At present, apoptosis is identified by membrane blebbing, DNA condensation, DNA laddering, Bcl-2 family protein expression, caspase expression and caspase activation.

3.1.1 *Membrane blebbing*

Membrane blebbing is an early event after the initiation of apoptosis. The outer membrane of the cell undergoes translocation of phosphatidylserine from the inner membrane to the outer membrane of the cell due to inhibition of the aminophospholipid translocase and the activation of scramblase and the increase in fodrin cleavage by caspase 3 (Martin *et al.*, 1995). The translocation of phosphatidylserine leads to the subsequent blebbing and budding off of the membrane to form small apoptotic bodies. Identification of membrane blebbing is assayed by binding of a biotin or fluorescein isothiocyanate (FITC) labelled annexin V molecule, which binds highly specifically to phosphatidylserine in a calcium dependent manner and is analysed by fluorescent microscopy or flow cytometry (Martin *et al.*, 1995; Clarke *et al.*, 2000). Annexin V binding may give false positive results and therefore over estimation of the number of apoptotic cells as annexin V molecules will

enter necrotic cells and stain untranslocated phosphatidylserine (Callahan *et al.*, 2000; Bai *et al.*, 2003). To counter this false staining of the cells it is required that a second stain be used to confirm that the cells have undergone apoptosis. This could be done using propidium iodide (Clarke *et al.*, 2000).

3.1.2 DNA condensation staining

The DNA in cells that undergo apoptosis condenses in the cell due to the cleavage of the high molecular weight chromatin by the endonuclease CAD. This condensed form of chromatin can be visualised by light, fluorescent or electron microscopy or quantified directly by flow cytometry (Wilson and Potten, 1999).

Light and fluorescent microscopy requires that the DNA must be stained for visualisation. In light microscopy, haematoxylin and thionin blue are used to stain fixed and wax embedded tissues. This method has good contrast in the tissue and stains the condensed chromatin heavily, but both stains also stain the mitotic cells in the sample giving false positives (Wilson and Potten, 1999).

Fluorescent microscopy is usually used to identify cells that have undergone apoptosis in cell culture. Four main fluorescent stains are used, (1) 4',6-Diamino-2-phenylindole (DAPI); (2) Hoechst stains 33258 and 33342 and (3) Acridine orange, (4) Terminal deoxynucleotidyl transferase mediated dUTP-biotin nick end labelling (TUNEL). Each

methodology has its own advantages and disadvantages (Table 4) (Wilson and Potten, 1999).

Table 4: Advantages and disadvantages of cell and DNA staining to identify apoptosis (Wilson and Potten, 1999).

Staining method	Advantages	Disadvantages
4' 6 – Diamino-2 phenylindole (DAPI).	Common, most used stain. Accepted as identifying apoptotic cells.	Stains mitotic and necrotic cells, making identification of apoptosis difficult.
Hoechst stains	Good at identifying the differences of two types of tissue (e.g. human and mouse).	Stains non-apoptotic cells.
Acridine orange	Excluded from viable cells making it ideal for studies on apoptosis.	Stains necrotic cells making exclusive identification of apoptotic cells difficult.
TUNEL staining	Terminal deoxynucleotide transferase (TDT) enzymatically labels all the “nicked” DNA ends. Detection is by specific antibody, therefore very sensitive.	Gives approx. 18% false negative results. Altering TDT concentration can produce false positive results.

The quantification of the cells after preparation for microscopy is normally conducted by a tally count of 500-1000 cells per slide from 10 random fields of vision or by flow cytometry (Wilson and Potten, 1999). Consistent criterion for the scoring of apoptosis is essential with most researchers only scoring the definite apoptotic events. These data are then analysed to calculate the percentage of total cells undergoing apoptosis (Wilson and Potten, 1999).

3.1.3 *DNA cleavage and strand breaks*

DNA cleavage by CAD to form the ~200 bp fragments is the most recognisable morphological change seen in apoptosis. To analyse this, agarose gel electrophoresis is normally used after isolation of the DNA from the cell to see a ~200bp “DNA ladder” (Wilson and Potten, 1999).

It has been noted however that different cells activate these biochemical changes at different time points during the induction of apoptosis. Therefore it was essential to optimise the assays that were to be used to assess apoptosis to gain a positive identification of apoptosis before moving onto further studies. Jurkat E6.1 cells were used initially to optimise the apoptosis assays that were going to be used due to the fast growing phenotype and their ability to readily undergo apoptosis (Gajate *et al.*, 2003, Handrick *et al.*, 2005, Subhashini *et al.*, 2005). To induce apoptosis in the Jurkat E6.1 cells different treatments were used. Treatments that were used targeted specific cellular processes known to induce

apoptosis e.g. COX-2 inhibition as described in section 1.4.4, creation of reactive oxygen species (Kwon *et al.*, 2002), and cellular micro-tubule formation (Copland *et al.*, 2005). Treated cells were cytopun and fluorescent microscopy, DNA ladder isolation, and caspase activation studies to assess apoptosis induction. Once this was achieved and apoptosis identified in the Jurkat E6.1 cells the inducer of apoptosis was tested in HUVECs.

3.2 *Aims*

- To optimise methodology of apoptosis analysis in Jurkat E6.1 cells and HUVECs.
- To identify an inducer of apoptosis that yields the specific biochemical apoptotic changes in HUVECs to use as a positive indication of apoptosis.

3.3 *Methods*

- Cell culture was carried out as detailed in Section 2.1.
- Condensation of chromatin was assessed following cytopinning of cells as described Section 2.3.
- Jurkat E6.1 cell DNA laddering was assayed using the DNA ladder Suicide track kit (Section 2.3.2) and caspase activation was measured as described in Section 2.3.4.
- DNA was isolated from HUVECs using the phenol/chloroform extraction (Section 2.3.3) and analysed by agarose gel electrophoresis (Section 2.8).
- Trypan blue exclusion assay was used to assess cell viability of treated HUVECs.

3.4 *Results*

3.4.1 *The induction of apoptosis by multiple stimuli*

Jurkat E6.1 cells were grown in fully supplemented media RPMI 1640 and treated with serum free medium with or without other stimuli. Serum free RPMI 1640 medium (SFRM) alone (Fig 3.1a), with hydrogen peroxide (20 μ M) (Wagner *et al.*, 2000) (Fig 3.1b), or staurosporine (0.1 μ M) (Cutolo *et al.*, 2005) (Fig 3.1c) did not produce a significant increase in condensed chromatin after 24 hr or 48 hr. DNA laddering assays with these treatments gave no induction of DNA laddering with SFRM or staurosporine; however hydrogen peroxide did produce some DNA laddering (Fig 3.2). In parallel experiments treatments with curcumin (50 μ M) (Smith, 2004) (Fig 3.1d), paracetamol (300 μ M) (Churchman *et al.*, 2001) (Fig 3.1e) and paclitaxel (500 μ M) (Copland *et al.*, 2005) (Fig 3.1f) were found to significantly induce chromatin condensation over 24 hr, which was slightly potentiated at 48 hr, and induced varying amounts of DNA laddering in the Jurkat E6.1 cells (Fig 3.2). However the DNA laddering observed with the curcumin and paracetamol were comparable to the DMSO controls. Caspase activation was confirmed by colorimetric assay with only paclitaxel showing any increase above the DMSO control levels after 24 hr, which was reduced to control levels at 48 hr (Fig 3.3a and 3.3b).

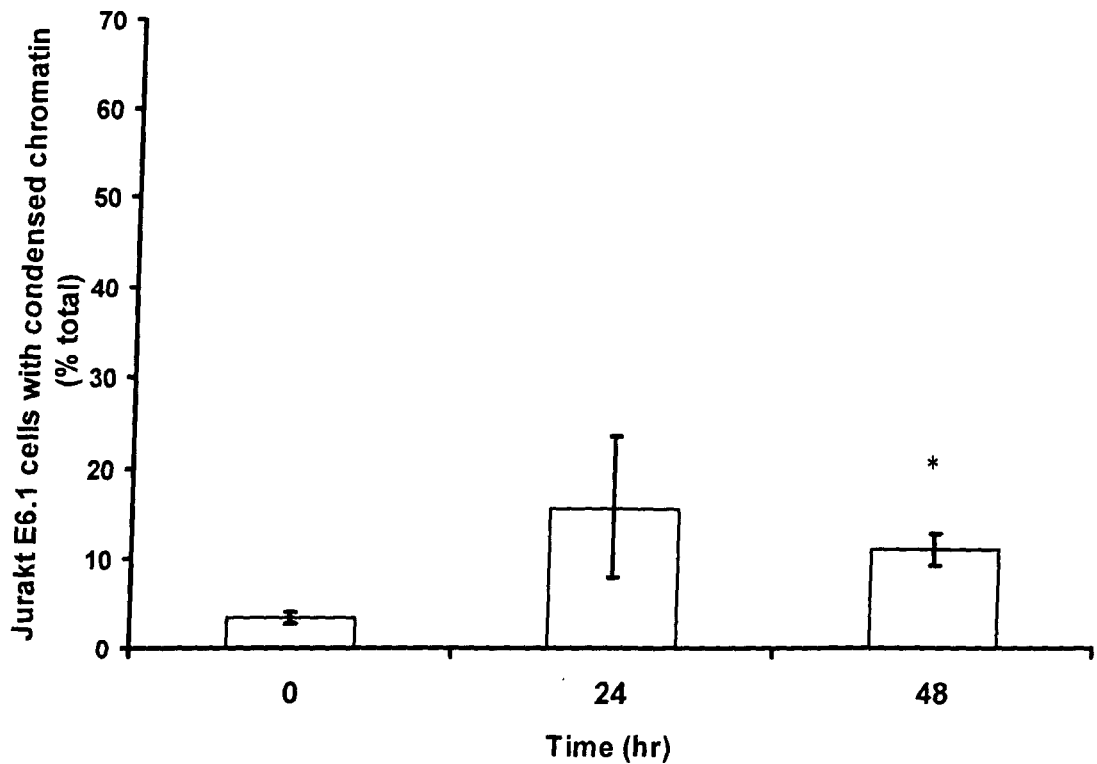


Figure 3.1a: Induction of chromatin condensation in Jurkat E6.1 cells with serum free RPMI 1640 medium. Jurkat E6.1 cells were treated with serum free medium RPMI 1640 (SFRM) over a 48 hr period prior to cytopinning and staining of the DNA with acridine orange. The data are the mean +/- s.e.m. of at least 3 experiments with 2 replicates in each. ANOVA was used to determine significance for all the data with Student's *t*-test identifying the individual points of significance. Significance is compared to SFRM 0 hr * $p < 0.05$.

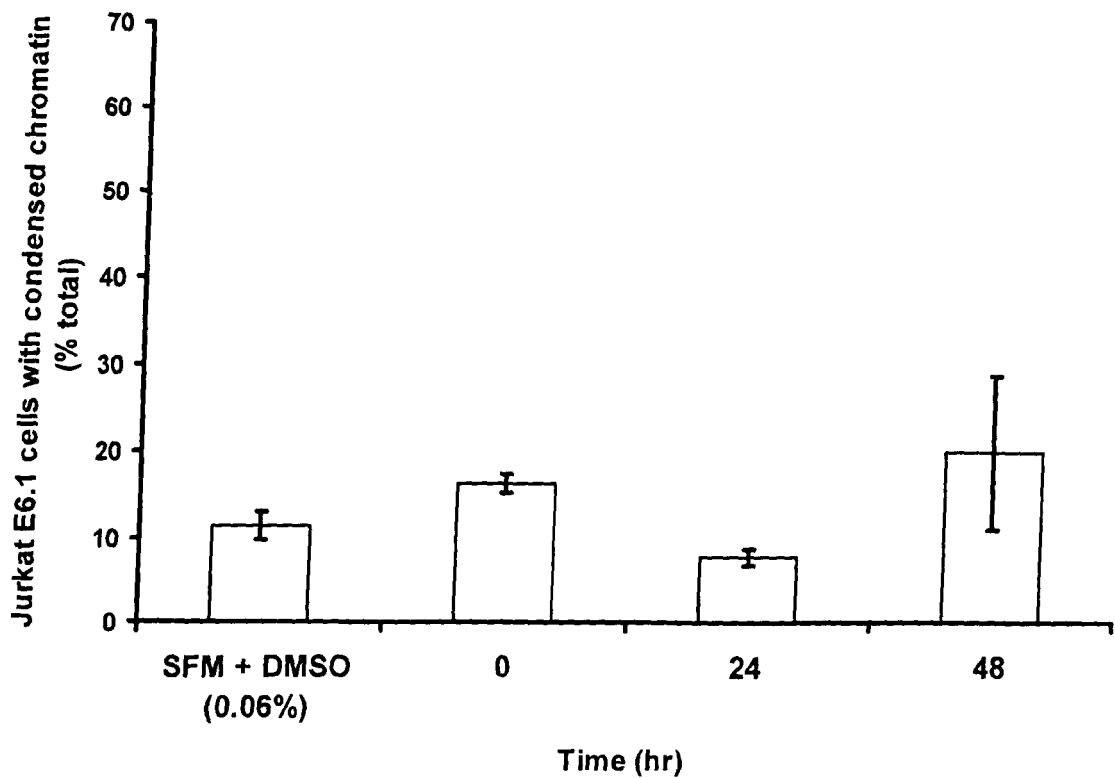


Figure 3.1b: Induction of chromatin condensation in Jurkat E6.1 cells with hydrogen peroxide (20 μ M). Treated cells were also incubated at 37°C for up to 48 hr prior to cytospinning and staining of the DNA with acridine orange. Controls were treated with serum free RPMI 1640 medium (SFRM) with DMSO (0.06%) for 48 hr at 37°C. The data are the mean \pm s.e.m. of at least 3 experiments with 2 replicates in each. ANOVA was used to determine significance for all the data with Student's t-test identifying the individual points of significance. Significance is compared to SFRM + DMSO (0.06%) * $p = < 0.05$.

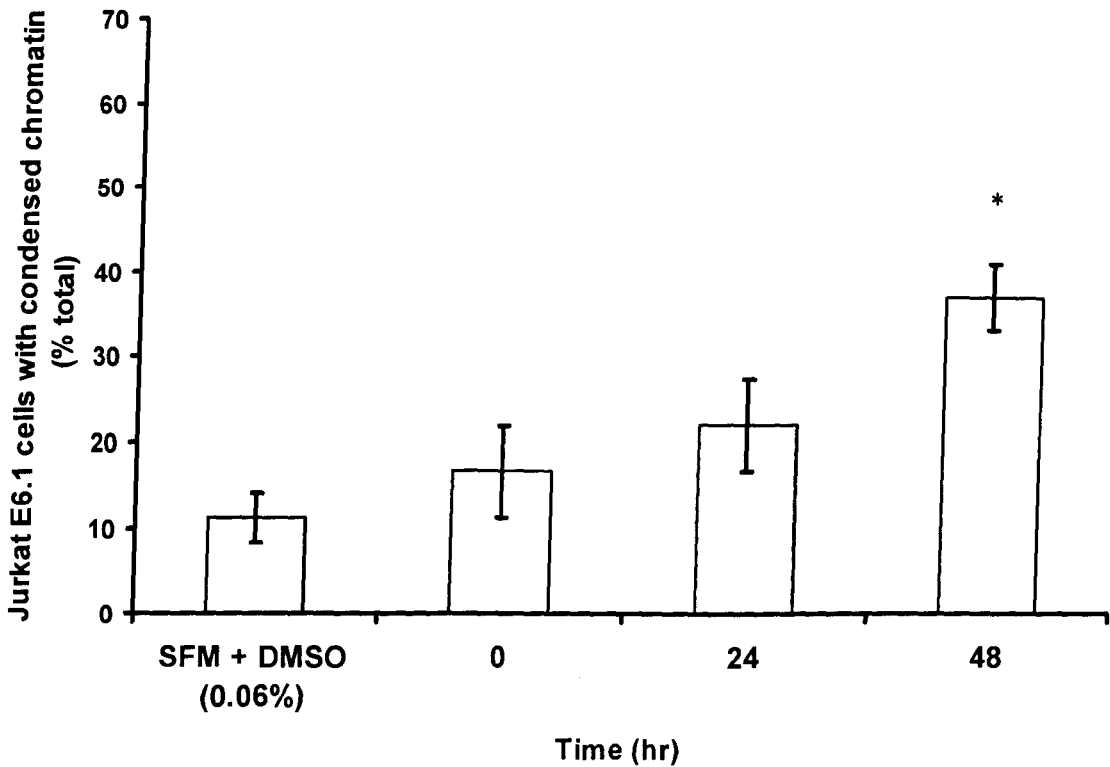


Figure 3.1c: Induction of chromatin condensation in Jurkat E6.1 cells with curcumin (50 μ M). Treated cells were also incubated at 37°C for up to 48 hr prior to cytospinning and staining of the DNA with acridine orange. Controls were treated with serum free RPMI 1640 medium (SFRM) with DMSO (0.06%) for 48 hr at 37°C. The data are the mean \pm s.e.m. of at least 3 experiments with 2 replicates in each. ANOVA was used to determine significance for all the data with Student's t-test identifying the individual points of significance. Significance is compared to SFRM + DMSO (0.06%) * $p < 0.05$.

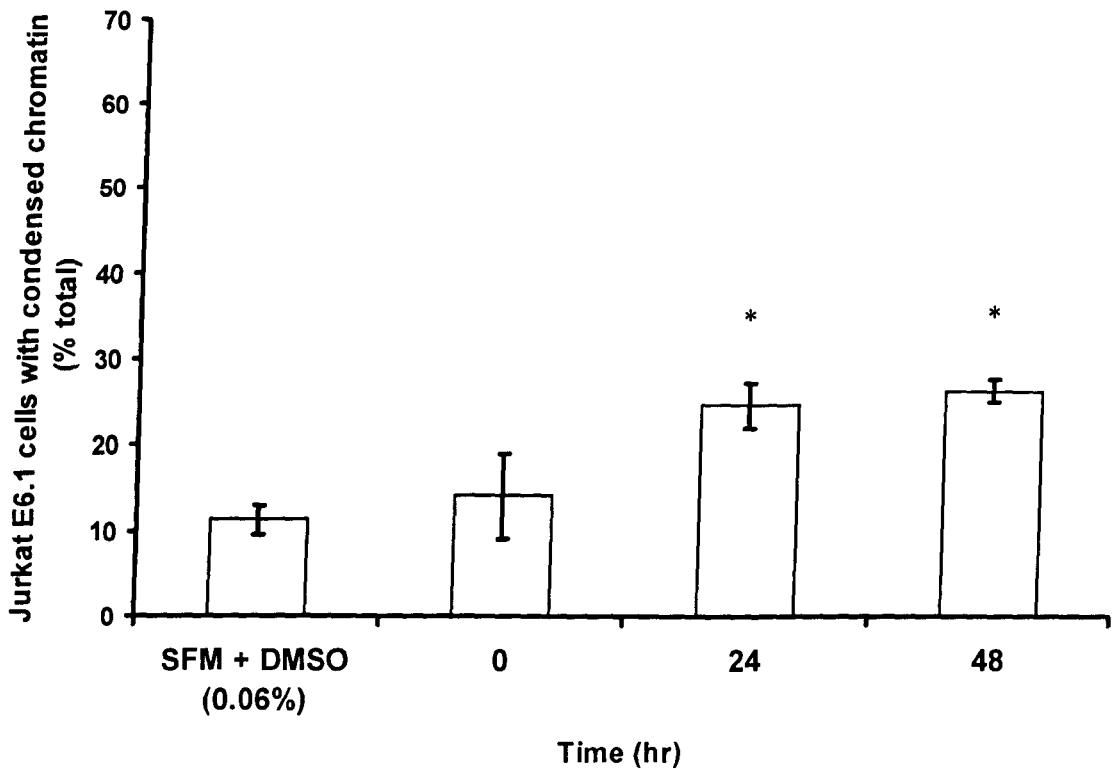


Figure 3.1d: Induction of chromatin condensation in Jurkat E6.1 cells with paracetamol (300 μ M). Treated cells were also incubated at 37°C for up to 48 hr prior to cytospinning and staining of the DNA with acridine orange. Controls were treated with serum free RMPI 1640medium (SFRM) with DMSO (0.06%) for 48 hr at 37°C. The data are the mean \pm s.e.m. of at least 3 experiments with 2 replicates in each. ANOVA was used to determine significance for all the data with Student's t-test identifying the individual points of significance. Significance is compared to SFRM + DMSO (0.06%) * $p < 0.05$.

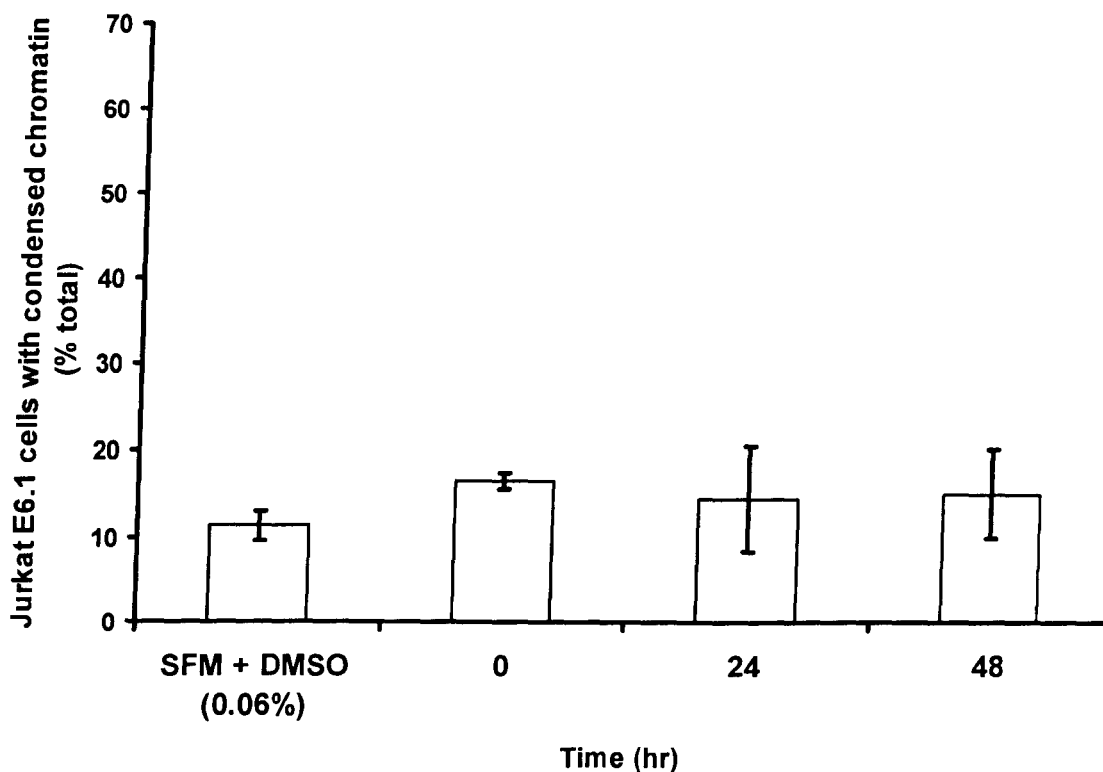


Figure 3.1e: Induction of chromatin condensation in Jurkat E6.1 cells with staurosporine (0.1 μ M). Treated cells were also incubated at 37°C for up to 48 hr prior to cytospinning and staining of the DNA with acridine orange. Controls were treated with serum free RPMI 1640 medium (SFRM) with DMSO (0.06%) for 48 hr at 37°C. The data are the mean \pm s.e.m. of at least 3 experiments with 2 replicates in each. ANOVA was used to determine significance for all the data with Student's t-test identifying the individual points of significance. Significance is compared to SFRM + DMSO (0.06%) * $p < 0.05$.

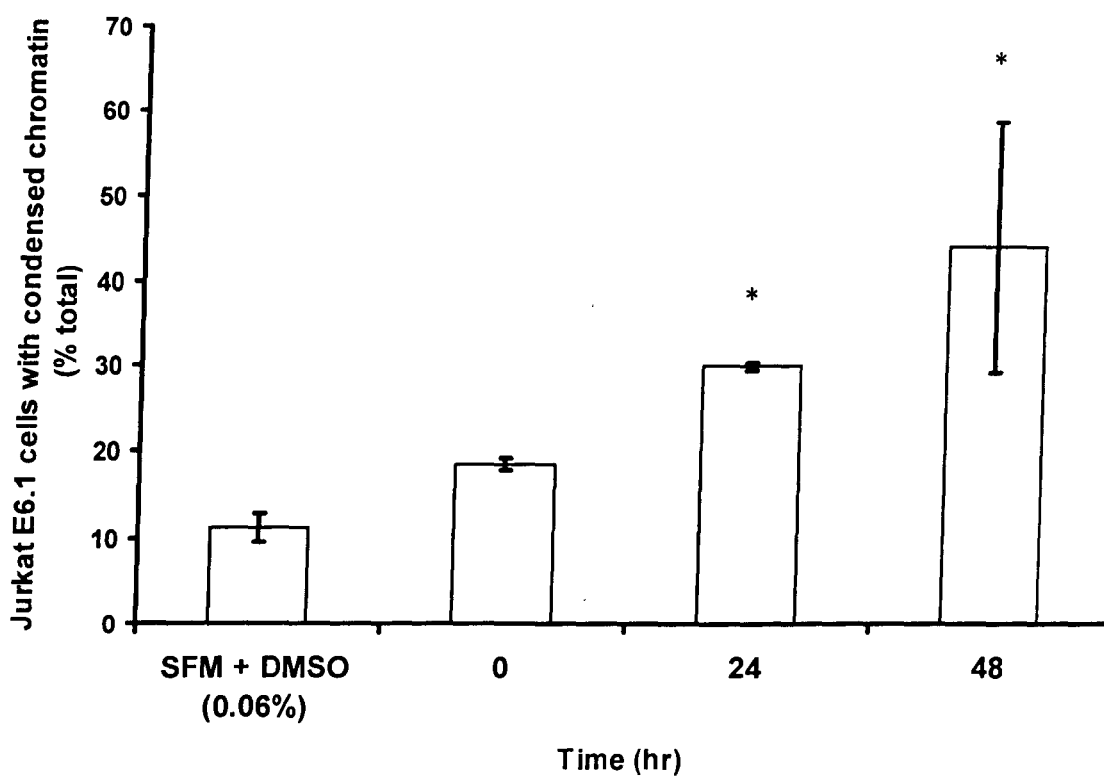


Figure 3.1f: Induction of chromatin condensation in Jurkat E6.1 cells with paclitaxel (500 μ M). Treated cells were incubated at 37°C for up to 48 hr prior to cytospinning and staining of the DNA with acridine orange. Controls were treated with serum free RPMI 1640 medium (SFRM) with DMSO (0.06%) for 48 hr at 37°C. The data are the mean \pm s.e.m. of at least 3 experiments with 2 replicates in each. ANOVA was used to determine significance for all the data with Student's t-test identifying the individual points of significance. Significance is compared to SFM + DMSO (0.06%) * $p < 0.05$.

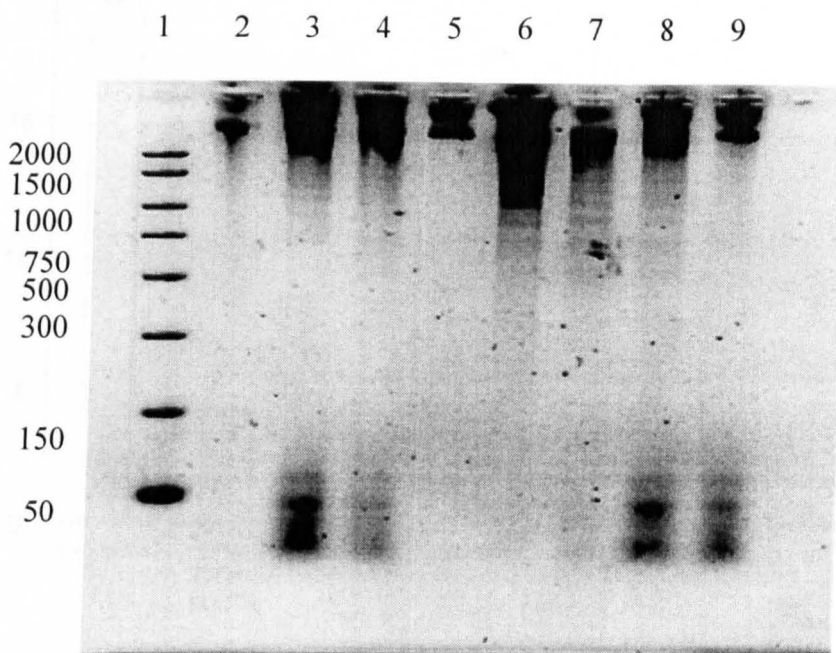


Figure 3.2: Induction of apoptotic DNA fragmentation in Jurkat E6.1 cells. Treatment with an apoptosis inducer were also incubated for 24hr at 37°C prior to DNA extraction using the DNA ladder Suicide track kit and visualised by 2% agarose gel electrophoresis and staining with ethidium bromide. Control cells were incubated at 37°C for 24hr with DMSO (0.06%). Lane (1) DNA ladder (100 bp) (2) Non serum media (3) Curcumin (1µM) (4) Hydrogen peroxide (20µM) (5) Staurosporine (0.1µM) (6) Paclitaxel (500µM) (7) Paracetamol (300mM) (8) DMSO (0.25%) (9) Untreated. The image is representative of 3 separate experiments.

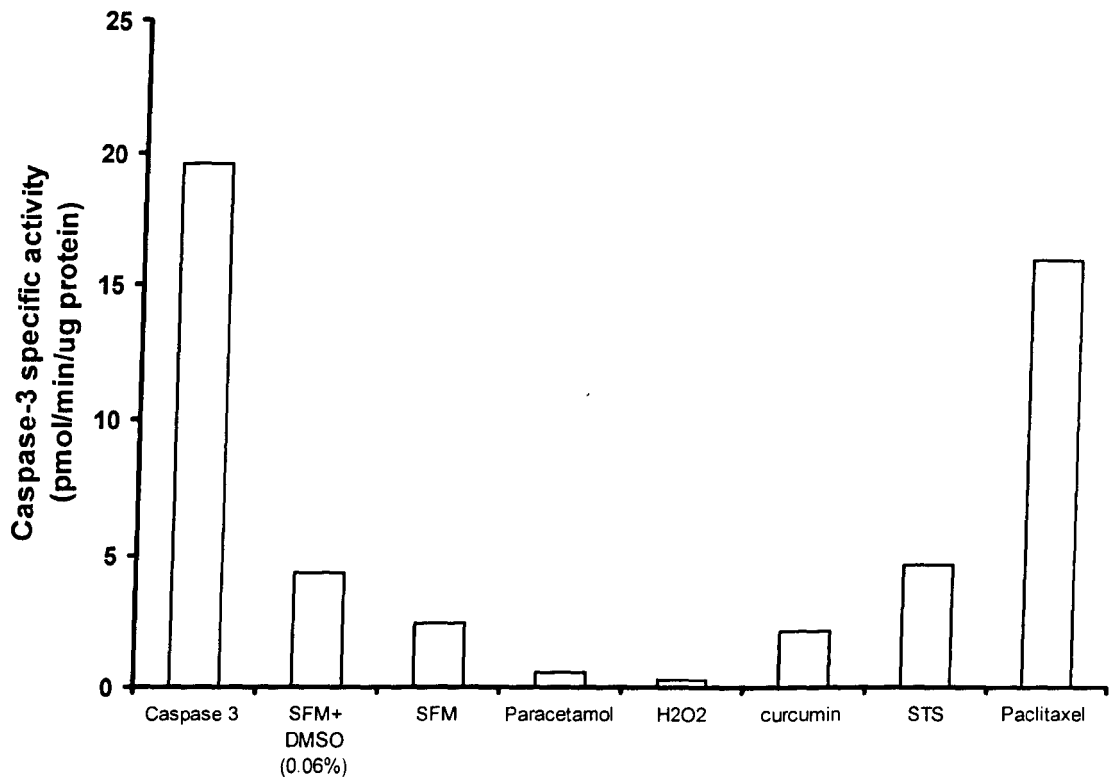


Figure 3.3a: Induction of caspase 3 activity by multiple stimuli in Jurkat E6.1 cells. Treated Jurkat E6.1 cells were incubated for 24 hr at 37°C prior to analysis of caspase 3 activity. Controls were incubated in serum free RPMI 1640 medium (SFRM) with DMSO (0.06%) for 24 hr at 37°C. The data is the mean 2 experiments with 2 replicates in each.

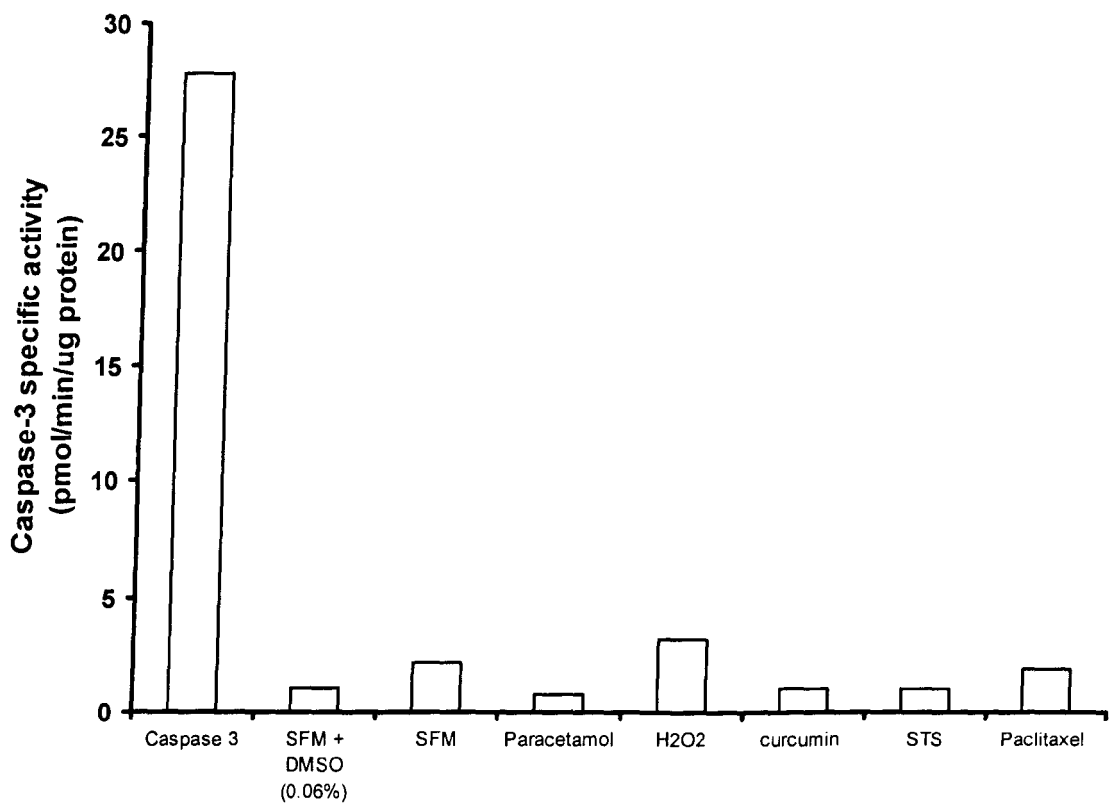


Figure 3.3b: Induction of caspase 3 activity by multiple stimuli in Jurkat E6.1 cells. Treated Jurkat E6.1 cells were incubated for 48 hr at 37°C prior to analysis of caspase 3 activity. Controls were incubated in serum free RPMI 1640 medium (SFRM) with DMSO (0.06%) for 48 hr at 37°C. The data is the mean 2 experiments with 2 replicates in each.

3.4.2 Effect of paclitaxel in Jurkat E6.1 cells

Treatment of Jurkat E6.1 cells for 24 hr with paclitaxel induced a significant dose dependent response on chromatin condensation between the concentrations of 1-1000nM (Fig 3.4a). Dose dependent DNA laddering was also observed in paclitaxel (50nM and 500nM) treated Jurkat E6.1 cells (Fig 3.4b).

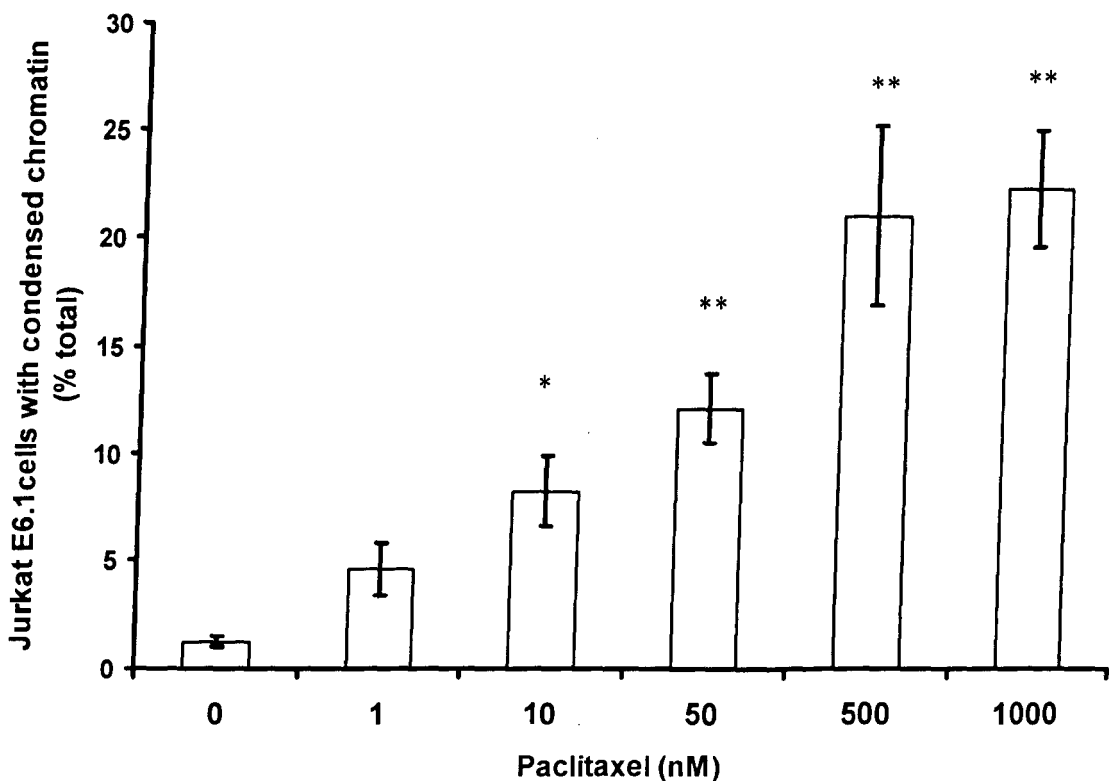


Figure 3.4a: Induction of chromatin condensation in Jurkat E6.1 cells with paclitaxel. Treated cells were also incubated at 37°C for up to 48 hr prior to cytospinning and staining of the DNA with acridine orange. Controls were treated with serum free RPMI 1640 medium (SFRM) with DMSO (0.06%) for 48 hr at 37°C. The data are the mean +/- s.e.m. of at least 3 experiments with 2 replicates in each. ANOVA was used to determine significance for all the data with Student's t-test identifying the individual points of significance. Significance is compared to SFRM + DMSO (0.06%) * $p < 0.05$, ** $p < 0.01$.

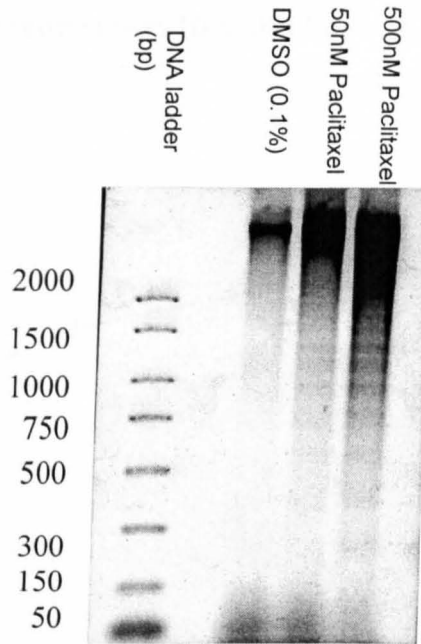


Figure 3.4b: Induction of apoptotic DNA fragmentation in Jurkat E6.1 cells. Jurkat E6.1 cells treated with paclitaxel (50/500nM) were also incubated for 24hr at 37°C. Control cells were incubated at 37°C for 24hr with DMSO (0.1%). DNA extraction was completed using the DNA ladder Suicide track kit and visualised by 2% agarose gel electrophoresis and staining with ethidium bromide. Lane (1) DNA ladder (1kB) (2) serum free media + DMSO (0.1%) (3) Paclitaxel (50nM) (4) Paclitaxel (500nM). The image is representative of 3 separate experiments

3.4.3 Effects of paclitaxel on HUVECs

Parallel experiments were carried out in HUVECs to assess the apoptotic effects of paclitaxel in these cells. A small but significant dose response was observed on chromatin condensation (Fig 3.5a). Interestingly, no DNA laddering occurred in any of the samples obtained from cells incubated with 10-5000 nM for 24 hr (Fig 3.5b).

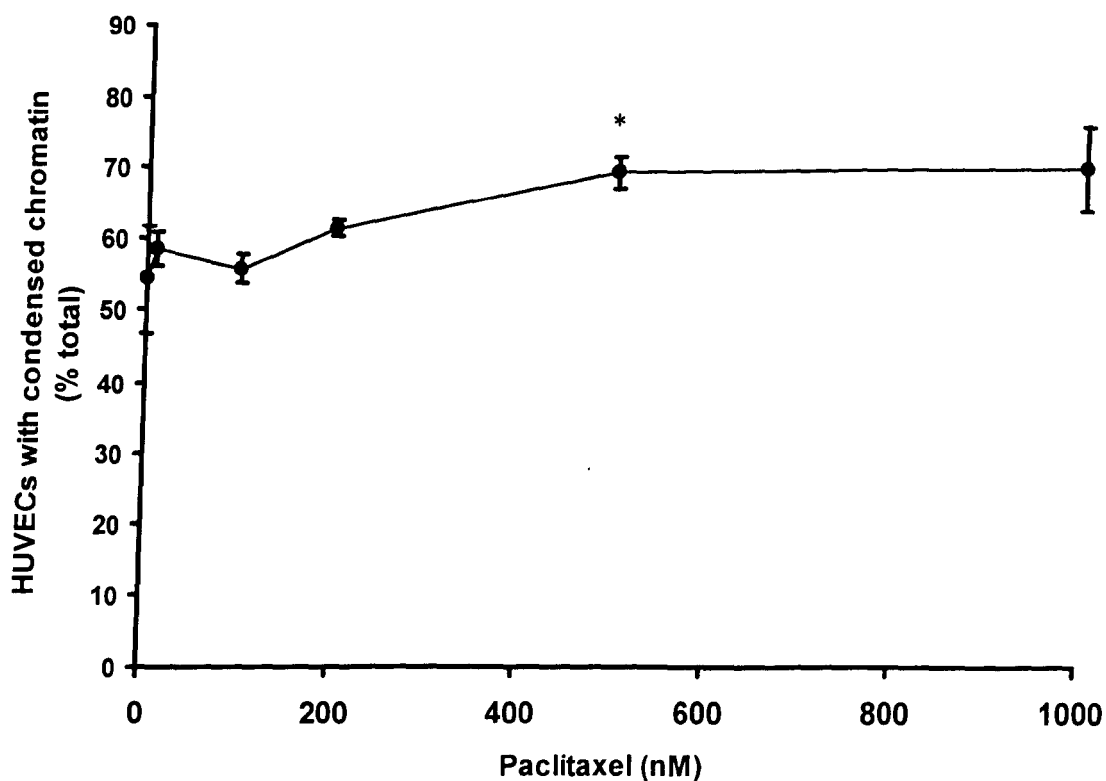


Figure 3.5a: Induction of chromatin condensation in HUVECs. Cells treated with paclitaxel were incubated for 24hr at 37°C prior to cytospinning and staining of the DNA with acridine orange. Control cells were incubated at 37°C for 24hr in serum free medium (SFM) + DMSO (0.01%). The data are the mean +/- s.e.m. of at least 3 experiments with 2 replicates in each. ANOVA was used to determine significance for all the data with Student's t-test identifying the individual points of significance. Significance is compared to SFM + DMSO (0.01%) * $p < 0.05$.

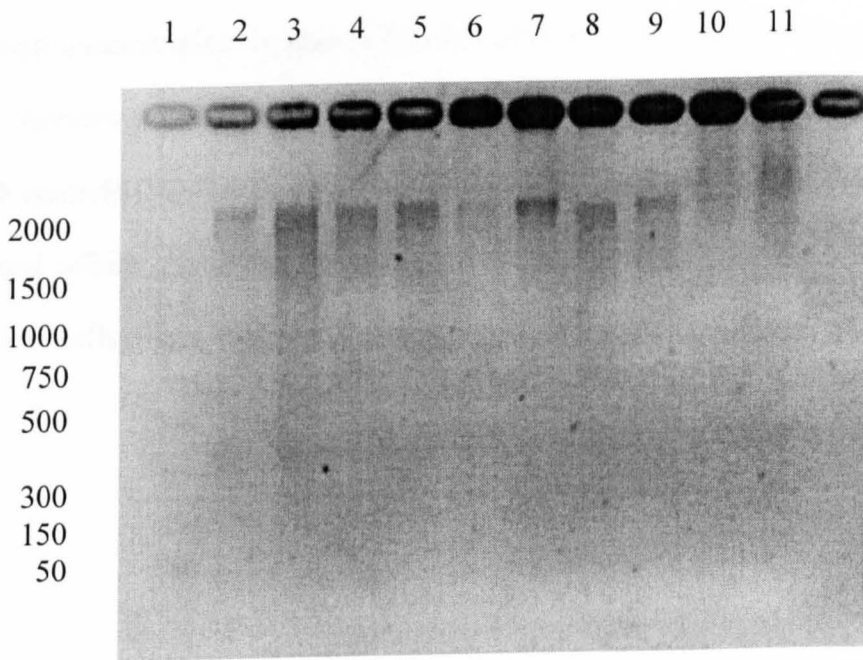


Figure 3.5b: Induction of apoptotic DNA fragmentation in HUVECs. Paclitaxel (10-5000nM) treated HUVECs were incubated for 24hr at 37°C. Control cells were incubated at 37°C for 24hr in serum free medium (SFM) 199 + DMSO (0.01%). DNA was extracted using the DNA ladder Suicide track kit and visualised by 2% agarose gel electrophoresis and staining with ethidium bromide. Lane (1) DNA ladder (1 Kb) (2) (3) 0.5% FCS media (4) 10nM (5) 100nM (6) 200nM (7) 500nM (8) 1000nM (9) 5000nM (10) Adherent cell sample of serum free media + DMSO (0.01%) treated cells. (11) Adherent cell sample of 5000nM treated cells. The image is representative of 3 separate experiments.

3.4.4 *Effects of actinomycin-D on HUVECs*

Because of the lack of significant effects with paclitaxel, HUVECs were treated with actinomycin-D as a positive control for the induction of apoptosis in these cells (Grafe *et al.*, 2001). In these studies, treatment of HUVECs with actinomycin-D for 24 hr induced a significant concentration-dependent (10-200 nM) increase in chromatin condensation (Fig 3.6a). Actinomycin-D (200 nM) also caused marked DNA laddering compared to the DMSO controls (Fig 3.6b). Trypan blue exclusion assays indicated that actinomycin-D decreased cellular membrane integrity in a dose dependent response (10-200 nM) when exposed to cells over a 24hr period (Fig 3.6c).

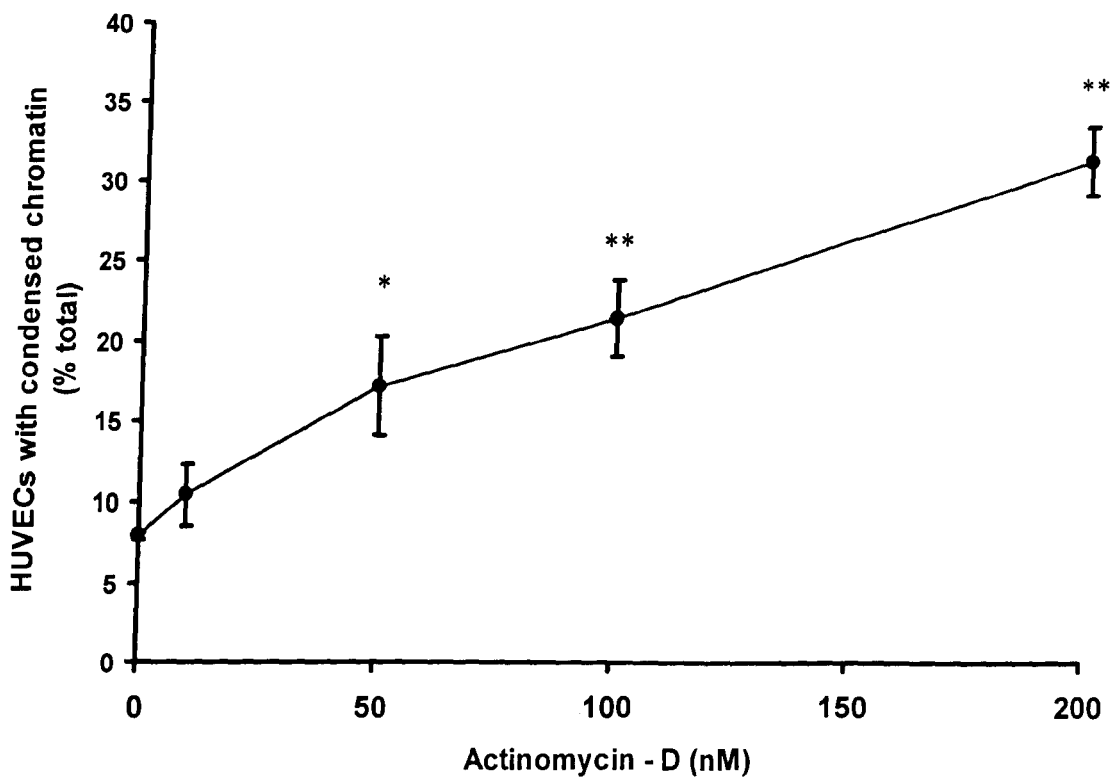


Figure 3.6a: Induction of chromatin condensation in HUVECs with actinomycin-D (10-200nM). Treated cells were incubated for 24hr at 37°C. Control cells were incubated at 37°C for 24hr in serum free medium (SFM) 199+ DMSO (0.0002%). HUVECs were cytospun and the DNA stained with acridine orange. The data are the mean +/- s.e.m. of 3 experiments with 2 replicates in each. ANOVA was used to determine significance for all the data with Student's t-test identifying the individual points of significance. Significance is compared to SFM + DMSO (0.01%) * $p < 0.05$, ** = $p < 0.01$.

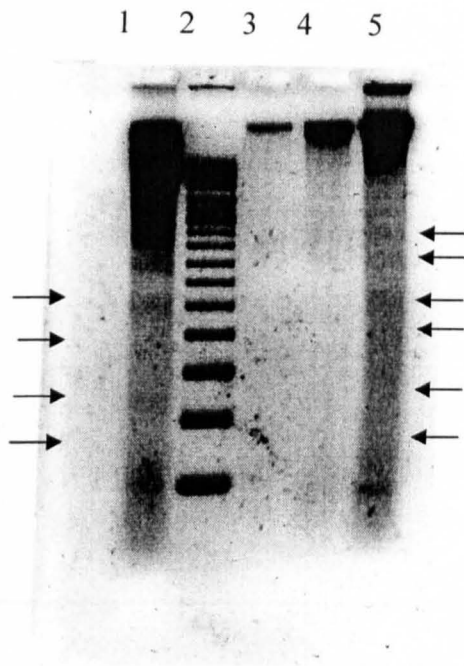


Figure 3.6b: Induction of apoptotic DNA fragmentation in HUVECs. Control cells were incubated at 37°C for 24hr with DMSO (0.0002%). HUVECs treated with actinomycin-D (200nM) were also incubated for 24hr at 37°C prior to DNA extraction using the phenol/chloroform method and visualised by 2% agarose gel electrophoresis and staining with ethidium bromide. Lane (1) Apoptotic positive HL-60 cells (2) DNA ladder (100bp) (3) Serum free media + DMSO (0.0002%) (4) Serum free media (5) Actinomycin-D (200nM). Arrows indicate darker DNA fragmentation in the sample. The image is representative of 3 separate experiments.

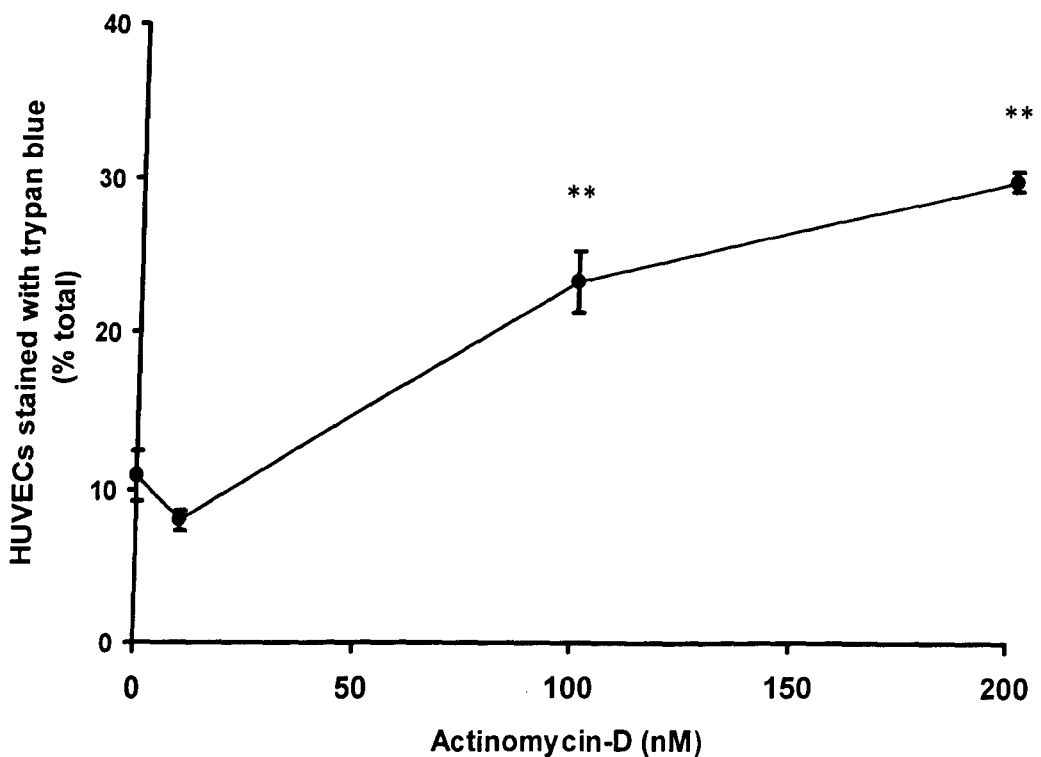


Figure 3.6c: Trypan blue staining of HUVECs treated with actinomycin-D (10-200nM). Treated cells were incubated for 24hr at 37°C. Control cells were incubated at 37°C for 24hr with serum free medium (SFM) 199 + DMSO (0.0002%). HUVECs were stained with trypan blue and counting by haemocytometer. The data are the mean +/- s.e.m. of 3 experiments with 2 replicates in each. ANOVA was used to determine significance for all the data with Student's t-test identifying the individual points of significance. Significance is compared to SFM + DMSO (0.01%) * $p < 0.05$, ** = $p < 0.01$.

3.5 *Discussion*

This chapter of experiments was involved in the optimisation techniques to be used for measuring apoptosis and identifying a suitable inducer of apoptosis in HUVECs. The present work indicates that actinomycin-D was a suitable inducer of apoptosis in HUVECs due to the induction of the characteristic morphological changes associated with this process e.g. DNA fragmentation and chromatin condensation.

Apoptosis was identified using chromatin condensation as the technique allows quantitative analysis of apoptotic and normal cells, which was confirmed by DNA fragmentation analysis. Initial studies of the different compounds investigated on Jurkat E6.1 cells gave varying amounts of chromatin condensation. Curcumin, paracetamol and paclitaxel were all shown to significantly increase chromatin condensation over 24 and 48 hr. Curcumin did not induce DNA fragmentation in to ~200 bp multimers in 24 hr or induce caspase 3 activity over 24 hr or 48 hr. Similar to the present study, Piwocka *et al.* (1999, 2001, and 2002) indicated that curcumin treatment of Jurkat E6.1 cells did not activate caspase 3 or induce lower molecular weight fragmentation of the DNA. Consequently combined with our studies this suggests that curcumin induces cell death through a caspase independent pathway and may be due to high glutathione levels in cells preventing caspase activation (Piwocka *et al.*, 2001).

In parallel studies, paracetamol induced chromatin condensation after 24 hr. However no further increase was seen at 48 hr. Paracetamol treatment of Jurkat E6.1 cells did not cause the activation of caspase 3 but did induce some slight DNA fragmentation to produce a characteristic DNA ladder associated with apoptosis. Similar to these

findings, Elder and Paraskeva (1999) indicated that traditional NSAIDs induced apoptosis in colorectal carcinoma cells *in vitro* with full DNA fragmentation. However, very high concentrations of the NSAIDs were used to induce apoptosis e.g. 1mM (Elder and Paraskeva, 1999) and therefore the dose of paracetamol used in the present experiments may not have been high enough to induce the full apoptotic morphological changes in Jurkat E6.1 cells.

Several studies have indicated paclitaxel may induce apoptosis through an increase in microtubule formation (Copland *et al.*, 2005; Markman *et al.*, 2005). In the present study, paclitaxel (0-500nM) did induce a dose dependent caspase-3-related chromatin condensation and DNA fragmentation at 24 hr in Jurkat E6.1 cells before caspase 3 activity declined back to control levels at 48 hr. Interestingly 24 hr treatment of HUVECs with paclitaxel (0-5000nM) did only cause a small significant increase in chromatin condensation but there was no DNA fragmentation. This finding is supportive of studies with paclitaxel in ARO and KAT-4 thyroid cancer cell lines in which paclitaxel did not induce caspase activation, DNA fragmentation or release cyt-c from the mitochondria (Pan *et al.*, 2001). Together with the current study this suggests clinically paclitaxel may not have an effect on the vasculature in the treatment of cancer prevention, but this is to be confirmed.

Further studies into actinomycin-D treatment of HUVECs resulted in a significant dose-dependent increase of apoptosis within 24 hr. Actinomycin-D treated HUVECs exhibited the characteristic morphological changes associated with apoptosis including chromatin condensation and DNA fragmentation in to the ~200 bp multimer DNA

“ladder”, which was consistent with previous studies that indicated an increase in TUNEL positive cells and DNA fragmentation in actinomycin-D treated HUVECs after 24 hr (Grafe *et al.*, 1999). The apoptotic mechanism proposed by Grafe *et al.* (1999) suggested a stimulation of free radical production which in turn activated the caspase cascade, but may be independent of protein synthesis as cycloheximide has been shown not to have an effect on the induced apoptosis (Grafe *et al.*, 1999).

Taken into consideration with our study it would suggest that treatment of endothelial cells with actinomycin-D does induce a caspase-dependent apoptosis. However, analysis of the DNA fragmentation by actinomycin-D (100-200nM) revealed smearing of some DNA in the phenol: chloroform extraction and agarose gel electrophoresis. These data implied that actinomycin-D may induce necrosis of the cells, which was confirmed by the membrane permeability study. Actinomycin-D (100nM-200nM) was shown to induce membrane permeability in ~20 % and ~30% of the cells respectively and therefore indicate a significant increase in necrosis at these concentrations.

It has been suggested that necrosis observed in an *in vitro* population of apoptotic cells may be due to cell culture being deficient in phagocytotic cells and therefore not clearing away apoptotic cells (Fadok *et al.*, 2001; Proskuryakov *et al.*, 2003). In this instance the apoptotic cells burst and undergo necrosis (Proskuryakov *et al.*, 2003). It may be in the present study that high doses of actinomycin-D may decrease the time taken to induce apoptosis in HUVECs and cause the cells to undergo post-apoptotic necrosis within the 24 hr studied and therefore appear necrotic, but this would require further time-dependent studies of caspase activation, chromatin condensation and DNA

fragmentation over 24 hr to confirm this hypothesis. However, actinomycin-D was selected as the positive control for the activation of apoptosis in HUVECs due to the reliable induction of the morphological changes associated with this process.

4.0 Effects of curcumin and 6-shogaol on VEGF₁₆₅ induced cyclooxygenase-2 expression and apoptosis in HUVECs

4.1 Introduction

Dietary compounds e.g. curcumin and 6-shogaol, have been found to exhibit anti-inflammatory properties and have been used in alternative therapies for certain inflammatory diseases such as rheumatoid arthritis. The anti-inflammatory properties of curcumin are thought to be due to the inhibition of the NF- κ B activation pathway of inflammatory enzymes including COX-2 and inducible nitric oxide synthase (iNOS) as described in section 1.2.12.1 (Fig. 1.2.17). However it has also been identified that the MAP kinase (p42/p44) pathway may also be inhibited by curcumin (Section 1.2.12.1). Recently compounds of similar structures have been identified and purified from ginger e.g. shogaols and gingerols, with 6-shogaol being most effective at inhibiting COX-2 specific prostaglandin production in lung epithelial cells (Section 1.2.12.2). It is not known if 6-shogaol acts in a similar way to curcumin by preventing signal transduction and transcription of the *COX-2* gene.

Apoptosis induction by curcumin has been shown in human melanoma cells (Bush *et al.*, 2001) potentially through the inhibition of COX-2 expression. COX-2 expression is an important factor in angiogenesis and HUVEC survival but it is not clear if curcumin has any effect on the inhibition of VEGF₁₆₅ induced COX-2 expression or if any inhibition of

COX-2 in HUVECs would induce apoptosis. Studies with 6-shogaol have indicated an inhibition of prostaglandin production (section 1.2.10) however no studies have been done to identify any pro-apoptotic effects on cells *in vitro* or if there are any effects on the inhibition of VEGF₁₆₅ induced COX-2.

4.2 *Aims*

- To investigate the effects of curcumin and 6-shogaol on VEGF₁₆₅ induced COX-2 expression.
- To investigate if curcumin and 6-shogaol induce apoptosis in HUVECs.

4.3 *Methods*

- Western blotting of COX-2 was carried out as described in section 2.4 using selective anti-COX-2 goat polyclonal IgG and anti- β -actin rabbit IgG at a concentration of 0.2 μ g/ml (a 1:1000 dilution of stock antibody). COX-2 antibody was detected by donkey anti-goat IgG-HRP at 0.08 μ g/ml (1:5000 dilution of stock antibody) and then visualised by ECL detection.
- Condensation of chromatin was assessed using the cytopinning technique described in Section 2.3.
- HUVEC DNA isolation was performed using the phenol/chloroform extraction of DNA (Section 2.3.3) and analysed by agarose gel electrophoresis (Section 2.8); Jurkat E6.1 DNA analysis was carried out by DNA ladder Suicide track kit ® (Section 2.3.2).

4.4 Results

4.4.1 Induction of COX-2 with VEGF₁₆₅ in HUVECs

HUVECs grown in fully supplemented medium 199 were quiesced for 16 hr in 1% FCS medium 199 and treated with 50ng/ml VEGF₁₆₅ for up to 24 hr. This resulted in the induction of COX-2 protein which was increased in a time-dependent manner, peaking at 8 hr and continuing until 24 hr (Fig 4.1).

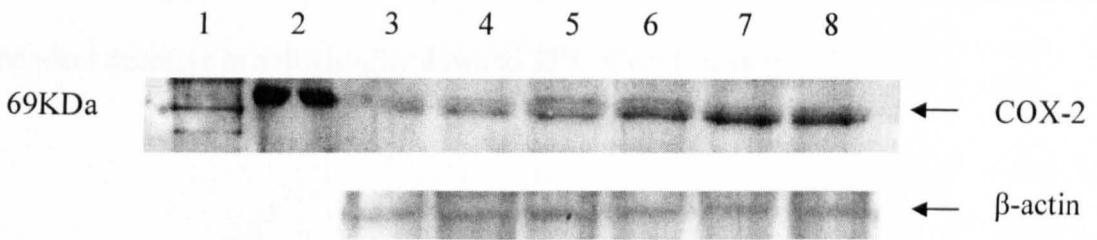


Figure 4.1: Induction of COX-2 expression in HUVECs with VEGF₁₆₅ (50ng/ml). Control cells were treated with 1% FCS medium 199 for 24 hr in a 37°C tissue culture incubator. VEGF₁₆₅ treated cells were incubated for up to 24 hr prior to cell lysis and western blotting of the samples. Lane (1) molecular weight marker, (2) J774 murine macrophages treated with LPS for 24 hr, (3) 0 hr, (4) 2 hr, (5) 4 hr (6) 6 hr (7) 8 hr (8) 24 hr VEGF₁₆₅. β -actin levels were assessed to show equal protein loading. The images are representative of 3 separate experiments

4.4.2 Inhibition of COX-2 by curcumin and 6-shogaol in HUVECs

VEGF₁₆₅ induced COX-2 expression was inhibited by curcumin in a dose independent manner with concentrations of 1.78 μ M, 3.12 μ M, 25 μ M and 50 μ M blocking VEGF

stimulated COX-2 expression (Fig 4.2a, c). However, 6.25 μ M and 12.5 μ M curcumin treatment had no effect on VEGF₁₆₅ induced COX-2 expression in HUVECs (Fig 4.2a, c).

6-shogaol induced a dose dependent response in the inhibition of VEGF₁₆₅ induced COX-2 in HUVECs. Expression of COX-2 was inhibited to unstimulated levels by low concentrations of the 6-shogaol and with the higher concentrations (12.5 μ M, 25 μ M and 50 μ M) reduced the expression below unstimulated levels by ~ 40% (Fig. 4.2b, c). Analysis of cell viability in 6-shogaol treated HUVECs using the MTT assay produced a dose dependent decrease in cell viability down to 33% of control values (Fig. 4.3).

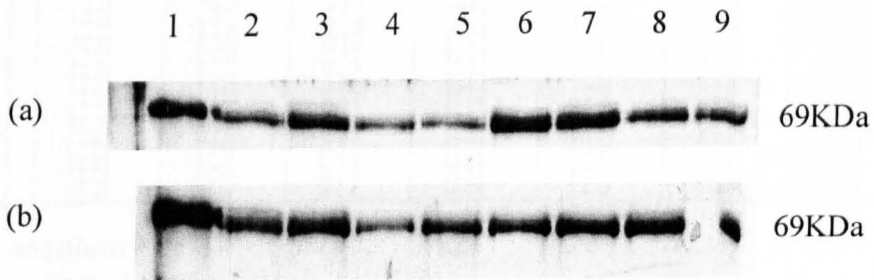


Figure 4.2a and b: Inhibition of VEGF₁₆₅ induced COX-2 expression in HUVECs by curcumin and 6-shogaol. VEGF₁₆₅ treated HUVECs in the presence or absence of curcumin (a) and 6-shogaol (b) were incubated at 37°C for 24 hr. Control cells were incubated with 1% FCS medium 199 + 0.2 % methanol (MeOH) for 24 hr at 37°C. Cells were lysed and western blotted. Lane (1) J774 murine macrophages treated with LPS for 24 hr, (2) 1% FCS medium 199+ MeOH (0.2%), (3) VEGF₁₆₅ (50ng/ml), (4) 50 μ M curcumin/6-shogaol, (5) 25 μ M, (6) 12.5 μ M, (7) 6.25 μ M, (8) 3.125 μ M, (9) 1.78 μ M. The image is representative of 2 separate experiments.

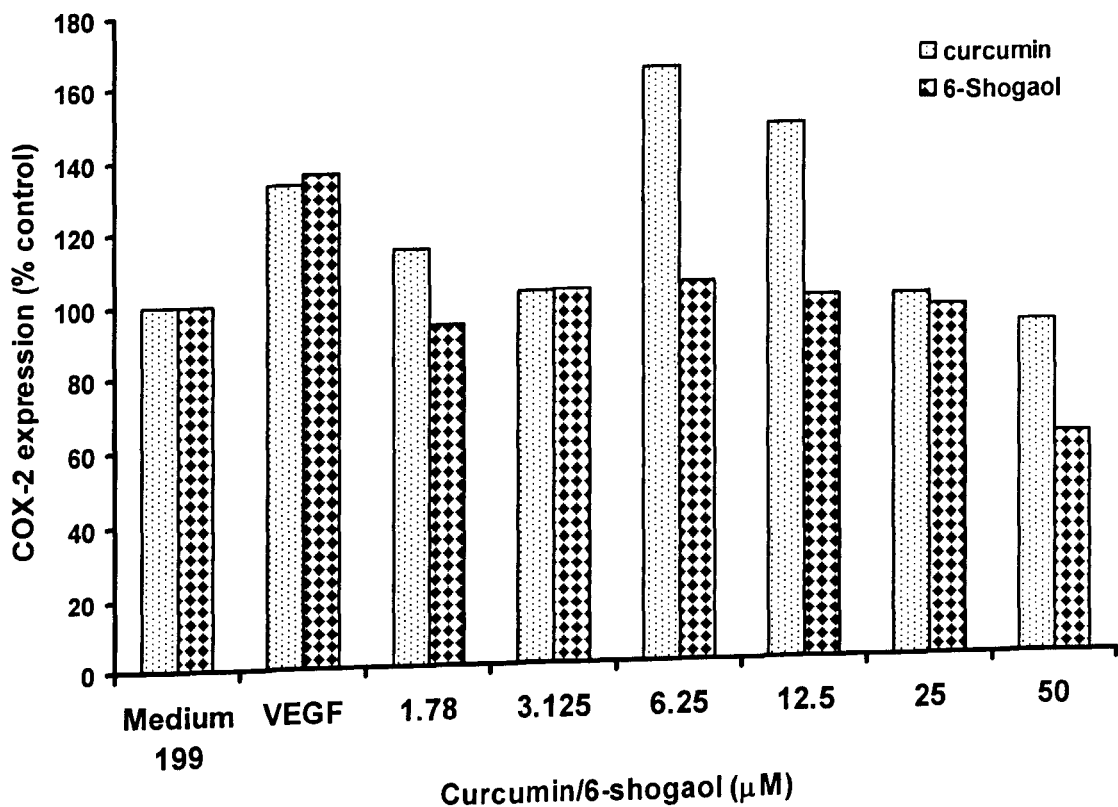


Figure 4.2c: Inhibition of VEGF₁₆₅ induced COX-2 expression in HUVECs by curcumin and 6-shogaol. VEGF₁₆₅ (50ng/ml) treated cells in the presence or absence of curcumin and 6-shogaol were incubated at 37°C for 24 hr. Control cells were incubated in 1% foetal calf serum (FCS) medium 199 + 0.2 % methanol for 24 hr at 37°C. Cells were lysed and western blotted and analysed by densitometry. The data is the mean of 2 experiments.

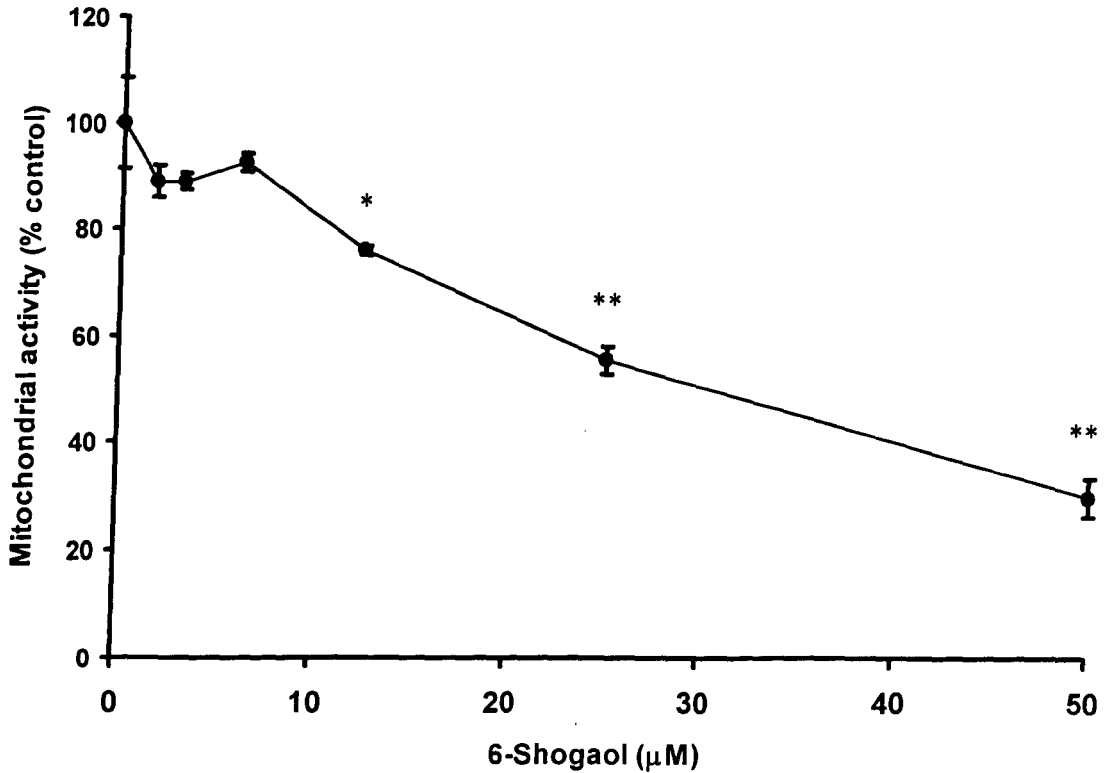


Figure 4.3: Mitochondrial activity in HUVECs treated with 6-shogaol. VEGF₁₆₅ (50ng/ml) and 6-shogaol treated cells were incubated at 37°C for 22 hr prior to addition of MTT and further incubation for 2 hr at 37°C. Control cells were treated with 20 % foetal calf serum medium 199 (complete medium) + methanol (MeOH) (0.002%) for 24 hr at 37°C. Crystal formation was assessed by colour change at 595nm. The data are the mean of 3 experiments +/- s.e.m with 2 replicates in each experiment. ANOVA was used to determine significance for all the data with Student's t-test identifying the individual points of significance. Significance is compared to complete medium 199 + MeOH (0.002%) * $p < 0.05$, ** $p < 0.01$.

4.4.3 *Induction of HUVEC apoptosis with curcumin and 6-shogaol*

In parallel studies curcumin was found to dose dependently induce significant chromatin condensation over 24 hr at 50 μ M (Fig 4.4a-d). 6-shogaol also induced a significant dose dependent increase in chromatin condensation over 24 hr peaking at 60% total cells with chromatin condensation (Fig 4.4a, e, and f). However treatment with 6-shogaol did not produce any HUVEC DNA fragmentation (Fig 4.5).

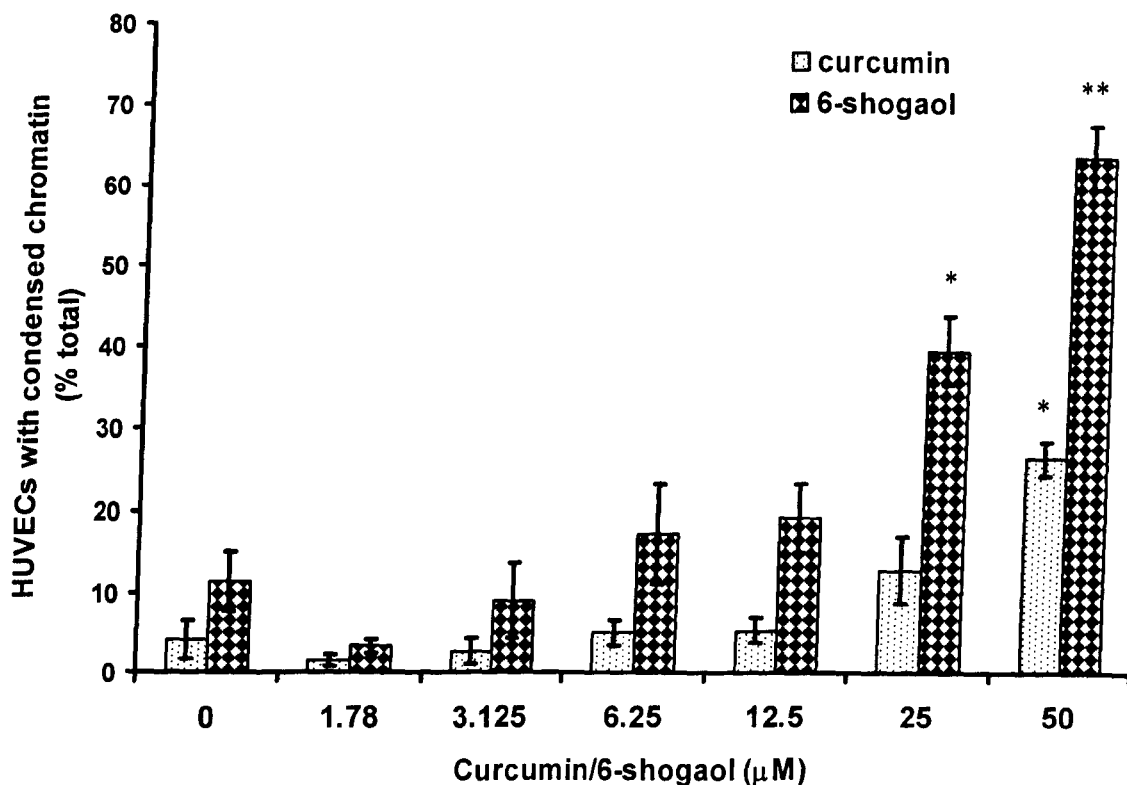


Figure 4.4a: Induction of chromatin condensation in HUVECs with curcumin and 6-shogaol. Treated cells were incubated in at 37°C for 24 hr. Control cells were treated with serum free medium (SFM) 199 + methanol (MeOH) (0.2%) for 24 hr at 37°C. HUVECs were cytopspun and the DNA stained with acridine orange. The data are the mean +/- s.e.m. of at least 3 experiments with 2 replicates in each. ANOVA was used to determine significance for all the data with Student's t-test identifying the individual points of significance. Significance is compared to SFM 199 + MeOH (0.2%) * $p < 0.05$, ** $p < 0.01$.

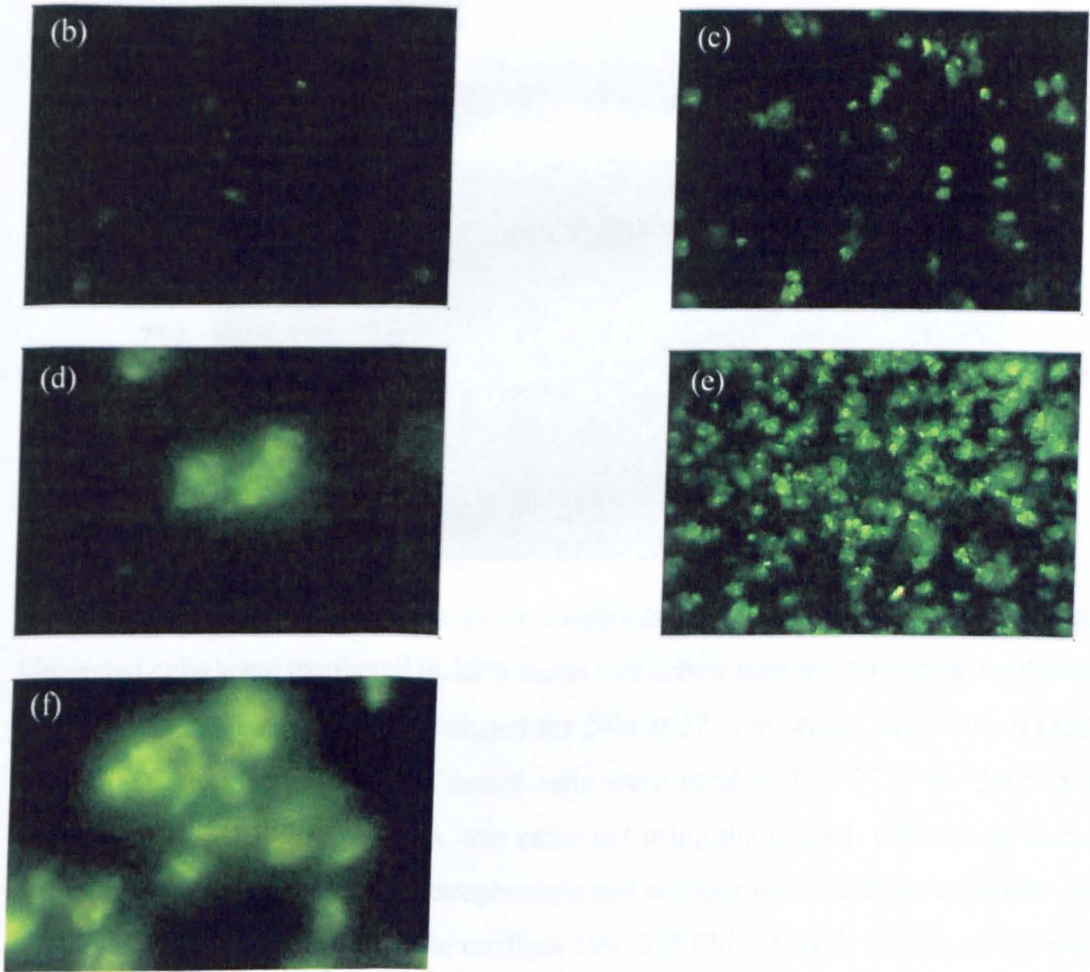


Figure 4.4b-f: Induction of chromatin condensation in HUVECs with curcumin and 6-shogaol. Controls were treated with serum free medium (SFM) 199 with methanol (MeOH) (0.2%) for 24 hr at 37°C (b). Curcumin (50 μ M) treated cells were also incubated at 37°C for 24 hr prior to cytopinning, staining of the DNA with acridine orange and viewed x100 (c) and x400 (d). 6-shogaol (50 μ M) treated cells were also incubated at 37°C for up to 24 hr prior to cytopinning, staining of the DNA with acridine orange and viewed x100 (e) and x400 (f). The images are representative of 3 separate experiments with 2 replicates in each.

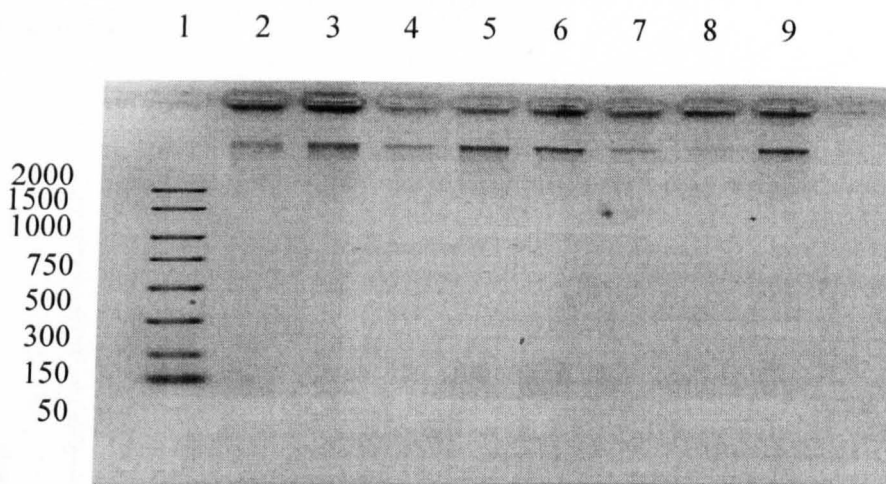


Figure 4.5: Induction of apoptotic DNA fragmentation in HUVECs treated with 6-shogaol. Untreated cells were incubated in 20% foetal calf serum medium (complete medium) for 24 hr at 37°C. Treated cells were incubated for 24hr at 37°C in serum free medium (SFM) 199 in the presence of 6-shogaol. Control cells were incubated at 37°C for 24hr in SFM + methanol (MeOH) (0.2%). DNA was extracted using the phenol: chloroform method and visualised by 2% agarose gel electrophoresis and staining with ethidium bromide. Lane (1) DNA ladder (100 bp) (2) complete medium 199 (3) SFM + MeOH (0.2%) (4 - 9) 6-shogaol 1.78μM, 3.12μM, 6.25μM, 12.5μM, 25μM, 50μM. The image is representative of 3 separate experiments.

4.4.4 *Effects of PGE₂ on curcumin and 6-shogaol induced HUVEC chromatin condensation*

Induction of HUVEC chromatin condensation by curcumin and 6-shogaol was not inhibited by exogenous PGE₂. Treatment of HUVECs with 50μM curcumin and 6-shogaol induced significant chromatin condensation (Fig 4.4, 4.5). To prevent this exogenous PGE₂ (10μM)

was added to the HUVECs simultaneously with the curcumin or 6-shogaol. Exogenous PGE₂ did not reduce the chromatin condensation induced by curcumin or 6-shogaol (Fig 4.6a, b, c, d, e).

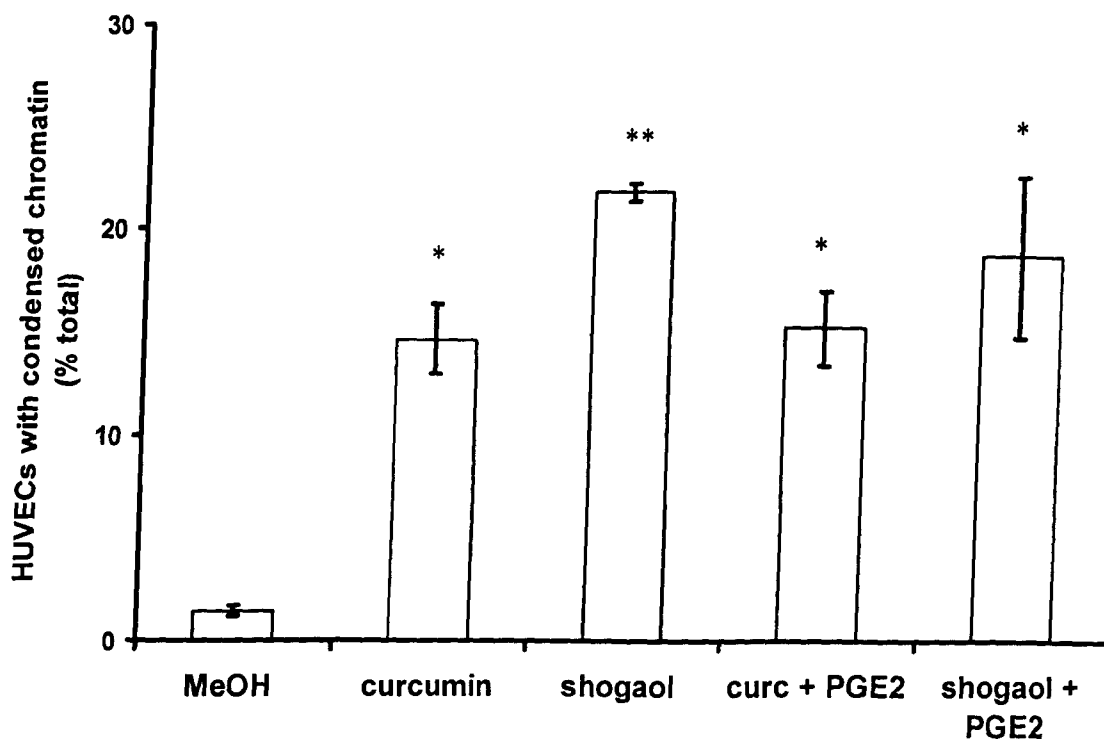


Figure 4.6a: Induction of chromatin condensation in HUVECs by curcumin and 6-shogaol. HUVECs treated in serum free medium (SFM) 199 with 6-shogaol (50 μ M) and curcumin (50 μ M) in the presence or absence of PGE₂ (10 μ M) were incubated at 37°C for 24 hr. Controls were treated with SFM + methanol (MeOH) (0.2%) for 24 hr at 37°C. HUVECs were cytopspun and the DNA stained with acridine orange. The data are the mean \pm s.e.m. of at least 3 experiments with 2 replicates in each. ANOVA was used to determine significance for all the data with Student's *t*-test identifying the individual points of significance. Significance is compared to SFM + MeOH (0.2%) * $p < 0.05$, ** $p < 0.01$.

4.4.5 Induction of apoptosis in HUVEC by curcumin and 6-shogaol
HUVEC cells treated with curcumin (50 μ M) + PGE₂ (10 μ M) showed chromatin condensation (Fig 4.7). The lack of chromatin condensation was observed in control HUVEC DNA following 24 hr treated with serum free medium (Fig 4.8). The induction of chromatin condensation is shown in Fig 4.9.

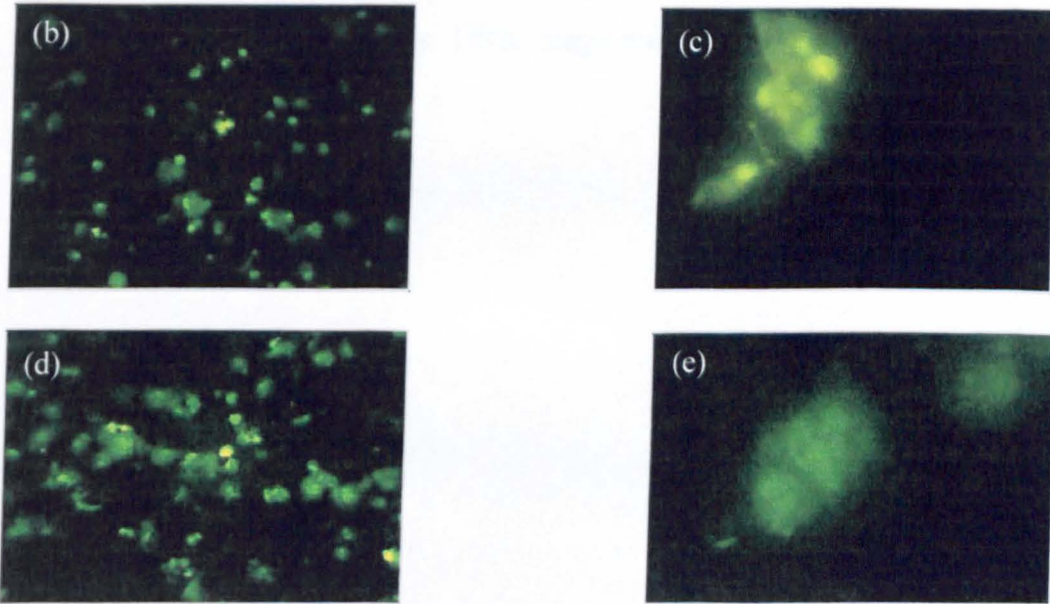


Figure 4.6b-e: Induction of chromatin condensation in HUVECs by curcumin and 6-shogaol. Controls were treated with serum free medium 199 with methanol (MeOH) (0.2%) for 24 hr at 37°C. 6-shogaol and curcumin with or without PGE₂ (10 μ M) treated cells were also incubated at 37°C for 24 hr prior to cytospinning and staining of the DNA with acridine orange. (b) curcumin (50 μ M) + PGE₂ (10 μ M) x100, (c) curcumin (50 μ M) + PGE₂ (10 μ M) x400, (d) 6-shogaol (50 μ M) + PGE₂ (10 μ M) x100, (e) 6-shogaol (50 μ M) + PGE₂ (10 μ M) x400.

4.4.5 *Induction of apoptosis in Jurkat E6.1 cells with curcumin and 6-shogaol*

Jurkat E6.1 cells treated with curcumin (50 μ M) did not induce significant chromatin condensation (Fig 4.7). The lack of chromatin condensation was accompanied by no significant DNA laddering in treated Jurkat E6.1 cells (Fig 4.8). In contrast 6-shogaol induced significant condensed chromatin at 50 μ M (Fig 4.7). Similarly to curcumin 6-shogaol did not produce any DNA fragmentation when examined by agarose gel electrophoresis (Fig 4.7b).

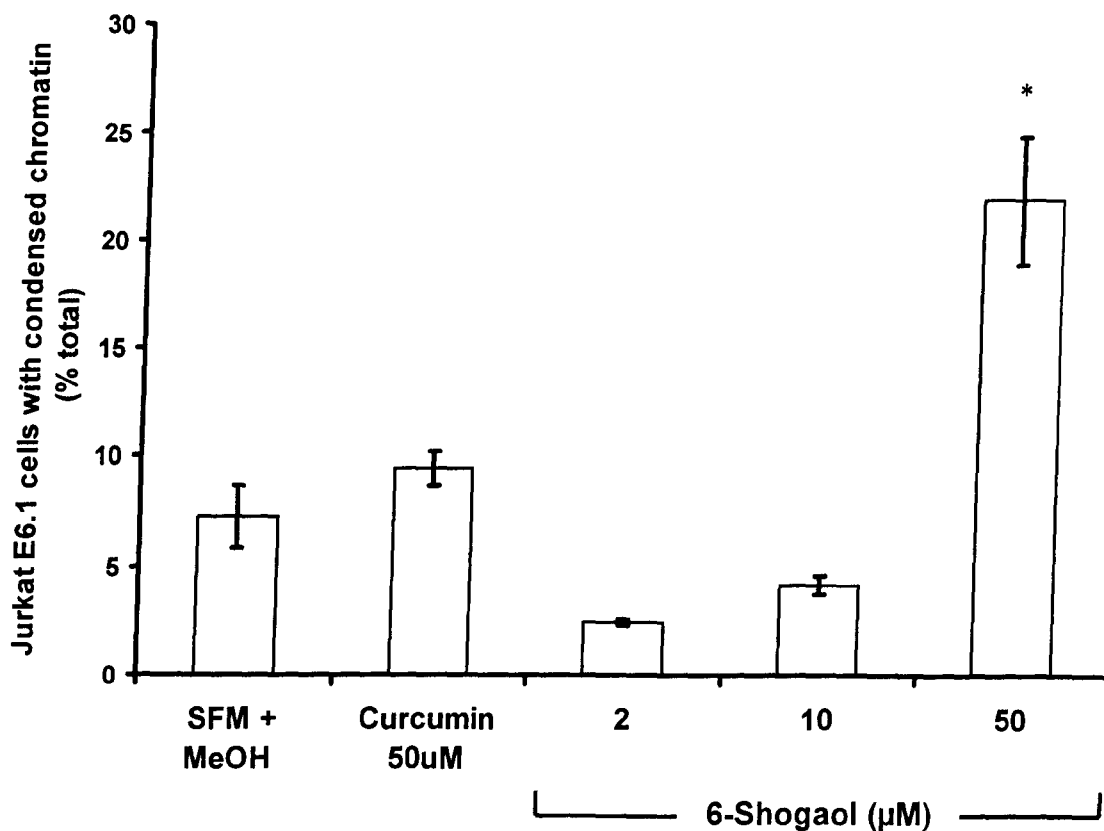


Figure 4.7a: Induction of chromatin condensation in Jurkat E6.1 cells by curcumin and 6-shogaol. 6-shogaol (2-50µM) and curcumin (50µM) treated cells were also incubated at 37°C for 24 hr prior to cytopinning and staining of the DNA with acridine orange. Controls were treated with serum free RPMI1640 medium (SFRM) + methanol (MeOH) (0.002%) for 24 hr at 37°C. The data are the mean +/- s.e.m. of at least 3 experiments with 2 replicates in each. ANOVA was used to determine significance for all the data with Student's t-test identifying the individual points of significance. Significance is compared to SFM + MeOH (0.002%) * $p < 0.05$, ** $p < 0.01$.

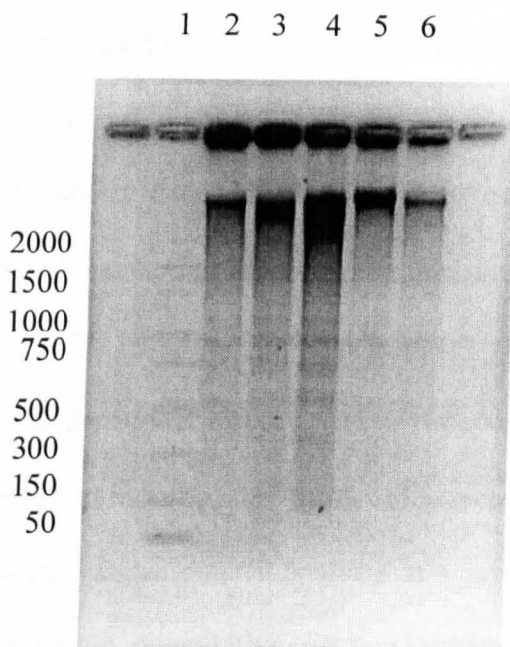


Figure 4.7b: Induction of apoptotic DNA fragmentation in Jurkat E6.1 cells by curcumin and 6-shogaol. Jurkat E6.1 cells treated with paclitaxel, 6-shogaol or curcumin were incubated for 24hr at 37°C. Control cells were incubated at 37°C for 24hr with methanol (0.002%). DNA extraction was completed using the DNA ladder Suicide track kit and visualised by 2% agarose gel electrophoresis and staining with ethidium bromide. Lane (1) DNA ladder (100 bp) (2) complete Medium RPMI1640 (3) serum free medium (SFM) + methanol (0.002%) (4) paclitaxel (500µM), (5) curcumin (50µM), (6) 6-shogaol (50µM). The image is representative of 3 separate experiments.

4.5 *Discussion*

The results presented in this chapter indicate that curcumin and shogaol induce a caspase-independent cell death in HUVECs. These effects were observed at concentrations higher than required to inhibit COX-2 possibly indicating a possible COX-2 independent mechanism of cell death.

Curcumin and 6-shogaol were found both to inhibit VEGF-induced COX-2 expression at low concentrations. Curcumin gave a bi-phasic effect of inhibition of COX-2. The western blot and densitometry data indicates no inhibition of VEGF induced COX-2 expression at 6.25 and 12.5 μM . Furthermore, the inhibition seen at 1.78 μM seems to be greater than at 3.125 μM . However, the densitometry analysis of the two replicate blots indicates and dose dependent effect at these two concentrations with 3.125 μM inhibiting COX-2 expression more than 1.78 μM . This inconsistency may be explained through the methodology. Densitometry analysis is a semi-quantitative method and may not give fully accurate quantitative data. Densitometry computer programs compare the density of the band chosen to the surrounding background. However, western blots may not have a uniform background behind the image of interest and this would interfere with the comparison of the band to the background producing a lesser or greater quantitative value than is seen elsewhere on the blot. Furthermore, the data is an average of two blots and again the background of different blots may vary no matter how similar the change in protein expression. This would also affect the data produced by computer program further altering the final results. It is therefore required that any inhibition suggested here must be confirmed by further experimentation. Moreover, any data produced by densitometry may need to be confirmed by more than by three

replicates if the changes in protein expression seen are not very clear. The curcumin data are comparable to other studies in mouse skin that show an inhibition of induced COX-2 expression by curcumin at both low (1-5 μ M) and at higher concentrations (25 μ M) (Chun *et al.*, 2003), though no studies were completed at intermediate concentrations. In contrast studies by Zhang *et al.*, (1999) indicated that curcumin had a dose dependent effect on phorbol 12-myristate 13 acetate induced COX-2 expression in human gastrointestinal epithelial cells and dose dependently inhibited PGE₂ formation. These studies indicate a possible curcumin inhibition of COX-2 expression and activity in HUVECs in a dose dependent mechanism though this remains to be confirmed by further experimentation.

6-Shogaol inhibited COX-2 expression at low concentrations < 10 μ M with a slight dose response effect. Similarly 6-shogaol was found to inhibit COX-2 activity in A459 cells with an IC₅₀ = 2.1 μ M (Tjendraputra *et al.*, 2001), possibly indicating a similar COX-2 inhibitory effect to that of curcumin. However the dose response effect on COX-2 expression by 6-shogaol in the current study was found to be due to cytotoxicity as determined by the MTT assay. The increase in cytotoxicity indicated a possible increase in apoptosis of the cells.

Curcumin and 6-shogaol both induced dose dependent chromatin condensation in HUVECs giving a maximum chromatin condensation of approximately 25% and 70% chromatin condensation respectively. Further studies with 6-shogaol did not induce DNA laddering in HUVECs or Jurkat E6.1 cells after 24 hr. Curcumin was also found not to induce DNA fragmentation in Jurkat E6.1 cells, which was similar to other

previous studies (Piwocka *et al.*, 1999; Piwocka *et al.*, 2000; Piwocka *et al.*, 2001 and *chapter 3*) that indicated a caspase independent cell death with no DNA laddering. In contrast to this Wei *et al.*, (2005) indicated an increase in DNA laddering upon treatment with 70 μ M 6-shogaol. However, the data presented by Wei *et al.*, (2005) does not appear to substantiate this suggestion with no apparent DNA laddering, but some smearing, on the agarose gel suggesting a caspase-independent fragmentation of the DNA. It has been suggested that the effects seen with curcumin may be due to a prevention of glutathione depletion and no cyt-c release (Piwocka *et al.*, 1999; Piwocka *et al.*, 2000; Piwocka *et al.*, 2001).

The investigation into the induction of chromatin condensation matches previous work by Smith (2004) that showed that similar concentrations of curcumin and 6-shogaol inhibited thymidine incorporation during DNA replication in HUVECs and therefore prevented HUVEC growth and replication. It is possible therefore that the inhibition of HUVEC replication seen in cells treated with curcumin and 6-shogaol is caused by the induction of cell death. Similarities in the effects observed with both curcumin and 6-shogaol treatments and the subsequently induced apoptotic morphology may be due to the comparable structures of the compounds.

As the structure of 6-shogaol is similar to curcumin (Tjendraputra *et al.*, 2001) it may be that cell death induced by 6-shogaol is through a similar mechanism. However, Wei *et al.*, (2005) have suggested that it is not the conserved phenyl ring seen in structures of 6-shogaol and 10-shogaol, and in curcumin (Zhang *et al.*, 1999), but the α,β -unsaturated ketone moiety. Together with the present study this would suggest that the enhanced

induction of chromatin condensation observed with 6-shogaol, compared to curcumin, may not be caused by the phenyl ring in both structures but by the α,β -unsaturated ketone moiety present in the structure of 6-shogaol and curcumin. However the phenyl ring may contribute to the activity of both 6-shogaol and curcumin. A hypothesis of how the two comparable structures may induce different effects in HUVECs may be due to the overall structures of the molecules. Curcumin consists of two phenyl rings connected by an alkyl chain (Zhang *et al.*, 1999). In contrast 6-shogaol does not have the second phenyl ring (Tjendraputra *et al.*, 2001) and therefore the free alkyl chain associated with 6-shogaol may be the cause of the enhanced levels of chromatin condensation. Mechanisms behind this effect would have to be confirmed but may be due to the increased lipophilicity of the 6-shogaol alkyl side chain making it possible for the molecule to enter cells easier than curcumin.

Chromatin condensation induced by 6-shogaol and curcumin also appears to be COX-2-independent. Simultaneous treatment of HUVECs with PGE₂ and 6-shogaol or curcumin did not prevent the chromatin condensation after 24 hr indicating that a prevention of PGE₂ formation was not the cause of apoptosis, though inhibition of another COX-2 product may have been the cause of the cell death. However, when considered with other studies, which indicate that curcumin and 6-shogaol inhibit COX-2 activity at lower concentrations than were used in this study (Zhang *et al.*, 1999, Tjendraputra *et al.*, 2001, Chun *et al.*, 2003), it may suggest that curcumin and 6-shogaol do not need to inhibit COX-2 to induce apoptosis. Furthermore, the current observations indicate that a 50% inhibition of COX-2 expression at low concentrations of curcumin and 6-shogaol did not induce chromatin condensation. This also supports a

caspase-independent mechanism as PGE₂ has been shown to increase Bcl-2 concentration and therefore prevent the mitochondrial apoptosis pathway being induced (Ghosh *et al.*, 2000, Hsu *et al.*, 2000, Johnson *et al.*, 2001, Basu *et al.*, 2005). Nevertheless this does not rule out the activation of the death receptor pathway of apoptosis or the activation of necrosis.

5.0 Comparison of selective and non-selective COX-2 inhibitors on angiogenesis and induction of apoptosis in HUVECs.

5.1 Introduction

Extended administration of non-steroidal anti-inflammatory drugs (NSAIDs) is implicated in the topical injury of the gastrointestinal (GI) tract e.g. gastric ulcers. Non-selective inhibition of the COX enzymes was found to be responsible with the decline in cytoprotective prostaglandins e.g. PGI₂ and PGE₂, causing the GI tract to become unregulated in secretions and blood flow, eventually leading to topical injury of the area. To prevent the GI damage induced by NSAIDs, selective COX-2 inhibitors were designed to prevent inflammation but spare COX-1 activity by binding to a “side-pocket” in the active site of the enzyme (described in section 1.2.8.2) therefore allowing the production of cytoprotective prostaglandins in the GI tract and maintain GI mucosal integrity. Rofecoxib and celecoxib are two selective COX-2 inhibitors that were approved for the treatment of osteoarthritis and rheumatoid arthritis respectively, and have been investigated for anti-cancer activity through the induction of apoptosis in the tumour cells (Hsu *et al.*, 2000; Blanke, 2002; Wu *et al.*, 2003) (discussed in section 1.2.8.3). However recent reports indicated that high concentrations of these two selective COX-2 inhibitors may produce apoptosis in cells *in vitro* and promote heart disease and vascular injury *in vivo* after extensive use. It is currently not known if this class of drugs induce apoptosis in endothelial cells at low concentrations *in vitro* or *in vivo*, or by what mechanisms they may induce apoptosis. Furthermore it is not known whether the specific inhibition of COX-2 alone could be responsible for the induction of apoptosis. Effects of selective COX-2 inhibitors on endothelial cell migration and tubule formation after potential damage to endothelial cells are also unknown.

5.2 *Aims*

- To compare the effects of the selective COX-2 inhibitor DuP-697 and of the non-selective COX inhibitor indomethacin on the induction of apoptosis and tubule formation in HUVECs.
- To determine if the induction of any apoptosis is due to selective COX-2 inhibition in the cells.
- To elucidate the pathways associated with the induction of apoptosis in HUVECs and if this induction can be inhibited by reversing COX-2 inhibition.

5.3 *Methods*

- Western blotting of COX-2 was carried out as described in section 2.4 using selective anti-COX-2 goat polyclonal IgG at a concentration of 0.2µg/ml (a 1:1000 dilution of stock antibody). COX-2 antibody was detected by donkey anti-goat IgG-HRP at 0.08µg/ml (1:5000 dilution of stock antibody) and then visualised by ECL detection.
- Western blotting of caspases was carried out using specific anti-caspase 3, 8 and 9 mouse monoclonal IgG at the concentration of 0.1µg/ml (1:1000 dilution of stock antibody).
- Condensation of chromatin was assessed using the cytopinning technique described in Section 2.3.
- HUVEC DNA isolation was performed using the phenol/chloroform extraction (Section 2.3.3) and analysis by agarose gel electrophoresis (Section 2.8).
- Matrigel tubule assay was carried out as described in Section 2.6.

5.4 Results

5.4.1 Expression of COX-2 in HUVECs

HUVECs grown in 20% serum-containing medium expressed low levels of COX-2 protein which did not change over a 24 hr incubation period as determined by western blot analysis (Fig 5.1). When quiesced cells were subsequently stimulated with VEGF there was a time-dependent increase in COX-2 expression with maximal expression occurring by 8 hr and maintained for 24 hr after the addition of VEGF (Fig 5.1).

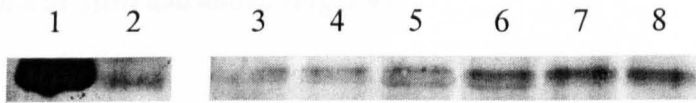


Figure 5.1: Cyclooxygenase-2 expression in HUVECs. HUVECs were quiesced for 16 hr in 1% FCS Medium 199 and then treated with VEGF for 0 - 24 hr. Lane (1) J774 murine macrophage treated with LPS for 24 hrs; (2) HUVECs cultured in 20% FCS Medium 199 for 24 hr; lanes (3)-(8) VEGF treated for 0hr, 2hr, 4hr, 6hr, 8hr and 24hr respectively. The blot is representative of 3 separate experiments.

5.4.2 Inhibition of prostaglandin E₂ production in unstimulated and VEGF₁₆₅ stimulated HUVECs by DuP-697

Treatment of cells with DuP-697 caused a dose dependent inhibition of PGE₂ production in unstimulated and VEGF treated HUVECs cultured in serum free medium (SFM), completely inhibiting PGE₂ production at 1 μ M (Fig 5.2). DuP-697 (in 20% foetal calf serum medium 199 (complete medium)) gave a small but significant inhibition (20%) of PGE₂ levels when compared to control values (Fig 5.3). Activation of HUVECs with VEGF was shown to increased PGE₂ production (23%) in complete medium which was inhibited by DuP-697 to 80% of control levels (Fig 5.3). In parallel studies, indomethacin caused a dose dependent inhibition of PGE₂ production, with complete inhibition obtained at concentrations of 3 μ M and above (Fig 5.4).

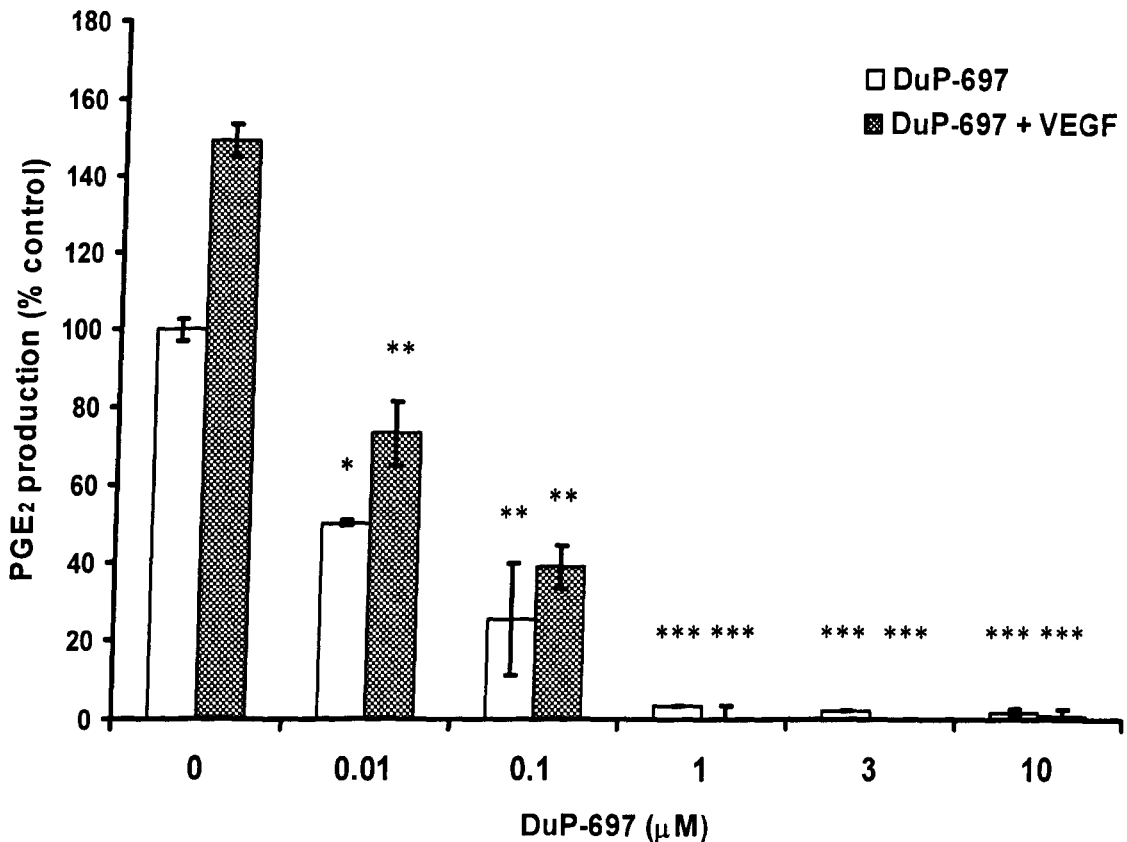


Figure 5.2: Inhibition of prostaglandin (PG) E₂ production in HUVECs by DuP-697 in serum free medium (SFM) 199. Treated cells were incubated for 24 hr at 37°C. VEGF treated cells were quiesced in 1% foetal calf serum (FCS) medium 199 for 16 hr prior to VEGF treatment in the presence or absence of DuP-697. Control cells were incubated with DMSO (0.01 %) for 24 hr at 37°C. PGE₂ levels were determined by ELISA. The data are the mean +/- s.e.m. of at least 3 experiments with 3 replicates in each. ANOVA was used to determine significance for all the data with Student's t-test identifying the individual points of significance. Significance was compared to SFM + DMSO (0.01%) +/- VEGF. **p*<0.05, ** *p*<0.01 and *** *p*<0.001.

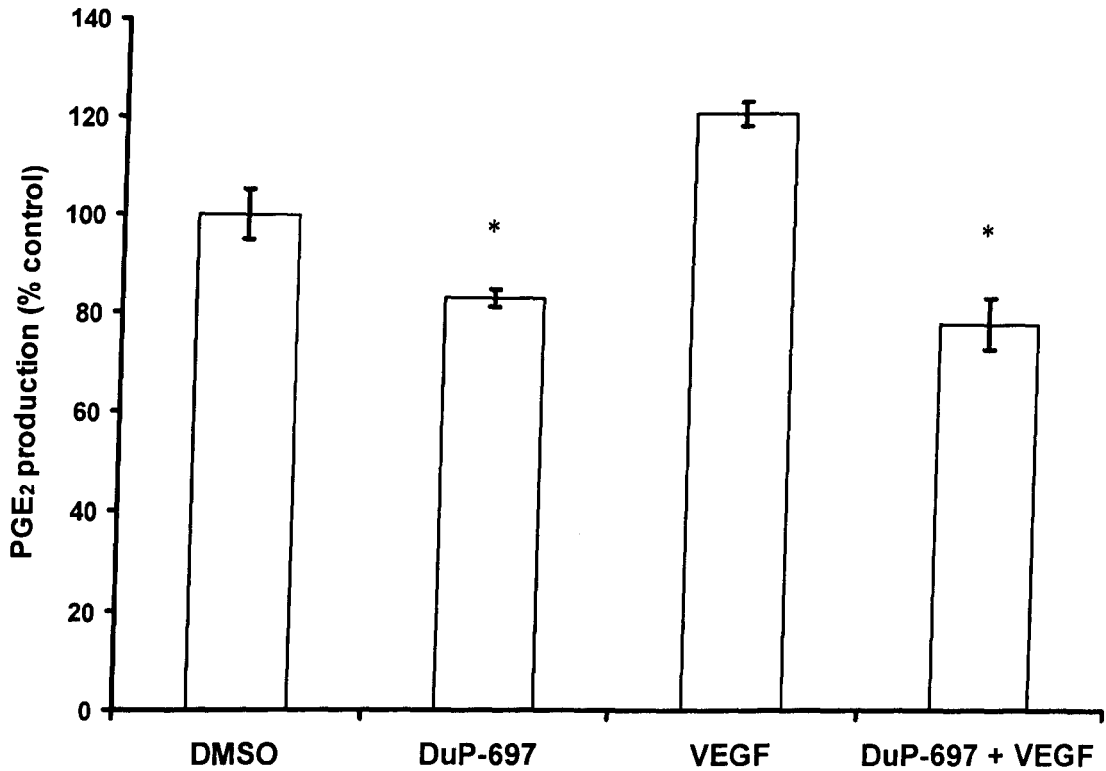


Figure 5.3: Inhibition of prostaglandin (PG) E₂ production in HUVECs by DuP-697 in 20% foetal calf serum medium (complete medium) 199. Treated cells were incubated for 24 hr at 37°C. VEGF treated cells were quiesced in 1% foetal calf serum (FCS) medium 199 for 16 hr prior to VEGF treatment in the presence or absence of DuP-697. Control cells were incubated with DMSO (0.01 %) for 24 hr at 37°C. PGE₂ levels were determined by ELISA. The data are the mean +/- s.e.m. of 3 experiments with 3 replicates in each. ANOVA was used to determine significance for all the data with Student's t-test identifying the individual points of significance. Significance was compared to complete medium + DMSO (0.01%) +/- VEGF. * $p < 0.05$.

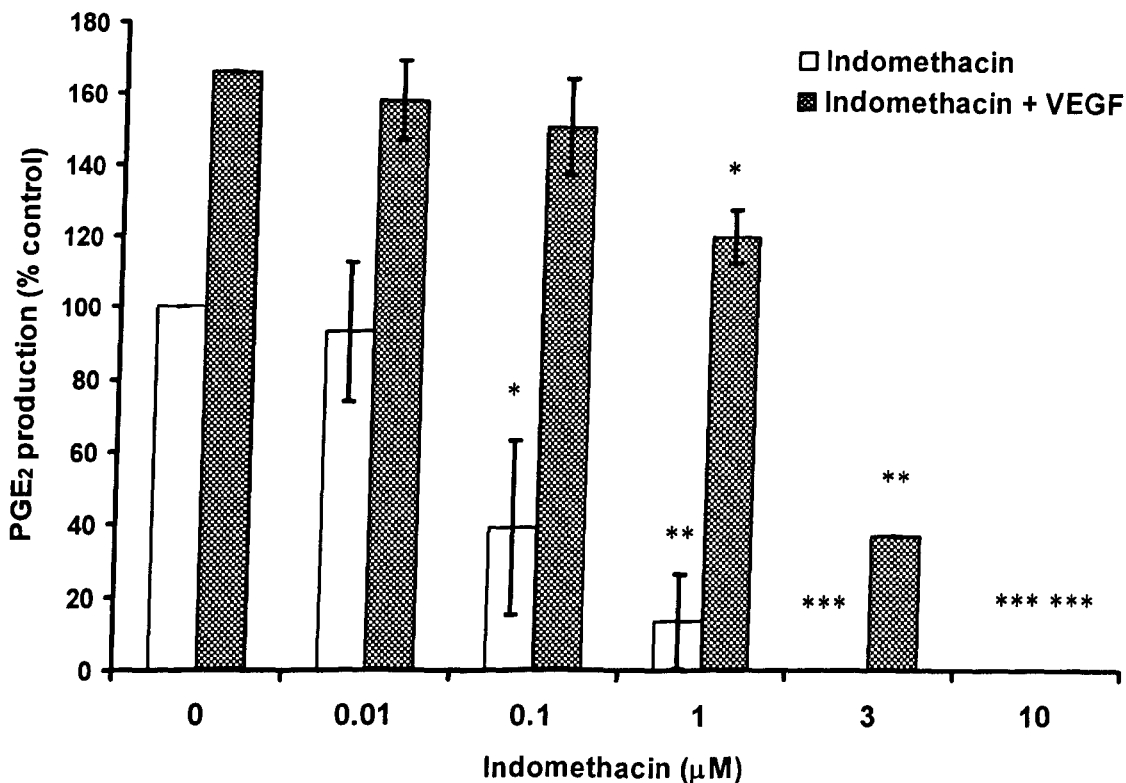


Figure 5.4: Inhibition of prostaglandin (PG) E₂ production in HUVECs cultured in serum free medium (SFM) by indomethacin. Treated cells were incubated at 37°C for 24 hr. Control cells were incubated with 0.01 % ethanol (EtOH) for 24 hr. PGE₂ levels were determined by ELISA. The data are the mean +/- s.e.m. of at least 3 experiments with 3 replicates in each. ANOVA was used to determine significance for all the data with Student's t-test identifying the individual points of significance. Significance was compared to serum free media (SFM) + DMSO (0.01%) +/- VEGF, * $p < 0.05$, ** $p < 0.01$ and *** $p < 0.001$.

5.4.3 Effects of DuP-697 on chromatin condensation in HUVECS

Treatment of HUVECs in SFM with 10 nM DuP-697 increased the amount of chromatin condensation in a dose dependent manner at concentrations of 0.0001-0.1 μ M (Fig. 5.5a-g). DuP-697 (10nM) caused high molecular weight DNA fragmentation as well as apoptotic DNA laddering after 24 hr (Fig. 5.6).

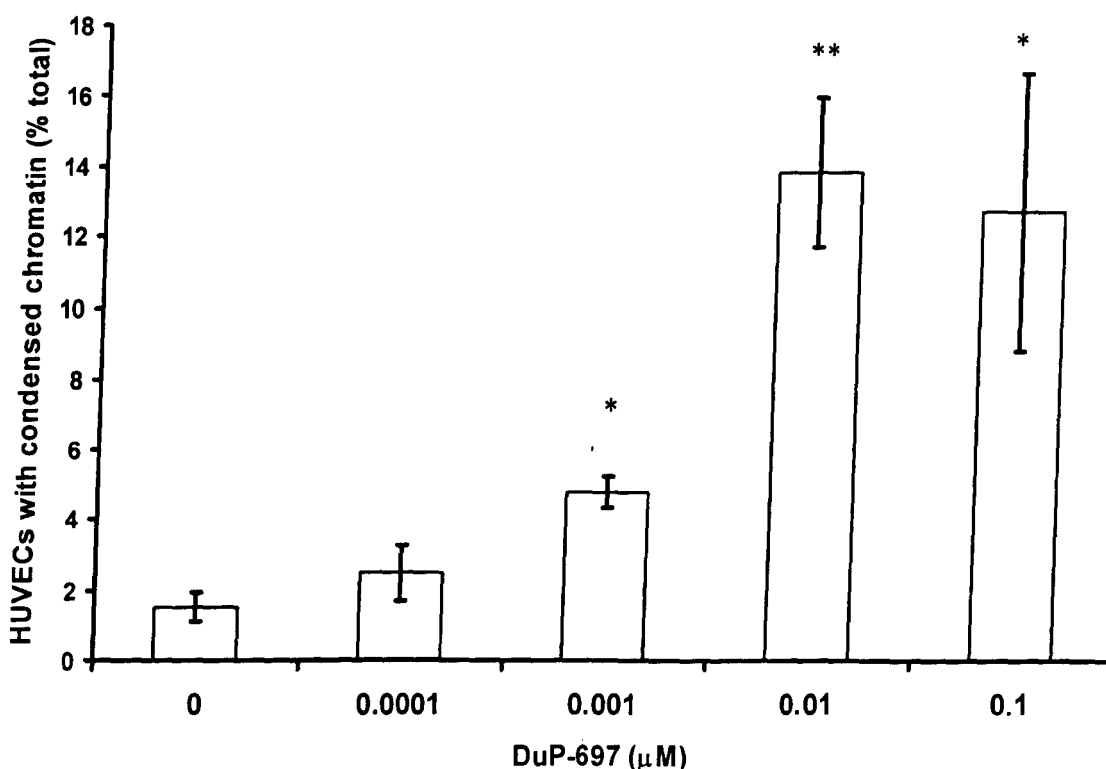


Figure 5.5a: Induction of chromatin condensation in HUVECs. Treated cells were incubated for 24 hr at 37°C. Control cells were incubated at 37°C for 24 hr with DMSO (0.01%). HUVECs were cytopspun and the DNA stained with acridine orange. The data are the mean \pm s.e.m. of 3 experiments with 2 replicates in each. ANOVA was used to determine significance for all the data with Student's t-test identifying the individual points of significance. Significance is compared to serum free media (SFM) + DMSO (0.01%) * $p < 0.05$ ** $p < 0.01$.

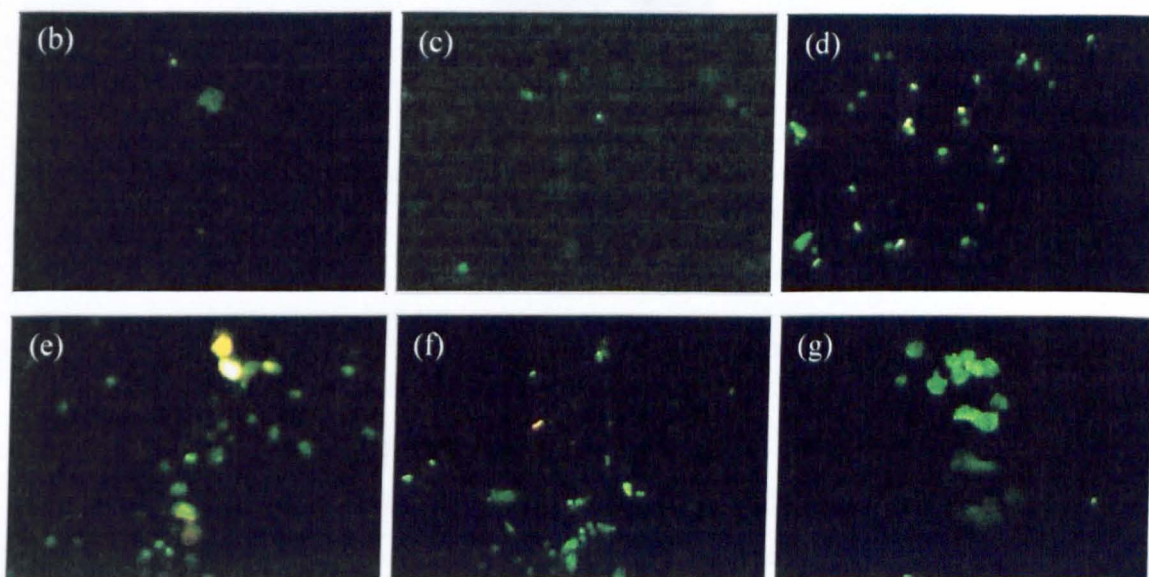


Figure 5.5b-g: Induction of chromatin condensation in HUVECs. Untreated cells were incubated in 20% foetal calf serum medium 199 (complete medium) for 24 hr (b). Control cells were incubated at 37°C for 24hr in serum free medium (SFM) + DMSO (0.01%) (c). HUVECs treated with DuP-697; 0.01 (d), 0.1 (e), 1 (f) and 10 μ M (g) were incubated for 24 hr at 37°C. HUVECs were cytopspun and the DNA stained with acridine orange. The images are representative of 3 experiments with 2 replicates in each.

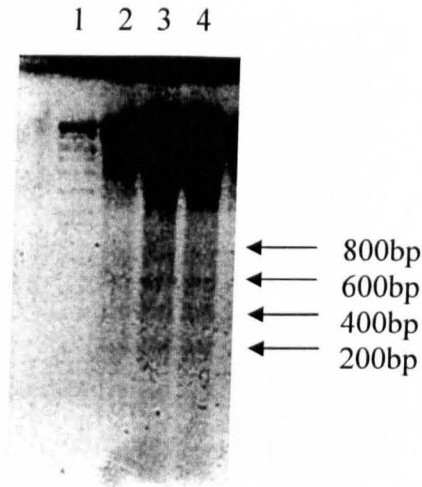


Figure 5.6: Induction of apoptotic DNA fragmentation in HUVECs. Treated HUVECs were incubated for 24 hr at 37°C. Control cells were incubated at 37°C for 24hr in serum free medium (SFM) + DMSO (0.01%). DNA was extracted using the phenol/chloroform method and visualised by 2% agarose gel electrophoresis and staining with ethidium bromide. Lane (1) DNA ladder (100bp) (2) SFM + DMSO (0.01%) (3) Actinomycin- D (200nM) apoptosis positive control (4) DuP-697 (10nM). The image is representative of 3 separate experiments.

5.4.4 Induction of apoptosis in HUVECs by indomethacin

Indomethacin induced a dose dependent chromatin condensation at concentrations of 3µM and above (Fig. 5.7 and 5.8a-g). These concentrations of indomethacin have been shown to inhibit COX-2 as well as COX-1 in whole cell systems (Mitchell *et al.*, 1994) and completely inhibited PGE₂ production in our studies (Fig. 5.4).

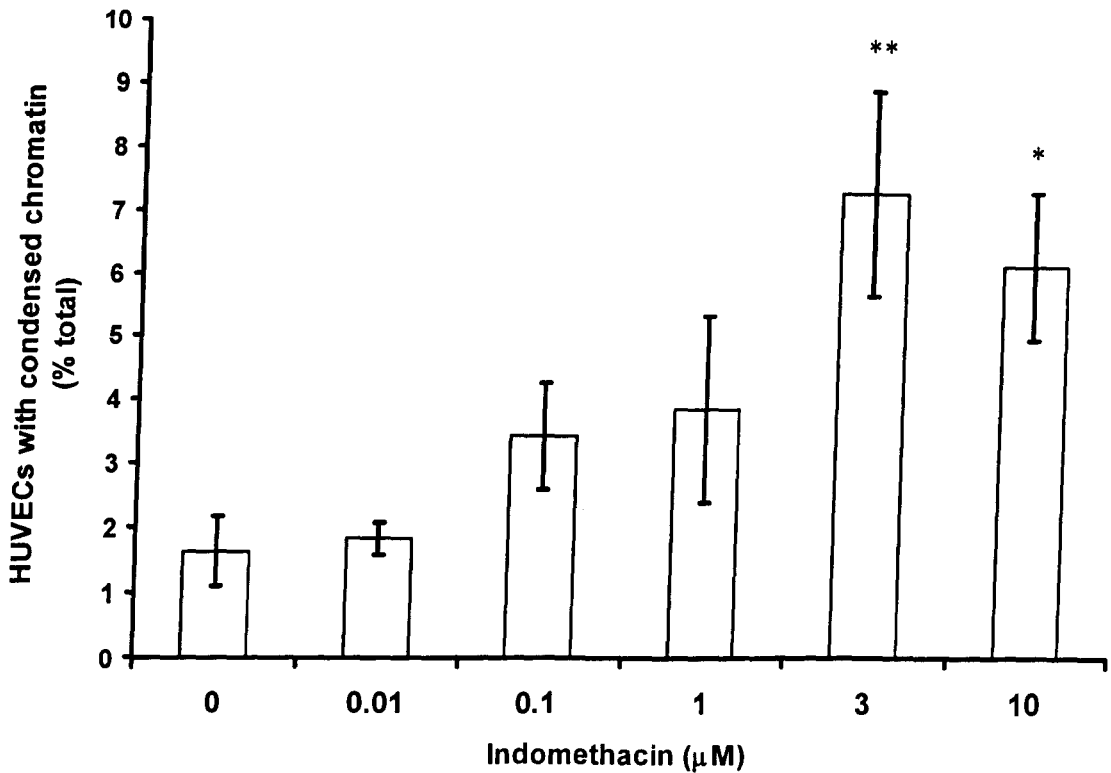


Figure 5.7a: Induction of chromatin condensation in HUVECs. Cells treated with indomethacin (0.01-10μM) were incubated for 24 hr at 37°C. Control cells were incubated at 37°C for 24hr with ethanol (EtOH) (0.01%). HUVECs were cytospun and stain with acridine orange. The data are the mean +/- s.e.m. of at least 3 experiments with 2 replicates in each. ANOVA was used to determine significance for all the data with Student's t-test identifying the individual points of significance. Significance is compared to serum free media (SFM) + EtOH (0.01%) * $p < 0.05$, ** $p < 0.01$.

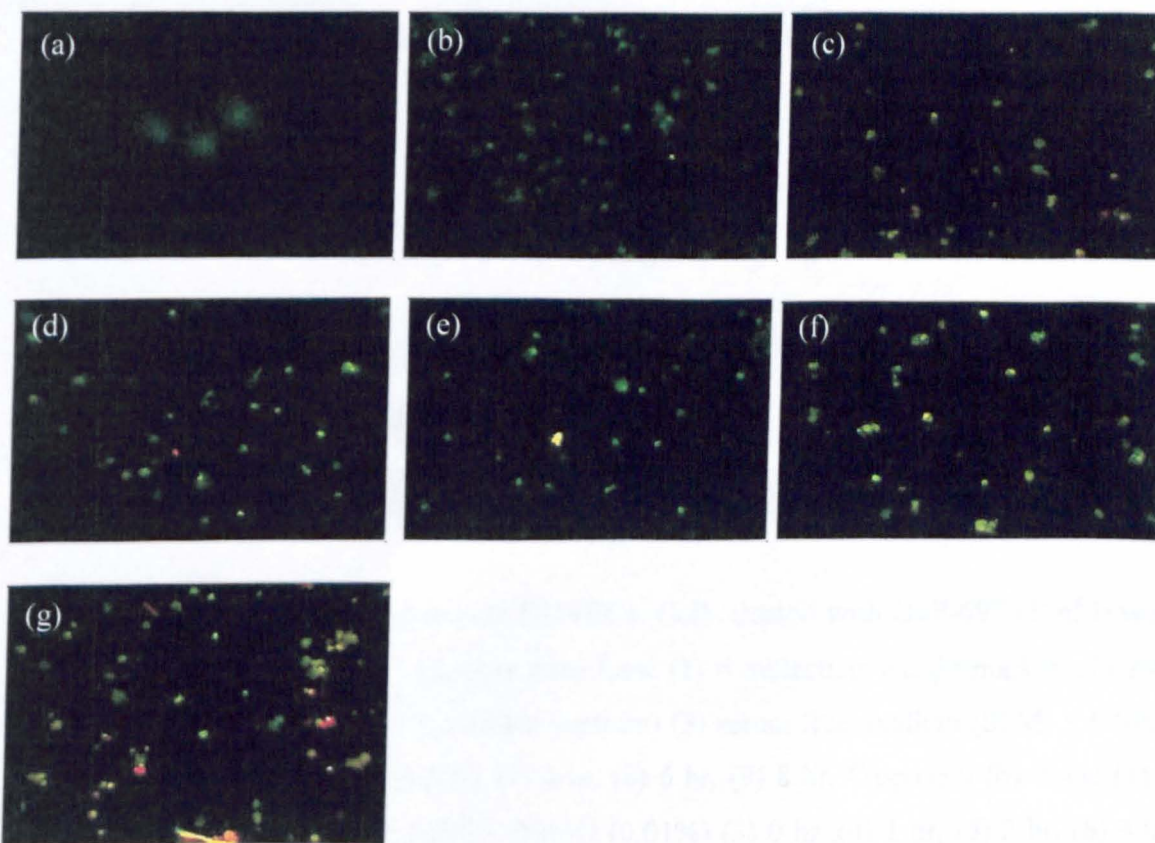


Figure 5.8a-g: Induction of chromatin condensation in HUVECs. Untreated HUVECs were incubated in 20% foetal calf serum medium 199 (complete medium) (a). Control cells were incubated at 37°C for 24hr in serum free medium (SFM) + ethanol (EtOH) (0.01%) (b). Cells treated with indomethacin; 0.01 (c) 0.1 (d), 1 (e), 3 (f) and 10 μ M (g) were also incubated for 24hr at 37°C. HUVECs were cytopspun and the DNA stained with acridine orange. The images are representative of 3 experiments with 2 replicates in each.

5.4.5 Effects of DuP-697 on caspase activation

Induction of caspase-8 (Fig 5.9a and d) and 9 (Fig 5.9b and d) occurred within 1 hr following DuP-697 treatment and peaked at 2 hrs, declining thereafter. By comparison, caspase 3 induction occurred at 2 hrs and remained elevated for up to 8 hr (Fig 5.9c and d).

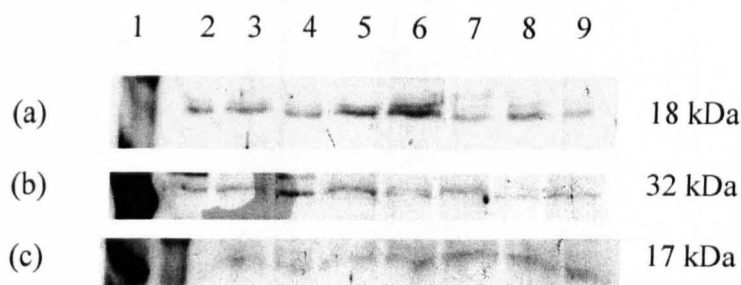


Figure 5.9a-c: Caspase expression in HUVECs. Cells treated with DuP-697 (10nM) were incubated at 37°C for 0-8 hr. Caspase 8 (a) Lane (1) = molecular weight marker, (2) 20% foetal calf serum medium 199 (complete medium) (3) serum free medium (SFM) + DMSO (0.01%), (4) 0 hr, (5) 1 hr, (6) 2 hr, (7) 4 hr, (8) 6 hr, (9) 8 hr. Caspase 9 (b) Lane (1) = molecular weight marker, (2) SFM + DMSO (0.01%) (3) 0 hr, (4) 1 hr, (5) 2 hr, (6) 4 hr, (7) 6 hr, (8) 8 hr, (9) complete medium. Caspase 3 (c) Lane (1) Jurkat E6.1 cells treated with 50µM paclitaxel positive control for 24 hr, (2) molecular weight marker, (3) SFM + DMSO (0.01%), (4) 0 hr, (5) 1 hr, (6) 2 hr, (7) 4 hr, (8) 6 hr, (9) 8 hr. The images are representative of 3 experiments.

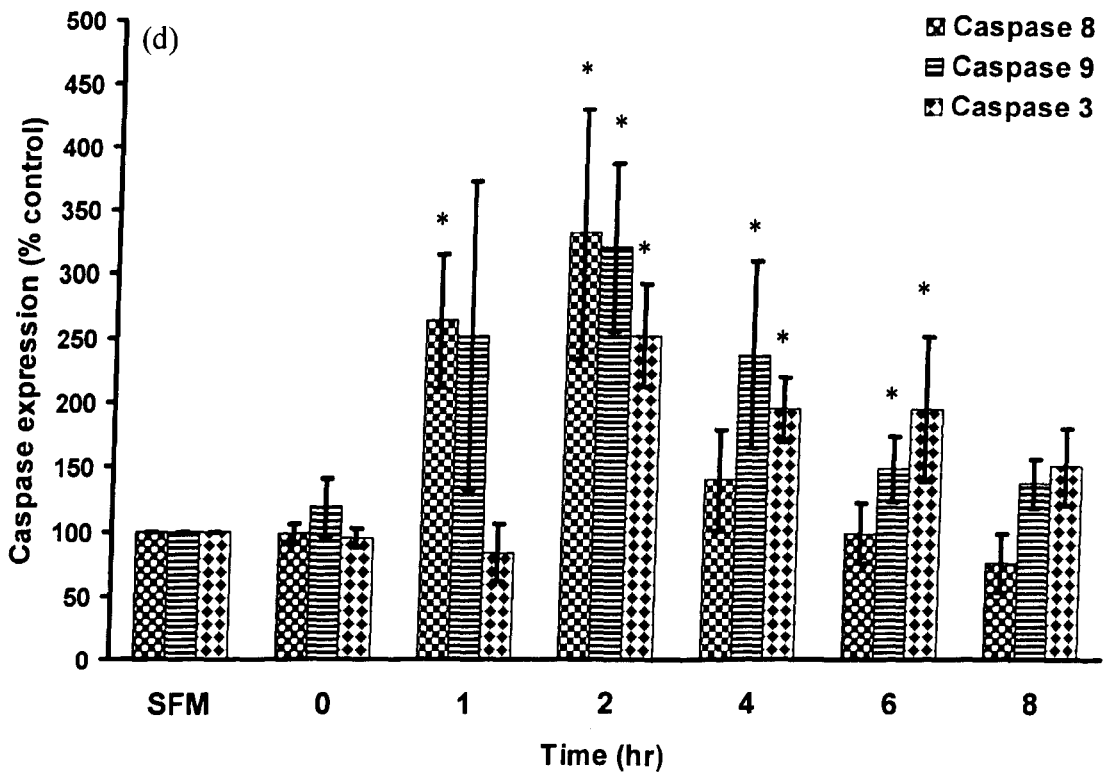


Figure 5.9d: Caspase expression in HUVECs. HUVECs were treated with DuP-697 (10nM) and incubated at 37°C for 0-8 hr. Control cells were incubated at 37°C for 8 hr in serum free medium (SFM) + DMSO (0.01%). HUVECs were lysed and analysed for caspase expression by western blotting and densitometry. The data are the mean +/- s.e.m. of 3 experiments. ANOVA was used to determine significance for all the data with Student's t-test identifying the individual points of significance. Significance is compared to serum free media (SFM) + DMSO (0.01%) * $p < 0.05$.

5.4.6 Effects of indomethacin on caspase activation

Induction of caspase 9 (Fig 5.10a and c) occurred within 1 hr following indomethacin treatment and peaked at 4 hrs, declining thereafter. Similarly caspase 3 induction occurred at 1 hr and levels declined to control levels over an 8 hr incubation period (Fig 5.10b and c).

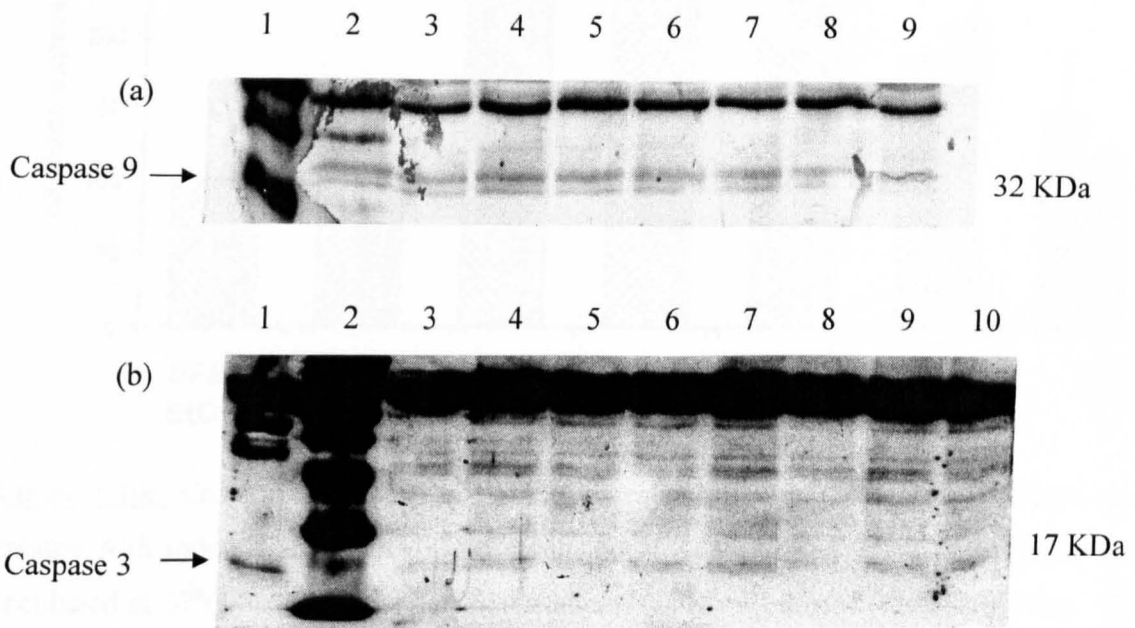


Figure 5.10a and b: Caspase expression in HUVECs treated with indomethacin. HUVECs were treated with indomethacin (3μM) and incubated at 37°C for 0-8 hr. Control cells were incubated at 37°C for 8 hr in serum free medium (SFM) + ethanol (EtOH) (0.01%). Caspase 9 (a); lane (1) molecular weight marker, (2) SFM + EtOH (0.01%), (3) 0 hr, (4) 1 hr, (5) 2 hr, (6) 4 hr, (7) 6 hr, (8) 8 hr, (9) 20 % foetal calf serum medium (complete medium). Caspase 3 (b); lane (1) Jurkat E6.1 cells treated with 50μM paclitaxel positive control, (2) molecular weight marker, (3) complete medium, (4) SFM + EtOH (0.01%), (5) 0 hr, (6) 1 hr, (7) 2 hr, (8) 4 hr, (9) 6 hr, (10) 8 hr. The images are representative of 3 experiments.

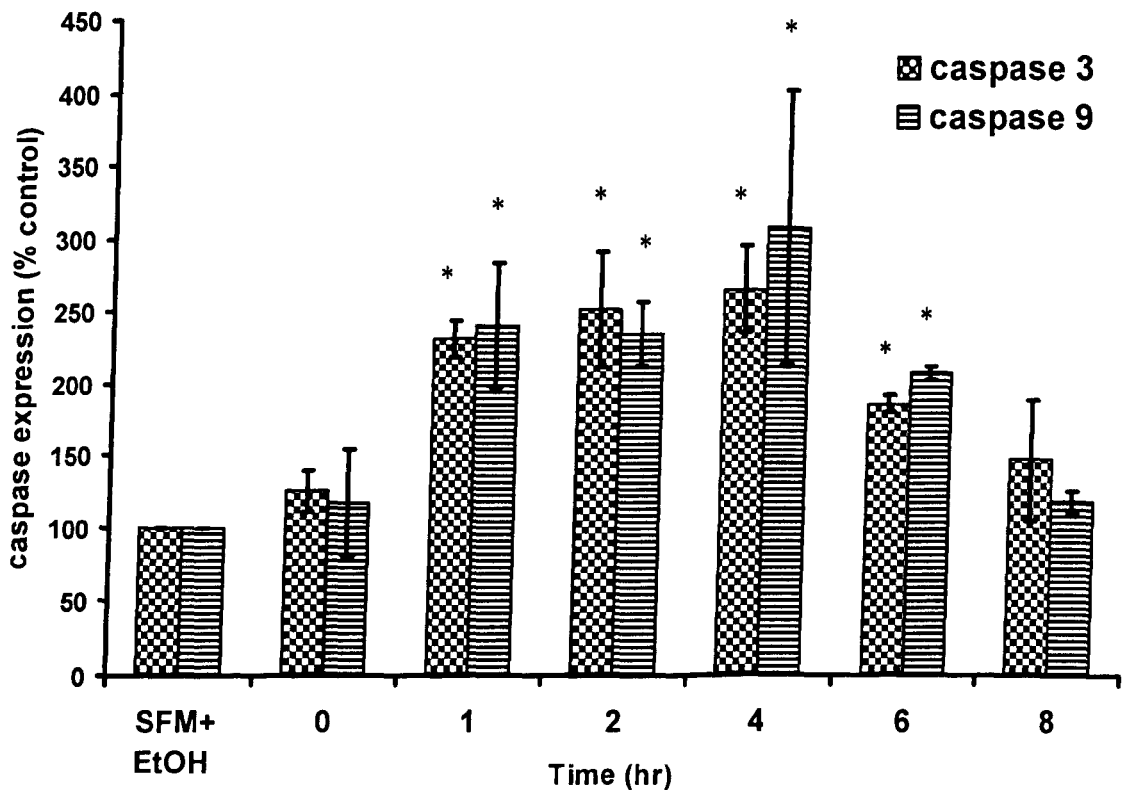


Figure 5.10c: Caspase expression in HUVECs treated with indomethacin. HUVECs were treated with indomethacin (3 μ M) and incubated at 37°C for 0-8 hr. Control cells were incubated at 37°C for 8 hr in serum free medium (SFM) + ethanol (EtOH) (0.01%). The data are the mean \pm s.e.m. of 3 experiments (caspase 9) and 2 experiments (caspase 3). ANOVA was used to determine significance for all the data with Student's t-test identifying the individual points of significance. Significance is compared to SFM + EtOH (0.01%) * $p < 0.05$.

5.4.7 Effects of PGE₂, VEGF₁₆₅ and CHO-DEVD on DuP-697 induced apoptosis in HUVECs

Prostaglandin E₂ (10 μ M) reversed chromatin condensation (Fig 5.11 and 5.12), caspase 8 and 9 activation (Fig 5.13) and DNA laddering (Fig 5.14) in HUVECs induced with DuP-

697 (10nM). A similar reversal was also observed following treatment of HUVECs with the specific caspase-3 inhibitor CHO-DEVD (12.5 μ M) as demonstrated by chromatin condensation (Fig. 5.11) and DNA laddering (Fig. 5.14). VEGF (50ng/ml) also reversed chromatin condensation (Fig. 5.15) and DNA laddering (Fig. 5.16).

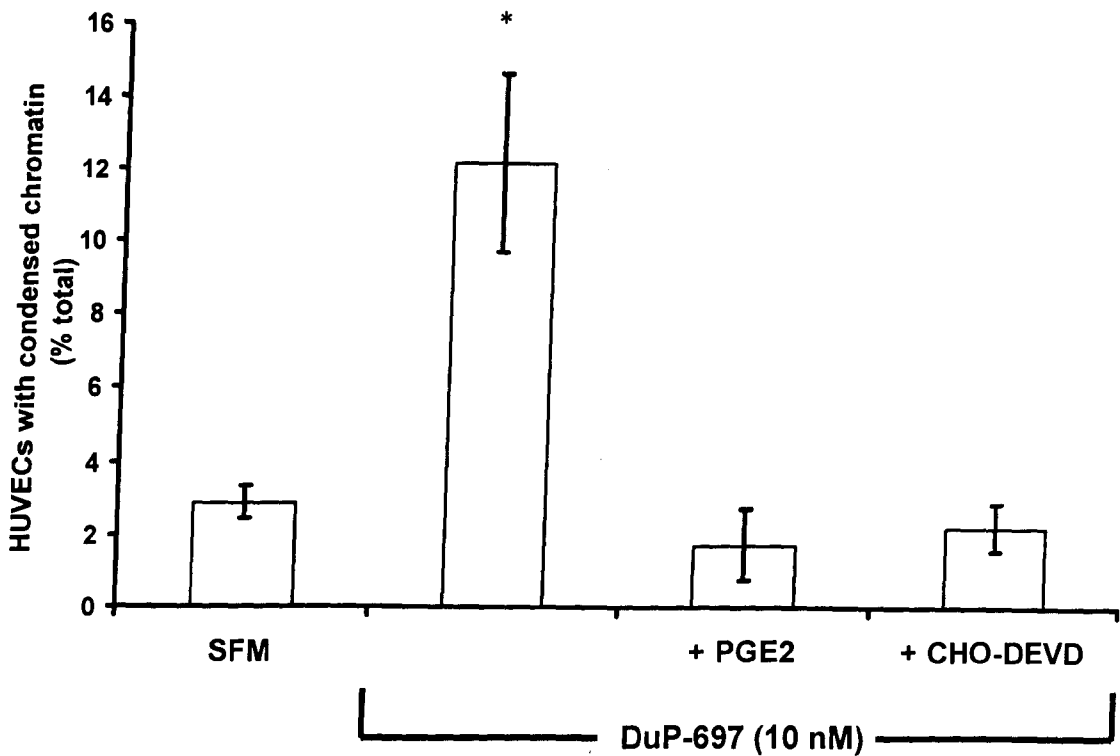


Figure 5.11: Reversal of DuP-697 induced chromatin condensation by PGE₂ and caspase 3 inhibitor (CHO-DEVD) in HUVECs. DuP-697 (10nM) treated cells were incubated at 37°C for 24 hr. In parallel experiments PGE₂ (10 μ M) or the caspase 3 inhibitor (CHO-DEVD) (12.5 μ M) were added to the HUVECs simultaneously with DuP-697 and incubated at 37°C for 24 hr. Cells were cytopun and stained with acridine orange. The data are the mean +/- s.e.m. of at least 3 experiments with 2 replicates in each. ANOVA was used to determine significance for all the data with Student's t-test identifying the individual points of significance. Significance is compared to serum free media (SFM) + DMSO (0.01%) * $p = < 0.05$.

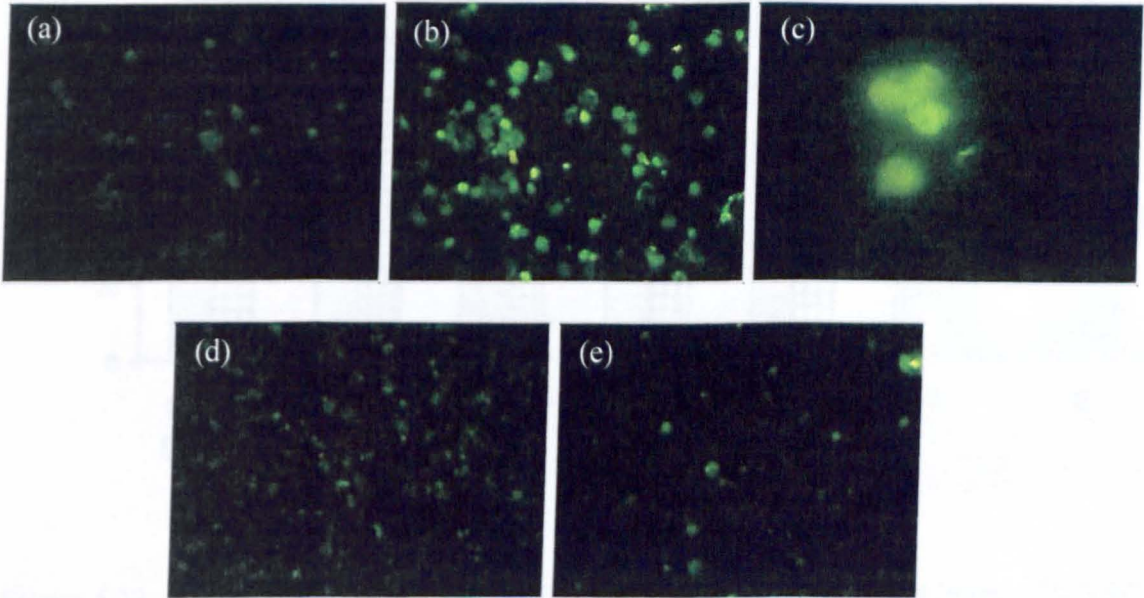


Figure 5.12: Reversal of DuP-697 induced chromatin condensation by PGE₂ and caspase 3 inhibitor (CHO-DEVD) in HUVECs. HUVECs were treated with DuP-697 (10nM) and incubated at 37°C in a tissue culture incubator for 24 hr (b) + (c). In parallel experiments PGE₂ (10µM) (d) or CHO-DEVD (12.5µM) (e) were added to the HUVECs simultaneously with DuP-697 and incubated at 37°C for 24 hr. Control cells (a) were incubated at 37°C for 24 hr in serum free medium (SFM) with DMSO (0.01%). HUVECs were cytopun and stained with acridine orange. The images are representative of 3 separate experiments.

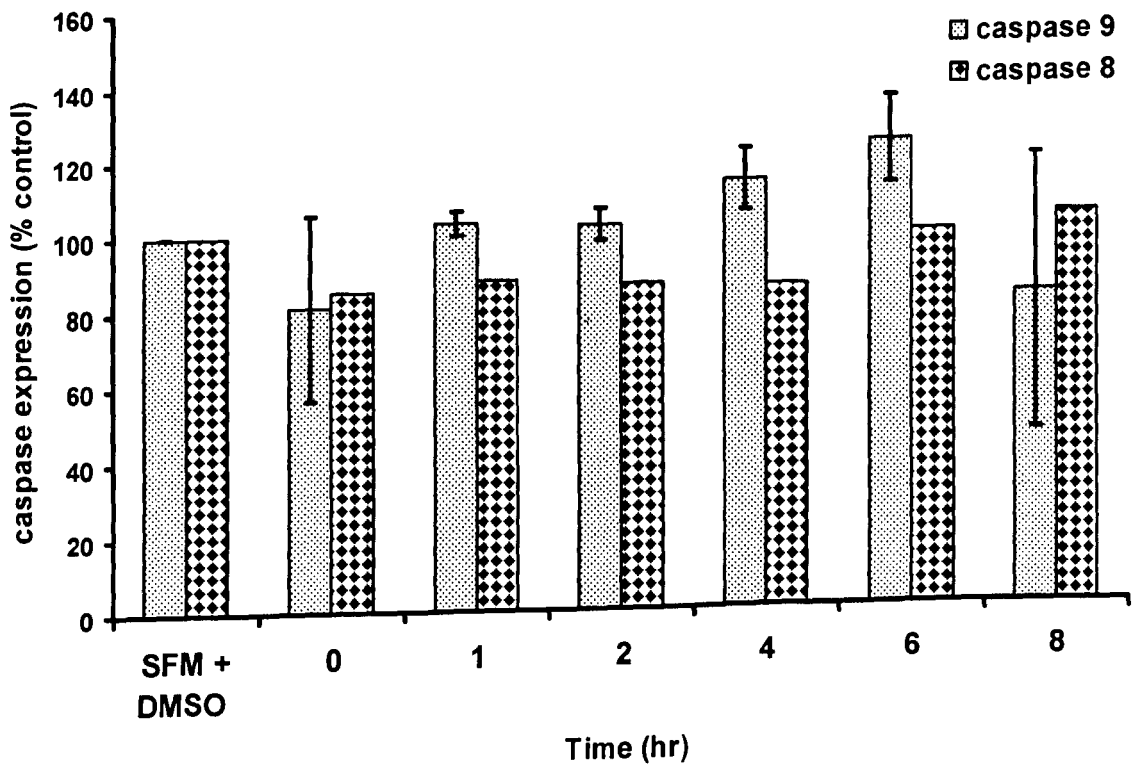


Figure 5.13: Caspase expression in HUVECs treated with DuP-697 and PGE₂. HUVECs were treated with DuP-697 (10nM) + PGE₂ (10μM) and incubated at 37°C for 24 hr. Control cells were incubated at 37°C for 24 hr with in serum free medium (SFM) + DMSO (0.01%). HUVECs were lysed and caspase expression was analysed by western blotting and densitometry. The data are the mean +/- s.e.m. of 3 experiments (caspase 9) and 2 experiments (caspase 8) respectively. ANOVA was used to determine significance for all the data with Student's t-test identifying the individual points of significance. Significance is compared to SFM + DMSO (0.01%) * $p < 0.05$.

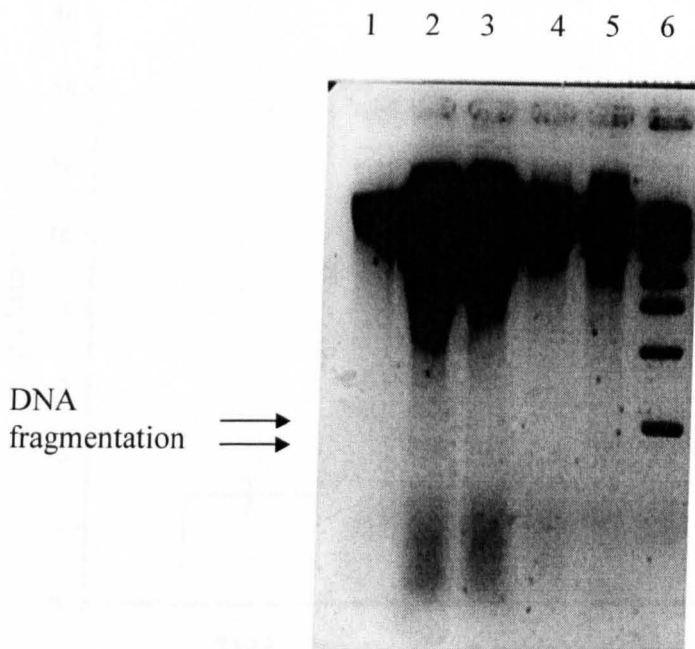


Figure 5.14: Induction of apoptotic DNA fragmentation in HUVECs. Control cells were incubated at 37°C for 24hr with DMSO (0.01%). DuP-697 (10nM) treated cells were incubated at 37°C for 24 hr. In parallel experiments PGE₂ or CHO-DEVD treatments were added simultaneously with DuP-697 and incubated for 24 hr at 37°C. Control cells were incubated at 37°C for 24 hr in serum free medium (SFM) with DMSO (0.01%). DNA was extracted using the phenol/chloroform method and visualised by 2% agarose gel electrophoresis stained with ethidium bromide. Lane (1) SFM + DMSO (0.01%) (2) Actinomycin- D (200nM) positive control (3) DuP-697 (10nM) (4) DuP-697 + PGE₂ (10 μM) (5) DuP-697 + CHO- DEVD (12.5 μM) (6) 1Kb Ladder. The image is representative of 3 separate experiments.

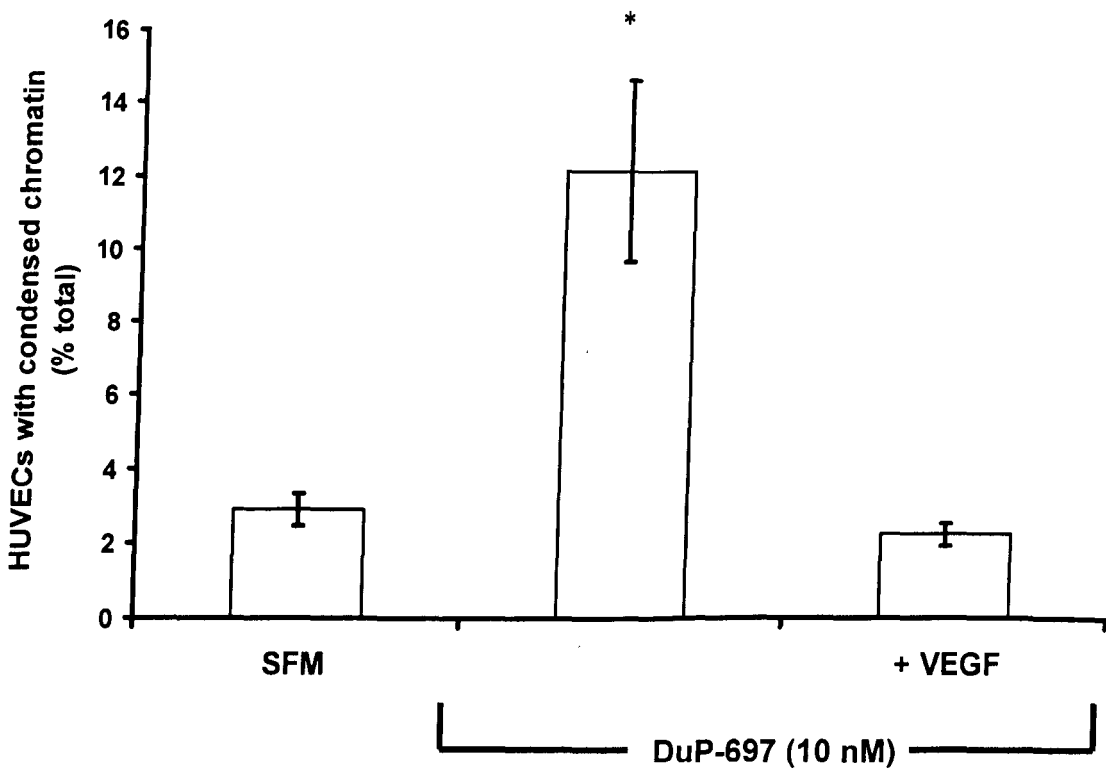


Figure 5.15a: Reversal of DuP-697 induced chromatin condensation by VEGF in HUVECs. DuP-697 (10nM) treated cells were incubated at 37°C for 24 hr. In parallel experiments VEGF (50ng/ml) was added to the HUVECs simultaneously with DuP-697 and incubated at 37°C for 24 hr. Control cells were incubated at 37°C for 24 hr in serum free medium (SFM) + DMSO (0.01%). HUVECs were cytospun and stained with acridine orange. The data are the mean +/- s.e.m. of 3 experiments with 2 replicates in each. ANOVA was used to determine significance for all the data with Student's t-test identifying the individual points of significance. Significance is compared to SFM + DMSO (0.01%) * $p < 0.05$.

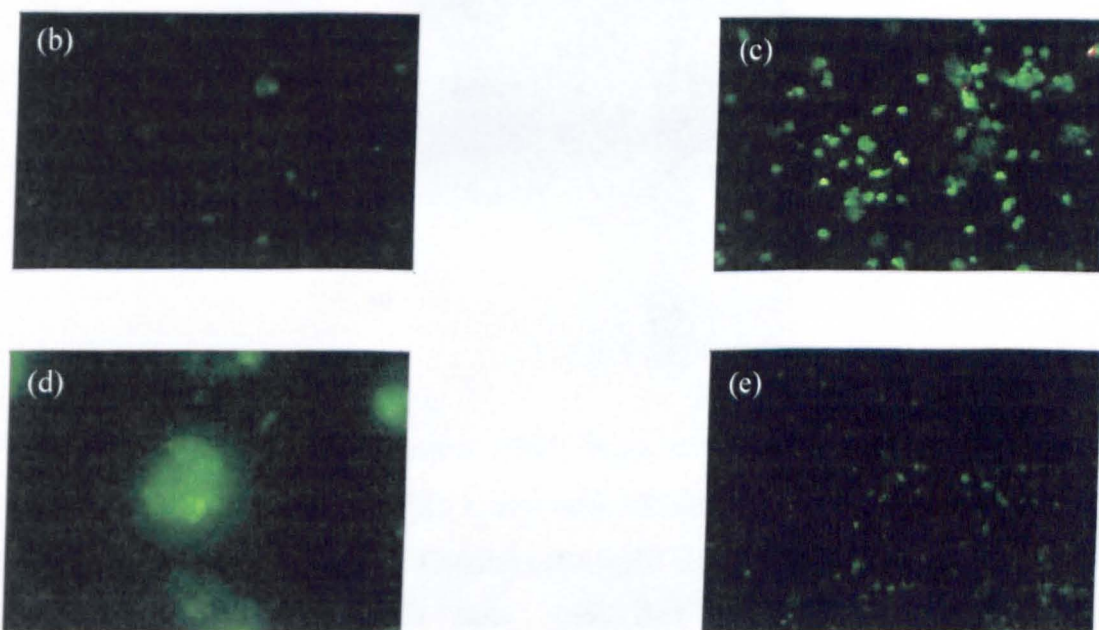


Figure 5.15b-e: Reversal of DuP-697 induced chromatin condensation by VEGF in HUVECs. DuP-697 (10nM) treated cells were incubated at 37°C in a tissue culture incubator for 24 hr (c) and (d). In parallel experiments VEGF (50ng/ml) was added to the HUVECs simultaneously with DuP-697 and incubated at 37°C for 24 hr (e). Control cells were incubated at 37°C for 24 hr in serum free medium (SFM) + DMSO (0.01%) (b). HUVECs were cytopun and stained with acridine orange. The images are representative of 3 separate experiments.

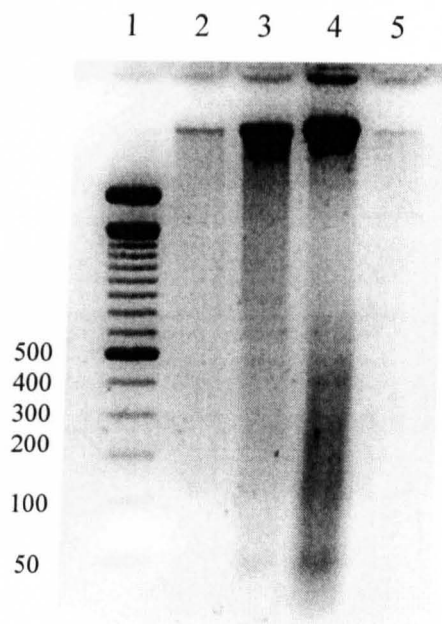


Figure 5.16: Induction of apoptotic DNA fragmentation in HUVECs. HUVECs treated with serum free medium (SFM) + DuP-697 (10nM) and/ or VEGF₁₆₅ (50ng/ml) were incubated for 24hr at 37°C. Control cells were incubated at 37°C for 24hr in SFM + DMSO (0.01%). HUVECs were lysed and DNA was extracted using the phenol/chloroform method and visualised by 2% agarose gel electrophoresis and staining with ethidium bromide. Lane (1) DNA Ladder (100 bp) (2) SFM + DMSO (0.01%) (3) Actinomycin- D (200nM) positive control (4) DuP-697 (10nM) (5) DuP-697 + VEGF₁₆₅ (50ng/ml). The image is representative of 3 separate experiments.

5.4.8 Induction of HUVEC membrane permeability by DuP-697

Cellular membrane permeability was assessed to assess cell viability using the trypan blue exclusion assay. Treatment for 24 hr with DuP-697 caused a dose dependent increase in the permeability of the HUVEC membrane to approximately 40% of all cells being stained (Fig 5.17).

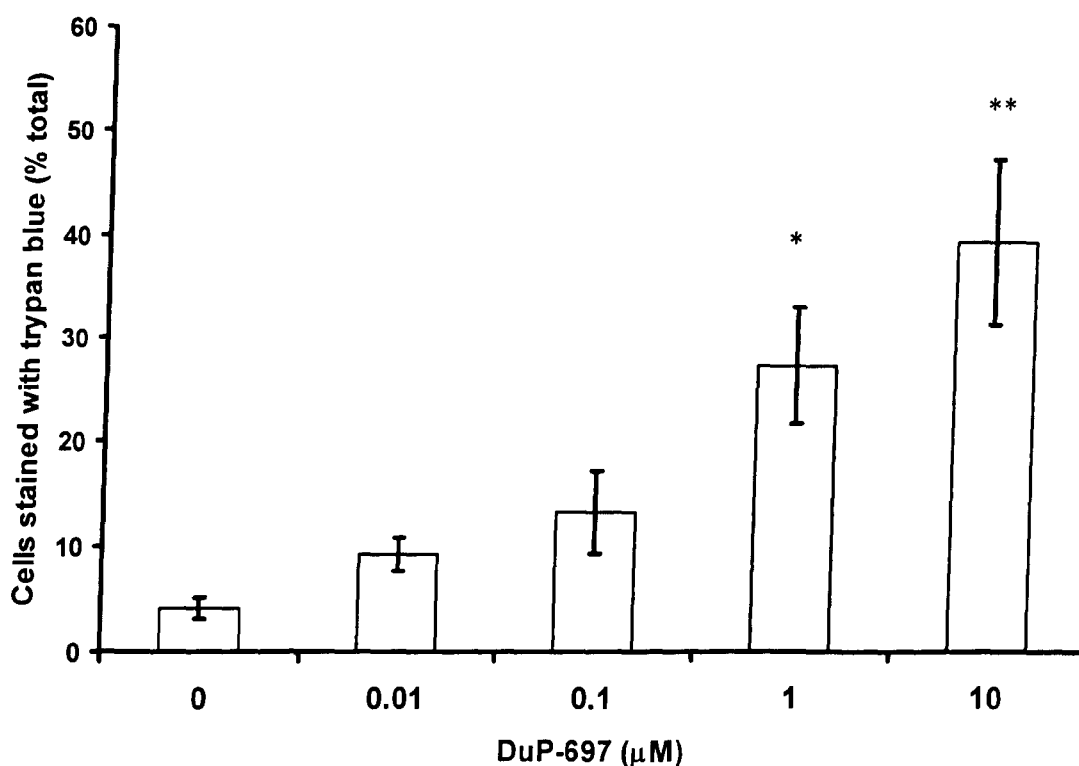


Figure 5.17: Induction of HUVEC membrane permeability by DuP-697. HUVECs treated with DuP-697 (0.01-10 µM) were incubated at 37°C for 24 hr. Control cells were incubated at 37°C for 24 hr in serum free medium (SFM) + DMSO (0.01%). HUVECs were counted by haemocytometer. The data are the mean +/- s.e.m. of 3 experiments with 2 replicates in each. ANOVA was used to determine significance for all the data with Student's t-test identifying the individual points of significance. Significance is compared to SFM + DMSO (0.01%) * $p < 0.05$, ** $p < 0.01$.

5.4.9 Effects of DuP-697 and indomethacin on tubule formation

Matrigel gel assays were used to assess angiogenic tubule formation of unstimulated and VEGF stimulated HUVECs (Fig 5.18). DMSO (0.01%) controls formed tubules in ECM gel (Fig 5.18a and b). DuP-697 (10nM) significantly inhibited the tubule formation of unstimulated HUVECs (Fig 5.18a and c). Prostaglandin E₂ (10μM) had no effect on tubule formation (Fig 5.18a and d) but significantly reversed the DuP-697 inhibition of tubule formation (Fig 5.18a and e). Activation of the HUVECs with VEGF (50ng/ml) increased the formation of the tubules relative to control levels (Fig 5.18a and f) and this increase was significantly reduced by DuP-697 (10nM) (Fig 5.18a and g). Addition of VEGF, PGE₂ and DuP-697 to HUVECs significantly increased tubule formation above control levels (Fig. 5.18a and h). The non-selective COX-2 inhibitor indomethacin only inhibited tubule formation at 3μM and above (Fig. 5.19a and 5.19b-i).

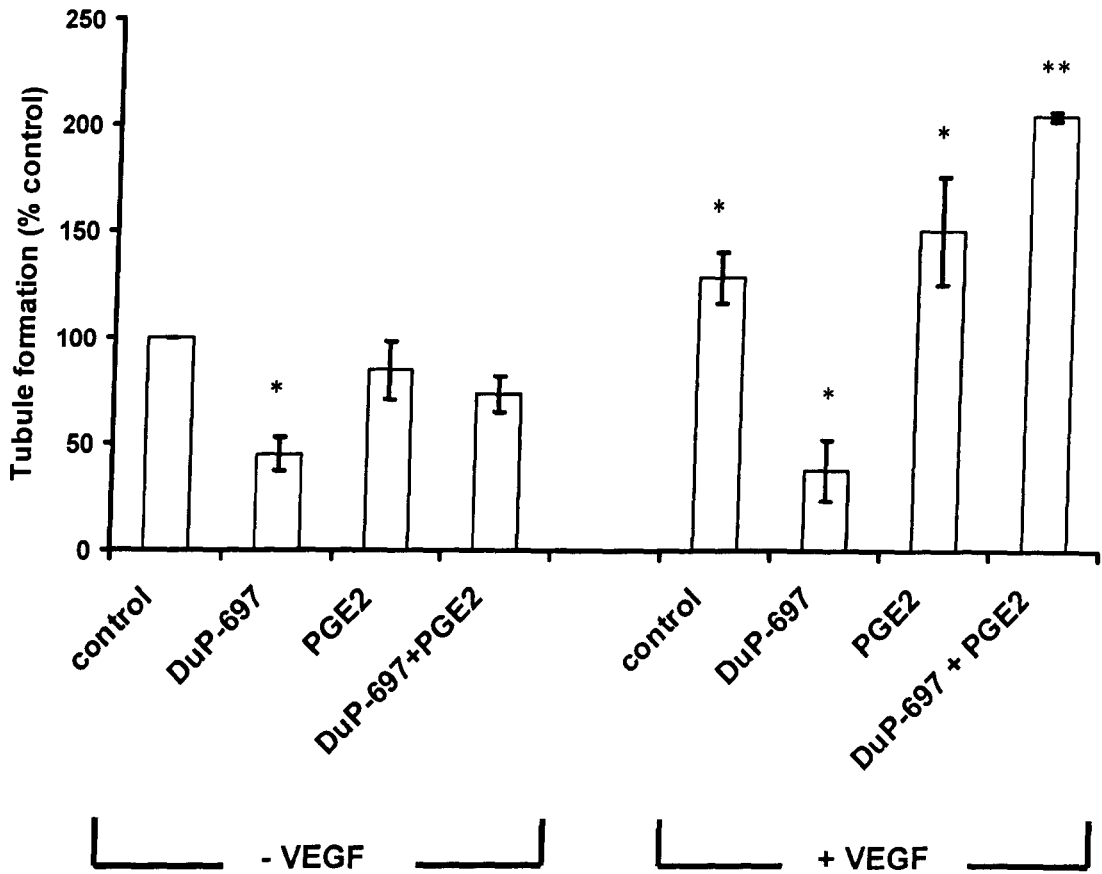


Figure 5.18a: Tubule formation of HUVECs treated with DuP-697. Treated HUVECs were incubated at 37°C for 8 hr. In parallel experiments PGE₂ (10µM) and/ or VEGF (50ng/ml) were added simultaneously with the DuP-697. Control cells were incubated at 37°C for 24 hr in 20% foetal calf serum medium 199 + DMSO (0.01%). The data are the mean +/- s.e.m. of at least 3 experiments with 2 replicates in each. ANOVA was used to determine significance for all the data with Student's t-test identifying the individual points of significance. Significance is compared to complete medium 199 + DMSO (0.01%) * $p < 0.05$, ** $p < 0.01$.

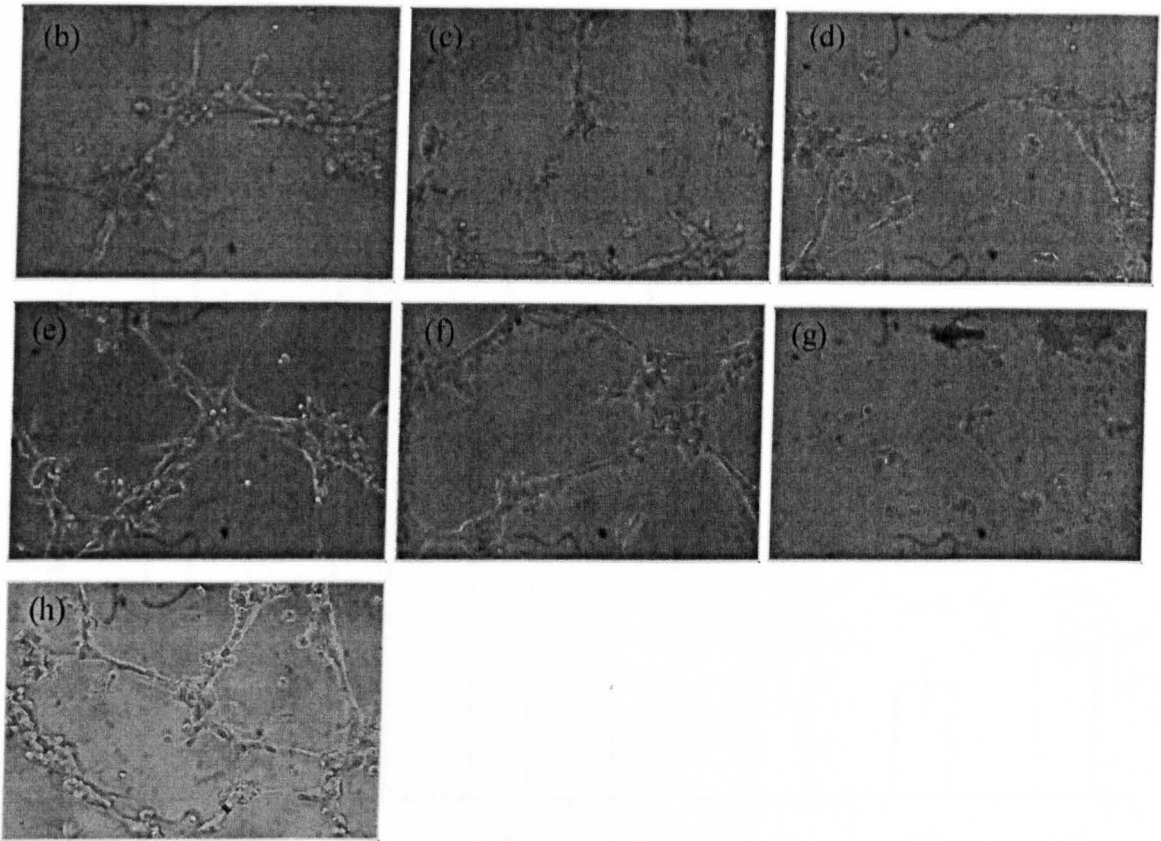


Figure 5.18b-h: Tubule formation of HUVECs treated with DuP-697. Control cells were incubated at 37°C for 24 hr in complete medium 199 + DMSO (0.01%) (b). Treated cells were incubated at 37°C for 8 hr. HUVECs were treated with DuP-697 (10nM) (c) or in the absence (d) or presence (e) of PGE₂ (10µM). HUVECs were treated VEGF (50ng/ml) in the absence (f) or presence (g) of DuP-697 and with a combination of all treatments (h). The images are representative of 3 separate experiments with 2 replicates in each experiment.

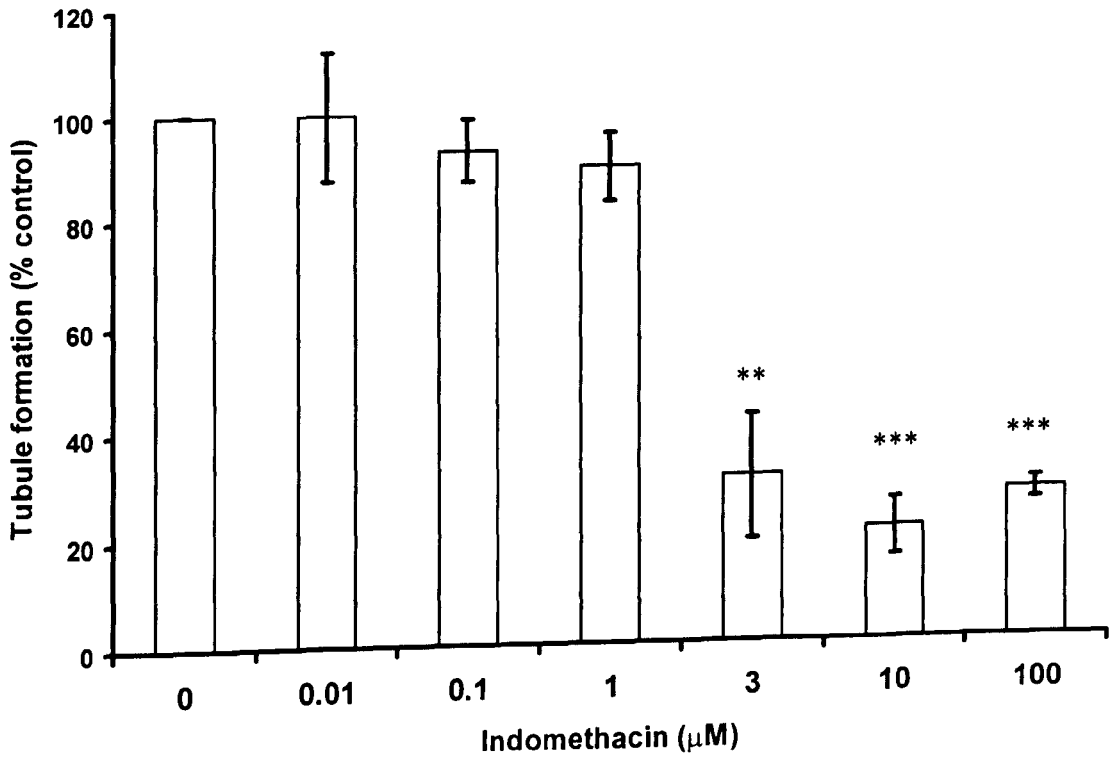


Figure 5.19a: Inhibition of HUVEC tubule formation by indomethacin. HUVECs were treated with indomethacin (0.01-100 µM) and incubated at 37°C for 8 hr. Control cells were incubated at 37°C for 24 hr in 20 % foetal calf serum medium (complete medium) with ethanol (EtOH) (0.01%). The data are the mean +/- s.e.m. of at least 3 experiments with 2 replicates in each. ANOVA was used to determine significance for all the data with Student's t-test identifying the individual points of significance. Significance is compared to complete medium 199 + EtOH (0.01%) * $p < 0.05$, ** $p < 0.01$, *** $p < 0.001$.

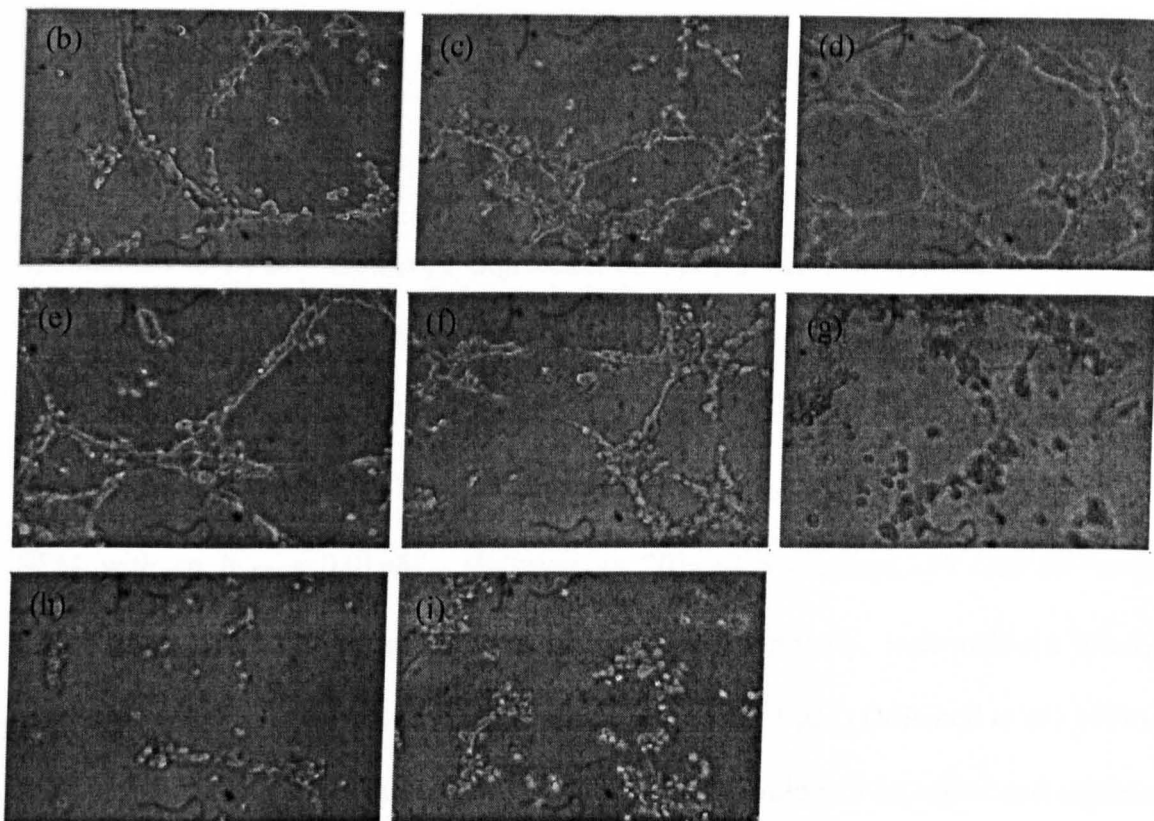


Figure 5.19b-i: Inhibition of HUVEC tubule formation by indomethacin. Untreated cells were incubated with 20 % foetal calf serum medium (complete medium) at 37°C for 8 hr (b). HUVECs treated with indomethacin 0.01 (d), 0.1 (e), 1 (f), 3 (g), 10 (h) and 100 μ M (i) were incubated at 37°C for 8 hr. Control cells were incubated at 37°C for 24 hr in complete medium + ethanol (EtOH) (0.01%) (c). The images are representative for 3 separate experiments with 2 replicates in each.

5.5 Discussion

The present studies show that DuP-697 induced apoptosis and inhibited capillary-like tubule formation in HUVECs. These effects were observed at a concentration of 10 nM DuP-697, the concentration equalling the IC_{50} value for inhibition of COX-2 activity *in vitro* (Gierse *et al.*, 1995).

COX-2 expression in HUVECs was induced by VEGF treatment over 8 hr and being maintained to 24 hr. However, expression of COX-2 was also seen in the untreated cells. This may be caused by the increased stress by trypsinisation of the cells or the incubation of the cells in SFM or 1% FCS medium 199 for 16 hr (Wheeler-Jones, 2005, personal communication). DuP-697 inhibited PGE₂ production dose dependently in SFM with an $IC_{50} = 0.01\mu\text{M}$. However, in 20% FCS medium 199 DuP-697 only inhibited ~ 20% of PGE₂ production in HUVECs. Similarly, indomethacin totally blocked PGE₂ production in SFM at the IC_{50} for COX-2 (3 μM) (Mitchell *et al.*, 1994). At this concentration of indomethacin 50% of COX-2 should still be active and capable of producing PGE₂. Further analysis of the PGE₂ concentrations from the SFM and 20% FCS medium studies indicate a 27% decrease in total PGE₂ production when HUVECs were incubated with SFM. This may possibly suggest that the enhanced inhibition of PGE₂ production seen in SFM by DuP-697 may be caused by a change in the expression levels of both COX-1 and COX-2. Incubation with SFM may increase COX-2 expression and decrease COX-1 expression. The change in expression profiles would decrease the production of COX-1 derived PGE₂ and make the majority of PGE₂ in the cells produced via COX-2. The effects seen by DuP-697 mediated inhibition of COX-2 would therefore be seem greater than the ~ 20% inhibition that was observed in

the 20% FCS medium studies. Parallel studies with DuP-697 on the inhibition of PGI₂ production gave no significant inhibition of PGI₂ levels in non-VEGF stimulated cells. However, in VEGF-stimulated cells a significant reduction of 20% was shown by 10 nM DuP-697. This indicates that in basal conditions COX-1 is responsible for the production of PGI₂ with COX-2 only producing PGI₂ under VEGF-stimulated conditions. Furthermore, this suggests that PGI₂ and PGE₂ production is regulated by the varying expression levels of COX-1 and COX-2 (Churchman *et al.*, 2006). To confirm this further research into the expression of COX-1 and COX-2 under stress conditions is required.

Results from various cell types indicate that inhibition of COX-2 is associated with the induction of apoptosis whereas the inhibition of COX-1 may not be involved. For instance, in U397 cells, inhibition of COX-1 did not induce apoptosis whereas inhibition of COX-2 was required to induce apoptosis *in vitro* (Riendeau *et al.*, 1997, Johnson *et al.*, 2001). In addition, COX-2 over-expression in endothelial cells has been shown to promote cell survival (Leahy *et al.*, 2002). In our studies we have found that the non-specific COX inhibitor indomethacin induced caspase activation and chromatin condensation only when used at concentrations known to inhibit COX-2 ($\geq 3 \mu\text{M}$; Mitchell *et al.*, 1994). This supports the notion that COX-2 may indeed be associated with cell survival and protection against apoptosis.

DuP-697 induced caspase dependent HUVEC chromatin condensation and DNA laddering. Similarly other selective COX-2 inhibitors, celecoxib and NS-398, have been shown to induce chromatin condensation and DNA fragmentation *in vitro* and *in*

vivo although at concentrations far higher than those reported to inhibit COX-2 *in vitro* (Wu *et al.*, 2003, Niederberger *et al.*, 2004, Zhang *et al.*, 2005).

In parallel with the above observations, the studies also revealed that PGE₂ or VEGF prevented the induction of chromatin condensation and DNA laddering in HUVECs by 10 nM DuP-697. Moreover, treatment of cells with VEGF stimulated PGE₂ production and resulted in a time-dependent induction of COX-2 protein which was only expressed at minimal basal levels in cells not stimulated with VEGF. These findings indicate that both PGE₂ and VEGF may protect against DuP-697 induced apoptosis in these cells. DuP-697 was able to inhibit PGE₂ production in HUVECs cultured in SFM and 20% FCS medium 199 by 50% and 23% when used at the concentrations that induced apoptosis, further suggesting a critical role for PGE₂ in cell survival. Previous studies have shown that exogenous PGE₂ can prevent apoptosis in HCA-7 human colon carcinoma cells induced by selective COX-2 inhibition (Sheng *et al.*, 1998). VEGF can induce expression of anti-apoptotic proteins Bcl-2 and A1 in HUVECs (Gerber *et al.*, 1998), which together with the actions of PGE₂ would suggest a pro-survival and anti-apoptotic actions of these two molecules.

Several studies implicate caspases as mediators of apoptosis induced by COX-2 inhibitors. Caspases 3, 8 and 9 were induced by DuP-697 in HUVECs and the apoptosis proved to be caspase 3 dependent as a selective caspase 3 inhibitor (CHO-DEVD) inhibited chromatin condensation and DNA fragmentation. Similarly, in several other studies, the induction of caspase dependent apoptosis by selective COX-2 inhibitors has been identified. For instance, Basu *et al.* (2005) and Dandekar *et al.* (2005) have

reported that 48 h treatment of MDA-MB-231, MDA-MB-468 breast cancer cells and PC3-MC prostate cancer cells respectively with celecoxib resulted in caspase 3, 7 and 9 activation during apoptosis.

Three possible pathways of caspase activation have been suggested in cells treated with selective COX-2 inhibitors. Selective COX-2 inhibitors (NS-398, celecoxib, rofecoxib) have been shown to inhibit cell signalling e.g. Akt and ERK, prevent production of PGE₂ and inhibit anti-apoptotic Bcl-2 protein expression (Ghosh *et al.*, 2000, Hsu *et al.*, 2000, Johnson *et al.*, 2001, Basu *et al.*, 2005). Nor *et al.* (1999) and Pai *et al.* (2001) have suggested that this inhibition of PGE₂ may lead to decreases in Bcl-2 protein expression and promote the mitochondrial pathway of apoptosis.

PGE₂ is also an important mediator in integrin binding to the ECM. Inhibition of PGE₂ decreases the expression of $\alpha\beta$ 3 integrin (Dormond *et al.*, 2002). The inhibition of $\alpha\beta$ 3 integrin binding to the ECM may result in two pathways being activated (1) inhibition of anti-apoptotic Bcl-2 protein expression, which precedes the activation of mitochondrial pathway apoptosis (Pollman *et al.*, 1999, Dormond *et al.*, 2002). (2) Fas receptor (Fas R) trimerisation and the activation of caspase 8 through the death receptor pathway of apoptosis (Aoudjit *et al.*, 2001).

It has also been shown that COX-2 sequesters p53 inhibiting apoptosis. Selective inhibition of COX-2 prevented the binding of p53 and increasing active caspase 9 expression (Choi *et al.*, 2001). Furthermore, in other studies Li *et al.* (2001) identified the mechanism for selective COX-2 inhibitor induced caspase activation in SW480 and

SW620 colon carcinoma cells as cyt-c and caspase 9 dependent. These two findings imply that COX-2 may be important in preventing mitochondrial permeability.

In relation to these three possible mechanisms of caspase activation, our findings that both caspase 8 and 9 were induced within 1 hr of DuP-697 treatment can support all of the mechanisms suggested. However, disruption of the $\alpha v\beta 3$ -ECM binding appears to promote the induction of both caspase 8 and 9 at the same time, which is similar to the current data. The decrease in integrin binding may induce an inhibition of anti-apoptotic Bcl-2 protein expression and promote Fas R trimerisation increasing the activation of caspase 9 and caspase 8 respectively. This suggestion would explain the activation of dual initiator caspases in the present study with no predominant apoptotic pathway being obvious.

Caspase activation may also be caused by the other possible mechanisms as stated above. Inhibition of COX-2 by DuP-697 is non-competitive (Rosenstock *et al.*, 1999), possibly changing the conformation of the enzyme by allosterism and preventing AA from entering the active site. If the conformation of COX-2 was changed this may also prevent COX-2 binding other proteins, for instance p53. The prevention of COX-2 binding would leave p53 to act as a transcription factor for the pro-apoptotic Bcl-2 proteins and increase mitochondrial pathway of apoptosis and activating caspase 9 (Choi *et al.*, 2001; Li *et al.*, 2001). Furthermore, this pathway would be promoted by a decrease in anti-apoptotic Bcl-2 proteins caused by a loss of PGE₂ production (Ghosh *et al.*, 2000, Hsu *et al.*, 2000, Johnson *et al.*, 2001, Basu *et al.*, 2005). However, this would possibly lead to a large increase in caspase 9 expression, which is not seen in the

current work. Further research would have to be conducted into the expression of Bcl-2 proteins and p53 sequestering to confirm the involvement of these pathways.

Selective COX-2 inhibition may promote the induction of HUVEC apoptosis as was further confirmed with indomethacin. In these studies indomethacin induced apoptotic chromatin condensation and caspase activation only at concentrations that inhibited COX-2 ($> 3\mu\text{M}$) (Mitchell *et al.*, 1994). However whether PGE₂ inhibition is the cause of the induction of apoptosis is unclear since indomethacin ($0.125\mu\text{M}$) inhibited PGE₂ production by 50% without inducing apoptosis. This concentration of indomethacin does not inhibit COX-2 activity (Mitchell *et al.*, 1994). It therefore may be suggested that PGE₂ may not be the only contributing factor in HUVEC survival, but it is clear that COX-2 activity is very important in cellular homeostasis.

COX-2 has been shown to be important in angiogenesis whereas COX-1 has no effect on this process (Bryant *et al.*, 1998; Pentland *et al.*, 2004). Treatment of HUVECs with DuP-697 (10 nM) prevented capillary-like tubule formation *in vitro* whereas the non-specific COX inhibitor indomethacin only inhibited angiogenesis at concentrations known to inhibit COX-2 ($\geq 3\mu\text{M}$). These data suggest that COX-2 is required for tubule formation. This action may be related to PGE₂ production since inhibition of tubule formation by DuP-697 was reversed by exogenous PGE₂ in our studies. Similarly, Leahy *et al.*, (2002) found that PGE₂ prevented the inhibition of *in vivo* rat cornea angiogenesis by celecoxib. PGE₂ has been shown to increase binding of endothelial cells to the ECM through $\alpha\beta 3$ dependent mechanism (Leahy *et al.*, 2002;

Yazawa *et al.*, 2005). Together with the present study these findings suggest a strong link between angiogenesis and PGE₂ production.

PGE₂ may induce VEGF expression through binding to the EP4 receptor and activating the JNK and HIF-1 α pathways (Ghosh *et al.*, 2000, Kuwano *et al.*, 2004, Huang *et al.*, 2005). Once induced, VEGF enhances COX-2 expression forming a positive feedback loop that regulates both VEGF production and COX-2 induction (Caughey *et al.*, 2001). The products of COX-2, including PGE₂ and TXA₂ may then play an important role in cellular migration and tubule formation and specific inhibition of PGE₂ and TXA₂ prevents proliferation and angiogenesis (Wu *et al.*, 2003, Jantke *et al.*, 2004). However, the induction of tubule formation by PGE₂ is probably independent of VEGF induction since there was no reversal of the inhibition of tubule formation in the presence of DuP-697 by VEGF. This suggests that PGE₂ may have a separate signalling pathway to affect tubule formation.

Similarly, previous studies with selective COX-2 inhibitors e.g. celecoxib and NS-398 have shown an inhibition of COX-2 activity, prostaglandin and thromboxane production and capillary-like tubule formation *in vitro* and angiogenesis *in vivo* by decreasing $\alpha v \beta 3$ integrin expression and binding to the ECM (Pollman *et al.*, 1999, Ghosh *et al.*, 2000, Dormond *et al.*, 2002, Leahy *et al.*, 2002, Yazawa *et al.*, 2005). Furthermore the inhibition of $\alpha v \beta 3$ integrin expression and binding to the VEGFR-2 decreased receptor phosphorylation upon VEGF₁₆₅ activation (Soldi *et al.*, 1999) preventing VEGFR-2 signalling; supporting our findings that VEGF₁₆₅ did not reverse DuP-697 inhibition of angiogenesis without PGE₂ treatment.

In summary, the selective COX-2 inhibitor DuP-697 has been found to induce apoptosis and prevent capillary-like tubule formation *in vitro* at pharmacologically relevant concentrations. The effects observed have been shown to be probably caused by the specific inhibition of COX-2. The induction of apoptosis is possibly caused by the inhibition of PGE₂ and $\alpha\text{v}\beta\text{3}$ integrin binding to the ECM. However this has to be fully established by further experimentation. The inhibition of capillary-like tubule formation does appear to be strongly linked to the expression of COX-2 derived PGE₂ possibly through a mechanism of $\alpha\text{v}\beta\text{3}$ integrin binding. The importance of other COX-2 metabolites that are expressed and the effects on angiogenesis must not be ruled out and further study must be done to confirm the role of PGE₂ and other COX-2 metabolites in tubule formation.

6.0 Isolation, growth and transfection of the apoptosis repressor with caspase recruitment domain (ARC)

6.1 *Introduction*

Apoptosis repressor with caspase recruitment domain (ARC) is a novel endogenous apoptosis inhibitor found to have high sequence similarity to some caspase binding proteins e.g. APAF-1 and FADD. The structural similarity observed by ARC causes interaction with pro-caspases and pro-apoptotic proteins e.g. Bax and APAF-1 preventing the activation of caspases and therefore apoptosis as described in section 1.3.5.1. Expression of the *ARC* gene has been characterised in heart and brain tissue in humans and varies in expression levels depending on cellular environment and experimental conditions. Expression in heart tissue may indicate that the vascular system may express ARC; however the vascular system beyond the heart tissue has not been tested for ARC. Possible ARC expression in endothelium may explain the slow cellular turnover rate and would give insight in to the mechanisms of endothelial cell apoptosis.

Transfection of primary HUVECs has been found to be difficult with cells not recovering from the procedure or not taking up sufficient plasmid to express the protein. Methods for the transfection of primary HUVECs therefore will have to be optimised before ARC transfection takes place.

6.2 *Aims*

- To isolate the plasmid containing the *ARC* gene.
- Transformation of competent bacteria with the *ARC* gene.
- To assess the size of *ARC* gene insert.
- To transfect primary HUVECs with the *ARC* gene.

6.3 *Methods*

- Plasmid pCDNA-3 containing the *ARC* gene was given as a gift from Professor Chen Xi (Division of Biochemistry, Cardiovascular Institute and Fu Wai Hospital, Chinese Academy of Medical Sciences & Peking Union Medical College, Beijing, China) on filter paper and was regenerated as described in Section 2.7.2.
- Preparation of competent cells and the pCDNA3-ARC and the transformation of competent DH5 α *E.coli* have all been described in Section 2.6.
- Restriction analysis (Section 2.6.6) was designed using the webcutter program and completed using Hinc II, Xba I, Not I, Hind III and Shb I digestions in a 10 μ l reaction with a concentration of 0.5 units/ μ l of restriction enzyme and analysed on a 1% agarose gel.
- Transfection methods used were as described in Section 2.7 and were optimised using green fluorescent protein and UV microscopy then ARC was transfected in to HUVECs.
- ARC expression in HUVECs was confirmed using western blotting (Section 2.4) with an anti-ARC rabbit polyclonal antibody (Merck biosciences) at a concentration of 1 μ g/ml.

6.4 Results

6.4.1 Expression of the ARC protein in HUVECs

Freshly isolated HUVECs from umbilical cords were lysed and different amounts of protein loaded on polyacrylamide gel during western blotting. Freshly isolated HUVECs were found to express ARC protein as determined by western blotting (Fig 6.1). Parallel samples from HUVECs grown in 20% FCS media over time (p0-p5) did not express the ARC protein (Fig 6.2- 6.4). HUVECs treated over 24 hr with serum free media also did not express the ARC protein (Fig 6.5).

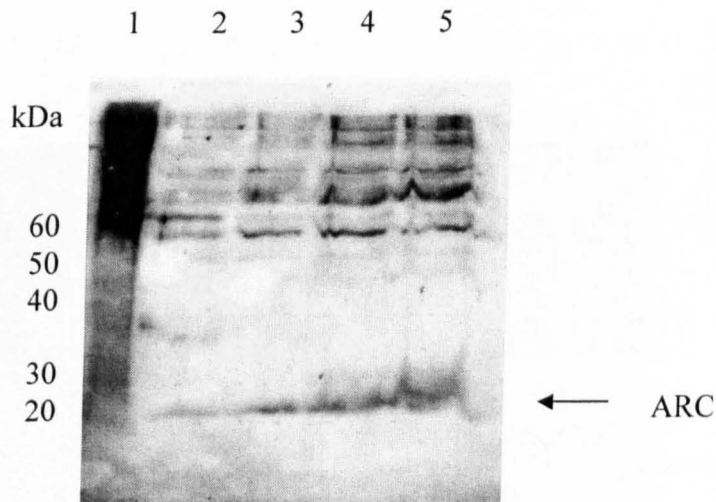


Figure 6.1: The expression of ARC in freshly isolated HUVECs. Lane (1) Molecular weight marker, (2) Freshly isolated HUVECs 20μg protein, (3) 40μg protein, (4) 60μg protein, (5) 80μg protein. The blot is representative of 3 separate experiments.

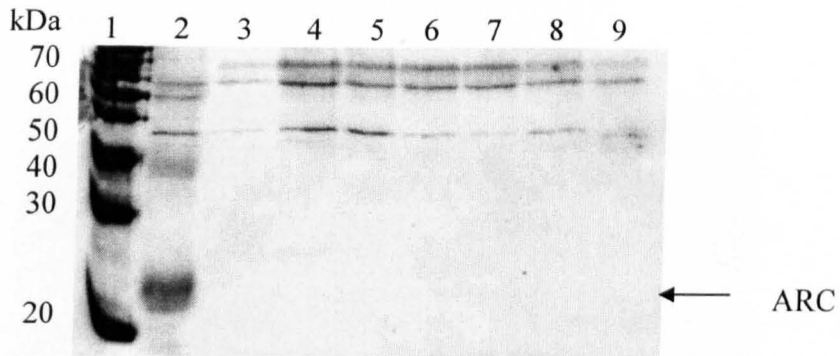


Figure 6.2: The expression of ARC in passage 0 HUVECs grown in 20% FCS medium 199 for up to 24 hr. Control cells were treated with 20% FCS medium 199. All other cells were quiesced for 16 hr with 1% FCS medium 199 for 16 hr before treatment with 20% FCS medium 199. Lane (1) Molecular weight marker, (2) Freshly isolated HUVECs, (3) control, (4) 0 hr, (5) 1 hr, (6) 2 hr, (7) 4 hr, (8) 8 hr, (9) 24 hr. The blot is representative of 3 experiments.

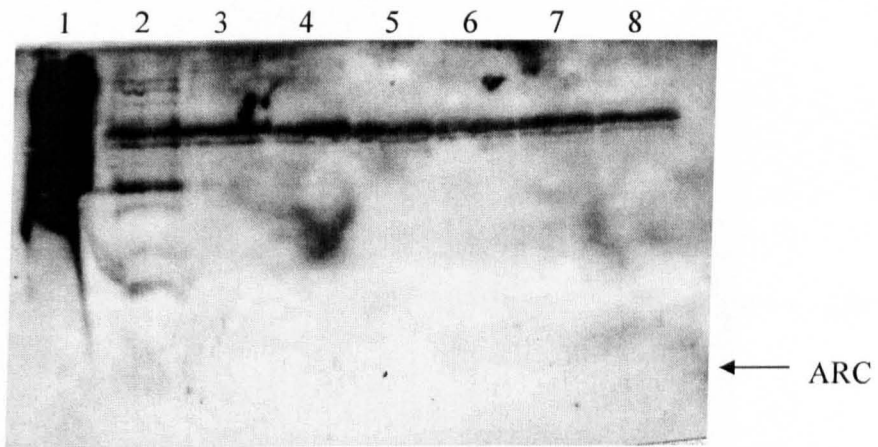


Figure 6.3: The expression of ARC in passage 1 HUVECs grown in 20% FCS medium 199 for up to 24 hr. Control cells were treated with 20% FCS medium 199. All other cells were quiesced for 16 hr with 1% FCS medium 199 for 16 hr before treatment with 20% FCS medium 199. Lane (1) Molecular weight marker, (2) control, (3) 0 hr, (4) 1 hr, (5) 2 hr, (6) 4 hr, (7) 8 hr, (8) 24 hr. The blot is representative of 3 experiments.

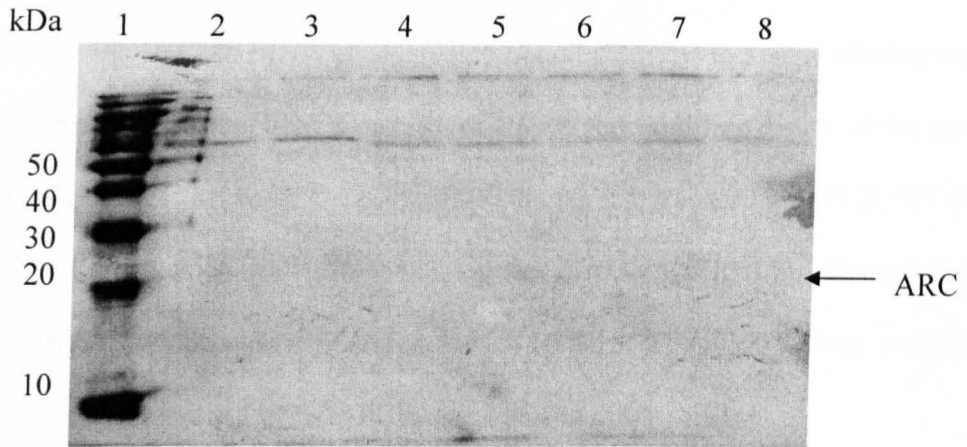


Figure 6.4: The expression of ARC in passage 5 HUVECs grown in 20% FCS medium 199 for up to 24 hr. Control cells were treated with 20% FCS medium 199. All other cells were quiesced for 16 hr with 1% FCS medium 199 for 16 hr before treatment with 20% FCS medium 199. Lane (1) Molecular weight marker, (2) control, (3) 0 hr, (4) 1 hr, (5) 2 hr, (6) 4 hr, (7) 8 hr, (8) 24 hr. The blot is representative of 3 experiments.

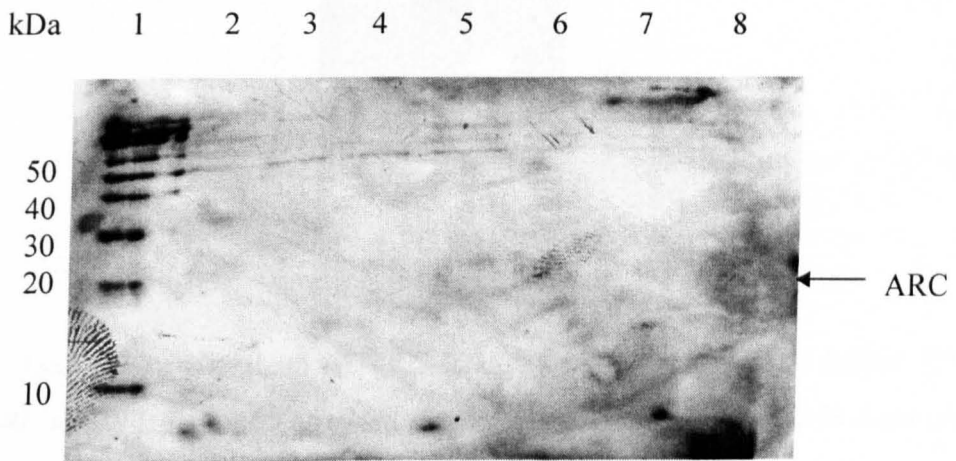


Figure 6.5: The expression of ARC in passage 5 HUVECs grown in 0% FCS medium 199 for up to 24 hr. Control cells were treated with 20% FCS medium 199. Lane (1) Molecular weight marker, (2) control, (3) 0 hr, (4) 1 hr, (5) 2 hr, (6) 4 hr, (7) 8 hr, (8) 24 hr. Image is representative of 3 experiments.

6.4.2 Analysis of *ARC* RNA transcription in HUVECs

Due to HUVECs not expressing the ARC protein in cultured cells RNA was extracted, as identified by the 18s and 28s rRNA bands, (Fig 6.6) and analysed to assess whether control of *ARC* gene expression is between transcription of the gene and translation of the protein. Following on from previous work (McKay, 2004) the reverse transcription-PCR (RT-PCR) of the HUVEC RNA at 55°C gave a 400 bp fragment of cDNA (Fig 6.7). Optimisation of the RT-PCR with different annealing temperatures, 50°C, 55°C and 60°C only produced a similar 400 bp cDNA band at the 50°C PCR reaction (Fig 6.8).

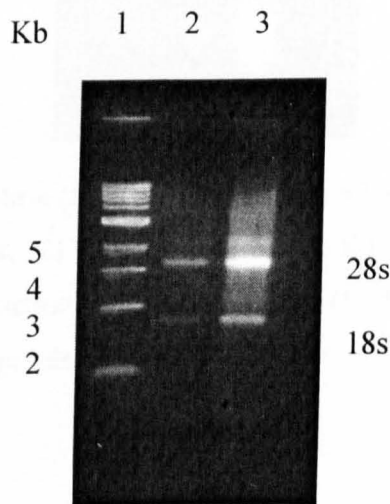


Figure 6.6: Isolation of passage 5 HUVEC RNA. Lane (1) 1 Kb DNA ladder, (2) 1:5 dilution of RNA, (3) 1:1 dilution of RNA. Samples were analysed on 1.2 % Agarose gel electrophoresed at 80v. The image is representative of 3 separate experiments.

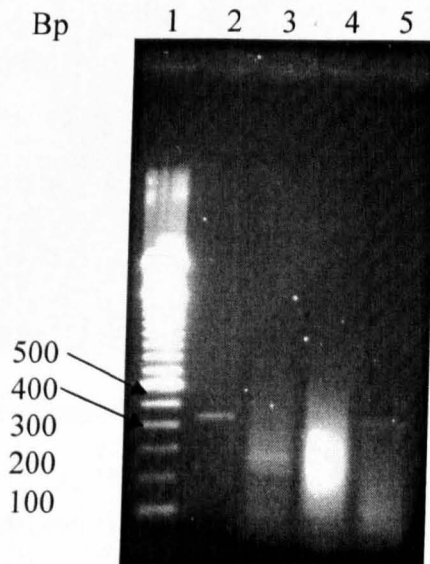


Figure 6.7: Reverse transcriptase (RT)-PCR of passage 5 HUVEC RNA for the *ARC* gene. Lane (1) 100 bp DNA ladder, (2) positive control (McKay, 2004) (3) Reaction – AMV-reverse transcriptase, (4) Reaction – RNA template, (5) 55°C reaction. Samples were analysed on 1.2 % Agarose gel electrophoresed at 80v. The image is representative of 3 separate experiments.

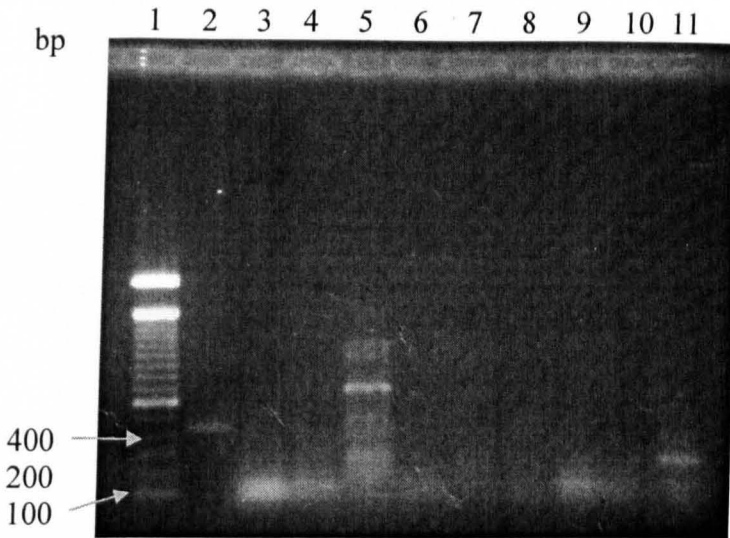


Figure 6.8: Reverse transcriptase (RT)-PCR of passage 5 HUVEC RNA using a gradient of annealing temperature. Lane (1) 1 Kb DNA ladder, (2) positive control (McKay, 2004) (3) 50°C reaction – AMV-reverse transcriptase, (4) 50°C reaction – RNA template, (5) 50°C reaction, (6) 55°C reaction – AMV-reverse transcriptase, (7) 55°C reaction – RNA template, (8) 55°C reaction, (9) 60°C reaction – AMV-reverse transcriptase, (10) 60°C reaction – RNA template, (11) 60°C reaction. Samples were analysed on 1.2 % Agarose gel electrophoresed at 80v. The image is representative of 3 separate experiments.

6.4.3 Transformation of competent *DH5α E.coli* with *ARC*

The plasmid pCDNA3-ARC was soaked from the filter paper in TE buffer and transformed into competent *DH5α E.coli*. After 24 hr incubation in ampicillin supplemented Luria-Bertani (LB) broth and mini prep isolation the plasmid was found to be amplified in the bacteria. Agarose gel analysis was run with 4:1 dilution of samples with loading buffer (Fig 6.9).

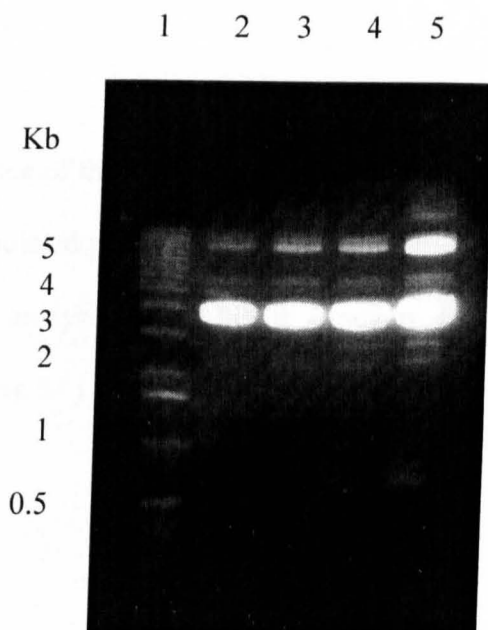


Figure 6.9: Isolation of pCDNA3-ARC from transfected DH5 α *E.coli* indicating the presence of the plasmid. Lane (1) 1Kb DNA ladder (2) Isolation 1 (0.16 μ g/ μ l DNA), (3) Isolation 2 (0.24 μ g/ μ l DNA), (4) Isolation 3 (0.24 μ g/ μ l DNA), (5) Isolation 4 (0.24 μ g/ μ l DNA). The image is representative of 3 experiments.

6.4.4 Restriction of pCDNA3-ARC isolated from transformed DH5 α *E.coli*

Treatment with Hinc II resulting in fragments of 200 bp, 661 bp, 840 bp, 1500 bp, 2274 bp, 3199 bp, and 3825 bp and possibly cut the *ARC* insert. Digestion with Xba I failed to restrict the plasmid as no bands except the control plasmid were visible on the gel. The Not I enzyme cut the plasmid giving two fragments of 7396 bp and 6000 bp. Hind III restriction gave 6000 bp and 820 bp fragments. Shb I restricted the plasmid resulting in fragments of 5233 bp, 804 bp and 583 bp (Fig 6.10). The Not I restriction digest indicated

that the size of the complete pCDNA3-ARC was approximately 7396 bp and with the size of pCDNA3 being 5446 bp (Invitrogen Life Technologies) estimated the size of the *ARC* gene insert as 1950 bp.

To confirm the presence of the *ARC* gene and to further confirm the size of the *ARC* gene insert the mini-prep isolated pCDNA3-ARC was amplified using *ARC* specific primers by PCR. Agarose gel analysis of the PCR products gave one major DNA band of approximately 2 Kb (Fig 6.11).

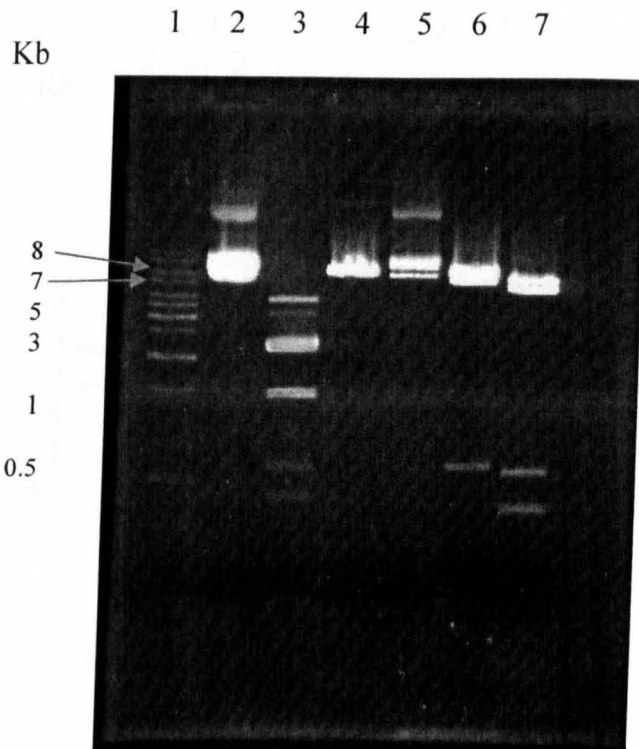


Figure 6.10: The digestion of pCDNA3-ARC with restriction enzymes to size the *ARC* gene insert in the pCDNA3.1 plasmid. Lane (1) 1Kb ladder, (2) pCDNA3-ARC, (3) Hinc II digestion, (4) Xba I digestion, (5) Not I digestion, (6) Hind III digestion, (7) Shb I digestion. The image is representative of 3 separate experiments.

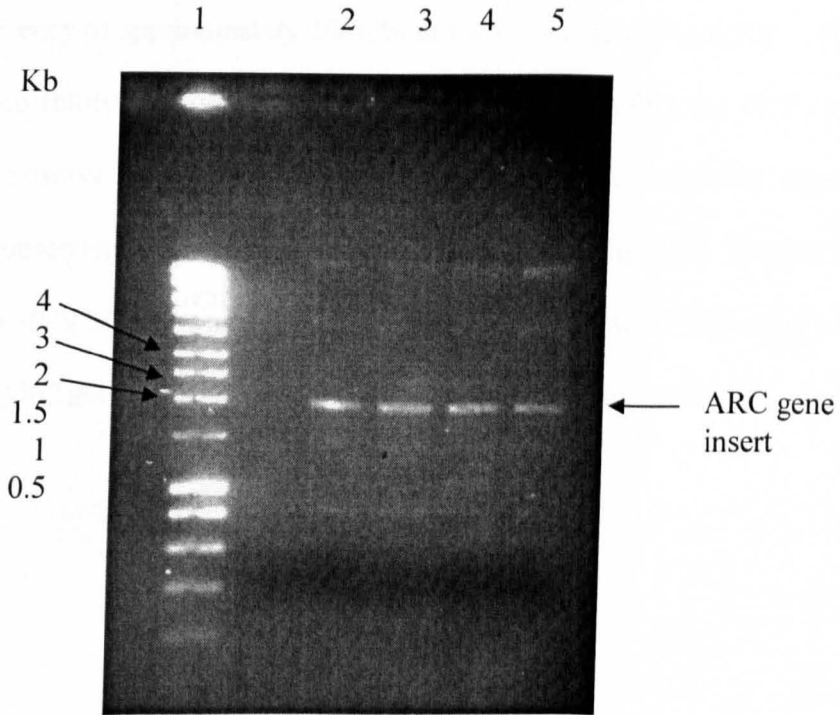


Figure 6.11: The PCR amplification of *ARC* gene insert from the isolated pCDNA3-*ARC* plasmid, indicating the presence of the *ARC* gene. Lane (1) 1 Kb ladder, (2) Plasmid isolation 1, (3) Plasmid isolation 2 (4) Plasmid isolation 3, (5) Plasmid isolation 4. Image is representative of 3 separate experiments.

6.4.5 *Transfection of HUVECs with pCDNA3-ARC*

Following the successful identification of the ARC gene in the pCDNA3-ARC construct cultured HUVECs (passage 1-4), which do not express ARC, were optimised for transfection with ARC using a number of techniques and the pCDNA3.1-GFP plasmid. HUVEC transfection using the JetPEI-HUVEC transfection reagent (Section 2.7.8) gave a transfection efficiency of approximately 20-30% of the cells plated (Fig 6.12). Following recombinant green fluorescent protein (GFP) expression in HUVECs the GFP expression was used as a positive control for successful transfection of following experiments. HUVECs were subsequently transfected with pCDNA3-ARC (Fig 6.13). Further analysis of the transfected HUVECs by western blotting gave a single protein band using a specific monoclonal anti-ARC antibody at approximately 30 kDa in size (Fig 6.14).

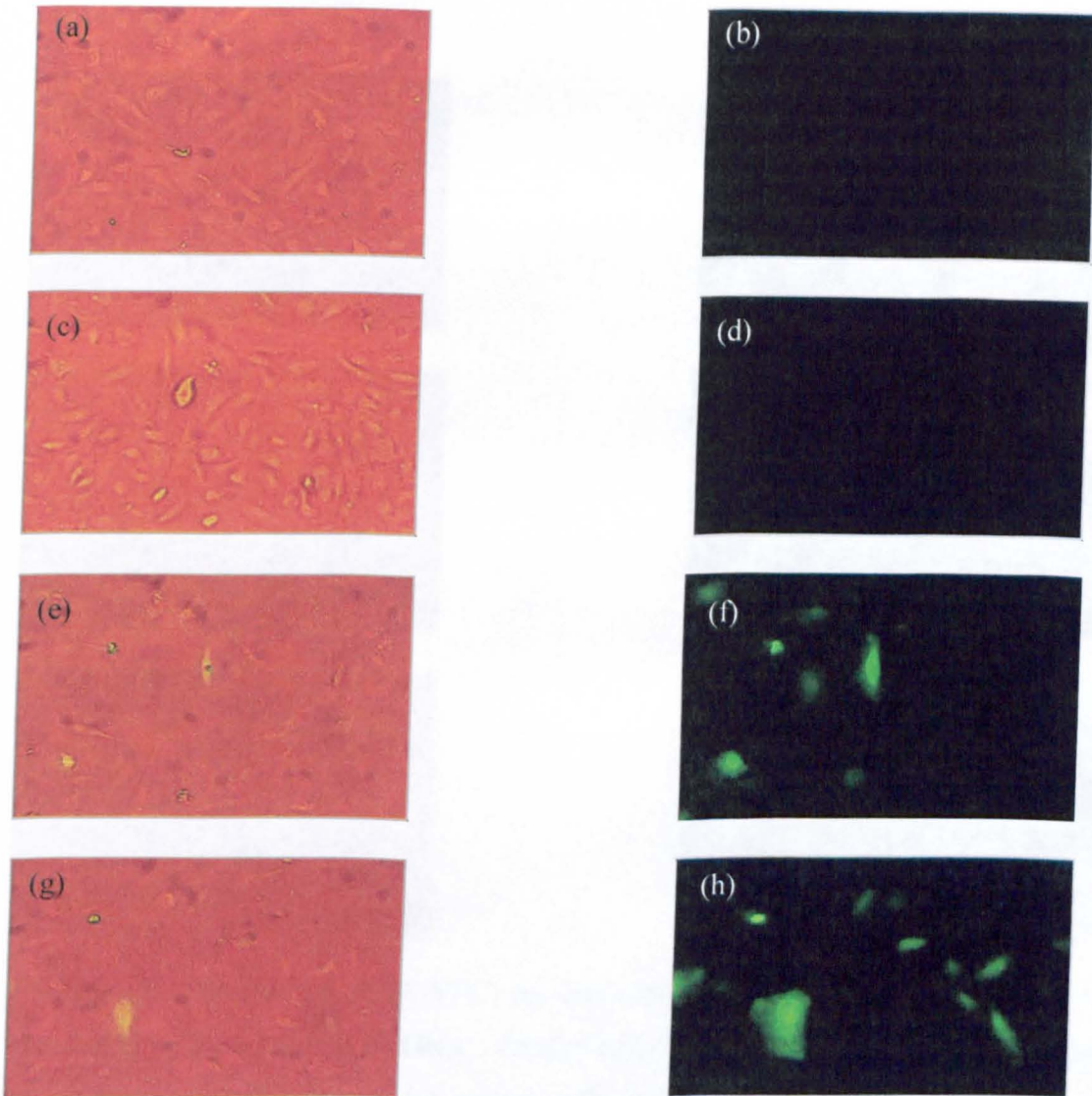


Figure 6.12: Transfection of HUVECs (passage 1-4) with pCDNA3.1-GFP to assess transfection efficiency. Control cells were transfected with no plasmid or DNA. Treated cells were transfected with vehicle plasmid and pCDNA3.1-GFP. Picture (a) control cells under light microscopy, (b) control cells under fluorescent microscopy, (c) HUVECs + pCDNA3.1 under light microscopy, (d) HUVECs + pCDNA3.1 under fluorescent microscopy (e, g) pCDNA3.1-GFP transfected HUVECs 1 and 2 under light and fluorescent microscopy, (f, h) pCDNA3.1-GFP transfected HUVECs 1 and 2 under fluorescent microscopy. Images are representative of 3 separate experiments.

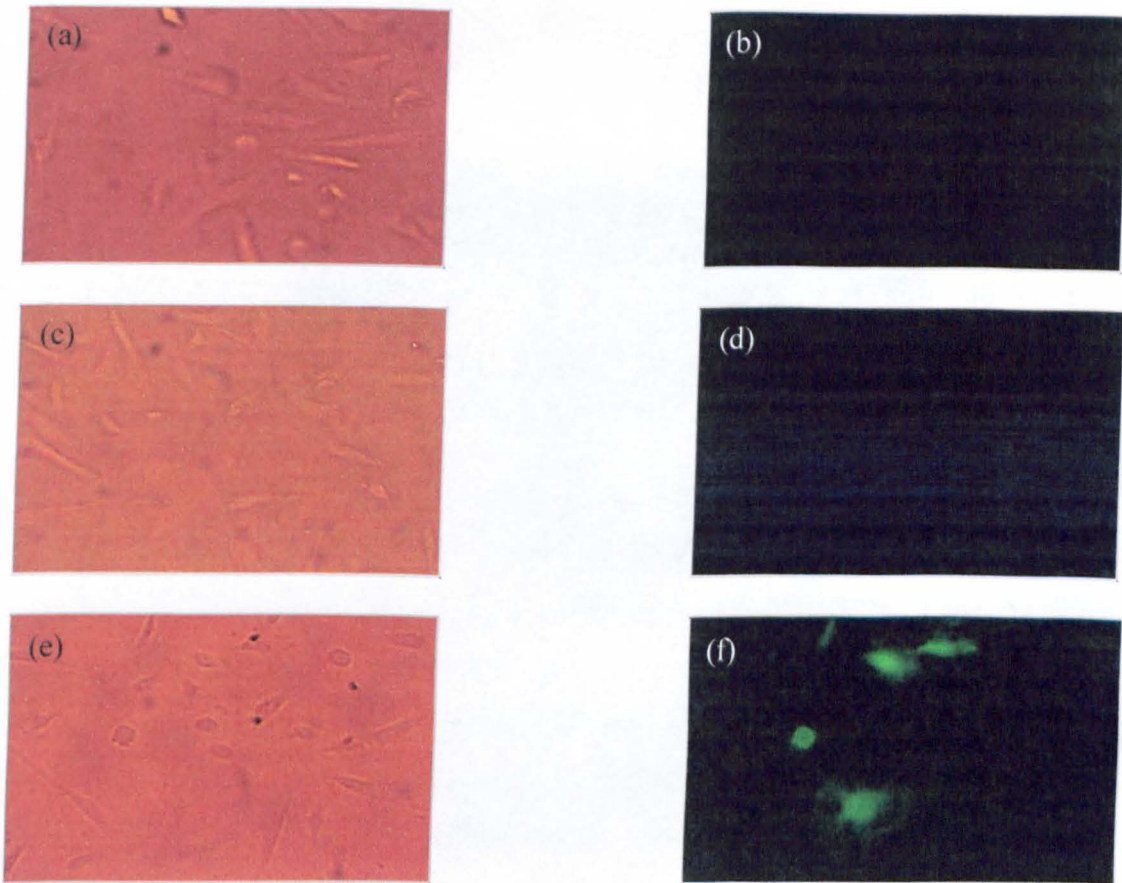


Figure 6.13: Transfection of HUVECs (p1-p4) with pCDNA3.1-GFP. Control cells were transfected with no plasmid or DNA. Treated cells were transfected with vehicle plasmid and pCDNA3.1-GFP. Picture (a) control cells under light microscopy, (b) control cells under fluorescent microscopy, (c) HUVECs + pCDNA3.1 under light microscopy, (d) HUVECs + pCDNA3.1 under fluorescent microscopy (e) pCDNA3.1-GFP transfected HUVECs under light microscopy, (f) pCDNA3.1-GFP transfected HUVECs under fluorescent microscopy. Images are representative of 3 separate experiments.

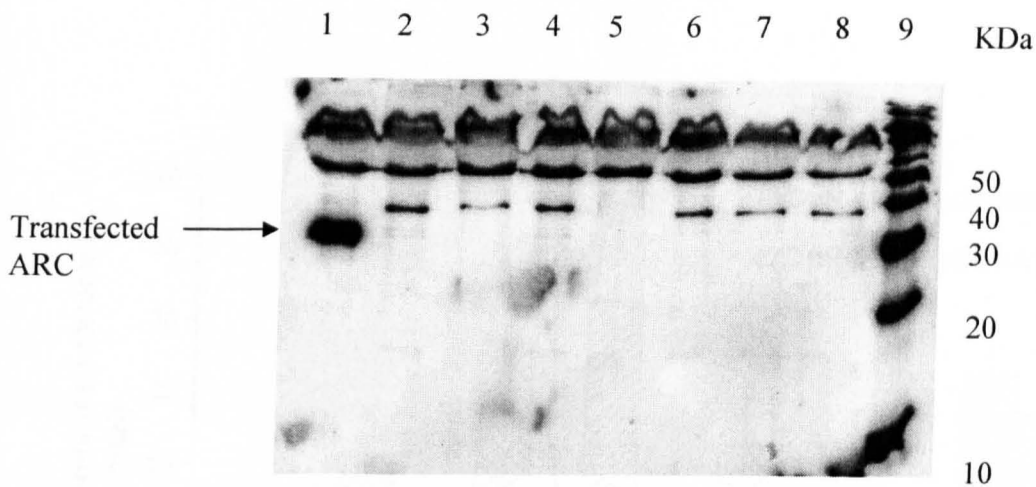


Figure 6.14: Expression of recombinant ARC protein in HUVECs. Lane (1) pCDNA3-ARC + JetPEI-HUVEC, (2) pCDNA3-ARC - JetPEI-HUVEC, (3) pCDNA3.1 + JetPEI-HUVEC, (4) pCDNA3.1 - JetPEI-HUVEC, (5) pCDNA3.1-GFP + JetPEI-HUVEC, (6) pCDNA3.1-GFP - JetPEI-HUVEC, (7) - plasmid + JetPEI-HUVEC, (8) - plasmid - JetPEI-HUVEC, (9) Molecular weight marker. The image is representative of 3 separate experiments.

6.4.6 *Inhibition of DuP-697 induced apoptosis in pCDNA3-ARC transfected HUVECs*

After successful transfection with the pCDNA3-ARC (Fig 6.13 and 6.14) HUVECs were treated with DuP-697 (0.01-1 μ M) for 24 hr. HUVECs treated with DuP-697 significantly induced ~ 27% chromatin condensation. Parallel studies with over-expression of the recombinant ARC protein and pCDNA3.1-GFP did not affect the levels of DuP-697 induced chromatin condensation (Fig 6.15). However, DMSO controls were also found to

induce significant (~20%) chromatin condensation when transfected with either pCDNA3.1-GFP or pCDNA3-ARC compared to the non-transfected cells.

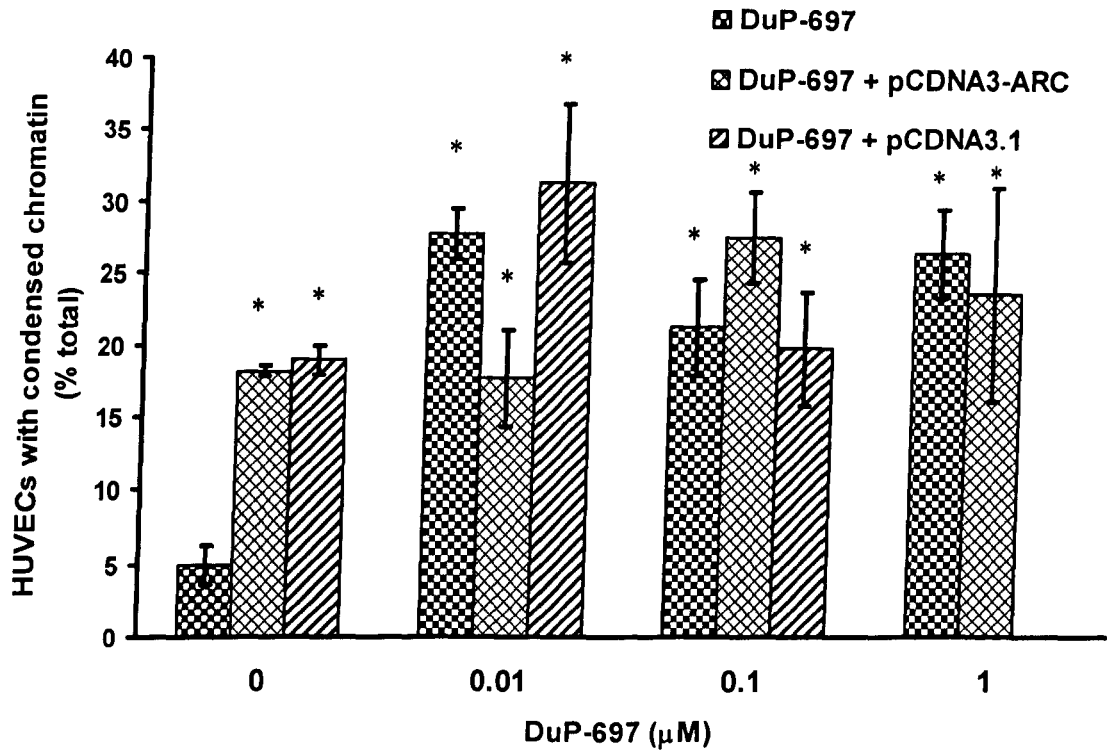


Figure 6.15: Induction of chromatin condensation by DuP-697 in HUVECs transfected with pCDNA3-ARC. Untransfected HUVECs were treated with serum free medium (SFM) + DuP-697 (10nM) for 24 hr at 37°C. HUVECs transfected with pCDNA3-ARC/pCDNA3.1 were incubated in 20% foetal calf serum medium (complete medium) for 24 hr prior to induction of chromatin condensation with DuP-697 (10nM) in SFM for 24 hr at 37°C. Control cells were treated with SFM + DMSO (0.01%). The data are representative of 3 separate experiments. ANOVA was used to determine significance for all the data with Student's t-test identifying the individual points of significance. Significance was compared to SFM + DMSO (0.01%) * $p < 0.05$.

6.5 *Discussion*

This chapter of results indicates that the apoptosis repressor with a CARD domain is endogenously expressed in HUVECs but is down regulated in tissue culture by possible transcriptional control of the *ARC* gene. Exogenous transfection of the *ARC* gene was shown to increase the expression of ARC in cultured HUVECs with little effect on DuP-697 induced chromatin condensation.

Several studies have shown that ARC is expressed in many different tissues e.g. cardiac tissue, skeletal muscle and some brain regions (Koseki *et al.*, 1998, Dowds and Sabban, 2001). Isolation of fresh HUVECs and immediate western blot analysis indicated that HUVECs *in vivo* endogenously express the ARC protein at low levels. The identification of a protein band of approximately 20 kDa proteins as ARC is consistent with Koseki *et al.* (1998) reporting that heart tissue transcribed the *ARC* gene with a predicted protein molecular weight of 22.6 kDa. This is however the first study to possibly identify the expression of the ARC protein in the vasculature.

The expression of ARC protein may be highly regulated and may require elements *in vivo* which are not present in our cell culture medium or the additional growth factors provided e.g. ECGF. This conclusion is based on the fact that expression of ARC rapidly disappeared when freshly isolated cells were incubated *in vitro* with the protein becoming undetectable even just after 24 hr in culture. Similarly it has been reported that the addition of growth factors into culture medium did not enhance ARC expression in PC12 cells (Dowds *et al.*, 2001), supporting the suggestion that culture medium does not contain the required supplements to induce ARC. Contrary to the study in PC12

cells by Dowds *et al.*, (2001) the present findings indicated that growth in serum free medium did not induce the expression of the ARC protein in tissue cultured HUVECs. This possibly suggests that the ARC protein may be expressed through stress activation, but incubation with serum free medium did not caused enough stress in HUVECs to activate transcription of the gene. Cell survival in HUVECs may be due to other possible mechanisms e.g. $\alpha\beta3$ integrin-ECM binding (Section 5.5).

Analysis of the transcription of the *ARC* gene (16q22.1) in cultured HUVECs did not indicate a clear and consistent cDNA band following RT-PCR analysis. These results possibly indicate that transcription of the *ARC* gene has been down regulated during tissue culture.

These findings suggest that down regulation of the ARC transcript and protein expression is not due to the presence of growth factors in the media. However at the moment the mechanism behind the down regulation of the gene transcription and protein expression is unclear.

The presence of the ARC insert in the pCDNA3 plasmid was confirmed by enzymatic restriction of the plasmid and by PCR. Restriction of the plasmid using different restriction enzymes indicated the total size of the plasmid was 7396 bp with the insert being ~1950 bp in size. This was confirmed by PCR which gave a product of ~ 2 Kb indicating the ARC gene was present in the plasmid.

Transfection of HUVECs with the pCDNA3-ARC plasmid produced a single protein band at ~30 kDa. The estimated molecular weight identified for the ARC protein is 22.6 kDa (Koseki *et al.*, 1998), however other studies have identified the transfected protein molecular weight in H9c2 cells at approximately 32 kDa (Neuss *et al.*, 2001), which supports our expressed protein in transfected HUVECs as ARC. Furthermore no protein of similar weight is expressed in any of the cells not transfected with the *ARC* gene indicating that the protein expressed in HUVECs is probably ARC.

Transfection of HUVECs with pCDNA3-ARC and the vector pCDNA3.1 induced a significant increase in chromatin condensation with further treatment of DuP-697 not having any additional effect. This is similar to levels of chromatin condensation seen in transfected HEK293 cells, SK-N-BE cells and H9c2 cells, which all indicate a 10-15% increase in condensed chromatin and cell death after transfection with ARC or empty vector (Li *et al.*, 2002, Gustafsson *et al.*, 2004, Jo *et al.*, 2004). This indicates that transfection of the HUVECs may have increased intracellular stress levels inducing some chromatin condensation without requiring DuP-697. The explanation for this may be possible starvation of the cells after transfection. It has been noted that transfection of bacteria increases the requirement of ATP to maintain the cells (Brown, 1998). This may also be the case in the transfected HUVECs and incubation in SFM may have induced chromatin condensation due to the lack of supplements in the medium.

In contrast to our findings, previous studies show that ARC transfected cells inhibited the all activation of chromatin condensation through preventing caspase dependent apoptosis (Koseki *et al.*, 1998, Neuss *et al.*, 2001, Li *et al.*, 2002, Gustafsson *et al.*,

2004, Jo *et al.*, 2004). However, treatment with DuP-697 did not give any additional induction of chromatin condensation above control levels for pCDNA3-ARC or pCDNA3.1-GFP transfected cells. This suggests that further chromatin condensation was possibly inhibited due to the transfection of the cells decreasing intracellular ATP levels and preventing the activation of the caspase cascade. Alternatively, it may be the chromatin condensation observed in the study is not due to apoptosis but necrosis and further confirmation of apoptosis by DNA fragmentation and caspase activation is required.

7 *General Discussion*

In recent years induction of endothelial cell apoptosis and inhibition of angiogenesis have been seen as a target for tumour treatment, rheumatoid arthritis and other inflammatory diseases (Carmeliet, 2000; Cao, 2001; Chavakis and Dimmeler, 2002; Folkman, 2003). The processes of angiogenesis and apoptosis are closely linked to each other with COX enzymes being influential in both pathways (Leahy *et al.*, 2002; Yazawa *et al.*, 2005 and *results chapter 5*) (Fig 7.1). The COX pathway has been identified as important in endothelial cell apoptosis with specific interest being given to COX-2. Increased expression of COX-2 by VEGF binding to endothelial cells has been shown to decrease apoptosis through the formation of COX-2 metabolites e.g. PGE₂ (Tsuji and Dubois 1995; Leahy *et al.*, 2002; King *et al.*, 2004; Lui *et al.*, 2004; Yazawa *et al.*, 2005). Furthermore, in this study it has been suggested that the expression profile of the COX enzymes may vary during cellular stress. Total PGE₂ production was shown to be decreased in HUVECs incubated with SFM compared to cells incubated in 20% FCS medium. This may possibly be caused by a decrease in the expression in COX-1 and increase COX-2 expression as explained previously (Section 5.5), suggesting further importance for COX-2 in cell homeostasis and survival.

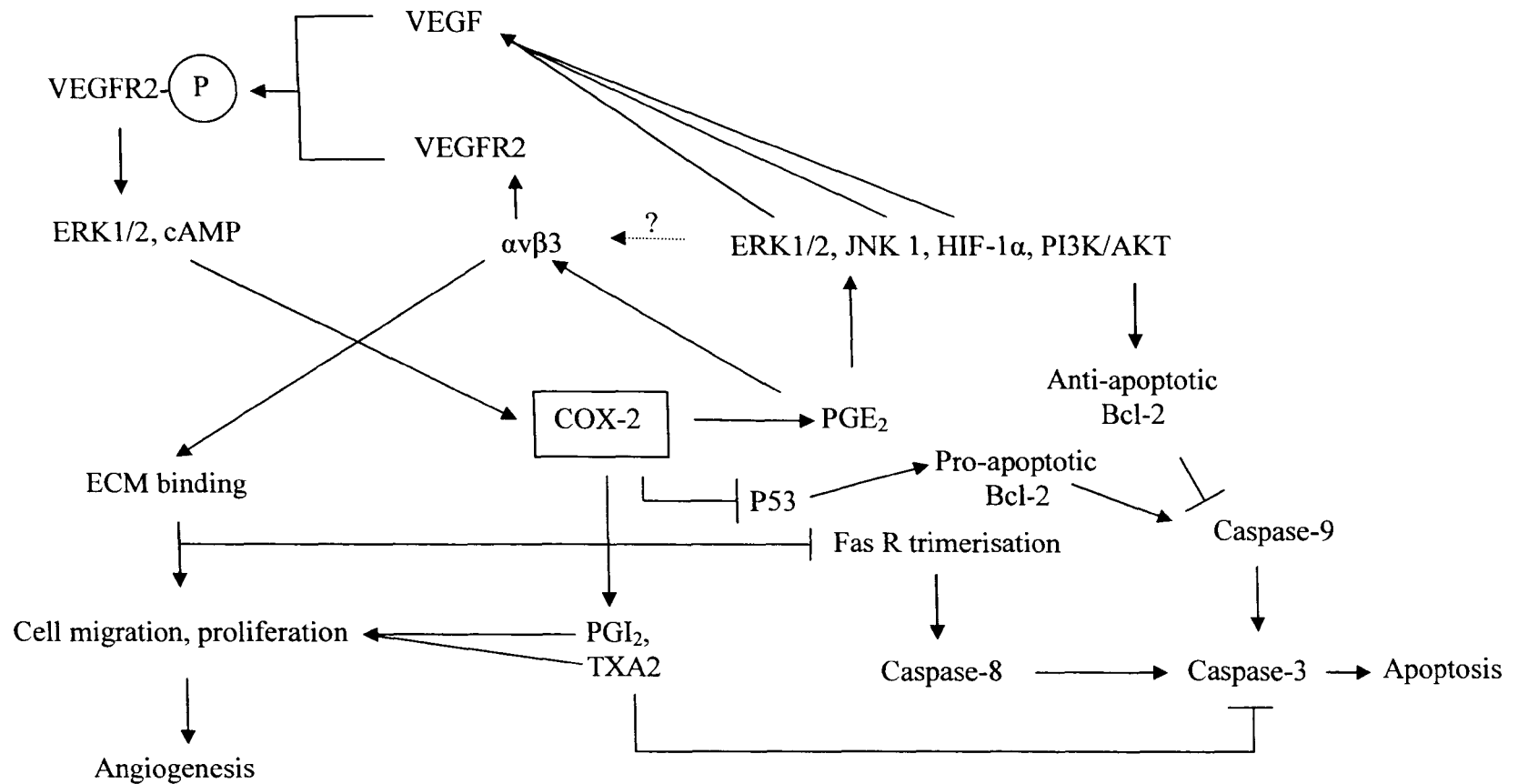


Figure 7.1: Schematic diagram of the role of COX-2 in the apoptosis and angiogenesis pathways. COX-2 involvement in angiogenesis and apoptosis is mediated through prostaglandin production specifically PGE₂, which may cause a positive feedback loop of VEGFR phosphorylation, cell survival, proliferation and migration (Nor *et al.*, 1999; Carmeliet, 2000; Aoudjit *et al.*, 2001; Choi *et al.*, 2001; Giordano and Johnson 2001; Lin *et al.*, 2001; Pai *et al.*, 2001; Gately and Li, 2004; Basu *et al.*, 2005).

Specific inhibition of COX-2 in endothelial cells induces a caspase-dependent apoptosis and inhibits *in vitro* and *in vivo* angiogenesis with no effect observed when only COX-1 is inhibited (Leahy *et al.*, 2002; Basu *et al.*, 2005; Yazawa *et al.*, 2005 and *results chapter 5*). Studies with paracetamol further indicated the induction of apoptosis through the inhibition of COX-2. Paracetamol used at a concentration known to inhibit COX-2 expression (300 μ M) (Churchman *et al.*, 2000) induced chromatin condensation and some DNA laddering without caspase 3 induction at 24 or 48 hr (*results chapter 3*). However, this may be that the treatment activated the caspase cascade transiently as seen in the DuP-697 and indomethacin studies. Therefore, caspase activation should have been identified as early as 1 hr for the samples that caused DNA laddering in the initial studies.

COX-2 specific effects have been shown to be reversed by exogenous PGE₂ indicating a role for PGE₂ in the prevention of apoptosis, as has previously been seen, and a specific role in angiogenesis other than increasing VEGF expression (Ghosh *et al.*, 2000; Hsu *et al.*, 2000; Johnson *et al.*, 2001; Basu *et al.*, 2005).

Previously proposed mechanisms to the induction of apoptosis through PGE₂ inhibition (Nor *et al.*, 1999; Pollman *et al.*, 1999; Choi *et al.*, 2001; Pai *et al.*, 2001; Dormond *et al.*, 2002) and the data acquired in this study do indicate a strong possibility that PGE₂ inhibition may be the cause of endothelial cell apoptosis in this case. However to assume that the mechanism of apoptosis activation is the inhibition of the anti-apoptotic effects of PGE₂ may be misleading as PGE₂ was only fractionally inhibited by DuP-697 and that other anti-apoptotic COX-2 metabolites e.g. TXA₂ would have been inhibited

by the selective COX-2 inhibitor (Wu *et al.*, 2003; Jantke *et al.*, 2004). The effects seen by treatment of endothelial cells with PGE₂ may be acting through a parallel pathway to reverse apoptosis and not solely reversing the specific inhibition of COX-2 caused by DuP-697. Similarly the effect of PGE₂ on selective COX-2 inhibited angiogenesis may be through a parallel pathway and inhibition of another COX-2 metabolite may be responsible for the decrease in capillary-like tubule formation e.g. TXA₂.

Further work could be completed to inhibit COX-1 and the specific PGE₂ synthase to identify whether induction of the endothelial cell apoptosis is a COX-2-PGE₂ specific effect or if the expression of the other prostaglandins and COX-2 metabolites are important in endothelial cell survival. The individual PG synthases may then be inhibited (Wheeler-Jones *et al.*, 2005, personal communication) to identify which of the COX-2 metabolites or which combination of metabolites is more important in the survival of endothelial cells. Studies into the inhibition of other prostaglandins e.g. PGI₂ by COX-2 inhibitors may also be useful in identifying the metabolites most important in apoptosis prevention. The other metabolites of COX-2 induce different pathways involved in cell migration, proliferation, adhesion and survival (Nor *et al.*, 1999; Carmeliet, 2000; Aoudjit *et al.*, 2001; Choi *et al.*, 2001; Giordano and Johnson, 2001; Lin *et al.*, 2001; Pai *et al.*, 2001; Gately and Li, 2004; Basu *et al.*, 2005). These other pathways induced by the other COX-2 metabolites may induce anti-apoptotic proteins e.g. XIAP or survivin, which may decrease the morphological changes observed in the present study (Chavakis and Dimmeler, 2002; Duval *et al.*, 2003).

To fully assess the potency of selective COX-2 inhibitors for inducing apoptosis a further dose response study would be carried out using lower concentrations than the present study. Furthermore, research into caspase expression and activation using western blots and colorimetric assays may be used to identify the pathways associated with selective COX-2 inhibitor induced apoptosis and the mechanisms behind VEGF and PGE₂ prevention of apoptosis. However, the current study does imply that clinical use of selective COX-2 inhibitors e.g. DuP-697 is potentially dangerous. Induction of endothelial cell apoptosis would induce weakening of the vascular system. Inhibition of subsequent angiogenesis would prevent any repair to damaged blood vessels. Both the induction of apoptosis and inhibition of angiogenesis may leave the vascular system subject to increased stress and damage.

Endothelial cells treated with natural products, curcumin and 6-shogaol, which have previously been shown to inhibit COX-2 activity (Tjendraputra *et al.*, 2001; Chun *et al.*, 2003), induced a caspase-independent form of cell death which was not mediated by COX-2 inhibition. Cell death was identified by chromatin condensation with no DNA laddering and no caspase 3 activation by curcumin in HUVECs and Jurkat E6.1 cells. This is similar to the previously done studies, which also indicated no caspase 3 activity or DNA laddering in curcumin treated cells although there was chromatin condensation (Piwocka *et al.*, 1999; Piwocka *et al.*, 2001). Curcumin and 6-shogaol may possibly act through similar mechanisms due to the similarities in the structures of the compounds (Section 4.5). Both compounds caused chromatin condensation at concentrations far higher than was required to inhibit COX-2 (Zhang *et al.*, 1999; Tjendraputra *et al.*,

2001; Chun *et al.*, 2003), but did not induce any other markers of apoptosis e.g. DNA laddering or caspase 3 activation.

Whether the morphological changes induced by curcumin and 6-shogaol can be identified as apoptosis is unclear, but it is clear that these compounds induce a form of cell death similar to apoptosis without the intracellular signalling to activate the caspases. Explanations for this type of cell death are speculative but may indicate possible pathways that are induced following 6-shogaol and curcumin treatment. The observed caspase-independent cell death induced by 6-shogaol and curcumin may be due to secondary necrosis, which occurs after the initiation of apoptosis.

Induction of secondary necrosis is initiated in cells which are undergoing apoptosis but fail to maintain ATP levels. Depletion of ATP inhibits full caspase activation preventing the caspase-cascade from completing the morphological changes associated with apoptosis and induces necrosis (Proskuryakov *et al.*, 2003). Pathways behind this have been speculated to be due to the formation of large DNA breaks, by intracellular ROS production or direct DNA damage by anti-cancer drugs, which induce production of poly (ADP-ribose) polymerase (PARP). PARP induction causes an increase in production of the PARP substrate (NAD⁺) resulting in depletion in ATP levels. This depletion then induces necrosis in the cells (Ha *et al.*, 1999; Walisser *et al.*, 1999; Proskuryakov *et al.*, 2003). Alternatively, other studies have suggested that opening of the mitochondrial permeability transient pore (MPTP) may be responsible for the induction of necrosis or apoptosis. Upon cellular stress e.g. oxidative stress the MPTP, formed from the VDAC and ANT proteins, opens increasing mitochondrial swelling

and rupture of the outer mitochondrial membrane releasing cyt-c. This release of cyt-c would therefore activate caspase 9. However if the cellular insult is very severe the MPTP may remain open depleting ATP stores and induce necrosis instead of closing and inducing apoptosis (Halestrap, 2005). Both of the pathways suggested strongly indicate a role for ATP depletion in the activation of a caspase-independent cell death. Furthermore, both pathways indicate a possible reason for the activation of chromatin condensation and DNA breaks in curcumin and 6-shogaol treated cells without the other morphological changes. However, as curcumin did not inhibit mitochondrial activity as identified by the MTT assay, it does not appear that mitochondrial disruption is the cause of the cell death in this case, though further investigation into the release of cyt-c, caspase expression and the activation of PARP would be required to confirm these mechanisms.

Future investigation into how curcumin and 6-shogaol induce chromatin condensation may focus around other endonucleases in the cell. It has been shown that endonuclease G, which has been identified in the mitochondria, can fragment DNA with out requiring caspase activation in other eukaryotes (Lily *et al.*, 2001; Parrish *et al.*, 2001). Other studies into the morphological changes e.g. annexin V binding to phosphatidylserine, organelle shrinking, and trypan blue exclusion could also be investigated to assess which pathways and enzymes are activated.

Clinically these compounds may be of some use to reduce angiogenesis. Induction of COX-2 independent chromatin condensation in HUVECs only occurs at high concentrations of curcumin and 6-shogaol, which may not be achievable *in vivo*, but

COX-2 activity would still be inhibited at low concentrations and possibly prevent angiogenesis (Yawaza *et al.*, 2005 and *results chapter 4*). Support for this hypothesis is indicated by previous studies which have shown the prevention of HUVEC replication by curcumin and 6-shogaol at concentration similar to this study (25-50 μ M) (Smith, 2004). Curcumin has also been shown to inhibit HUVECs forming capillary-like tubules *in vitro* (0-25 μ M) and angiogenesis *in vivo* (10mM) (Thaloor *et al.*, 1998; Gururaj *et al.*, 2002). 6-Shogaol is more potent in the inhibition of COX-2 activity, IC_{50} = 2.1 μ M, than curcumin (Tjendraputra *et al.*, 2001) and this may indicate that this compound is more effective at inhibiting angiogenesis and could be further investigated through *in vitro* capillary-tubule formation assays and *in vivo* angiogenesis research using lower concentrations than were studied in this thesis.

The investigated effects of the ARC protein are unclear in HUVECs, though this study does indicate that ARC may possibly be expressed in the vasculature. Further work would include the further identification of the native HUVEC and transfected protein as ARC by protein sequencing. Investigation into transcription of the *ARC* gene may be studied through RT-PCR using ARC specific primers and subsequent sequencing of the cDNA produced. Mechanisms of tissue culture induced inhibition of ARC expression could also be addressed by these methods. The anti-apoptotic effects of ARC would have to be reassessed using a stimulus that is known to be blocked by the protein ARC e.g. FasL, to prove the protein activity. Furthermore, different strategies for the transfection of ARC may have to be considered e.g. adenovirus (Wheeler-Jones, 2005, personal communication), to prevent cytotoxicity in the cells induced during transfection with pCDNA3-ARC. It is possible that the transfection increased the

requirement for supplemented medium (Section 6.5) and it was the incubation with SFM that caused the increase in chromatin condensation observed. Possible mechanisms for this may be similar to the secondary necrosis pathways discussed above, with a decrease in ATP inducing chromatin condensation. However this would require further investigation as suggested previously.

In summary this study indicates the pathways of apoptosis activated in endothelial cells have been shown to be dependent on the stimulus used, e.g. actinomycin-D, curcumin and 6-shogaol, DuP-697 or indomethacin (*results chapter 3, 4 and 5*). The different pathways identified were similar to previous studies, which proposed that certain pathways of cell death induced different morphological and biochemical changes in the cells with some of the changes associated with apoptosis, e.g. DNA fragmentation and caspase activation, not occurring (Collins *et al.*, 1992; Oberhammer *et al.*, 1993; Zakeri *et al.*, 1993; Taylor *et al.*, 2001). Three different pathways of cell death have been identified in this study; (1) caspase-dependent apoptosis that gives the associated morphological and biochemical changes e.g. DNA “laddering”, chromatin condensation and membrane blebbing, (2) caspase-independent cell death with chromatin condensation and no DNA laddering or smearing, (3) necrosis, which was assessed positive by trypan blue staining of the cells and by DNA smearing when visualised by agarose gel electrophoresis.

The present study also identified that COX-2 inhibition may not be the only stimulus required to induce cell death in endothelial cells, though COX-1 inhibition has no effect on endothelial cell apoptosis. However selective COX-2 inhibitors induced caspase-

dependent apoptosis through one or more mechanisms that can be inhibited by PGE₂. COX-2 inhibition is required to inhibit *in vitro* capillary-like tubule formation and cell replication with PGE₂ having a specific role in angiogenesis.

8.0 References

- Abe, M., and Sato, Y., (2001) cDNA microarrays analysis of the gene expression profile of VEGF-activated human umbilical vein endothelial cells, *Angiogenesis*, **4**, 289-98.
- Abmayr, S., Crawford, RW., Chamberlain, JS. (2004) Characterisation of ARC, apoptosis repressor interacting with CARD, in normal and dystrophin-deficient skeletal muscle, *Human Mol Gen*, **13** (2), 213-21.
- Akarasereenont, P., Techatraisak, K., Thauorn, A. and Chortewuthakorn, S. (2002) The expression of COX-2 in VEGF-treated endothelial cells is mediated through protein tyrosine kinase, *Meds of Inflamm*, **11**, 17-22.
- Allison, MC., Howatson, AG., Torrance, CJ., Lee, FD, Russell, RI. (1992) Gastrointestinal damage associated with the use of nonsteroidal anti-inflammatory drugs, *N Eng J Med*, **327** (11), 749-54.
- Aoudjit, F., and Vuori, K., (2001) Matrix attachment regulates Fas-induced apoptosis in endothelial cells: A role for c-flip and implications for anoikis, *J Cell Biol*, **152**, 633-43.
- Ashkenazi, A. and Dixit, V. M. (1998) Death Receptors: Signaling and Modulation, *Science*, **281**, 1305-1308.
- Bai, M., Tsanou, E., Agnantis, N., Chaidos, A., Dimou, D., Skyrilas, A., Dimou, S., Vlychou, M., Galani, V. and Kanavaros, P. (2003) Expression of cyclin D3 and cyclin E and identification of distinct clusters of proliferation and apoptosis in diffuse large B-cell lymphomas, *Histology and Histopathology*, **18**, 449-57
- Basu, GD., Pathangey, LB., Tinder, TL., Gendler, SJ., Mukerjee, P. (2005) Mechanisms underlying the growth inhibitory effects of the cyclooxygenase-2 inhibitor celecoxib in human breast cancer cells, *Breast Cancer Res*, **7**, R422-35.
- Bates, DO., and Harper, SJ. (2003) Regulation of vascular permeability by vascular endothelial growth factors, *Vascular Pharmacol*, **39**, 225-37.
- Bierhaus, A., Chen, J., Liliensiek, B., and Nawroth, PP. (2000) LPS and cytokine-activated endothelium, *Sem Thromb and Haemostasis*, **26** (5), 571-87.
- Bishop- Bailey, D., and Hla, T. (1999) Endothelial cell apoptosis induced by peroxisome proliferator-activated receptor (PPAR) ligand 15-deoxy- $\Delta^{12,14}$ -prostaglandin J₂, *J Biol Chem*, **274**, 17042-48.

- Blanke, CD. (2002) Celecoxib with chemotherapy in colorectal cancer, *Oncol*, **16** (4), 17-21.
- Blatt, N. B. and Glick, G. D. (2001) Signaling pathways and effector mechanisms pre-programmed cell death, *Bioorg Med Chem*, **9**, 1371-1384.
- Boldin, M., Goncharov, T., Goltsev, Y. and Wallach, D. (1996) Involvement of MACH, a novel MORT1/FADD-interacting protease, in Fas/APO-1- and TNF receptor-induced cell death., *Cell*, **85**, 803-15.
- Bortner, C. D. and Cidlowski, J. A. (1998) A necessary role for cell shrinkage in apoptosis, *Biochem Pharmacol*, **56**, 1549-1559
- Brown, TA. (1998) Gene Cloning: an introduction. Stanley Thornes (publishers) Ltd. Cheltenham, UK.
- Bryant, CE., Appelton, I., and Mitchell, JA. (1998) Vascular endothelial growth factor upregulates constitutive cyclooxygenase-1 in primary bovine and human endothelial cells, *Life Sci*, **62**, 2195-2201.
- Budihardjo, I., Oliver, H., Lutter, M., Luo, X. and Wang, X. (1999) Biochemical pathways of caspase activation during apoptosis, *Annu Rev Cell Dev Biol*, **15**, 269-90.
- Bush, J.A., Chung, KJ. and Li, G. (2001) Curcumin induces apoptosis in human melanoma cells through a Fas receptor/ caspase 8 pathway independent of p53, *Exp. Cell Res*, **271**, 305-314.
- Callahan, M., Williamson, P. and Schlegel, R. (2000) Surface expression of phosphatidylserine on macrophages is required for phagocytosis of apoptotic thymocytes, *Cell Death Differ*, **7**, 645-53.
- Cao, Y. (2001) Endogenous angiogenesis inhibitors and their therapeutic implications, *Int. J. Biochem Cell Biol*, **33**, 357-69
- Carmeliet, P. (1999) Basic concepts of (Myocardial) angiogenesis: Role of vascular endothelial growth factor and angiopoietin, *Curr Interv Cardiol Rep*, **1**, 322-335.
- Carmeliet, P. (2000) Mechanism of angiogenesis and arteriogenesis, *Nat Med*, **6**, 389-95.

- Carmeliet, P., and Collen, D. (2000) Molecular basis of angiogenesis: Role of VEGF and VE-cadherin, *Ann NY Acad Sci*, **902**, 249-64.
- Carmeliet, P. and Jain, R. (2000) Angiogenesis in Cancer and other diseases, *Nature*, **407**, 249-57
- Caughey, GE., Cleland, LG., Penglis, PS., Gamble, JR., James, MJ. (2001). Roles of cyclooxygenase (COX)-1 and COX-2 in prostanoid production by human endothelial cells: selective up-regulation of prostacyclin synthesis by COX-2. *J Immunol*, **167** (5), 2831-8.
- Chan, CC., Boyce, S., Brideau, C., Charlston, S., Cromlish, W., Ethier, D., Evans, J., Ford-Hutchinson, AW., Forrest, MJ., Gauthier, JY., Gordon, R., Gresser, M., Guay, J., Kargman, S., Kennedy, B., LeBlanc, Y., Leger, S., Mancini, J., O'Neill, GP., Ouellet, M., Patrick, D., Percival, MD., Perrier, H., Prasit, P., Rodger, I., Tagari, P., Therien, M., Vickers, P., Visco, D., Wang, Z., Webb, J., Wong, E., Xu, LJ., Young, RN., Zambona, R., Reindeau, D. (1999) Rofecoxib [Vioxx, MK-0966; 4-(4'-Methylsulfonylphenyl)-3-phenyl-2-(5H)-furanone]: A potent and orally active cyclooxygenase-2 inhibitor. Pharmacological and biochemical profiles, *J Pharmacol and Exp Ther*, **290**, 551-60.
- Chatterjee, S., Bish, LT., Jayasankar, V., Stewart, AS., Woo, YJ., Crow, MT., Gardner, TJ., Sweeney, HL. (2003) Blocking the development of postischemic cardiomyopathy with viral gene transfer of the apoptosis repressor with caspase recruitment domain, *J Thoracic Cardio. Surg*, **125**, 1461-69.
- Chavakis, E. and Dimmeler, S. (2002) Regulation of Endothelial cell Survival and Apoptosis During Angiogenesis, *Arterio, Thromb vascular biol*, **22**, 887-893.
- Chen, J., Flannery, J. G., LaVail, M. M., Steinberg, R. H., Xu, J. and Simon, M. I. (1996) Bcl-2 overexpression reduces apoptotic photoreceptor cell death in three different retinal degenerations, *PNAS*, **93**, 7042-7047.
- Choi, EM., Heo, JI., Oh, JY., Kim, YM., Ha, KS., Kim, JI., Han, JA. (2001) COX-2 regulates p53 activity and inhibits DNA damage-induced apoptosis, *Biochem Biophys Res Comms*, **328**, 1107-12.
- Chou, JJ., Li, H., Salvesen, G., Yuan, J. and Wagner, G. (1999) Solution structure of BID, an intracellular amplifier of apoptotic signaling, *Cell*, **96**, 615-24.

- Chun, K., Keum, Y., Han, S., Song, Y., Kim, S. and Surh, Y. (2003) Curcumin inhibits phorbol ester-induced expression of cyclooxygenase-2 in mouse skin through suppression of extracellular signal-regulated kinase activity and NF-kappaB activation, *Carcinogenesis*, **24**, 1515-24.
- Churchman, A., Mallison, H., Clifford, R. H., Fütter, L. E., Del Soldato, P., Moore, P. K. and Baydoun, A. R. (2000) Regulation of COX-2 and iNOS expression by novel NO-NSAIDs., *Inflamm Res*, **50**, S221.
- Churchman, A., Baydoun, A.R. & Hoffman, R. (2006) Inhibition of angiogenic tubule formation and induction of apoptosis in human endothelial cells by the selective cyclooxygenase-2 inhibitor 5-bromo-2-(4-fluorophenyl)-3-(methylsulfonyl) thiophene (DuP-697)., *B J Pharmacol.*, **In press**.
- Clarke, R., Lund, E., Johnson, I. I. and Pinder, A. (2000) Apoptosis can be detected in attached colonic adenocarcinoma HT29 cells using annexin V binding, but not by TUNEL assay or sub-G0 DNA content, *Cytometry*, **40**, 252.
- Collins, R.J., Harmon, B.V., Gobe, G.C., Kerr, JFR. (1992) Internucleosomal DNA cleavage should not be the sole criterion for identifying apoptosis, *Int J Radiation Biol*, **61**, 451-453.
- Colville-Nash, P.R. and Gilroy, D. (2000) COX-2 and the cyclopentone prostaglandins: - A new chapter in the book of inflammation?, *Prostaglandins other lipid meds*, **62**, 33-43.
- Copland, J.A., Marlow, L.A., Kurakata, S., Fujiwara, K., Wong, A.K., Keinest, P.A., Williams, S.F., Haugen, B.R., Klopper, J.P., Smallridge, R.C. (2005) Novel high-affinity PPAR gamma agonist alone and in combination with paclitaxel inhibits human anaplastic thyroid carcinoma tumor growth via p21 (WAF1/CIP1), **Dec epub ahead of print**.
- Cowling, V. and Downward, J. (2002) Caspase-6 is the direct activator of caspase-8 in the cytochrome c-induced apoptosis pathway: absolute requirement for removal of caspase-6 prodomain, *Cell Death Differ*, **9**, 1046-56.
- Cutolo, M., Capellino, S., Montagna, P., Ghiorzo, P., Sulli, A. and Villaggio, B. (2005) Sex hormone modulation of the cell growth and apoptosis of the human monocytic/ macrophage cell line, *Arthritis Res & Therap*, **7**, R1124-1132.

- Dandekar, DS., Lopez, M., Carey, RI., Lokeshwar, BL. (2005) cyclooxygenase-2 inhibitor celecoxib augments chemotherapeutic drug-induced apoptosis by enhancing activation of caspase-3 and -9 in prostate cancer cells, *Int J Cancer*, **115**, 484-92.
- Davis, TW., O'Neal, JM., Pagel, MD., Zweifel, BS., Mehta, PP., Heuvelman, DM., Masferrer, JM. (2004) Synergy between celecoxib and radiotherapy results from inhibition of cyclooxygenase-2-derived prostaglandin E₂, a survival factor for tumour and associated vasculature, *Cancer Res*, **64**, 279-285.
- Desagher, S., Osen-Sand, A., Nichols, A., Eskes, R., Montessuit, S., Lauper, S., Maundrell, K., Antonsson, B. and Martinou, J.-C. (1999) Bid-induced Conformational Change of Bax Is Responsible for Mitochondrial Cytochrome c Release during Apoptosis, *J. Cell Biol.*, **144**, 891-901.
- Dong, YG., Chen, DD., He, JG., Guan, YY. (2004) Effects of 15-deoxy- $\Delta^{12,14}$ -prostaglandin J₂ on cell proliferation and apoptosis in ECV304 endothelial cells, *Acta Pharmacol*, **25** (1), 47-53.
- Dor, Y., Djonov, V. and Keshet, E. (2003) Making vascular networks in the adult: branching morphogenesis without a roadmap, *Trends in Cell Biol*, **13**, 131-136.
- Dormond, O., Bezzi, M., Mariotti, A., Ruegg, C. (2002) Prostaglandin E₂ promotes integrin α V β 3-dependent endothelial cell adhesion, Rac-activation and spreading through cAMP/PKA-dependent signalling, *J Biol Chem*, **277**, 45838-46.
- Dowds, TA., and Sabban, EL. (2001) Endogenous and exogenous ARC in serum withdrawal mediated PC12 cell apoptosis: a new pro-apoptotic role for ARC, *Cell death and Diff*, **8**, 640-48.
- Duval, H., Harris, M., Li, J., Johnson, N., and Print C. (2003) New insights into the function and regulation of endothelial cell apoptosis, *Angiogenesis*, **6**, 171-183.
- Earnshaw, W., Martins, L. and Kaufmann, S. (1999) Mammalian caspases: structure, activation, substrates, and functions during apoptosis., *Annu Rev Biochem*, **68**, 383-424.
- Egeblad, M. and Werb, Z. (2002) New functions for the matrix metalloproteinases in cancer progression, *Nat Rev Cancer*, **2**, 161-74.

- Elder, DJE., and Paraskeva, C. (1999) Induced apoptosis in the prevention of colorectal cancer by non-steroidal anti-inflammatory drugs, *Apoptosis*, **4**, 365-72.
- Emery, P. (1999) Clinical aspects of COX-2 inhibitors, *Drugs Today*, **35**, 267-74.
- Enari, M., Sakahira, H., Yokoyama, H., Okawa, K., Iwamatsu, A. and Nagata, S. (1998) A caspase-activated DNase that degrades DNA during apoptosis, and its inhibitor ICAD., *Nature*, **391**, 43-50.
- Engidawork, E., Gulesserian, T., Yoo, BC., Cairns, N., Lubec, G. (2001) Alteration of caspases and apoptosis-related proteins in brains of patients with Alzheimer's disease, *Biochem Biophys Res Comms*, **281**, 84-93.
- Erl, W., Weber, C., Zerneck, A., Neuzil, J., Vosseler, CA., Kim, HJ., and Weber, PC. (2004) cyclopentone prostaglandins induce endothelial cell apoptosis independent of peroxisome proliferators-activated receptor- γ , *European J Immun*, **34**, 241-50.
- Fadok, VA., Bratton, DL., Rose, DM., Pearson, A., Ezekewitz, RAB., and Henson, PM. (2000) A receptor for phosphatidylserine-specific clearance of apoptotic cells., *Nature*, **405**, 85-90.
- Fadok, VA., de Cathelineau, A., Daleke, DL., Henson, PM., and Bratton DL. (2001) Loss of phospholipid asymmetry and surface exposure of phosphatidylserine is required for phagocytosis of apoptotic cells by macrophages and fibroblasts., *J Biol Chem*, **276** (2), 1071-77.
- Ferrara, N. (2001) Vascular endothelial growth factor and the regulation of angiogenesis, *Recent Prog in Hormone Res*, **55**, 15-35.
- Ferrara, N., Berber, HP., LeCouter, J., (2003) The biology of VEGF and its receptors, *Nat Med*, **9** (6), 669- 76.
- Fitzgerald, GA. (2002) cardiovascular pharmacology of nonselective nonsteroidal anti-inflammatory drugs and c ϕ xibs: clinical considerations, *Am J Pharmacol*, **89**, 26D-32D.
- Folkman, J. (1971) Tumor angiogenesis: therapeutic implications, *N Engl J Med*, **285**, 1182-6.
- Folkman, J. (2003) Angiogenesis and apoptosis, *Sem in Cancer Biol*, **13**, 159-167

- Frisch, S. and Francis, H. (1994) Disruption of epithelial cell-matrix interactions induces apoptosis, *J. Cell Biol.*, **124**, 619-626.
- Gajate, C., An, F. and Mollinedo, F. (2003) Rapid and selective apoptosis in human leukemic cells induced by aplidine through a Fas/CD95- and mitochondrial-mediated mechanism, *Clin Cancer Res*, 1535-45.
- Gans, KR., Galberaith, W., Roman, RJ., Haber, SB., Kerr, JS., Schmidt, WK., Smith, C., Hewes, WE., Ackerman, NR., (1990) Anti-inflammatory and safety profile of DuP 697, a novel orally effective prostaglandin synthesis inhibitor, *J Pharmacol and Exp Therap*, **254**, 180-87.
- Gately, S. (2000) The contributions of cyclooxygenase to tumour angiogenesis, *Cancer and metastasis Rev*, **19**, 19-27.
- Gately, S. and Kerbel, R. (2003) Therapeutic potential of selective cyclooxygenase -2 inhibitors in the management of tumour angiogenesis, *Prog Exp Tum Res*, **37**, 179-92.
- Gerber, HP., Dixit, V., Ferrara, N. (1998) Vascular endothelial growth factor induces expression of the anti-apoptotic proteins Bcl-2 and A1 in vascular endothelial cells, *J Biol Chem*, **273**, 13313-16.
- Ghosh, AK., Hirasawa, N., Niki, H., and Ohuchi, K. (2000) Cyclooxygenase-2-mediated angiogenesis in carrageenin-induced granulation tissue in rats, *J Pharmacol and Exp Therap*, **295**, 802-09.
- Gierse, AK., Hauser, SD., Creely, DP., Koboldt, C., Rangwala, SH., Isakson, PC., Seibert, K. (1995) Expression and selective inhibition of the constitutive and inducible forms of human cyclooxygenase. *Biochem J*, **305**, 479
- Gilroy, D., Tomlinson, A. and Willoughby, D. (1998) Differential effects of inhibitors of cyclooxygenase (cyclooxygenase 1 and cyclooxygenase 2) in acute inflammation, *Eur J Pharmacol*, **355**, 211-7.
- Giordano, F. and Johnson, R. (2001) Angiogenesis: The role of the microenvironment in flipping the switch., *Curr opin in genetics and dev*, **11**, 35-40.
- Goldstein, JL., Silverstein, FE., Agrawal, NM., Hubbard, RC., Kaiser, J., Maurath, CJ., Verburg, KM., Geis, GS. (2000) Reduced risk of gastrointestinal ulcer complications with celecoxib, a novel COX-2 inhibitor, *Am J Gastroenterol*, **95** (7), 1681-90.

- Grafe, M., Steinheider, G., Desaga, U., Warnecke, C., Lehmkuhl, H., Regitz-Zagrosek, V., Hildebrandt, A. and Fleck, E. (1999) Characterization of two distinct mechanisms for induction of apoptosis in human vascular endothelial cells, *Clin Chem Lab Med*, **37**, 505-10.
- Green, J. and Reed, D. (1998) Mitochondria and Apoptosis, *Science*, **281**, 1309-1312.
- Gross, A., Jockel, J., Wei, M. C. and Korsmeyer, S. J. (1998) Enforced dimerization of BAX results in its translocation, mitochondrial dysfunction and apoptosis, *EMBO J.*, **17**, 3878-3885.
- Gross, A., McDonnell, J. and Korsmeyer, S. (1999) BCL-2 family members and the mitochondria in apoptosis, *Genes Dev*, **13**, 1899-911.
- Gupta, S. (2001) Molecular steps of death receptor and mitochondrial pathways of apoptosis., *Life sci*, **69**, 2957-2964.
- Gururaj, AE., Belakavadi, M., Venkatesh, DA., Marme, D., Salimath, BP., (2002) Molecular mechanisms of anti-angiogenic effect of curcumin, *Biochem and Biophys Res Comms*, **297**, 934-42.
- Gustafsson, AB., Tsai, JG., Logue, SE., Crow, MT., and Gottlieb, RA. (2004) ARC protects against cell death by interfering with Bax activation, *J Biol Chem*, **279**, 21233-38.
- Ha, HC. and Synder, SH. (1999) Poly(ADP-ribose) polymerase is a mediator of necrotic cell death by ADP depletion, *Proc Natl Acad Sci USA*, **96**, 13978-82.
- Handrick, R., Rudner, J., Muller, I., Eibl, H., Belka, C. and Jendrossek, V. (2005) Bcl-2 mediated inhibition inhibition of erucylphosphochlorine-induced apoptosis depends on its subcellular localisation, *Biochem Pharmacol*, **70**, 837-50.
- Halestrap, A. (2005) A pore way to die, *Nature*, **434**, 578-579.
- Hata, AN., and Breyer, RM. (2004) Pharamcology and signalling of prostaglandin receptors: Multiple roles in inflammation and immune modulation, *Pharamcol and Therap*, **103**, 147-66.
- Hertig, A. (1935) Angiogenesis in the early human chorine and in the primary placenta of the macaque monkey, *Contib to Embryol*, **146**, 37-81.

- Ho, L., Osaka, H., Aisen, P. S. and Pasinetti, G. M. (1998) Induction of cyclooxygenase (COX)-2 but not COX-1 gene expression in apoptotic cell death, *J Neuroimmunol*, **89**, 142-149.
- Hong, YM., Jo, DG., Lee, JY., Chang, JW., Nam, JH., Noh, JY., Koh, JY., Jung, YK. (2003) Down regulation of ARC contributes to vulnerability of hippocampal neurons to ischemia/hypoxia, *FEBS Letters*, **543**, 170-73.
- Hsu, AL., Ching, TT., Wang, DS., Song, X., Rangnekar, VM., and Chen, CS. (2000) The cyclooxygenase-2 inhibitor celecoxib induces apoptosis by blocking Akt activation in human prostate cancer cells independently of Bcl-2, *J Biol Chem*, **15**, 11397-403.
- Ide, T., Egan, K., Bell-Parikh, C., FitzGerald, GA. (2003) Activation of nuclear receptors by prostaglandins, *Thrombosis Res*, **110**, 311-15.
- Iniguez, M., Rodriguez, A., Volpert, O., Fresno, M. and Redondo, J. (2003) Cyclooxygenase-2: a therapeutic target in angiogenesis, *Trends in Mol Med*, **9**, 73-78.
- Inoue, H., Yokoyama, C., Hara, S., Tone, Y. and Tanabe, T. (1995) Transcriptional Regulation of Human Prostaglandin-endoperoxide Synthase-2 Gene by Lipopolysaccharide and Phorbol Ester in Vascular Endothelial Cells, *J. Biol. Chem.*, **270**, 24965-24971.
- Inoue, H., Tanabe, T., Umesono, K. (2000) Feedback control of cyclooxygenase-2 expression through PPAR- γ , *J. Biol. Chem*, **275**, 28028-32.
- Inoue, H., Taba, Y., Miwa, Y., Yokota, C., Miyagi, M. & Sasaguri, T. (2002) Transcriptional and posttranslational regulation of cyclooxygenase-2 expression by fluid shear stress in vascular endothelial cells., *Arterioscler Thromb Vasc Biol.*, **22**, 1415-20.
- Jabbour, HN., Kelly, RW., and Boddy, SC. (2002) Autocrine/paracrine regulation of apoptosis in epithelial cells by prostaglandin E₂, *Prostaglandins, Leukotrienes and Essential Fatty Acids*, **67 (5)**, 357-363.
- Jantke, J., Landehoff, M., Kurzel, F., Zapf, S., Kim, E., and Giese, A. (2004) Inhibition of the arachidonic acid metabolism blocks endothelial cell migration and induces apoptosis, *Acta Neurochir*, **146**, 483-94.
- Jendrossek, V., Handrick, R., and Belka C. (2003) Celecoxib activates a novel mitochondrial apoptosis signalling pathway, *FASEB J*, **17**, 1547-49.

- Jo, D.G., Jun, J.I., Chang, J.W., Hong, Y.M., Song, S., Cho, D.H., Shim, S.M., Lee, H.J., Cho, C., Kim, D.H. & Jung, Y.K. (2004) Calcium binding of ARC mediates regulation of caspase 8 and cell death., *Mol Cell Biol.*, **24**, 9763-70.
- Johnson, A.J., Song, X., Hsu, A.L., and Chen, C.S. (2001) Apoptosis signalling pathways mediated by cyclooxygenase-2 inhibitors in prostrate cancer cells, *Adv Enz Reg*, **41**, 221-35.
- Jones, M., Wang, H., Peskar, B., Levin, E., Itani, R., Sarfeh, I. and Tarnanski, A. (1999) Inhibition of angiogenesis by non-steroidal anti-inflammatory drugs: Insight into mechanisms and implications for cancer growth and ulcer healing, *Nat Med*, **5**, 1418-23.
- Kalluri, R. (2003) Basement membranes: Structure, assembly and role in tumour angiogenesis, *Nat Rev*, **3**, 422-33.
- Kerr, J., Wyllie, A. and Currie, A. (1972) Apoptosis: a basic biological phenomenon with wide-ranging implications in tissue kinetics., *B J Cancer*, **26**, 239-57.
- King, A.R., Rowe, S.J., Francis, S.E., Whyte, M.K.B., Crossman, D.C. (2004) Human umbilical vein cell (HUVEC) resistance to apoptosis is mediated by activation of NF- κ B, *Cardio Pathol*, S127.
- Kirsch, D. G., Doseff, A., Chau, B. N., Lim, D.-S., de Souza-Pinto, N. C., Hansford, R., Kastan, M. B., Lazebnik, Y. A. and Hardwick, J. M. (1999) Caspase-3-dependent Cleavage of Bcl-2 Promotes Release of Cytochrome c, *J. Biol. Chem.*, **274**, 21155-21161.
- Kirtikawa, K., Raghov, R., Laulederkind, S.J.F., Goorha, S., Kanekura, T., and Ballou, L.R. (2000) Transcriptional regulation of cyclooxygenase-2 in the human microvascular endothelial cell line HMEC-1: Control by the combinatorial actions of AP2, NF-IL-6 and CRE elements, *Mol Cell Biochem*, **203**, 41-51.
- Koseki, T., Inohara, N., Chen, S. and Nunez, G. (1998) ARC, an inhibitor of apoptosis expressed in skeletal muscle and heart that interacts selectively with caspases, *PNAS*, **95**, 5156-5160.
- Krammer, P. (1999) CD95(APO-1/Fas)-mediated apoptosis: live and let die, *Adv Immunol*, **71**, 163-210.
- Kuwano, T., Nakao, S., Yamamoto, H., Tsuneyoshi, M., Yamamoto, T., Kuwano, M., Ono, M. (2004) Cyclooxygenase 2 is a key enzyme for inflammatory cytokine induced angiogenesis, *FASEB J*, **18**, 300-10.

- Kwon, KB., Yoo, SJ., Ryn, DG., Yang, JY., Kim, JS., Park, JW., Kun, HR., Park, BH. (2002) Induction of apoptosis by diallyl disulphide through activation of caspase 3 in human leukaemia HL-60 cells, *Biochem Pharmacol*, **63**, 41-7.
- Leahy, KM., Ormberg, RL., Wang, Y., Zweifel, BS., Koki, AT., Masferrer JM. (2002) Cyclooxygenase-2 inhibition by celecoxib reduces proliferation and induces apoptosis in angiogenic endothelial cells *in vivo*, *Cancer Res*, **62**, 625-31.
- Li, PF., Li, J., Muller, EC., Otto, A., Dietz, R., von Harsdorf R. (2002) Phosphorylation by protein kinase CK2: A signalling switch for the caspase-inhibiting protein ARC, *Mol Cell*, **10**, 247-258.
- Lichenburger, LM. (2001) Where is the evidence that cyclooxygenase inhibition is the primary cause of non-steroidal anti-inflammatory drug (NSAID)-induced gastrointestinal injury? Topical injury revisited, *Biochem Pharmacol*, **61**, 631-37.
- Lily, Y., Luo, X., Wang, X. (2001) Endonuclease G is an apoptotic DNase when released from mitochondria, *Nature*, **412**, 95-99.
- Lingen, M. (2001) Role of leukocytes and endothelial cells in the development of angiogenesis in inflammation and wound healing., *Arch Pathol Lab Med*, **125**, 67-71.
- Liu, D., Jai, H., Holmes, DIR., Stannard, A., Zachary, I. (2003) Vascular endothelial growth factor-regulated gene expression in endothelial cells: KDR-mediated induction of Egr3 and the related nuclear receptors Nur77, Nurr1 and Nor1, *Atherosclerotic and Thrombotic Vascular Biol*, **23**, 2002-07.
- Lui, XH., Kirschenbaum, A., Yu, K., Yao, S., Levine, AC. (2004) Cyclooxygenase-2 suppresses hypoxia-induced apoptosis via a combination of direct and indirect inhibition of p53 activity in a human prostate cancer cell line, *J. Biol. Chem*, **Nov 18**, 1-31
- Markman, M., Blessing, J., Rubin, SC., Connor, J., Parviz, H. and Waggoner, S. (2005) Phase II trial of weekly paclitaxel (80 mg/m²) in platinum and paclitaxel-resistant ovarian and primary peritoneal cancers: A gynecological oncology group study, *Gynecologic Oncol*, e-pub.
- Marnett, L., Rowlinson, S., Goodwin, D., Kalgutkar, A. and Lanzo, C. (1999) Arachidonic acid oxygenation by COX-1 and COX-2, *J. Biol. Chem*, **274**.
- Marnett, L. (2002) Cyclooxygenase mechanism, *Curr opin chem biol*, **4**, 545-552.

- Marsden, V., and Strasser, A. (2003) Control of apoptosis in the immune system: Bcl-2, BH3-only proteins and more., *Annu Rev Immunol*, **21**, 71-105.
- Martin, S. J., O'Brien, G. A., Nishioka, W. K., McGahon, A. J., Mahboubi, A., Saido, T. C. and Green, D. R. (1995) Proteolysis of Fodrin (Non-erythroid Spectrin) during Apoptosis, *J. Biol. Chem.*, **270**, 6425-6428.
- Marzo, I., Brenner, C., Zamzami, N., Jürgensmeier, J. M., Susin, S. A., Vieira, H. L. n. A., Prévost, M.-C., Xie, Z., Matsuyama, S., Reed, J. C. and Kroemer, G. (1998) Bax and Adenine Nucleotide Translocator Cooperate in the Mitochondrial Control of Apoptosis, *Science*, **281**, 2027-2031.
- Masferrer, JL., Zweifel, BS., Manning, PT., hauser, SD., Leahy, KM., Smith WG., Isakson, PC., Seibert, K. (1994) Selective inhibition of inducible cyclooxygenase 2 in vivo is anti-inflammatory and nonulcerogenic, *Proc. Natl. Acad. Sci. USA*, **91**, 3228-32.
- Masferrer, J. (2001) Approach to Angiogenesis Inhibition based on Cyclooxygenase -2, *Cancer J*, **7**, S144-S152.
- McKay, E. (2004) Isolation and identification of apoptosis repressor with CARD (ARC) in HUVECs, MSc. Research Project, University of Hertfordshire.
- Mestre, J. R., Rivadeneira, D. E., Mackrell, P. J., Duff, M., Stapleton, P. P., Mack-Strong, V., Maddali, S., Smyth, G. P., Tanabe, T. and Daly, J. M. (2001) Overlapping CRE and E-box promoter elements can independently regulate COX-2 gene transcription in macrophages, *FEBS Letters*, **496**, 147-151.
- Mitchell, JA., Akarasereenont, P., Thiemermann, C., Flower, RJ., Vane, JR., (1994) Selectivity of nonsteroidal anti-inflammatory drugs as inhibitors of constitutive and inducible cyclooxygenase. *Proc Natl Acad Sci U S A*, **90** (24), 11693-97.
- Moore, B. and Simmons, D. (2000) Cyclooxygenase 2 inhibition, apoptosis, and chemoprevention by non-steroidal anti-inflammatory drugs, *Curr med chem*, **7**, 1131-1144.
- Morgan DM, 1996, Isolation and culture of human umbilical cord endothelial cells. *Methods in molecular medicine: Human cell culture protocols*. Ed. Picot J. pg. 105-106, Humana press inc. Totowa, NJ: USA.

- Morita, I., Schindler, M., Regier, M. K., Otto, J. C., Hori, T., DeWitt, D. L. and Smith, W. L. (1995) Different Intracellular Locations for Prostaglandin Endoperoxide H Synthase-1 and -2, *J. Biol. Chem.*, **270**, 10902-10908.
- Mukherjee, D., Nissen, SE., Topol, EJ. (2001) Risk of cardiovascular events associated with selective COX-2 inhibitors. *JAMA*, **286**, 954-9.
- Murakami, M. and Kudo, I. (2004) Recent advances in molecular biology and physiology of the prostaglandin E2-biosynthetic pathway, *Prog in Lipid Res*, **43**, 3-35.
- Murphy, J. and Fitzgerald, D. (2001). Vascular endothelial growth factor induces cyclooxygenase- dependent proliferation of endothelial cells via the VEGF-2 receptor, *FASEB J*, **15**, 1667-69.
- Neisisus, U., Olsson, R., Rukwied, R., Lischetki, G., Schmelz, M. (2001). Prostaglandin E2 induces vasodilation and pruritus, but no protein extravasation in atopic dermatitis and controls, *J Am Acad of Dermatol*, **47**, 28-32.
- Neufeld, G., Cohen, T., Gengrinovitch, S., Poltorak, Z. (1999) Vascular endothelial growth factor (VEGF) and its receptors, *FASEB J*, **13**, 9-22.
- Neuss, M., Monticone, R., Lundberg, M. S., Chesley, A. T., Fleck, E. and Crow, M. T. (2001) The Apoptotic Regulatory Protein ARC (Apoptosis Repressor with Caspase Recruitment Domain) Prevents Oxidant Stress-mediated Cell Death by Preserving Mitochondrial Function, *J. Biol. Chem.*, **276**, 33915-33922.
- Nicholson, D. W. and Thornberry, N. A. (1997) Caspases: killer proteases, *Trends in Biochem Sci*, **22**, 299-306.
- Niederberger, E., Manderscheid, C., Grosch, S., Schmidt, H., Ehnert, C., Geisslinger, G. (2004) Effects of the selective COX-2 inhibitors celecoxib and rofecoxib on human vascular cells, *Biochem Pharmacol*, **68**, 341-50.
- Nor, JE., Christensen, J, Mooney, DJ., and Polverini, PJ. (1999) Vascular endothelial growth factor (VEGF)- mediated angiogenesis is associated with enhanced endothelial cell survival and induction of Bcl-2 expression, *Am Jof Pathol*, **154** (2), 375-82.

- Nor, JE., Christensen, J, Liu, J., Peters, M., Mooney, DJ., Strieter, RM., and Polverini, PJ. (2001) Up-regulation of Bcl-2 in microvascular endothelial cells enhances intratumoral angiogenesis and accelerates tumour growth, *Cancer Res*, **61**, 2183-88.
- Oberhammer, F., Wilson, JW., Dive, C., Morris, ID., Hickman, JA., Wakeling, AE., Walker, PR., Sikorska, M. (1993) Apoptotic death in epithelial cell: cleavage of DNA to 300 and/or 50 kb fragments prior to or in the absence of internucleosomal fragmentation, *EMBO J*, **12**, 3679-84.
- Orth, K., O'Rourke, K., Salvesen, G. S. and Dixit, V. M. (1996) Molecular Ordering of Apoptotic Mammalian CED-3/ICE-like Proteases, *J. Biol. Chem.*, **271**, 20977-20980.
- Ottonello, L., gonella R., Dapino, P., Sacchetti, C., Dallegri, F. (1998) Prostaglandin E2 inhibits apoptosis in human neutrophilic polymorphonuclear leukocytes: role of intracellular cyclic AMP levels, *Exp Haematol*, **26 (9)**, 895-902.
- Pai, R., Szabo, IL., Soreghan, BA., Atay, S., Kawanaka, H., and Tarnawski, AS. (2001) PGE2 stimulates VEGF expression in endothelial cells via ERK2/JNK1 signalling pathways, *Biochem and Biophys Res Comms*, **286**, 923-28.
- Pairet, M. (1999) In *Inducible enzymes*, Vol. 1 London, UK.
- Parrish, J., Li, L., Klotz, K., Ledwich, D., Wang, X., Xue, D. (2001) Mitochondrial endonuclease G is important for apoptosis in *C.elegans*, *Nature*, **412**, 90-94.
- Pan, J., Xu, G., Yeung, SCJ. (2001) Cytochrome-c release is upstream of activation of caspase-9, caspase-8 and caspase-3 in the enhanced apoptosis of anaplastic thyroid cancer cells induced by manumycin and paclitaxel, *J Clin Endocrinol and Metabol*, **86 (10)**, 4731-40.
- Pang, L., and Hoult, JRS. (1997) Repression of inducible nitric oxide synthase and cyclooxygenase-2 by prostaglandin E2 and other cyclic AMP stimulants in J774 macrophages, *Biochem Pharmacol*, **53**, 493-500.
- Paper, D. (1998) Natural Products as Angiogenesis Inhibitors, *Planta Medica*, **64**, 686-695.
- Parfenova, H., Parfenova, VN., Shlopov, BV., Levine, V., Falkos, S., Pourcyrous, M., Leffler, CW. (2001) Dynamics of nuclear localisation sites for COX-2 in vascular endothelial cells, *Am J Physiol: Cell Physiol*, **281**, C166-78.

- Pasyk, KA. and Jakobczak, BA. (2004) Vascular endothelium: Recent advances, *European J Dermatol*, **14**, 209-13.
- Penning, TD., Talley, JJ., Bertenshaw, SR., Carter, JS., Collins, PW., Docter, S., Graneto, MJ., Lee, LF., Malecha, JW., Miyashiro, JM., Rogers, RS., Koboldt, CM., Perkins, WE., Seibert, K., Veenhuizen, AW., Zhang, YY., Isakson, PC. (1997) Synthesis and biological evaluation of the 1,5-Diarylpyrazole class of cyclooxygenase-2 inhibitors: Identification of 4-[5-(4-methylphenyl)-3-(trifluoromethyl)-1H-pyrazol-1-yl]benzenesulfonamide (SC-58635, celecoxib), *J Med Chem*, **40**, 1347-65.
- Pentland, AP., Scott, G., VanBuskirk, J., Tanck, C., LaRossa, G., and Brouxhons S. (2004) Cyclooxygenase-1 deletion enhances apoptosis but does not protect against ultraviolet light-induced tumours, *Cancer Res*, **64**, 5587-91.
- Perez-Sala, D. and Lamas, S. (2001) Regulation of cyclooxygenase -2 expression by nitric oxide in cells, *Antioxidants and Redox sig*, **3**, 231-48.
- Piwocka, K., Zablocki, K., Weickowski, M., Skierski, J., Feiga, I., Szorpa, J., Drela, N., Wojczack, L. and Sikora, E. (1999) A novel apoptosis like pathway, independent of mitochondria and caspases, induced by curcumin in human lymphoblastoid T (Jurkat) cells, *Exp Cell Res*, **249**.
- Piwocka, K., Jarugu, E., Skierski, J., Gradzka, I. and Sikora, E. (2001) Effect of glutathione depletion on caspase - 3 independent apoptosis pathway induced by curcumin in Jurkat cells, *Free Radical Biol and Med*, **31**, 670-678.
- Piwocka, K., Bielak-Zmijenska, A. and Sikora, E. (2002) Curcumin induces caspase-3 independent apoptosis in human multi-drug resistant cells, *Ann. NY. Acad. Sci*, **973**, 250-254.
- Pluda, JM. (1997) Tumour-associated angiogenesis: Mechanisms, clinical implications, and therapeutic strategies, *Sem Oncol*, **24**, 203-18.
- Plummer, SM., Holloway, KA., Manson, MM., Munks RJL., Kaptein, A., Farrow, S., Howells, L. (1999) Inhibition of cyclooxygenase 2 expression in colon cells by the chemopreventive agent curcumin involves inhibition of NF- κ B activation via the NIK/IKK signalling complex, *Oncogene*, **18**, 6013-20.
- Pollman, MJ., Naumovski, L., Gibbons, GH. (1999) Endothelial cell apoptosis in capillary network remodelling, *J Cell Physiol*, **178**, 359-70.

- Proskuryakov, SY., Gabai, VL., Konoplyannikov, AG. (2002) Necrosis is an active and controlled form of programmed cell death, *Biochemistry*, **67**, 387-408.
- Purdy, KE., Arendshorst, WJ. (2000) EP1 and EP4 receptors mediate prostaglandin E₂ actions in the microcirculation of rat kidney, *Am J Physiol: Renal Physiol*, **279**, F755-64.
- Rak, J., Mitsuhashi, Y., Sheehan, C., Tamir, A., Vilorio-Petit, A., Filmus, J., Mansour, S. J., Ahn, N. G. and Kerbel, R. S. (2000) Oncogenes and Tumor Angiogenesis: Differential Modes of Vascular Endothelial Growth Factor Up-Regulation in ras-transformed Epithelial Cells and Fibroblasts, *Cancer Res*, **60**, 490-498.
- Rao, L., Perez, D. and White, E. (1996) Lamin proteolysis facilitates nuclear events during apoptosis, *J. Cell Biol.*, **135**, 1441-145.
- Riendeau, D., Charleson, W., Cromish, W., Mancini, JA., Wong, E., and Guay, J. (1997) Comparison of the cyclooxygenase-1 inhibitory properties of non-steroidal anti-inflammatory drugs (NSAIDs) and selective COX-2 inhibitors, using sensitive microsomal and platelet assays, *Can. J Physiol Pharmacol*, **75**, 1088-95.
- Rosenstock, M., Danon, A., Rimon, G. (1999) PGHS-2 inhibitors, NS398 and DuP-697, attenuate the inhibition of PGHS-1 by aspirin and indomethacin without altering its activity, *Biochimica et Biophysica Acta*, **1440**, 127-37.
- Rosenstock, M., Danon, A., Rubin, M., Rimon, G. (2001) Prostaglandin H synthase-2 inhibitors interfere with prostaglandin H synthase-1 inhibition by nonsteroidal anti-inflammatory drugs, *European J Pharmacol*, **414**, 101-108.
- Rotonda, J., Nicholson, D., Fazil, K., Gallant, M., Gareau, Y., Labelle, M., Peterson, E., Rasper, D., Ruel, R., Vaillancourt, J., Thornberry, N. and Becker, J. (1996) The three-dimensional structure of apopain/CPP32, a key mediator of apoptosis, *Nat Struct Biol*, **3**, 619-25.
- Ruegg, C., Dormond, O. and Mariotti, A. (2004) Endothelial cell integrins and COX-2: mediators and therapeutic targets of tumour angiogenesis, *Biochimica et Biophysica*, **1654**, 51-67.
- Rusnak, JM., Calmels, TP., Hoyt, DG., Kondo, Y., Yalowich, JC., Lazo, JS. (1996) genesis of discrete higher order DNA fragments in apoptotic human prostatic carcinoma cells, *Mol Pharmacol*, **49** (2), 244-52.

- Sakahira, H., Takemura, Y. and Nagata, S. (2001) Enzymatic Active Site of Caspase-Activated DNase (CAD) and It's Inhibition by Inhibitor of CAD, *Archives Biochem and Biophys*, **388**, 91-99.
- Sakamoto, C. (1998) Roles of COX-1 and COX-2 in gastrointestinal pathophysiology, *J Gastroenterol*, **33**, 618-24.
- Salvesen, G. and Dixit, V. (1997) Caspases: intracellular signaling by proteolysis, *Cell*, **91**, 443-6.
- Savill, J., Fadok, V., Henson, P., Haslett, C. (1993) Phagocyte recognition of cells undergoing apoptosis, *Immunol Today*, **14 (3)**, 131-36.
- Sawaoka, H., Tsuji, S., Tsuji, M., Gunauen, E., Sasaki, Y., Kawano, S. and Hori, M. (1999) Cyclooxygenase inhibitors suppress angiogenesis and reduce tumour growth in vivo, *Lab Invest*, **79**, 1469-77.
- Schultz, DR., and Harrington, WJ. (2003) Apoptosis: Programmed cell death at a molecular level, *Sem in Arthritis and Rheumatism*, **32 (6)**, 345-69.
- Sheng, H., Shao, J., Morrow, JD., Beauchamp, RD., Dubois, RN. (1998) Modulation of apoptosis and Bcl-2 expression by prostaglandin E₂ in human colon cancer cells, *Cancer Res*, **58 (2)**, 363-6.
- Shi, Y. (2001) A structural view of mitochondria-mediated apoptosis, *Nature Structural Biol*, **8**.
- Shi, Y. (2002) Mechanisms of caspase activation and inhibition during apoptosis, *Mol Cell*, **9**, 459-70.
- Shikama, Y., Mai, U., Miyashita, T. and Yamada, M. (2001) Comprehensive Studies on Subcellular Localizations and Cell Death-Inducing Activities of Eight GFP-Tagged Apoptosis-Related Caspases, *Exp Cell Res*, **264**, 315-325.
- Shimizu, S., Narita, M. and Tsujimoto, Y. (1999) Bcl-2 family proteins regulate the release of apoptogenic cytochrome c by the mitochondrial channel VDAC, *Nature*, **399**, 483-487.
- Shimizu, S., Shinohara, Y. and Tsujimoto, Y. (2000) Bax and Bcl-xL independently regulate apoptotic changes of yeast mitochondria that require VDAC but not adenine nucleotide translocator, *Oncogene*, **19**, 4309-18.
- Simon, L. (1999) Role and regulation of cyclooxygenase-2 during inflammation, *Am J Med*, **106**, 37s-42s.

- Singh, AK., Sidhu, GS., Deepa, T., Maheshwari, RK. (1996) Curcumin inhibits the proliferation and cell cycle progression of human umbilical vein endothelial cell, *Cancer Letters*, **107**, 109-15.
- Smith, EJ. (2004) Identification and characterisation of anti-angiogenic protein fragments in venous leg ulcer fluid, *PhD thesis*, University of Hertfordshire.
- Smith, W. L. and Langenbach, R. (2001) Why there are two cyclooxygenase isozymes? *J. Clin. Invest.*, **107**, 1491-1495.
- Smith, WL. (1986) Prostaglandin biosynthesis and its compartmentation in vascular smooth muscle and endothelial cells, *Annu Rev Physiol*, **48**, 251-62.
- Smith, C. J., Zhang, Y., Koboldt, C. M., Muhammad, J., Zweifel, B. S., Shaffer, A., Talley, J. J., Masferrer, J. L., Seibert, K. and Isakson, P. C. (1998) Pharmacological analysis of cyclooxygenase-1 in inflammation, *PNAS*, **95**, 13313-13318.
- Smith, W., DeWitt, D. and Garavito, R. (1999) Cyclooxygenases: structural, cellular, and molecular biology, *Annu Rev Biochem*, **69**, 145-82.
- Soldi, R., Mitola, S., Strasly, M., Defilippi, P., Tarone, G., Bussolino, F. (1999) Role of $\alpha V\beta 3$ integrin in the activation of vascular endothelial growth factor receptor-2, *EMBO J*, **18** (4), 882-92.
- Soler, M., Camacho, M., Escudero, JR., Iniguez, MA., Vila, L., (2000) human vascular smooth muscle cells but not endothelial cells express prostaglandin E synthase, *Circulation Res*, **Sept 15**, 504-07.
- Song, X., Lin, HP., Johnson, AJ., Tseng, PH., Yang, YT., Kulp, SK., and Chen, CS. (2002) Cyclooxygenase-2. player or spectator in cyclooxygenase-2 inhibitor- induced apoptosis in prostrate cancer cells, *J National Cancer Institute*, **94**, 585-91.
- Stack, E. and Dubois, R. (2001) Regulation of cyclo-oxygenase-2, *Best Prac Res Clin Gastroenterol*, **15**, 787-800
- Steele, VE., Hawk, ET., Viner, JL., Lubet, RA. (2003) Mechanisms and applications of non-steroidal anti-inflammtory drugs in the chemoprevention of cancer, *Mut Res*, **523-4**, 137-44.
- Subhashini, J., Malupal, SV. and Reddanna, P. (2005) Anti-proliferative and apoptotic effects of celecoxib on human chronic myeloid leukaemia in vitro, *Cancer Letters*, **224**, 31-43.

- Sun, Y., Tang, XM., Half, E., Kuo, MT., and Sinicrope, FA. (2002) Cyclooxygenase-2 overexpression reduces apoptotic susceptibility by inhibiting the cytochrome c-dependent apoptotic pathway in human colon cancer cells, *Cancer Res*, **62**, 6323-28.
- Surh, Y.-J., Chun, K.-S., Cha, H.-H., Han, S. S., Keum, Y.-S., Park, K.-K. and Lee, S. S. (2001) Molecular mechanisms underlying chemopreventive activities of anti-inflammatory phytochemicals: down-regulation of COX-2 and iNOS through suppression of NF-[kappa]B activation, *Mut Res/Fundamental Mol Mech of Mutagen*, **480-481**, 243-268.
- Tamura, M., Sebastian, S., Gurates, B., Yang, S., Fang, Z. and SE, B. (2002) Vascular endothelial growth factor up-regulates cyclooxygenase-2 expression in human endothelial cells, *J Clin Endocrinol Metab*, **87**, 3504-7.
- Tanabe, T. and Tohnai, N. (2002) Cyclooxygenase isozymes and their gene structures and expression, *Prostaglandins and Other Lipid Med*, **68-69**, 95-114.
- Taylor, EL., Megson, IL., Haslett, C., Rossi, AG. (2001) Dissociation of DNA fragmentation from the other hallmarks of apoptosis in nitric oxide-treated neutrophils: Differences between individual nitric oxide donor drugs, *Biochem Biophys Res Comms*, **289**, 1229-36.
- Thaloor, D., Singh, AK., Sidhu, GS., Prasad, PV., Kleinman, HK., Maheshwari, RK. (1998) Inhibition of angiogenic differentiation of human umbilical vein endothelial cells by curcumin, *Cell Growth and Diff*, **9**, 305-12.
- Thornberry, N., Rosen, A. and Nicholson, D. (1997) Control of apoptosis by proteases, *Adv Pharmacol*, **41**, 155-77.
- Thurston, G., Maas, K., Labarbara, A., Mclean, JW., McDonald, DM. (2000) Microvascular remodelling in chronic airway inflammation in mice, *Clin Exp Pharmacol Physiol*, **27**, 836-41.
- Tjendraputra, E., Tran, V., Liu-Brennan, D., Roufogalis, B. and Duke, C. (2001) Effect of Ginger constituents and synthetic analogues on cyclooxygenase 2 enzyme in intact cells., *Bioorg Chem*, **29**, 156-63.
- Totzke, G., Schulze-Osthoff, K., Janicke, RU. (2003) Cyclooxygenase-2 (COX-2) inhibitors sensitize tumour cells specifically to death receptor-induced apoptosis independently of COX-2 inhibition, *Oncogene*, **22** (39), 8021-30.

- Tsujii, M. and Dubois, RN. (1995) Alterations in cellular adhesion and apoptosis in epithelial cells overexpressing prostaglandin endoperoxidase synthase 2, *Cell*, **83**, 493-501.
- Uracz, W., Uracz, D., Olszanecki, R., Gryglewski, RJ. (2002) Interleukin 1 β induces functional prostaglandin E synthase in cultured human umbilical vein endothelial cells, *J Physiol Pharmacol*, **53**, 643-54.
- Urban, MK. (2000) COX-2 specific inhibitors offer improved advantages over traditional NSAIDs, *Orthopedics*, **23** (7), s761-64.
- van Loo, G., Saelens, X., Matthijssens, F., Schotte, P., Beyaert, R., Declercq, W. and Vandenaabeele, P. (2002) Caspases are not localized in mitochondria during life or death, *Cell Death Differ*, **9**, 1207-11.
- Varner, JA., Brooks, PC. and Cherish, DA. (1995) The integrin alpha V beta 3: Angiogenesis and apoptosis, *Cell Adhesion Comms*, **3**, 367-74.
- Wagner, BA., Buettner, GR., Oberley, LW., Darby, CJ., Burns, CP. (2000) Myeloperoxidase is involved in H₂O₂-induced apoptosis of HL-60 human leukaemia cells, *J. Biol. Chem*, **275**, 22461-69.
- Walisser, JA. and Thies, RL. (1999) Poly(ADP-ribose) polymerase inhibition in oxidant-stressed endothelial cells prevents oncosis and permits caspase activation and apoptosis, *Exp Cell Res*, **251**, 401-13.
- Wallace, JL. (1999) Distribution and expression of cyclooxygenase (COX) isoenzymes, their physiological roles, and the categorization of the nonsteroidal anti-inflammatory drugs (NSAIDs), *Am J Med*, 11s-15s.
- Ward, C., Dransfield, I., Murray, J., Farrow, SN., Haslett, C., Rossi, AG. (2002) Prostaglandin D₂ and its metabolites induce caspase-dependent granulocyte apoptosis that is mediated via inhibition of I κ B α degradation using a peroxisome proliferator-activated receptor- γ -independent mechanism, *J Immunol*, **168**, 6232-43.
- Wary, KK., Thakker, GD., O'Humtsoe, J., Yang, J. (2003) Analysis of VEGF-responsive genes involved in the activation of endothelial cells, *Mol Cancer*, **2**, 1-12.
- Wei, QY., Ma, JP., Cai, YJ., Yang, L., Lui, ZL. (2005) Cytotoxic and apoptotic activities of diarylheptanoids and gingerol-related compounds from the rhizome of Chinese ginger, *J Ethnopharmacol*, **102**, 177-84.
- Weir, MR., Froch, I. (2000) Weighing the renal effects of NSAIDs and COX-2 inhibitors, *Clin Dilemmas*, **1**, 3-12.

- Wheeler-Jones, C., Abu-Ghazaleh, R., Cospedal, R., Houlston, RA., Martin, J. and Zachary, I. (1997) Vascular endothelial growth factor stimulates prostacyclin production and activation of cytosolic phospholipase A2 in endothelial cells via p42/p44 mitogen activated kinase, *FEBS letters*, **420**, 28-32.
- Williams, CS., Tsujii, M., Reese, J., Dey, SK., and Dubois, RN. (2000) Host cyclooxygenase-2 modulates carcinoma growth, *J Clin Invest*, **105**, 1589-1594.
- Willoughby, D. A., Moore, A. R., Colville-Nash, P. R. and Gilroy, D. (2000) Resolution of inflammation, *Int J Immunopharmacol*, **22**, 1131-1135.
- Wilson, J. and Potten, C. (1999) In *Apoptosis: A practical approach* (Ed, Studzinski, G.) Humana, London.
- Wu, GS., Zou, SQ., Liu, ZR., Tang, ZH., Wang JH. (2003) Celecoxib inhibits proliferation and induces apoptosis via prostaglandin E2 pathway in human cholangiocarcinoma cell lines, *World J Gastroenterol*, **9** (6), 1302-06.
- Yamamoto, K., Arakawa, T., Ueda, N. and Yamamoto, S. (1995) Transcriptional Roles of Nuclear Factor kappaB and Nuclear Factor-Interleukin-6 in the Tumor Necrosis Factor alpha-Dependent Induction of Cyclooxygenase-2 in MC3T3-E1 Cells, *J. Biol. Chem.*, **270**, 31315-320.
- Yazawa, K., Tsuno, NH., Kitayama, J., Kawai, K., Okaji, Y., Asakage, M., Sunami, E., kaisaki, S., Hori, N., Wantanabe, T., Takahashi, K., Nagawa, H. (2005) Selective inhibition of cyclooxygenase (COX)-2 inhibits endothelial cell proliferation by induction of cell cycle arrest, *Int J Cancer*, **113**, 541-48.
- Yoshida, H., Kong, Y., Yoshida, R., Elia, A., Hakem, A., Hakem, R., Penninger, J. and Mak, T. (1998) Apaf1 is required for mitochondrial pathways of apoptosis and brain development., *Cell*, **94**, 739-50.
- Zakeri, ZF., Quaglino, D., Latham, T., Lockshin, RA. (1993) Delayed internucleosomal DNA fragmentation in programmed cell death, *FASEB J*, **7**, 470-78.
- Zamzami, N. and Kroemer, G. (2003) Apoptosis: Mitochondrial Membrane Permeabilization - The (W)hole Story?, *Curr Biol*, **13**, R71-R73
- Zha, S., Yegnasubramanian, V., Nelson, WG., Isaacs, WB., De Marzo, AM. (2004) Cyclooxygenases in cancer: progress and perspective, *Cancer Lectures*, **215**, 1-20.

- Zhang, F., Altorki, N., Mestre, J., Subbaramaiah, K. and Dannenberg, A. (1999) Curcumin inhibit cyclooxygenase -2 transcription in bile acid and phorbol ester treated human gastrointestinal epithelial cells, *Carcinogenesis*, **20**, 445-51.
- Zheng, T. S. and Flavell, R. A. (2000) Divinations and Surprises: Genetic Analysis of Caspase Function in Mice, *Exp Cell Res*, **256**, 67-73.
- Zimmermann, K. C., Bonzon, C. and Green, D. R. (2001) The machinery of programmed cell death, *Pharmacol Therap*, **92**, 57-70.
- Zou, H., Li, Y., Liu, X. and Wang, X. (1999) An APAF-1·Cytochrome c Multimeric Complex Is a Functional Apoptosome That Activates Procaspase-9, *J. Biol. Chem.*, **274**, 11549-11556.

9.0 Appendix A: Products and Supplier List

<u>Product</u>	<u>Supplier</u>
<u>Primary antibodies</u>	
Anti apoptosis repressor with CARD polyclonal rabbit IgG	Merck Biosciences
Anti Caspase-3 monoclonal mouse IgG	Merck Biosciences
Anti Caspase-8 monoclonal mouse IgG	Merck Biosciences
Anti Caspase-9 monoclonal mouse IgG	Merck Biosciences
Anti Cyclooxygenase-2 polyclonal goat IgG	Santa Cruz
<u>Secondary antibodies</u>	
Anti goat IgG-HRP conjugate	Santa Cruz
Anti mouse IgG-HRP conjugate	Merck Biosciences
Anti rabbit IgG-HRP conjugate	Merck Biosciences
<u>Assay kits</u>	
BCA protein assay kit	Pierce
Caspase-3 cellular activity assay kit	Merck Biosciences
DNA suicide track ® kit	Merck Biosciences
JetPEI-HUVEC transfection reagent	Autogen Bioclear
PGE ₂ ELISA Kit	R & D Systems

Cell culture and isolation

Collagenase (type 2a)	Sigma
Endothelial cell growth factor	Sigma
Foetal bovine serum	Sigma
Gelatin	Sigma
L-Glutamine	Sigma
Media 199	Sigma
Penicillin/streptomycin	Sigma
RPMI 1640 media	Sigma
Trypsin-EDTA	Sigma
Matrigel	Sigma

Cytospinning and cell staining

Acridine orange	Sigma
Glycerol	Sigma
Glass slides	Menzel-Glaser

Gel electrophoresis and western blotting

Acrylamide/ Bisacrylamide (37.5:1)	Sigma
Ammonium persulphate	BDH
Bromophenol blue	BDH
Bovine serum albumin	Sigma
Photographic developer	Amersham
	Pharmacia
	Biotech
Dithiothreitol	BDH
Enhanced Chemiluminescence Reagents	Amersham
	Pharmacia
	Biotech
ECL photographic film	Kodak
Photographic fixer	Amersham
	Pharmacia
	Biotech

Glycine	BDH
Methanol	Fischer Scientific
Nitrocellulose membrane	Biorad
Non fat dried milk	Marvel
Phosphate buffered saline tablets	Sigma
Polyoxyethylene sorbitan monolaurate/Tween 20	Sigma
Sodium dodecyl sulphate (SDS)	Sigma
Tetramethylethylenediamine/TEMED	BDH
Trizma -Base	BDH
<u>Miscellaneous</u>	
Actinomycin-D	BDH
Agarose	Sigma
CHO-DEVD (specific caspase 3 inhibitor)	Sigma
Curcumin	Sigma
DuP-697	Toocris Cookson
Ethidium bromide	Sigma
Hydrogen peroxide	Sigma
Indomethacin	Sigma
Lipopolysaccharide (LPS)	Sigma
Paclitaxel (Taxol ®)	Sigma
Paracetamol	Sigma
6-Shogaol	
Sodium chloride	BDH

10.0 Appendix B: Solutions and Reagents

<u>E.coli Growth Media</u>		
<u>LB Agar</u>	Tryptone	10g/ L
	Yeast extract	5g/ L
	NaCl	10g/ L
	Bacterial agar N ^o . 1	20g/ L
<u>LB Broth</u>	Tryptone	10g/ L
	Yeast extract	5g/ L
	NaCl	10g/ L
<u>Ampicillin</u>		50mg/ml diluted to 50 µg/ml

<u>DNA gel analysis</u>			
			Final Concentration
<u>TAE buffer</u>	Tris (base)	4.84g/ L	0.04 M
	EDTA	0.372g/ L	0.001M
	pH 8.0 with glacial acetic acid		
<u>TE buffer</u>	1M Tris-Hcl pH7.4	10 ml	0.01M
	0.5M EDTA pH8.0	2 ml	0.001M

<u>Western Blotting</u>			
			Final Concentration
<u>SDS-PAGE</u> <u>Electrode Buffer</u>	Tris (Base)	6g/ L	0.05 M
	Glycine	28.8g/ L	0.384 M
	SDS	1g/ L	0.1 % (w/v)
<u>Blotting Buffer</u>	Tris (Base)	3.03g/ L	25mM
	Glycine	14.41g/ L	192mM
	Methanol	0.2 L/ L	20% (v/v)

<u>SDS-PAGE gels</u>			
<u>Resolving gel (x2)</u>		12.5% acrylamide	15% acrylamide
	1.875 M Tris-Hcl pH 8.8	2 ml	2 ml
	Distilled H ₂ O	3.65 ml	2.85 ml
	30% Acrylamide/ Bis-acrylamide	4.2 ml	5 ml
	10% SDS (w/v)	100 µl	100 µl
	10% ammonium persulphate (w/v)	50 µl	50 µl

<u>SDS-PAGE gels</u>		
<u>Stacking gel (x2)</u>		4% acrylamide
	0.6 M Tris-Hcl pH 6.8	0.5 ml
	Distilled H ₂ O	3.75 ml
	30% Acrylamide/ Bis-acrylamide	0.68 ml
	10% SDS (w/v)	50 µl
	10% ammonium persulphate (w/v)	25 µl